

A Performance-Related Specification for Hot-Mixed Asphalt

DETAILS

185 pages | | PAPERBACK

ISBN 978-0-309-21364-6 | DOI 10.17226/22835

AUTHORS

BUY THIS BOOK

FIND RELATED TITLES

Visit the National Academies Press at NAP.edu and login or register to get:

- Access to free PDF downloads of thousands of scientific reports
- 10% off the price of print titles
- Email or social media notifications of new titles related to your interests
- Special offers and discounts



Distribution, posting, or copying of this PDF is strictly prohibited without written permission of the National Academies Press. (Request Permission) Unless otherwise indicated, all materials in this PDF are copyrighted by the National Academy of Sciences.

NCHRP REPORT 704

**A Performance-Related
Specification for
Hot-Mixed Asphalt**

FUGRO CONSULTANTS INC.
Austin, TX

ARIZONA STATE UNIVERSITY
Tempe, AZ

Subscriber Categories

Highways • Materials • Construction

Research sponsored by the American Association of State Highway and Transportation Officials
in cooperation with the Federal Highway Administration

TRANSPORTATION RESEARCH BOARD

WASHINGTON, D.C.

2011

www.TRB.org

NATIONAL COOPERATIVE HIGHWAY RESEARCH PROGRAM

Systematic, well-designed research provides the most effective approach to the solution of many problems facing highway administrators and engineers. Often, highway problems are of local interest and can best be studied by highway departments individually or in cooperation with their state universities and others. However, the accelerating growth of highway transportation develops increasingly complex problems of wide interest to highway authorities. These problems are best studied through a coordinated program of cooperative research.

In recognition of these needs, the highway administrators of the American Association of State Highway and Transportation Officials initiated in 1962 an objective national highway research program employing modern scientific techniques. This program is supported on a continuing basis by funds from participating member states of the Association and it receives the full cooperation and support of the Federal Highway Administration, United States Department of Transportation.

The Transportation Research Board of the National Academies was requested by the Association to administer the research program because of the Board's recognized objectivity and understanding of modern research practices. The Board is uniquely suited for this purpose as it maintains an extensive committee structure from which authorities on any highway transportation subject may be drawn; it possesses avenues of communications and cooperation with federal, state and local governmental agencies, universities, and industry; its relationship to the National Research Council is an insurance of objectivity; it maintains a full-time research correlation staff of specialists in highway transportation matters to bring the findings of research directly to those who are in a position to use them.

The program is developed on the basis of research needs identified by chief administrators of the highway and transportation departments and by committees of AASHTO. Each year, specific areas of research needs to be included in the program are proposed to the National Research Council and the Board by the American Association of State Highway and Transportation Officials. Research projects to fulfill these needs are defined by the Board, and qualified research agencies are selected from those that have submitted proposals. Administration and surveillance of research contracts are the responsibilities of the National Research Council and the Transportation Research Board.

The needs for highway research are many, and the National Cooperative Highway Research Program can make significant contributions to the solution of highway transportation problems of mutual concern to many responsible groups. The program, however, is intended to complement rather than to substitute for or duplicate other highway research programs.

NCHRP REPORT 704

Project 09-22
ISSN 0077-5614
ISBN 978-0-309-21364-6
Library of Congress Control Number 2011940562

© 2011 National Academy of Sciences. All rights reserved.

COPYRIGHT INFORMATION

Authors herein are responsible for the authenticity of their materials and for obtaining written permissions from publishers or persons who own the copyright to any previously published or copyrighted material used herein.

Cooperative Research Programs (CRP) grants permission to reproduce material in this publication for classroom and not-for-profit purposes. Permission is given with the understanding that none of the material will be used to imply TRB, AASHTO, FAA, FHWA, FMCSA, FTA, or Transit Development Corporation endorsement of a particular product, method, or practice. It is expected that those reproducing the material in this document for educational and not-for-profit uses will give appropriate acknowledgment of the source of any reprinted or reproduced material. For other uses of the material, request permission from CRP.

NOTICE

The project that is the subject of this report was a part of the National Cooperative Highway Research Program, conducted by the Transportation Research Board with the approval of the Governing Board of the National Research Council.

The members of the technical panel selected to monitor this project and to review this report were chosen for their special competencies and with regard for appropriate balance. The report was reviewed by the technical panel and accepted for publication according to procedures established and overseen by the Transportation Research Board and approved by the Governing Board of the National Research Council.

The opinions and conclusions expressed or implied in this report are those of the researchers who performed the research and are not necessarily those of the Transportation Research Board, the National Research Council, or the program sponsors.

The Transportation Research Board of the National Academies, the National Research Council, and the sponsors of the National Cooperative Highway Research Program do not endorse products or manufacturers. Trade or manufacturers' names appear herein solely because they are considered essential to the object of the report.

Published reports of the

NATIONAL COOPERATIVE HIGHWAY RESEARCH PROGRAM

are available from:

Transportation Research Board
Business Office
500 Fifth Street, NW
Washington, DC 20001

and can be ordered through the Internet at:

<http://www.national-academies.org/trb/bookstore>

Printed in the United States of America

THE NATIONAL ACADEMIES

Advisers to the Nation on Science, Engineering, and Medicine

The **National Academy of Sciences** is a private, nonprofit, self-perpetuating society of distinguished scholars engaged in scientific and engineering research, dedicated to the furtherance of science and technology and to their use for the general welfare. On the authority of the charter granted to it by the Congress in 1863, the Academy has a mandate that requires it to advise the federal government on scientific and technical matters. Dr. Ralph J. Cicerone is president of the National Academy of Sciences.

The **National Academy of Engineering** was established in 1964, under the charter of the National Academy of Sciences, as a parallel organization of outstanding engineers. It is autonomous in its administration and in the selection of its members, sharing with the National Academy of Sciences the responsibility for advising the federal government. The National Academy of Engineering also sponsors engineering programs aimed at meeting national needs, encourages education and research, and recognizes the superior achievements of engineers. Dr. Charles M. Vest is president of the National Academy of Engineering.

The **Institute of Medicine** was established in 1970 by the National Academy of Sciences to secure the services of eminent members of appropriate professions in the examination of policy matters pertaining to the health of the public. The Institute acts under the responsibility given to the National Academy of Sciences by its congressional charter to be an adviser to the federal government and, on its own initiative, to identify issues of medical care, research, and education. Dr. Harvey V. Fineberg is president of the Institute of Medicine.

The **National Research Council** was organized by the National Academy of Sciences in 1916 to associate the broad community of science and technology with the Academy's purposes of furthering knowledge and advising the federal government. Functioning in accordance with general policies determined by the Academy, the Council has become the principal operating agency of both the National Academy of Sciences and the National Academy of Engineering in providing services to the government, the public, and the scientific and engineering communities. The Council is administered jointly by both Academies and the Institute of Medicine. Dr. Ralph J. Cicerone and Dr. Charles M. Vest are chair and vice chair, respectively, of the National Research Council.

The **Transportation Research Board** is one of six major divisions of the National Research Council. The mission of the Transportation Research Board is to provide leadership in transportation innovation and progress through research and information exchange, conducted within a setting that is objective, interdisciplinary, and multimodal. The Board's varied activities annually engage about 7,000 engineers, scientists, and other transportation researchers and practitioners from the public and private sectors and academia, all of whom contribute their expertise in the public interest. The program is supported by state transportation departments, federal agencies including the component administrations of the U.S. Department of Transportation, and other organizations and individuals interested in the development of transportation. www.TRB.org

www.national-academies.org

COOPERATIVE RESEARCH PROGRAMS

CRP STAFF FOR NCHRP REPORT 704

Christopher W. Jenks, *Director, Cooperative Research Programs*
Crawford F. Jencks, *Deputy Director, Cooperative Research Programs*
Edward T. Harrigan, *Senior Program Officer*
Melanie Adcock, *Senior Program Assistant*
Eileen P. Delaney, *Director of Publications*
Margaret B. Hagood, *Editor*

NCHRP PROJECT 09-22 PANEL

Field of Materials and Construction—Area of Bituminous Materials

Larry L. Michael, *Hagerstown, MD (Chair)*
Dale S. Decker, *Dale S. Decker, LLC, Eagle, CO*
James P. Delton, *Arizona DOT, Phoenix, AZ*
Stacey D. Diefenderfer, *Virginia DOT, Charlottesville, VA*
W. M. “Mike” Lackey, *Topeka, KS*
Rebecca S. McDaniel, *Purdue University, West Lafayette, IN*
David E. Newcomb, *National Asphalt Pavement Association, Lanham, MD*
Charles F. Potts, *Heritage Group, Indianapolis, IN*
Ronald A. Sines, *Oldcastle Materials, Leominster, MA*
James M. Warren, *Asphalt Contractors Association of Florida, Inc., Tallahassee, FL*
Dean C. Weitzel, *MACTEC Engineering & Consulting, Inc., Reno, NV*
John D’Angelo, *D’Angelo Consulting, LLC, Annandale, VA*
Michael R. Smith, *FHWA Liaison*
Frederick Hejl, *TRB Liaison*

FOREWORD

By Edward Harrigan

Staff Officer

Transportation Research Board

This report provides a proposed performance-related specification (PRS) for hot-mix asphalt (HMA) in the form of the Microsoft Windows®-based Quality-Related Specification Software (QRSS). The report details the research performed and illustrates the development of the QRSS and its ability to carry out pay adjustment factor and payment computations by comparing the as-built pavement performance with that of the as-designed pavement. Thus, the report will be of immediate interest to staff of state highway agencies, materials suppliers, and paving contractors with responsibility for specification and construction of HMA pavements.

NCHRP Project 9-22, “Beta Testing and Validation of HMA PRS,” was awarded to Fugro Consultants, Inc., Austin, Texas; major contributions to the research were made by subcontractor Arizona State University, Tempe, Arizona.

The objective of this research was to develop a HMA PRS based on spreadsheet solutions of the Mechanistic-Empirical Pavement Design Guide (MEPDG) originally developed in NCHRP Project 9-19, “Superpave Support and Performance Models Management,” as specification criteria for HMA rutting and fatigue cracking performance tests. This HMA PRS is now available as the QRSS.

The QRSS is a stand-alone program for Microsoft Windows (versions XP and 7) that employs a database of pre-solved solutions of the MEPDG. The program is capable of (1) calculating the predicted rutting, fatigue cracking, and low-temperature (thermal) cracking of an HMA pavement from the mix volumetric and binder and aggregate properties of the as-designed HMA (typically the job mix formula) and (2) comparing them with predictions calculated from the contractor’s lot or sub-lot quality assurance data for the same properties. The volumetric and materials properties are entered in the Witczak Predictive Equation to estimate values of the dynamic modulus (E^*) that, in turn, are used to predict the development of rutting and fatigue cracking and the pavement service life based on the development of these distresses over time. For prediction of low-temperature cracking, the same volumetric and materials properties are used to estimate HMA creep and strength behavior. Finally, pay factor adjustment factors and payments (penalty/bonus) are derived from the predicted service life differences for each as-built lot or sub-lot.

The QRSS gives project-specific performance predictions; the program accounts for climate, traffic, pavement structure, and the desired or expected pavement life in terms of distress limits assigned by the owner agency. Further, the distress predictions are stochastic; they are calculated through a Monte Carlo procedure that uses standard deviations of the input properties to account for construction and testing variabilities when assigning risk between the owner agency and the contractor and computing pay adjustment factors and payments.

The report fully documents the research leading to the development of the QRSS proposed for review and possible adoption by AASHTO. In addition, five appendixes and the QRSS program are available for download from the NCHRP Project 9-22 web page at <http://apps.trb.org/cmsfeed/TRBNetProjectDisplay.asp?ProjectID=958>:

APPENDIX A: Raw Data for Permanent Deformation Model Analysis

APPENDIX B: Raw Data for Fatigue Cracking Model Analysis

APPENDIX C: Summary of Results for Level 3 Creep Compliance Predictive Equations

APPENDIX D: Hardening Ratio Database

APPENDIX E: QRSS User's Manual

CONTENTS

1	Chapter 1 Research Overview
1	1.1 Introduction
1	1.1.1 Background
1	1.1.2 Performance-Related Specification
2	1.1.3 Project History and Objectives
3	1.1.4 Organization of this Report
4	1.2 Scope of Study
4	1.2.1 MEPDG Based HMA Distress Prediction
4	1.2.2 Volumetrics-Based Performance Prediction in the QRSS
5	1.3 QRSS Overview
5	1.3.1 Development of a Probabilistic Methodology for Performance Pay Factors
5	1.3.2 Dynamic Modulus
6	1.3.3 Effective Temperature
6	1.3.4 MEPDG Closed Form Solutions
7	1.3.5 Probabilistic Solution
9	1.3.6 Service Life Prediction
9	1.3.7 Comparison of Mix Design and As-Built Mix Predicted Life Difference (PLD)
10	1.3.8 Determination of Pay Adjustment Factors
10	1.3.9 IRI in Pay Adjustment
11	1.3.10 Final Cost
14	Chapter 2 Development of the QRSS Performance Models
14	2.1 Introduction
14	2.2 General Variables
14	2.2.1 Effective Temperature
21	2.2.2 Determination of Dynamic Modulus (E^*)
25	2.2.3 Determination of Creep Compliance
26	2.2.4 Frequency-Depth Relationship
31	2.3 Performance Model Development for Permanent Deformation
31	2.3.1 Introduction
31	2.3.2 Selection of Variables Affecting Rutting
33	2.3.3 Sub-Layering Scheme
35	2.3.4 Development of MEPDG Database
42	2.4 Performance Model Development for Fatigue Cracking
42	2.4.1 Introduction
42	2.4.2 Fatigue Distress Variables
47	2.4.3 Database Analysis and Results

56	2.5 Performance Model Development for Thermal Cracking
56	2.5.1 Introduction
56	2.5.2 Sensitivity Study
57	2.5.3 Mechanistic-Based Fracture Model Process
58	2.5.4 Input
59	2.5.5 Analysis
60	2.5.6 Output
60	2.5.7 Results
63	Chapter 3 Development of the Quality Related Specification and Software
63	3.1 Introduction
63	3.2 Determination of Deterministic Solution
66	3.2.1 Mix Design
69	3.2.2 E* Testing Temperature and Frequency
69	3.2.3 Dynamic Modulus-Distress Relationship for Rutting
69	3.2.4 Dynamic Modulus-Distress Relationship for FC
71	3.3 Determination of a Probabilistic Solution
71	3.3.1 Analysis of Variance for Significance of Regression
73	3.3.2 Monte Carlo Simulation
73	3.3.3 Rosenblueth Method
77	3.3.4 Historical Variance of Variables
77	3.3.5 Use of Beta Distribution
80	3.4 Application of Stochastic Methods in Performance Prediction
80	3.4.1 Application of Stochastic Methods to Dynamic Modulus
84	3.4.2 E* Variability Calculation
85	3.4.3 Application of Stochastic Methods on Rutting and FC
85	3.4.4 Application of Stochastic Methods to Thermal Cracking
87	3.5 Determination of Service Life and the Predicted Life Difference (PLD)
87	3.5.1 Conversion of Distress to Service Life for Rutting Distress
89	3.5.2 Conversion of Distress to Service Life for FC Distress
91	3.5.3 Conversion of Distress to Service Life for Thermal Cracking Distress
91	3.5.4 Comparison Between the As-Designed (JMF) Mix and the As-Built Mix Data
93	3.6 Pay Adjustment Factor and Payment (Penalty/Bonus) Computation
93	3.6.1 Three Distresses
95	3.6.2 Inclusion of IRI
99	Chapter 4 QRSS General Procedure
99	4.1 Introduction
99	4.2 Detailed Procedure
99	4.2.1 Mode Selection and General Information
99	4.2.2 User Input
105	4.2.3 Mix Design
106	4.2.4 Pay Adjustment Analysis (Stochastic Analysis of the As-Designed Mix)
115	4.2.5 Pay Performance Analysis (Stochastic Analysis for As-Built Mix)
123	4.2.6 Run Solution

130	Chapter 5 Summary, Conclusions, and Future Research
130	5.1 Summary
130	5.2 Conclusions
131	5.3 Proposed Future Research
132	References
134	Appendices A, B, C, D
135	Appendix E Quality Related Specification Software (QRSS) User's Manual

Note: Many of the photographs, figures, and tables in this report have been converted from color to grayscale for printing. The electronic version of the report (posted on the Web at www.trb.org) retains the color versions.

CHAPTER 1

Research Overview

1.1 Introduction

1.1.1 Background

Historically, transportation departments have used a variety of hot mix asphalt (HMA) construction specifications that consider pavement performance. Traditionally, HMA production and construction specifications require the measurement of volumetric properties of the HMA, typically air voids, asphalt content, and aggregate gradation, that are assumed to be related to an arbitrary level of performance. Specifications in which materials and construction (M&C) variables¹ also known as acceptance quality characteristics (AQC)s², are used to control quality primarily tie the AQC's to performance through intuition, engineering judgment, or both. Minimum in-situ density is an AQC used in specifications where the relationship to better performance is intuitive, i.e., higher in situ densities generally mean better performance. At present, HMA quality is typically defined by how close the as-built mixture meets the requirements of the job mix formula (JMF), i.e., the as-designed mix. Expected future performance is inferred from the differences between the as-designed and as-built HMA properties. Consequences accrue to the contractor for not satisfying the specification. Typically, the problem would have to be remedied to the satisfaction of the engineer, the defective pavement would have to be removed and replaced, or the contractor would have to accept a reduced payment.

In recent years there has been interest in the paving industry in defining the quality of the mix and pavement in terms of performance, where the contractor responsible for production

and placement would then be paid on the basis of the difference in service life between the as-designed and as-built pavement. In this case, the specifications state the AQC as a measure of pavement performance. Such a specification describes how the finished product should perform over time. Warranty or guarantee specifications, by which the contractor agrees to build and maintain the pavement for a specified period of time, are also used. In these types of specifications, a time period is identified during which the AQC's are expected to be maintained at satisfactory levels. In general, this approach to specifications has not yet been widely accepted in the industry.

1.1.2 Performance-Related Specification

In Reference 32, a performance-related specification (PRS) is defined as a quality acceptance (QA) specification that describes the desired levels of key AQC's that have been found to correlate with fundamental engineering properties that predict performance. Thus, the selection of a particular AQC by itself does not make the specification performance related. Rather, there must be a direct connection to performance through field validated empirical or mechanistic prediction models that account for the effect of deviations of the as-built AQC level from the as-designed AQC level. A comprehensive PRS requires the development of relationships between M&C variables such as HMA layer thickness, strength, and smoothness and pavement response and distress. This process requires a significant amount of work including the definition of the specification criteria that will be included in the PRS; establishment of the relationships between M&C variables, pavement response, and performance; and selection of testing methodologies for material characterization. Other factors such as environment, traffic, pavement cross section, and variability also must be considered in a comprehensive PRS. To implement the PRS, pavement performance must be predicted based on the initial design (as-designed) and the as-built properties. The difference in predicted performance

¹Defined in Reference 32 as "A characteristic of materials and/or construction that can be controlled directly or indirectly."

²Reference 32 defines a quality characteristic as "That characteristic of a unit or product that is actually measured to determine conformance with a given requirement. When the quality characteristic is measured for acceptance purposes, it is an acceptance quality characteristic . . ."

between the as-designed and as-built pavement then is used as a basis for acceptance.

In 1994 the FHWA funded the design, construction, and loading of a test track project to provide the basis for the development of a prototype HMA PRS (the last several years of the project were conducted through NCHRP Project 9-20, "Performance-Related Specifications for Hot-Mix Asphalt Construction"). Entitled *WesTrack* and constructed in Nevada, the primary objective of the project was to provide data to quantify the effects of deviations in M&C variables on the overall performance of the HMA layers. This study was also tasked with verifying the Superpave mixture design method developed during the SHRP Asphalt Research Program using field performance data. All constituent materials including asphalt binder and aggregates were thoroughly characterized along with the HMA. The primary performance emphasis was on the load-associated distresses of permanent deformation and fatigue cracking. The research conducted during the *WesTrack* project included basic volumetric testing of HMA in addition to performance testing of laboratory mixed/laboratory compacted (LMLC), field mixed/laboratory compacted (FMLC), and field mixed/field compacted (FMFC) specimens from the test track sections. The volumetric properties of the as-produced and in situ HMA material were determined through a comprehensive lab testing program. Component material characteristics were determined for the mixtures. These results were utilized to develop simple empirical relationships for performance prediction to support a PRS; these relationships provided the basis for the prediction models used in HMA Spec, the software implementation of the PRS.

This PRS-based HMA Spec Version 1.0 (or alpha version) software developed during the *WesTrack* project required a thorough beta test to determine programming errors and deficiencies. The HMA Spec software also needed to be robust as well as easy to understand to facilitate broad implementation of the PRS. The original *WesTrack* team identified numerous limitations of this alpha version of the HMA Spec program: the pavement lot size was fixed, only the lowest level I pavement prediction models were incorporated in the alpha version; user-defined maintenance and rehabilitations were not thoroughly tested; limited rehabilitation options were available and an asphalt concrete (AC) overlay had to be utilized for the life cycle cost analysis (LCCA) to work properly; determination of the present worth of future rehabilitation treatments was limited to real dollars and a real discount rate; and only U.S. customary units were utilized.

1.1.3 Project History and Objectives

The contract for NCHRP Project 9-22, "Beta Testing and Validation of HMA PRS," was awarded to Fugro Consultants LP (Fugro) in October 2000. Its original objective was to

evaluate and refine the HMA PRS and HMA Spec software developed through the *WesTrack* project in a series of field trials in order to calibrate and validate its Levels I and II performance models.

After careful evaluation of the existing HMA Spec, the decision was made by the NCHRP project panel in April 2001 to use the Mechanistic-Empirical Pavement Design Guide (MEPDG) software produced in NCHRP Project 1-37A, "Development of the 2002 Guide for the Design of New and Rehabilitated Pavement Structures: Phase II," as the "engine" for performance prediction models in the HMA PRS. The NCHRP project panel modified the objectives and scope of work to allow for the integration of the MEPDG performance prediction system into the NCHRP Project 9-22 HMA PRS. The primary objective of the project was revised to accomplish integration of the flexible pavement performance prediction system of the MEPDG into the PRS. The MEPDG contains models for predicting HMA permanent deformation, fatigue cracking, and thermal cracking. Smoothness is then calculated based on the other distresses predicted as well as the original, initial as-built smoothness level of the project. In addition, this prediction system incorporates multiple levels of predictive complexity as a function of the roadway classification.

Once the MEPDG software was released in 2004, the project team made significant progress towards integration of its HMA models into the HMA Spec software. In March 2004, ARA Inc. was selected as a prime subcontract to Fugro and worked on the input and output (reporting) modules of HMA Spec so that all MEPDG inputs were included. At this point, the MEPDG models were developed in a straightforward Monte Carlo stochastic analysis for use within the HMA Spec. However because of the computational methodology developed for the original MEPDG program, the addition of a Monte Carlo simulation to the HMA Spec program resulted in a program that required days to complete the analysis of a single project. This problem was discussed with the NCHRP project panel in May 2004. The project team and the panel agreed to cease work on NCHRP 9-22 project until a peer-reviewed and faster version of the MEPDG Software was available.

Around this time, researchers at Arizona State University (ASU) were working on the development of a rapid, spreadsheet-based program for prediction of AC rutting distress that had multi-functional applications. The spreadsheet program utilized pre-solved solutions of the MEPDG as the basis for predicting rutting. The plan was to implement the spreadsheet-based program as a QA tool for AC construction. As it was noted that this simplified program could significantly reduce program runtime, NCHRP suggested that the Fugro project team visit ASU, discuss the issues, and prepare an analysis of the capabilities of the spreadsheet program and how it might be used in a final NCHRP Project 9-22 product. This visit took place in April 2005.

This and subsequent visits led to a plan for replacing the MEPDG software component in the HMA Spec software with spreadsheet solutions developed by ASU for rutting, fatigue cracking, and thermal cracking. These solutions would be originally coded as Excel spreadsheets that could provide instantaneous estimates of the AC distresses in flexible pavements. One of the major benefits of this approach is that it finally tied together the structural distress (performance) prediction of a pavement system to the real properties of the mixtures used in the system methodology. This solution methodology was derived from predictive (closed form) models developed from a comprehensive set of factorial runs of the MEPDG software. Therefore, using identical MEPDG inputs, solutions are quickly obtained from the database, eliminating the need to actually run the MEPDG program. The spreadsheet solution for HMA rutting was extremely quick, with thousands of simulations taking but a few seconds. The closed form spreadsheet solutions developed by ASU produced rut depth predictions very close to those predicted by the MEPDG program. In addition to the spreadsheet developed by ASU for AC rutting, the plan was expanded to include tasks for ASU to develop and integrate similar solutions for AC fatigue (bottom-up alligator) cracking and AC thermal cracking. For purposes of NCHRP Project 9-22, a probabilistic version of the spreadsheet solution was developed for each key distress.

It is important to recognize that there are several computational differences among the ASU spreadsheet solutions, the original HMA Spec, and the MEPDG program, and in particular the traffic inputs, number of HMA layers, and analysis period. The ASU spreadsheet solutions use ESALs to characterize traffic, whereas the HMA Spec allowed the user to input traffic in a manner similar to that of the MEPDG. HMA Spec allowed the user to enter several HMA layers in the pavement structure though only one layer was considered in the PRS analysis. The ASU spreadsheet solutions are based on using up to three AC layers (identical to the MEPDG) and each layer can be used in the PRS analysis. Given the deficiencies of the HMA Spec software at this juncture, it was anticipated that developing a new user interface to work with the ASU spreadsheet solutions would take less time and effort than modifying the HMA Spec to reflect the new parameters and capabilities specific to the ASU spreadsheet solutions.

The revised plan and budget for finalizing the spreadsheet solutions and integrating these solutions into a new working version of the PRS software was submitted to NCHRP and approved in August 2005 with the following tasks:

- Task 5—Development of Spreadsheet Solutions (AC Rutting, Fatigue Cracking, Thermal Cracking)
- Task 6—Preliminary Integration of Spreadsheet Solutions into PRS Program

Task 7—Application of PRS Spec Prototype in the Field by FHWA

Task 8—Prepare PRS Spec Beta Version

Task 9—Beta Test PRS Spec Beta Version

Task 10—Final Report and Presentation of Results to NCHRP Panel

At a project panel meeting held in April 2006 it was decided to convert the closed form Excel spreadsheet solutions to an integrated, user-friendly program written in the C# programming language that could run as an independent program in the Microsoft Windows operating system. It was also agreed at this meeting to use the name Quality Related Specification Software (QRSS) for the new stand-alone program.

The field project data sets collected in the initial stages of the project by the FHWA mobile laboratory were not as extensive and complete as needed for validation of the QRSS. The research team requested the state highway agencies to provide the QA data sets for this purpose and such data were ultimately collected from 10 states including Alabama, Arizona, Indiana, Kansas, Kentucky, Maine, Maryland, Mississippi, Oklahoma, and Texas. These data were used in the final beta testing and field validation of the QRSS, which are being accomplished in NCHRP Projects 9-22(01), “Facilitating Implementation of the Quality-Related Specification Software (QRSS),” and 9-22A, “Evaluation of the Quality Related Specification Software (QRSS) Version 1.0.”

1.1.4 Organization of this Report

This report presents a detailed technical exposition of the QRSS and instructions and examples of its use as a PRS. This Chapter 1 describes NCHRP Project 9-22, the main features of the QRSS, and its basis in the MEPDG. Chapters 2 and 3 are comprehensive technical discussions of the development of the performance models in the QRSS and its use of deterministic and probabilistic solutions to arrive at performance predictions, service life estimates, and pay adjustment factors. Chapter 4 describes the use of the QRSS to develop pay factors for HMA construction projects from a comparison of the predicted service life of the as-designed and as-built pavement. Chapter 5 provides a project summary, conclusions, and proposed future research activities. Appendix E is a user manual for the QRSS.

Appendixes A: Raw Data for Permanent Deformation Model Analysis, B: Raw Data for Fatigue Cracking Model Analysis, C: Summary of Results of Level 3 Creep Compliance Predictive Equations, and D: Hardening Ratio Database, are available for download from NCHRP Project 9-22 web page³.

³<http://apps.trb.org/cmsfeed/TRBNetProjectDisplay.asp?ProjectID=958>.

1.2 Scope of Study

This section discusses the state of the art technologies of the MEPDG software (developed in NCHRP Projects 1-37A and 1-40) used by the QRSS to achieve the goal of a probabilistic Quality Related Specification for HMA construction.

1.2.1 MEPDG Based HMA Distress Prediction

The MEPDG, using four major input parameters of traffic, structure, climate, and material, is capable of predicting HMA pavement distress over its design life. The key HMA pavement distress predictions in the MEPDG are rutting (permanent deformation), fatigue cracking, thermal cracking, and International Roughness Index (IRI).

1.2.1.1 Rutting

Rutting describes any distortion in the HMA pavement surface as a result of the accumulated traffic loading. It is important to note that rutting does not occur only in AC layers; it can also occur in any of the underlying pavement layers. However, the QRSS analyzes only rutting occurring in the AC layers.

1.2.1.2 Fatigue Cracking

Short longitudinal cracks that appear in the wheel path and then spread quickly to become interconnected, exhibiting a cracking pattern similar to alligator skin, are called fatigue cracking or alligator cracking. Due to load-induced tensile stresses and strains caused by bending of the AC layers, these cracks initiate at the bottom of the AC and propagate to the surface under repeated load applications.

1.2.1.3 Thermal Cracking

Cracking in flexible pavements, developed due to a sudden (rapid) temperature drop in the AC surface, is classified as thermal cracking. Typically, thermal cracking is caused when the tensile strains caused by rapid low temperature changes exceed the tensile strength of the material at the specific temperature of occurrence. The MEPDG predicts transverse thermal cracking.

1.2.1.4 International Roughness Index (IRI)

The MEPDG calculates the IRI for HMA pavements over the design life of the pavement as a function of the predicted distresses (rutting, alligator fatigue cracking, longitudinal cracking, and transverse cracking) and a site factor to count for the climatic changes. However, the QRSS uses the initial IRI in its analyses since the QRSS is concerned with construction quality and not the change in IRI over time.

1.2.2 Volumetrics-Based Performance Prediction in the QRSS

The dynamic modulus, a fundamental engineering property of the AC layer, is a direct measure of performance. The dynamic modulus equation used in both the lower levels of MEPDG analysis and the QRSS is the Witczak Predictive Equation (WPE) (1). The WPE is a function of the aggregate gradation, volumetric properties, and binder viscosity of the AC layer. These variables are also the main properties typically used in HMA QA specifications.

1.2.2.1 Aggregate Gradation

One of the most influential aggregate characteristics in determining pavement performance is the particle size distribution or gradation of aggregates in the HMA. It is widely accepted that uniformity in the HMA mixture is of primary importance in pavement performance, and state agencies have developed a band of gradation for HMA mixture design. Gradation information is required for the determination of almost every important HMA property. In the WPE, the key sieve sizes required for prediction of the HMA dynamic modulus are $\frac{3}{4}$ ", $\frac{3}{8}$ ", #4 and # 200.

1.2.2.2 Volumetric Properties

An important component in the HMA mixture volumetrics is the asphalt content. In general, deviations from the optimum asphalt content (either plus or minus) may be responsible for the development of distresses. The effective asphalt content of the mixture is the total asphalt binder content of the HMA less the portion of asphalt binder that is lost by absorption into the aggregate. In assessing the performance of HMA mixtures, it is absolutely critical to understand that HMA performance is driven by the *effective* asphalt content in the mix and not the total asphalt content. To ensure the right amount of asphalt content in the as-placed HMA, several measures of the mix volumetrics, such as voids in the mineral aggregate (VMA), voids filled with asphalt (VFA), and percent air voids (V_a) of laboratory compacted samples, are required.

The air voids content is a measure of the air voids in the HMA mixture expressed as a percentage of the total mix volume. Bulk specific gravity (G_{mb}) and theoretical maximum specific gravity (G_{mm}) are used to determine the air voids in the mixture. VMA is a measure of the voids in between the mineral aggregate particles in a compacted mixture. It is determined from the bulk density of the sample, the bulk gravity of the aggregate, and the mixture asphalt content. Setting a minimum VMA is an approach that is used to ensure that adequate asphalt is available to the mixture. The other mixture property that is important is the portion of

the VMA filled with asphalt. Generally the voids filled with asphalt should be high enough to provide a durable mix and one that resists the flow of air and water through the mixture. However, it should be low enough to avoid the bleeding and rutting that may occur under heavy traffic. These mixture volumetrics are then used to determine the effective asphalt content, which is a primary component in ensuring the performance of the mixture and in the prediction of the HMA dynamic modulus.

A most important tool in the QA of HMA construction is measurement of the in situ density of the HMA. This density measurement, combined with knowledge of the theoretical maximum density, will allow computation of the air voids of the compacted mixture in situ. For the prediction of dynamic modulus of the as-built mixture, the initial in situ air voids content measured after construction is used.

1.2.2.3 Binder Viscosity

Viscosity or stiffness of the binder is another important parameter in determining the dynamic modulus of the HMA mixture. This parameter is typically obtained by laboratory testing. If the direct measure of binder viscosity or shear stiffness is not available, the regression parameters A and VTS can be used instead to estimate the binder stiffness.

1.3 QRSS Overview

The approach used to develop the QRSS is summarized in this section and discussed in detail in Chapters 2 and 3.

1.3.1 Development of a Probabilistic Methodology for Performance Pay Factors

The QRSS uses a probabilistic performance pay factor methodology founded on several important concepts:

1. The concept of effective temperature is used to evaluate the climatic effects on the HMA dynamic modulus and so predict the anticipated deformation and fatigue distresses for a particular pavement structure and project location. There are different effective temperatures for rutting and fatigue cracking.
2. Simulation of the MEPDG distress prediction is the basis for developing closed form solutions (CFS) for the three major distresses (rutting, fatigue cracking, and thermal cracking). The CFS for rutting and fatigue cracking are based on relating the dynamic modulus calculated with the respective effective temperature to the pavement distress. The solution for thermal cracking is based on relating the calculated creep compliance (D) to the pavement distress.

3. For the job mix formula (JMF), heretofore referred to as the as-designed mix, a Monte Carlo simulation is conducted on the dynamic modulus using the mean and historical variance of the HMA volumetric properties and aggregate gradation. This is done separately for rutting and fatigue cracking. An alternative type of simulation, the Rosenblueth point estimate method, is conducted on the creep compliance for thermal cracking.
4. From the CFS and the two simulations, the pavement distresses for the as-designed mix are estimated.
5. A relationship is developed between each predicted distress level and pavement life. These relationships are then used to estimate the pavement life of the as-designed mix.
6. Similarly, for the constructed mix, heretofore referred to as the as-built mix, the lot data (daily production) are used in the simulations to estimate each distress and predict pavement life for each lot.
7. The cumulative probability distributions of the as-designed and as-built pavement lives are compared to calculate the pavement life difference (PLD) for each lot.
8. The Pay Factor Penalty/Bonus is then estimated from the PLD for each lot. The criterion for each distress between the PLD and Pay Factor is solely defined by the user agency. The summation of the pay factors for the lots will provide the total project pay factor.
9. Only the IRI value (actual degree of smoothness obtained by the contractor) is used to adjust the pay factor.

The QRSS methodology developed in NCHRP Project 9-22 is based on simplifying assumptions compared to the comprehensive MEPDG solution. The assumptions are:

1. Traffic is represented by ESALs.
2. No seasonal changes are allowed for the unsaturated modulus of any unbound layer (base, subbase, or subgrade). Rather, an effective modulus of all unbound layers is estimated.
3. The accuracy of the CFS is almost equivalent to that of the MEPDG. However, the MEPDG will give the more accurate distress predictions.
4. The QRSS will predict one value of each distress at the end of the design life.

These assumptions do not critically affect the HMA distress predictions. The following sections discuss each concept and the steps in the development of probabilistic methodology for Performance Pay Factors.

1.3.2 Dynamic Modulus

The dynamic modulus is a fundamental material property of the AC layer used in the MEPDG. The dynamic modulus

equation that has been adopted in this work, as well as the lower levels of analysis in the MEPDG, is the WPE shown in Equation 1 (1). The WPE is a function of the volumetric properties, aggregate gradation, and binder viscosity (stiffness) of the AC layer. These are also the main properties used in QA specifications for AC construction.

$$\begin{aligned} \log E^* = & -1.249937 + 0.029232 p_{200} - 0.001767 (p_{200})^2 \\ & - 0.002841 p_4 - 0.058097 V_a - 0.8022 \frac{V_{beff}}{(V_{beff} + V_a)} \\ & + \frac{3.87197 - 0.0021 p_4 + 0.003958 p_{38} - 0.000017 (p_{38})^2 + 0.00547 p_{34}}{1 + e^{(-0.603313 - 0.31335 \log(f) - 0.393532 \log(\eta))}} \end{aligned} \quad (1)$$

where

- E^* = Asphalt Mix Dynamic Modulus, in 10^5 psi
- η = bitumen viscosity in 10^6 poise
- f = loading frequency in Hz
- V_a = air voids in the mix, by volume, %
- V_{beff} = effective bitumen content, by volume, %
- p_{34} = cumulative % retained on the $\frac{3}{4}$ inch sieve
- p_{38} = cumulative % retained on the $\frac{3}{8}$ -inch sieve
- p_4 = cumulative % retained on the No. 4 sieve
- p_{200} = % passing the No. 200 sieve

1.3.3 Effective Temperature

The concept of effective temperature is used to evaluate climatic effects on the dynamic modulus to determine the critical temperature and moduli used to predict the anticipated rutting and fatigue cracking distresses for a particular pavement structure and project location (2). There are two different effective temperature equations: one for rutting (Equation 2) and another for fatigue cracking (Equation 3):

For rutting:

$$\begin{aligned} T_{eff} = & 14.62 - 3.361 \ln(Freq) - 10.940(z) + 1.121(MAAT) \\ & + 1.718(\sigma MMAT) - 0.431(Wind) + 0.333(Sunshine) \\ & + 0.08(Rain) \end{aligned} \quad (2)$$

For fatigue cracking:

$$\begin{aligned} T_{eff} = & -13.995 - 2.332(Freq)^{0.5} + 1.006(MAAT) \\ & + 0.876(\sigma MMAT) - 1.186(Wind) \\ & + 0.549(Sunshine) + 0.071(Rain) \end{aligned} \quad (3)$$

where

- T_{eff} = modified Witzczak T_{eff} , °F
- z = critical depth, inch
- Freq = loading frequency, Hz
- MAAT = mean annual air temperature, °F
- $\sigma MMAT$ = standard deviation of the mean monthly air temperature
- Rain = annual cumulative rainfall depth, inches
- Sunshine = mean annual percentage sunshine (%)
- Wind = mean annual wind speed (mph)

Using the effective temperature to estimate the dynamic modulus provides an easy, accurate way to account for the effects of climatic and temperature change on the AC pavement layers.

1.3.4 MEPDG Closed Form Solutions

Since a great amount of time would be required to execute the number of MEPDG runs needed to assess the predicted distress of the as-designed and as-built mixes, the use of CFS evolved in related NCHRP projects conducted by ASU for mix design and performance testing and these were adapted to the QRSS. These CFS were developed from the results of a comprehensive set of factorial runs of the MEPDG and hence estimate the minimum required AC dynamic modulus necessary to conform to a user-specified distress criteria for rutting and fatigue cracking. The CFS are based on relating the dynamic modulus calculated using the effective temperature to rutting and fatigue cracking distress.

1.3.4.1 Rutting

Rutting can occur in any of the underlying pavement layers, apart from the rutting in the AC layers. However, only rutting in the AC layers is considered in the QRSS since the objective of the NCHRP 9-22 was to develop a QRS for HMA construction. The rutting prediction using the CFS is based on a database created from the results of 864 runs of the MEPDG over a wide range of conditions. These results are then interpolated to find the rutting corresponding to the specific pavement structure and climate in question. Details of the rutting prediction methodology can be found in Sotil (3) and El-Basyouny and Jeong (4). The correlation between the MEPDG prediction and the CFS rutting solution of NCHRP Project 9-22 is excellent, with a regression coefficient of 0.996 as shown in Figure 1.

1.3.4.2 Fatigue Cracking

Classical fatigue cracking (alligator cracking) that is caused by load-induced tensile strains that initiate at the bottom of

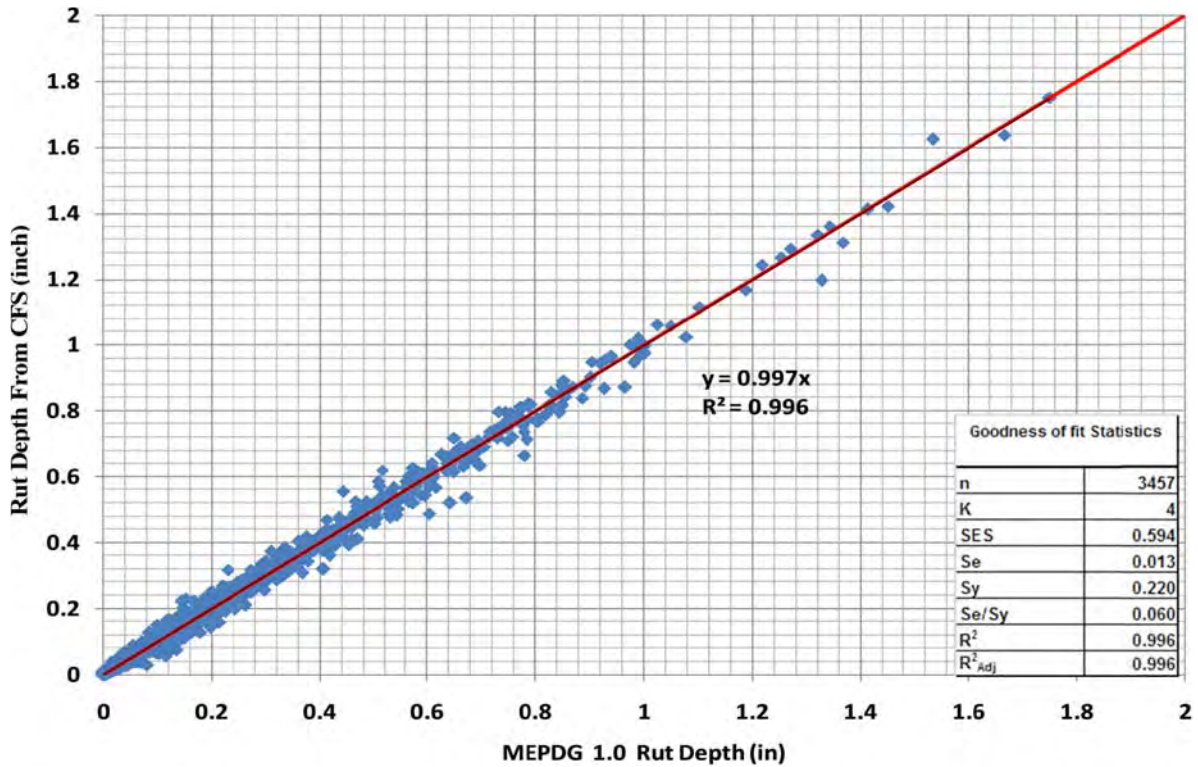


Figure 1. MEPDG versus QRS rutting prediction comparison.

the AC layer and propagate to the surface under repeated load applications is considered in the QRSS. As this point in time, top-down fatigue cracking (longitudinal) is not considered.

A CFS was developed to predict fatigue cracking. A total of 7,776 MEPDG simulation runs were used to develop the fatigue model in the CFS; details can be found in El-Badawy et al. (5). The correlation between the MEPDG prediction and the CFS fatigue cracking solution of NCHRP Project 9-22 is excellent, with a regression coefficient of 0.998 as shown in Figure 2.

1.3.4.3 Thermal Cracking

Several attempts were made to develop a CFS for the thermal cracking in NCHRP Project 9-22, but it proved difficult to obtain an accurate prediction with any prediction model attempted. Accordingly, a module similar to that in the MEPDG was developed to analyze the thermal cracking. This module requires the hourly temperature and is not dependent on an effective temperature. Figure 3 shows the comparison between the prediction of thermal cracking by the MEPDG and the QRSS model. The prediction is almost identical, with a nominal regression coefficient of 1. For more details on the thermal cracking prediction model, the reader is referred to Jeong et al. (6).

1.3.5 Probabilistic Solution

For as-designed mix, a Monte Carlo simulation is conducted on the dynamic modulus using the mean and historical variance of the HMA volumetric properties and aggregate gradation. Separate simulations are done for rutting and fatigue cracking.

A key requirement in the development of the pay factor methodology is the use of a probabilistic solution. The probabilistic solution accounts for the variability of the material properties in the as-designed as well as the as-built pavement. With the CFS solutions developed in NCHRP Project 9-22, probabilistic Monte Carlo simulations can be easily accomplished in minutes.

The Monte Carlo simulations are used for rutting and fatigue cracking while the Rosenbluth probabilistic point estimate method is used for the thermal cracking simulation. It was the original intention of the project team to use Monte Carlo simulation for all three distress prediction modules. This would have been possible if the thermal cracking module was developed in a closed-form solution where a number of simulations for both D and distress prediction would be completed within a very short duration of time. However, this became impossible to do because the thermal cracking module was developed as a stand-alone subroutine. This subroutine needs hourly-based climatic data, which are retrieved

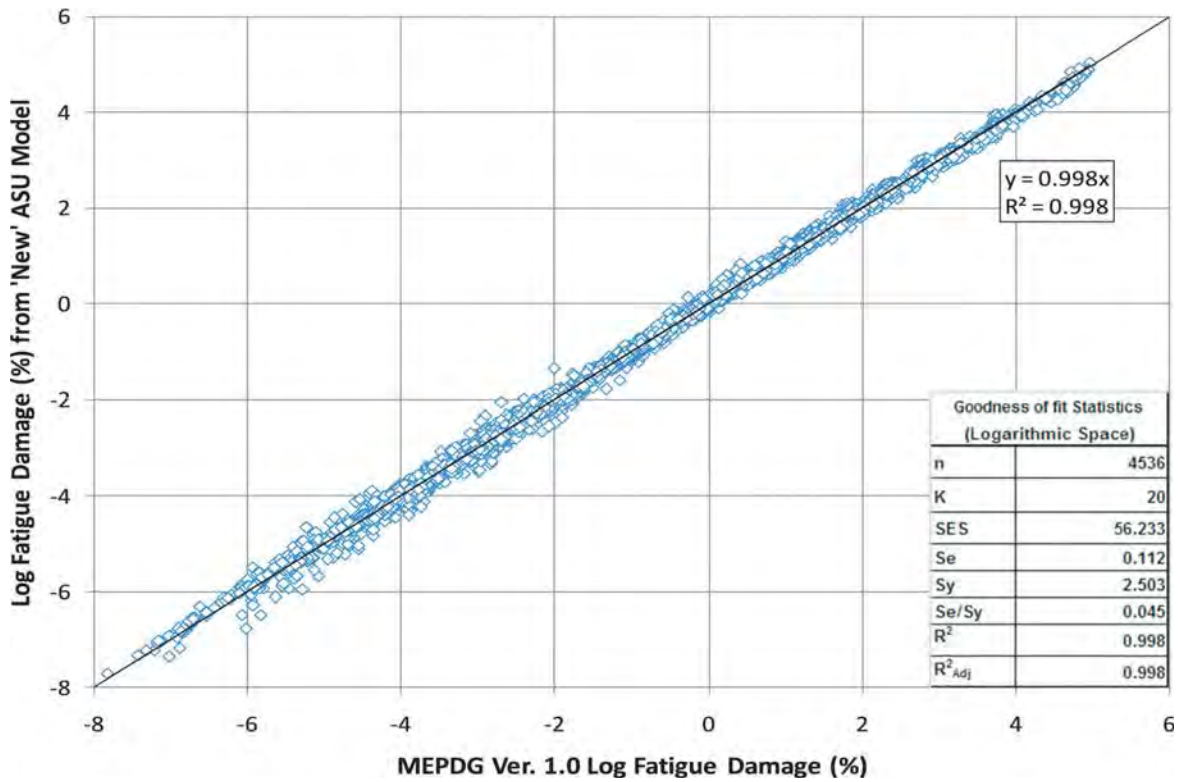


Figure 2. MEPDG versus QRS fatigue cracking prediction comparison.

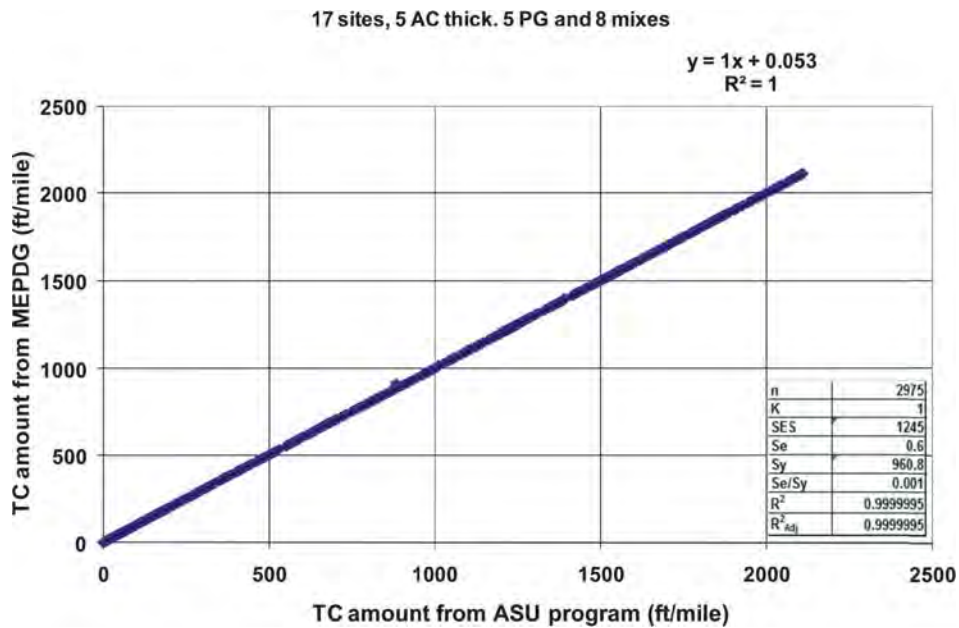


Figure 3. MEPDG versus QRS thermal cracking prediction comparison.

from actual weather stations, for the entire design service life. This required at least several seconds per simulation. As a result, to complete hundreds of Monte Carlo simulations a considerable amount of time would be required (e.g., 2 seconds per simulation * 1,000 simulations requires approximately half an hour). Note that this probabilistic simulation is required several times throughout the quality evaluation process for both the as-designed mix and the as-built mix of each lot. For this reason, the Rosenblueth method was selected as an alternative in order to reduce the simulation time, and yet provide an accurate statistical analysis.

All probability simulation is based on using the mean and variance of different variables to predict the variability in the predictor. The following section will summarize the two simulations. For more details of the probabilistic solutions, refer to Jeong and El-Basyouny (7).

The probabilistic simulations require the mean and standard deviation of the material properties such as the air voids, binder content, aggregate gradation, and binder viscosity. When the simulation is done on the as-designed mix, historical standard deviations are used. When the as-built data is used, the variance of the property within each lot is used.

1.3.5.1 Monte Carlo Simulation

The Monte Carlo simulation for rutting and fatigue cracking is conducted on the dynamic modulus equation (the WPE). For each simulation, the modulus is calculated using random number generation for normal probability distributions. The rutting and fatigue cracking distribution (mean and variance) are then estimated using the CFS. Finally, the service life of the pavement is calculated. One thousand Monte Carlo simulation runs are used to obtain the mean and variance of each predicted distress.

1.3.5.2 Rosenblueth Method

The Rosenblueth method involves the determination of the probability distribution of a complex function $f(x)$ using linear combinations of powers of adequately selected point estimates around any desired value x (8). In practice either a "2 point" or "3 point" solution can be used (9). The main consideration is the computational time required by a 3^{nv} factorial compared to a 2^{nv} factorial. Uncertainty is expressed by incorporating the central tendency and dispersion of the thermal cracking and service life estimated by the Rosenblueth method.

The number of primary variables for the thermal cracking solution was selected to be 4 (air voids, effective binder content, AC thickness, and binder type). This yields $2^4 = 16$ Rosenblueth simulations to be used to assess the variability in the thermal cracking prediction over a given time period.

1.3.6 Service Life Prediction

A relationship was developed to relate the predicted distress to the pavement life, which is then used to estimate the pavement life for the as-designed mix. To assess the impact of the difference in the distress predictions, the service life of the pavement is calculated using Equation 4 for rutting and Equation 5 for fatigue cracking.

$$Y = \frac{\log\left(\left(\frac{RUT}{RUT_c} * \frac{E^*}{E_c^*}\right)^{1/0.479244} \left((1+r)^{Y_c} - 1\right) + 1\right)}{\log(1+r)} \quad (4)$$

$$Y = \frac{\log\left(\frac{N_f}{N_{fc}} \left((1+r)^{Y_c} - 1\right) + 1\right)}{\log(1+r)} \quad (5)$$

where

Y = predicted service life

Y_c = design life

RUT = rut depth

RUT_c = rut depth criterion value, deterministically predicted

N_f = allowable failure traffic repetitions

N_{fc} = criterion value for failure traffic repetitions

E^* = dynamic modulus

E_c^* = dynamic modulus criterion value

r = growth rate (rate of traffic increase per year)

Similarly, for the as-built pavement, the Monte Carlo simulation is run to estimate each distress and the pavement service life for each lot.

1.3.7 Comparison of Mix Design and As-Built Mix Predicted Life Difference (PLD)

The cumulative probability distributions of the as-designed pavement life and the as-built pavement life are compared to calculate the PLD for each lot. The probabilistic solutions provide the mean and variance of the predicted distress for a given distress type for the as-designed and as-built mixes. A probability distribution can then be formed from the mean and variance for the pavement service life obtained from each distress.

A cumulative frequency distribution is then created for the as-designed mix. A similar distribution is created for each lot representing the as-built lot variability. Figure 4 shows sample cumulative frequency distributions for both as-designed and as-built pavements. The normal distribution is used for the rutting, while the beta distribution is used for the fatigue cracking due to the fact that fatigue cracking has a minimum of zero and a maximum value of 100%. Similarly, thermal cracking uses a beta distribution as the distress has a minimum of zero and a maximum of 2,112 ft/mile.

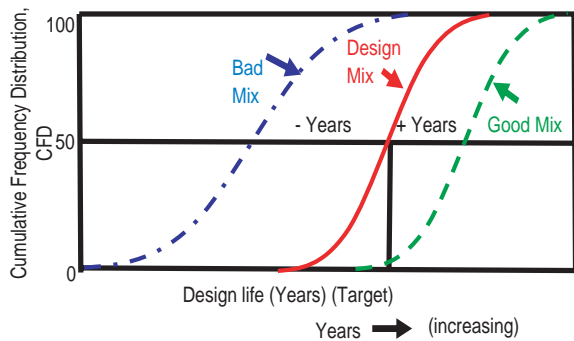


Figure 4. As-built and as-designed cumulative frequency distribution.

To assess the difference between the as-designed and as-built distributions a variable called the predicted life difference (PLD) is introduced. The PLD is defined as the difference in predicted service life between the as-designed mix and the as-built mix. This parameter has a unique algebraic sign, depending upon whether the as-built mix is of greater or lesser quality (Service Life) than the as-designed mix. Finally, this PLD is used as the basis for establishing the Pay Factor Penalty/Bonus for each distress type.

1.3.8 Determination of Pay Adjustment Factors

The Pay Factor Penalty/Bonus is estimated from the PLD for each lot. The criterion relating the PLD and the Pay Factor (PF) for each distress is solely defined by the user agency. The summation of the pay factors for the lots provides the total project pay factor. The Pay Factor (PF) is based on the loss or gain in the service life. Figure 5 shows the relationship between the PF and the PLD.

Table 1 shows typical values of the parameters needed to set the PF-PLD relationship. It is important to note that the

Table 1. Typical value of pay adjustment factors.

TYPICAL PAY ADJUSTMENT FACTORS	
Max. Bonus (%), Y1	7
Max. Penalty (%), Y2	20
Max. PLD (Years), X1	5
Min. PLD (Years), X2	-5
PLD for no Bonus, X3	2.5
PLD for no Penalty, X4	-2.5
PLD for Remove and Replace, X5	-10

precise coordinates of each point and of the shape of the relationship are defined by the user agency.

First, maximum and minimum PF values need to be determined by the agency, which has complete latitude to change these values. Then, relationships between the PLD and the pay adjustment factor can be developed. There might be a region where there is no bonus or penalty, e.g., the region between (X3) and (X4) in Figure 5. Also, there should be a value (X5) at which removal and replacement of the as-built section is required.

The PLD value calculated from each lot is then used to calculate the PF by lot. The lot PF is then summed up for each distress to calculate the total PF by distress. The PF-PLD relationship can be tailored by the agency (or between the agency and contractor) on the basis of experience and policy.

1.3.9 IRI in Pay Adjustment

The IRI also is used in adjusting the PF. IRI is considered a standard measure of pavement smoothness as it correlates well with user-panel serviceability ratings and can be easily measured from elevation data along the wheel path. A pavement roughness index computed from a longitudinal profile measurement using a quarter-car simulation at a simulation speed of 50 mph is defined as the IRI. Smoothness is accounted for in the MEPDG program by considering the initial smoothness at construction and subsequent changes over the pavement life by summing the damaging effect of distress. In the QRSS, unlike other distresses, IRI is not predicted over time but included as an additional distress. The inclusion of IRI into the QRSS is straightforward; only the initial IRI₀ at the time of construction is considered in the calculation of the final pay adjustment. The actual measured average initial IRI₀ at each milepost in the project is required for the evaluation of the smoothness of the as-built road surface. The fundamental concept used in the QRSS follows the traditional state DOT approach.

The payment approach used in the QRSS for IRI is to adjust the Penalty/Bonus based upon the initial IRI measured

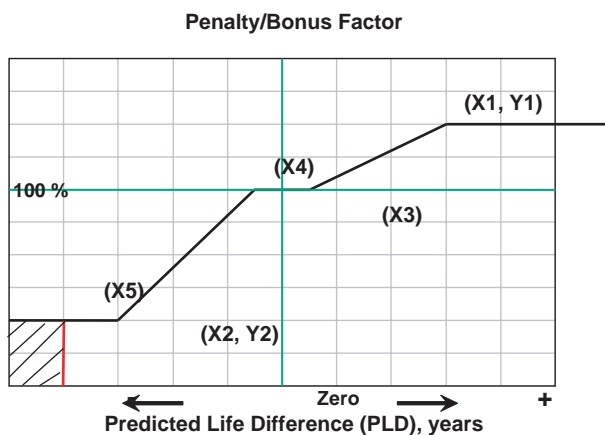


Figure 5. Penalty/Bonus versus pavement life difference relationship.

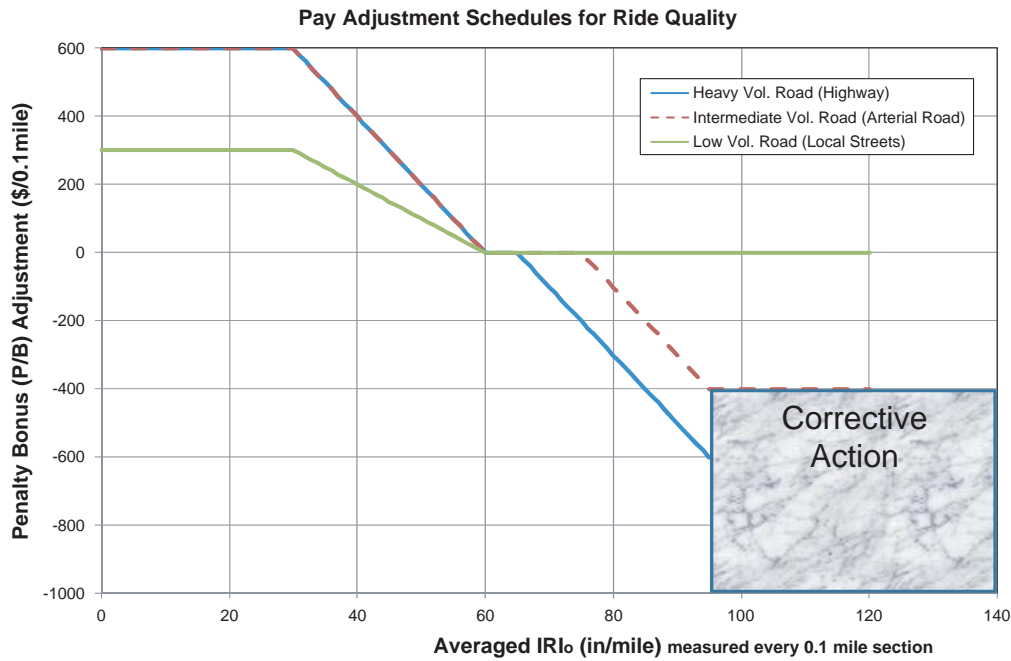


Figure 6. Penalty/Bonus versus pavement life difference relationship for IRI.

over 0.1 mile at every milepost. Three different payment schedules have been included to allow the user to adjust the Penalty/Bonus values as a function of traffic volume as shown in Figure 6. Table 2 is the QRSS recommended payment schedule as a function of traffic volume and IRI₀. Table 3 is an example of the Penalty/Bonus costs determined from the measured IRI₀ values for a project.

The total penalty/bonus cost for the IRI is calculated with Equation 6.

$$C_{PB2} = \sum_{i=1}^L \sum_{j=1}^{L_p/0.1} (P/B)_{IRI_{ij}} \quad (6)$$

where

L = number of total lanes

L_p = length of project (mile)

(P/B)_{IRI_{ij}} = penalty or bonus (\$) for IRI_{ij}

IRI_{ij} = average IRI₀ for ith lane and jth mile post

1.3.10 Final Cost

The final incentive or disincentive is calculated in dollars by considering all individual distress pay factors. The first correction is related to the lot definition. If a statistical lot is defined as a fixed tonnage, no correction is needed. However,

Table 2. Initial IRI₀ pay adjustment in QRSS.

Average IRI for each 0.1 mile of Traffic Lane (in/mile)	Pay Adjustment (\$/0.1 mile of Traffic Lane)		
	Schedule 1 (High Traffic Volume)	Schedule 2 (Intermediate Traffic Volume)	Schedule 3 (Low Traffic Volume)
≤ 30	600	600	300
31	580	580	290
32	560	560	280
33	540	540	270
...
74	-180	0	0
75	-200	0	0
76	-220	-20	0
77	-240	-40	0
78	-260	-60	0

Table 3. Initial measured IRI₀ and penalty/bonus cost.

Mile Post	Unit Mileage (mile)	Lane 1		Lane 2	
		Average Initial IRI	Penalty/Bonus (\$)	Average Initial IRI	Penalty/Bonus (\$)
1	0.1	33	+540	74	-180
2	0.1	34	+520	76	-220
3	0.1	32	+560	77	-240
4	0.1	35	+500	75	-200
5	0.1	33	+540	74	-180
Sum	0.5		+2,660		-1,020

if a lot is defined as a day’s production (i.e., potentially a different tonnage each day) then the tonnage correction in Equation 7 is applied. The Total Penalty/Bonus in Equation 7 simply represents a weighted average Penalty/Bonus of all lots in a given project by tonnage.

$$Total P / B = \frac{\sum(n_i)(P/B)_i}{N_t} \quad (7)$$

where

- Total P/B = total penalty/bonus (%)
- n_i = tonnage of each lot
- (P/B)_i = penalty/bonus (%) of each lot
- N_t = total tonnage

Equation 7 is rearranged to Equation 8 to include the construction cost:

$$C_{PB} = \left(\frac{\sum(n_i)(P/B)_i}{N_t} - 1 \right) C_{AC} \quad (8)$$

where

- C_{PB} = Final Penalty/Bonus cost for a given project
- C_{AC} = Construction cost for AC pavement

Since the QRSS considers three major distresses as well as up to three AC layers for rutting, Equation 8 can be expanded to the general form in Equation 9. Equation 9 utilizes the total Penalty/Bonus cost for three distresses and for rutting in three AC layers.

$$C_{PB} = \beta_r \left\{ P_{r-s} \left(\frac{\sum n_k (P/B)_{rk}}{N_{t(AC-s)}} - 1 \right) C_{AC-s} + P_{r-m} \left(\frac{\sum n_l (P/B)_{rl}}{N_{t(AC-m)}} - 1 \right) C_{AC-m} + P_{r-b} \left(\frac{\sum n_m (P/B)_{rm}}{N_{t(AC-b)}} - 1 \right) C_{AC-b} \right\} + \beta_f \left(\frac{\sum n_m (P/B)_{fm}}{N_{t(AC-b)}} - 1 \right) C_{AC-b} + \beta_{tf} \left(\frac{\sum n_k (P/B)_{tk}}{N_{t(AC-s)}} - 1 \right) C_{AC-s} \quad (9)$$

where

- k, l, and m = lot number for surface, middle, and bottom layer
- N_{t(AC-s)}, N_{t(AC-m)}, and N_{t(AC-b)} = tonnage for surface, middle, and bottom layers
- C_{AC-s}, C_{AC-m}, and C_{AC-b} = construction cost for surface, middle, and bottom layers
- P_{r-s}, P_{r-m}, and P_{r-b} = rutting contribution factor for surface, middle, and bottom layers
- β_r, β_f and β_{tf} = regional calibration factors

Equation 9 has five terms; the first three terms are involved with rutting, while the fourth and fifth terms are related to fatigue cracking and thermal cracking, respectively. The subscripts *s*, *m*, and *b* denote the surface, middle, and bottom layers.

Another factor introduced in Equation 9 is termed the layer rutting contribution factor, P_{ri}. When rutting occurs in a pavement due to excessive loading or poor mix design, the rutting observed on the pavement surface is a cumulative rut depth that has occurred within the total AC pavement layer. In the majority of AC pavements, the majority of the rutting occurs within the upper portion of the total AC thickness. Thus, the rutting magnitude of rutting within each AC layer or AC mix type is highly variable. Because of this, the layer rutting contribution factors have been introduced as layer weighting values.

Also, Equation 9 contains a regional calibration factor, β, for each distress; these are calibration factors for the distress prediction. For the national calibration used in the MEPDG, β_r = β_f = β_{tf} = 1.0. However, if the agency has done a local or regional calibration of the MEPDG distress models, the new calibration factors may be substituted in Equation 9 to properly weight the three distresses.

The final Penalty/Bonus cost is determined by adding the IRI₀ Penalty/Bonus cost—calculated with Equation 6—to the Penalty/Bonus costs found with Equation 9 for the three distresses. Equation 10 represents the final Penalty/Bonus equation implemented in the QRSS.

$$C_{PB} = C_{PB1} + C_{PB2} \quad (10)$$

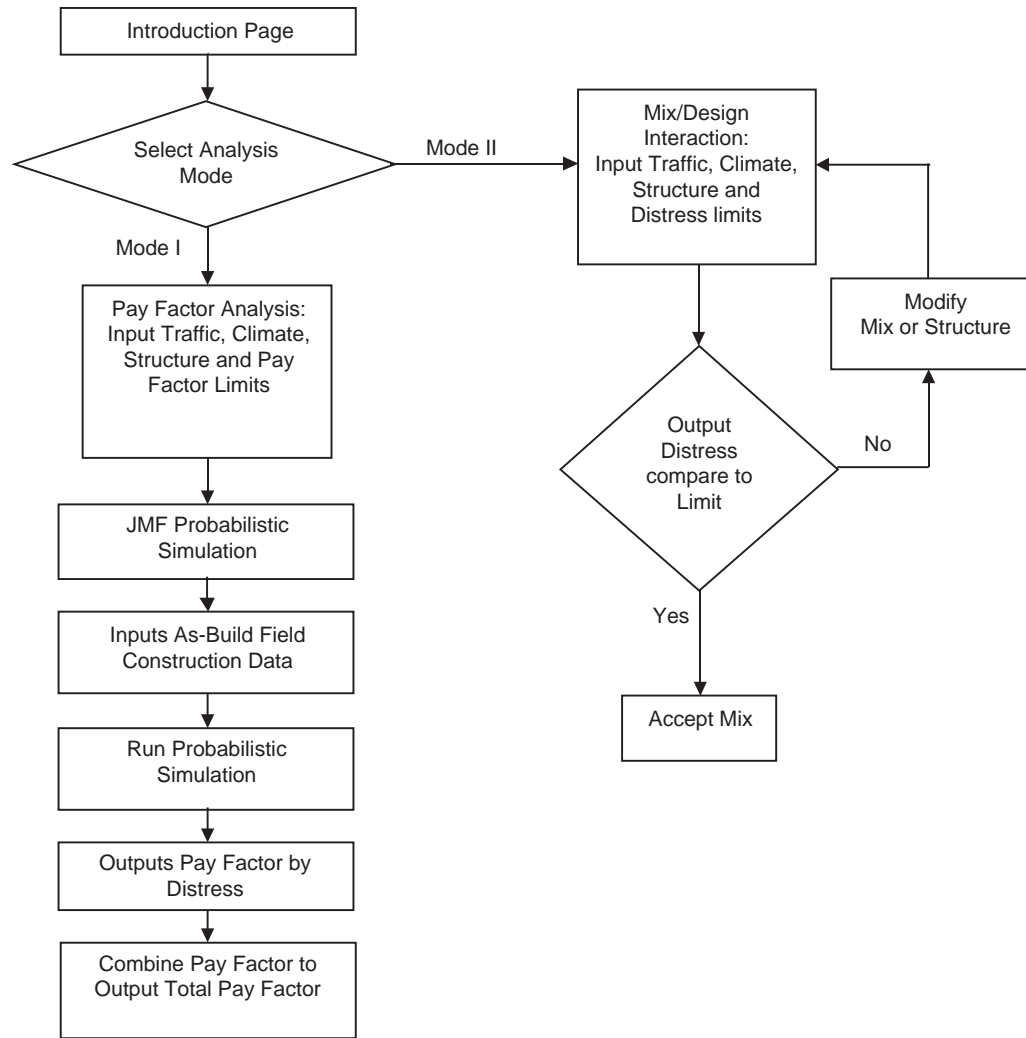


Figure 7. Flow diagram of QRSS performance pay factor methodology.

where

C_{PB} = final penalty/bonus cost for a given project

C_{PB1} = penalty/bonus cost associated with the three distresses—Equation 9

C_{PB2} = penalty/bonus cost associated with IRI_0 —Equation 6

The QRSS represents a true first step in integrating HMA mixture design and pavement structural design. It is

also a first step in relating construction quality to pavement performance over the life of the pavement. Figure 7 shows a general flowchart of the performance pay factors methodology. A study using actual pavement construction and QA data from projects in several states is underway in NCHRP Project 9-22A to assess the validity of the methodology and its suitability for use by the state DOTs.

CHAPTER 2

Development of the QRSS Performance Models

2.1 Introduction

The QRSS is based on the use of performance predictions obtained with the MEPDG. However, running the MEPDG can require hours of computational time to obtain the distress predictions. Accordingly, performance prediction models were needed that could produce the needed predictions in seconds rather than hours. This chapter describes the development of closed form solutions (CFS) for each of the three HMA distresses (rutting, fatigue cracking, and thermal cracking) predicted by the MEPDG.

The following section defines and discusses the general variables used in the development of the QRSS performance models.

2.2 General Variables

2.2.1 Effective Temperature

The determination of a single test temperature for HMA mixtures to simulate major distresses commonly observed on flexible pavements (e.g., rutting, fatigue cracking, and thermal cracking) is of great significance in their design and analysis. It is obvious that the use of a single test temperature would greatly reduce testing time as well as the necessary analytical efforts in the mixture evaluation process and lead to an increase in practicality and efficiency.

The presence of a single temperature at which HMA mixtures can be evaluated has been termed the “Effective Temperature” in the literature. Effective temperature (T_{eff}) can be defined as a single test temperature at which an amount of a given type of distress, within a given pavement system, would be equivalent to that which would occur from the seasonal temperature fluctuation throughout the annual temperature cycle. It should be noted that the amount of distress in this context is cumulative damage caused during a given pavement design life. Also note that the effective temperature is unique for each distress type. Hence, the rutting effective temperature

is not necessarily the same as the fatigue cracking effective temperature.

A methodology for the T_{eff} prediction was developed over the years by Witczak and colleagues. The T_{eff} solution was originally developed as part of SHRP Project A-001, “Improved Asphaltic Materials, Experiment Design, Coordination and Control of Experimental Materials,” and represented the fundamental methodology used to evaluate rutting and fatigue cracking in the SHRP A-407 report (10, 11). The initial T_{eff} approach considered a comprehensive analytical framework involving a factorial of environmental locations, effective depths to compute the T_{eff} value, pavement structural system, various mix properties and responses, tire pressures, and models of permanent strain behavior in asphalt mixtures. As a result, the methodology represented a comprehensive approach to determine T_{eff} . However, limitations of the initial T_{eff} model introduced by the absence of the traffic loading frequency concept (vehicle speed) and the limited use of a variety of climatic characteristics [i.e., in addition to the Mean Annual Air Temperature (MAAT)] motivated a further enhancement of the T_{eff} model. Most importantly, the T_{eff} had to be unique to a given distress type and magnitude. In other words, the predictive distress methodology of the design and analysis system becomes an integral part of the T_{eff} approach. Thus the T_{eff} results presented in this report are uniquely tied to the calibrated performance models found in the MEPDG (Ver. 1.0) (12).

The following sections present a review of the initial Witczak T_{eff} approach followed by the introduction of a new T_{eff} model approach developed for rutting and fatigue cracking distresses.

2.2.1.1 Rutting Effective Temperature

Initial Witczak Effective Temperature Model. A fundamental approach used to obtain the initial Witczak T_{eff} was to find design factors that are believed to significantly influence

Table 4. Factorial design for initial Witczak T_{eff} model development.

Factors	Level Type	Number of Levels
Geographical Location	Barrow (Alaska), Kapuskaging (Ontario), Richmond (Virginia), and Bahrain (Kingdom of Bahrain)	4
Effective Pavement Depth	1, 2, and 3 inches	3
Pavement Cross Section	hac = 4, 8, and 12 inches Subgrade Modulus = 5, 15, and 30 psi	9
Asphalt Quality Level	Dense Graded, Open Graded, and Sand Graded	3
Tire Pressure	80 and 150 psi	2

the relationship between rutting distress and T_{eff} . For this initial stage of T_{eff} development, the effects of five major factors were evaluated. These factors and their levels are shown in Table 4.

A comprehensive sensitivity analysis for the effect of these factors on the T_{eff} concluded that the T_{eff} for rutting of asphalt concrete mixes was only influenced by selection of the critical depth (z) for an environmental location represented by the historic average MAAT. A multiple regression predictive equation for the T_{eff} was obtained with those two variables. Thus, for any desired critical depth, z , the design T_{eff} was initially expressed by:

$$T_{eff} (\text{°F}) = 58.0 - 5.5(z) + 0.92(MAAT) \tag{11}$$

This initial Witczak T_{eff} model was validated with the AC rutting prediction models in the MEPDG (Version 0.7, released in 2005). Twelve environmental locations were selected to observe the correlation between MEPDG rut depth prediction and T_{eff} . From Figure 8 and Table 5, it appears that the general trend of T_{eff} to the predicted rut depth was reasonable (i.e., the predicted

rut depth increases with increasing T_{eff}). However, it was also observed that a more accurate solution to the rutting problem required improvement of the model for high temperature locations.

It is clear that the MEPDG AC rut prediction (0.131 inches) for Phoenix, AZ ($T_{eff} = 117.84$), is higher than the ones corresponding to Key West, FL ($T_{eff} = 121.08$ and AC Rut Prediction = 0.097 inches), and Jackson, MS ($T_{eff} = 108.95$ and AC Rut Prediction = 0.106 inches). However, the predicted rutting at Jackson is higher than that at Key West, despite the fact the effective temperature for Jackson is 12°F below that for Key West.

The following inputs were used to predict the relationship shown in Figure 8:

- AC Rut Predictions for the sublayer between 1 inch and 2 inches ($z = 1.5$ inch) in a 5.9-in Pavement Structure
- Number of Traffic Repetitions = 7,500,000 ESALs
- Average Traffic Speed = 45 mph
- Binder Type = Conventional PG 82-10
- Air Voids = 7%
- Effective Binder Content = 10%

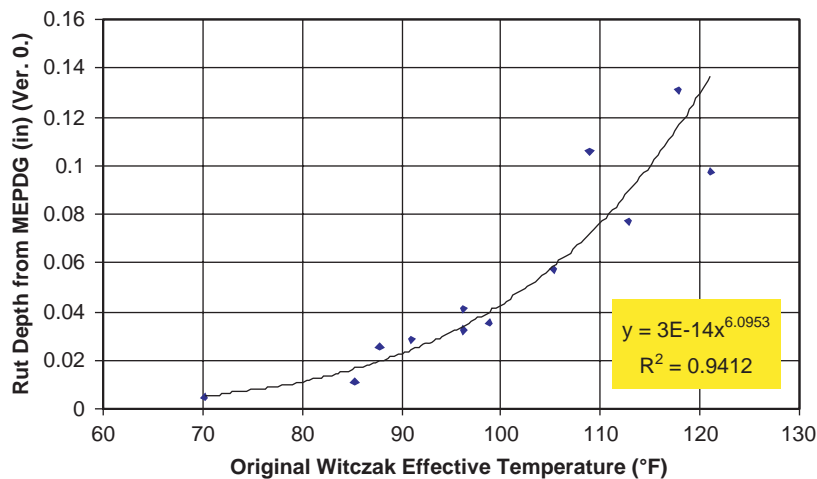


Figure 8. Relationship between T_{eff} (Initial Model) and rut depth (MEPDG Ver.0.7).

Table 5. MAAT and T_{eff} for various locations (z = 1.5 inch).

Locations	MAAT (°F)	Original Witczak T _{eff} (Equation (1)) (°F)
Kotzebue, Alaska	21.9	69.9
Homer, Alaska	38.5	85.2
Grand Forks, ND	41.7	88.1
Great Falls, Montana	45.9	92.0
Chicago, Illinois	51.4	97.0
Hartford, Connecticut	51.5	97.1
Indianapolis, Indiana	54.1	99.5
Oklahoma City, OK	61.1	106.0
Jackson, Mississippi	64.9	109.5
Houston, Texas	69.0	113.2
Phoenix, Arizona	74.9	118.7
Key West, Florida	77.9	121.4

- Retained Sieve ¾ = 0%
- Retained Sieve ⅜ = 26.8%
- Retained Sieve No. 4 = 46.4%
- Passing Sieve No. 200 = 8.24%

In addition, Table 5 summarizes the MAAT and the subsequent T_{eff} value from the original Witczak Equation for the 12 sites shown in Figure 8.

Revised Effective Temperature Model (2005). The initial T_{eff} model was reevaluated to increase its prediction accuracy. This reevaluation began by considering the environmental terms used in the MEPDG (Version 0.7): air temperature, wind speed, rainfall, sunshine percentage, and relative humidity (12), which are recorded hourly and stored within the MEPDG for hundreds of environmental sites within the United States. Therefore, it seemed reasonable to think that the correlations between T_{eff} and MEPDG predictions of AC Rut Depth might significantly improve if all the aforementioned environmental terms were included in the T_{eff} approach.

In addition to the consideration of the environmental terms, it was also decided to incorporate the influence of the typical traffic load and corresponding frequency (time of loading). A major reason for this was the recognition that the original Witczak T_{eff} (Equation 11) was developed for a single loading frequency of 1 Hz. Therefore, it was necessary to assess the effect of different traffic speeds (i.e., the frequency of loading) and to incorporate this term in the T_{eff} model.

The frequency was first incorporated within Equation 11 (with MAAT still as the environmental conditions characterization factor). The format of this equation, with the frequency term incorporated into the model is presented in Equation 12:

$$T_{eff} = 58 - 5.5 \left\{ \underbrace{[a_1z + a_2] \text{Ln}(Freq) + [a_3z + a_4]}_{\substack{\text{Term replaces "5.5 z" in} \\ \text{Equation 11}}} \right\} + \underbrace{\left\{ [a_5z + a_6] (Freq)^{[a_7z + a_8]} \right\}}_{\substack{\text{Term replaces "0.92 MAAT" in} \\ \text{Equation 11}}} MAAT \quad (12)$$

where

T_{eff} = modified Witczak T_{eff}, °F

z = critical depth, inch

Freq = loading frequency, Hz

MAAT = Mean Annual Air Temperature, °F

a₁~a₈ = regression constants to be determined

Sotil (3) presents the detailed development of Equation 12. The next step was to replace the MAAT variable with a linear combination of the five environmental terms used by the MEPDG, with their corresponding regression coefficients. A pilot study with respect to the inclusion of a loading frequency term and the five environmental terms showed that a slight improvement occurred but the problems noted in Figure 8 (e.g., rut depths at Jackson higher than those at Key West) were still observed. Thus, it was decided to include the standard deviation of the mean monthly air temperature (σ_{MMAT}) as an additional factor. This allowed consideration of the range of high temperatures possibly experienced in the summertime at a given site, as well as its variability, in support of the MAAT term already included.

The MEPDG rut depth results were used to determine the 14 regression coefficients (eight from Equation 12, five for the environmental terms used by the MEPDG, and one for the additional factor, σ_{MMAT}). The MEPDG Version 0.7 was used to produce the rutting results for the wide range of pavement conditions shown in Table 6. In addition, the study used 52 of the 72 LTPP Sections used in the national calibration of the MEPDG AC Rut Depth Prediction Model for the model validation study (13). Therefore, the total number of simulated sections was 724 (= 672+52).

The 14 regression coefficients were determined for the following equation:

$$T_{eff} = 58 - 5.5 \left\{ [a_1z + a_2] \text{Ln}(Freq) + [a_3z + a_4] \right\} + \left\{ [a_5z + a_6] (Freq)^{[a_7z + a_8]} \right\} T_f \quad (13a)$$

where

$$T_f = a_9(MAAT) + a_{10}(\sigma_{MMAT}) + a_{11}(\text{Rain}) + a_{12}(\text{Sunshine}) + a_{13}(\text{Wind}) + a_{14}(\text{R.H.}) \quad (13b)$$

T_f = temperature factor, °F

σ_{MMAT} = standard deviation of the mean monthly air temperature

Table 6. Matrix of rutting analysis (MEPDG Ver. 0.7).

Factors	Number of Levels	Level Type
Environmental locations	12	Hot to cold region (Alaska ~ Arizona)
Number of traffic repetitions	1	10,000,000 ESALs
Asphalt layer thickness	7	1, 2, 3, 4, 6, 8, 12 inches
Vehicle speed	4	0.5, 15, 45, 60 mph
Asphalt binder	2	PG 82-10, PG 52-40

Total number of Runs: $12 \times 1 \times 7 \times 4 \times 2 = 672$

Rain = annual cumulative rainfall depth, inches
 Sunshine = mean annual percentage sunshine (%)
 Wind = mean annual wind speed (mph)
 R.H. = mean annual relative humidity (%)
 $a_1 \sim a_{14}$ = regression coefficients

The final database of simulated AC rut depth predictions was then reduced to include only sections with a total AC Rut Depth less than 0.50 inches. This resulted in a final number of 468 data points that were used in the study. A non-linear optimization scheme yielded the following final equation:

$$T_{eff} = 41.534 - 3.261 \ln(Freq) - 9.021(z) + 1.11(MAAT) + 1.254(\sigma_{MMAT}) - 1.132(Wind) + 0.337(Sunshine) + 0.071(Rain) \quad (14)$$

This 2005 revised Witzcak T_{eff} model modified the relationship in Figure 8 to a much more accurate correlation, as shown in Figure 9. The fitted equation had an improved R^2 value (from 0.9412 in Figure 8 to 0.9930 in Figure 9) and the discrepancies

previously observed disappeared (that is, the rutting properly increased with temperature as defined by the T_{eff}).

New Revised Effective Temperature Model (2008). MEPDG Version 1.0 became available in 2008. One of the major changes found in Version 1.0 was an upgraded climatic database with more climatic data from each U.S. weather station. Since the previous effective model developed in 2005 was based upon version MEPDG Version 0.7, it was again necessary to reevaluate the previous T_{eff} model with the new rut depth results predicted by Version 1.0.

It should be noted that the new revised T_{eff} model uses the same model form as before. That is, the only modification from the previous model was to recalibrate the model by obtaining new coefficients from the non-linear optimization process. Simulations were conducted with the MEPDG Version 1.0 according to the matrix shown in Table 6, except that two more AC thicknesses, 2.75 and 20 inches, were added. Thus, the total number of simulations increased to 864. Environmental terms for the 12 environmental sites for the new

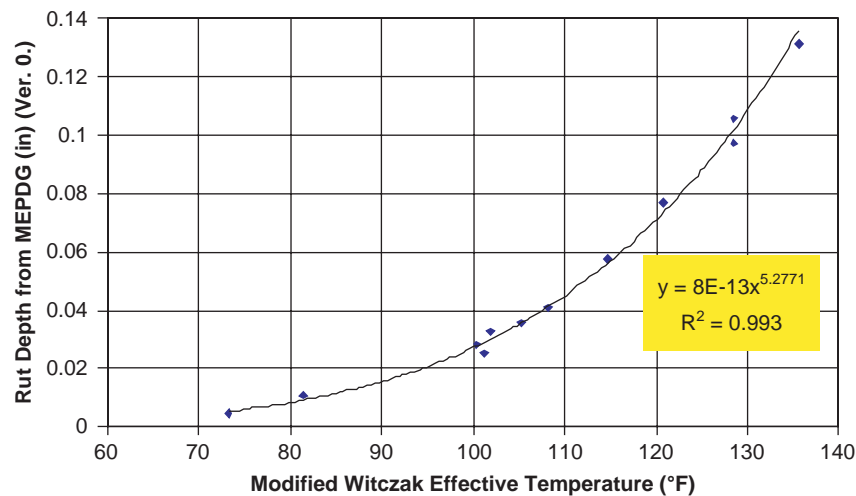


Figure 9. Relationship between T_{eff} (2005 Revised Model) and rut depth (MEPDG ver. 0.7).

Table 7. Climatic summary of the 12 environmental sites.

Location	MAAT (°F)	Wind Speed (mph)	Sunshine (%)	Rainfall (inches)	σMMAT (°F)
Kotzebue, Alaska	23.4	9.9	39.4	11.0	20.6
Homer, Alaska	39.8	5.5	33.4	24.7	11.2
Grand Forks, ND	40.1	9.0	53.8	19.5	21.6
Great Falls, Montana	45.0	9.9	62.1	12.8	15.6
Chicago, Illinois	50.5	8.1	37.1	29.8	17.2
Hartford, Connecticut	51.4	5.8	58.2	43.3	15.8
Indianapolis, Indiana	53.3	8.3	37.2	40.4	16.4
Oklahoma City, OK	60.2	9.7	48.4	30.9	15.6
Jackson, Mississippi	64.2	4.7	66.7	51.5	12.6
Houston, Texas	68.8	5.9	38.0	47.5	11.2
Phoenix, Arizona	74.7	5.3	60.8	6.6	14.8
Key West, Florida	77.7	8.4	72.6	36.8	5.6

T_{eff} model were retrieved from the MEPDG Version 1.0. A summary of the environmental terms used for each of the twelve geographic locations is presented in Table 7.

Equation 15 is the final form of the revised T_{eff} model for rutting. The T_{eff} values computed for the 12 locations across the nation are correlated with the corresponding rut depths as shown in Figure 10. As expected, the accuracy of the model is not improved from the previous model because the new model merely changed coefficients according to the rutting predicted from the MEPDG Version 1.0 (12).

$$T_{eff} = 14.62 - 3.361Ln(Freq) - 10.940(z) + 1.121(MAAT) + 1.718(\sigma_{MMAT}) - 0.431(Wind) + 0.333(Sunshine) + 0.08(Rain) \quad (15)$$

The specific inputs used to determine the relationship shown in Figure 10 are as follows:

- AC rutting predictions for the sublayer between 1 inch and 2 inches ($z=1.5$ inch) in a 4-in. pavement structure
- Number of traffic repetitions = 10,000,000 ESALs
- Average traffic speed = 45 mph
- Binder type = conventional PG 82-10
- Air voids = 7%
- Effective binder content = 10%
- Retained on sieve $\frac{3}{4}$ " = 0%
- Retained on sieve $\frac{3}{8}$ " = 26.8%
- Retained on sieve No. 4 = 46.4%
- Passing sieve No. 200 = 8.24%

Sensitivity of the Rutting Effective Temperature. A sensitivity analysis was performed to investigate the impact of the variables in the effective temperature equation. The rutting T_{eff} was calculated for the variables of AC thickness (thin vs. thick), binder type (soft vs. hard), and traffic speed (slow vs. fast) at the 12 locations listed in Table 7. Figure 11 depicts the results of the

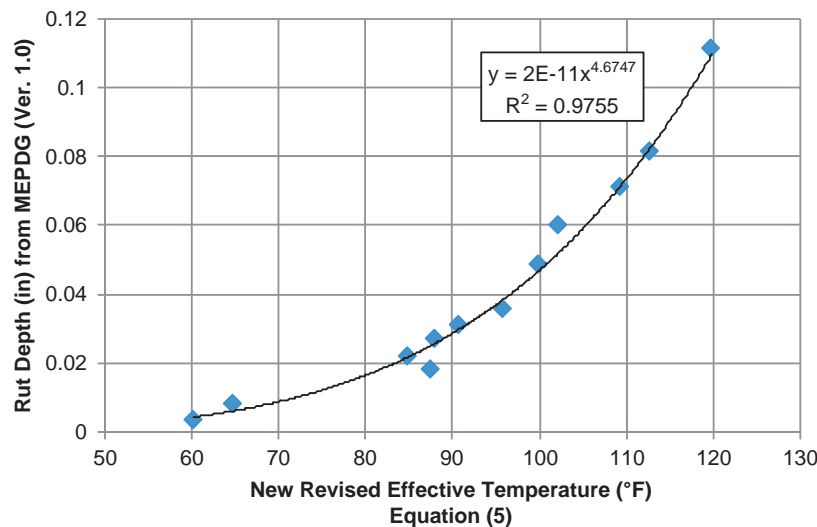


Figure 10. Relationship between T_{eff} (2008 Revised Model) and rut depth (MEPDG ver. 1.0).

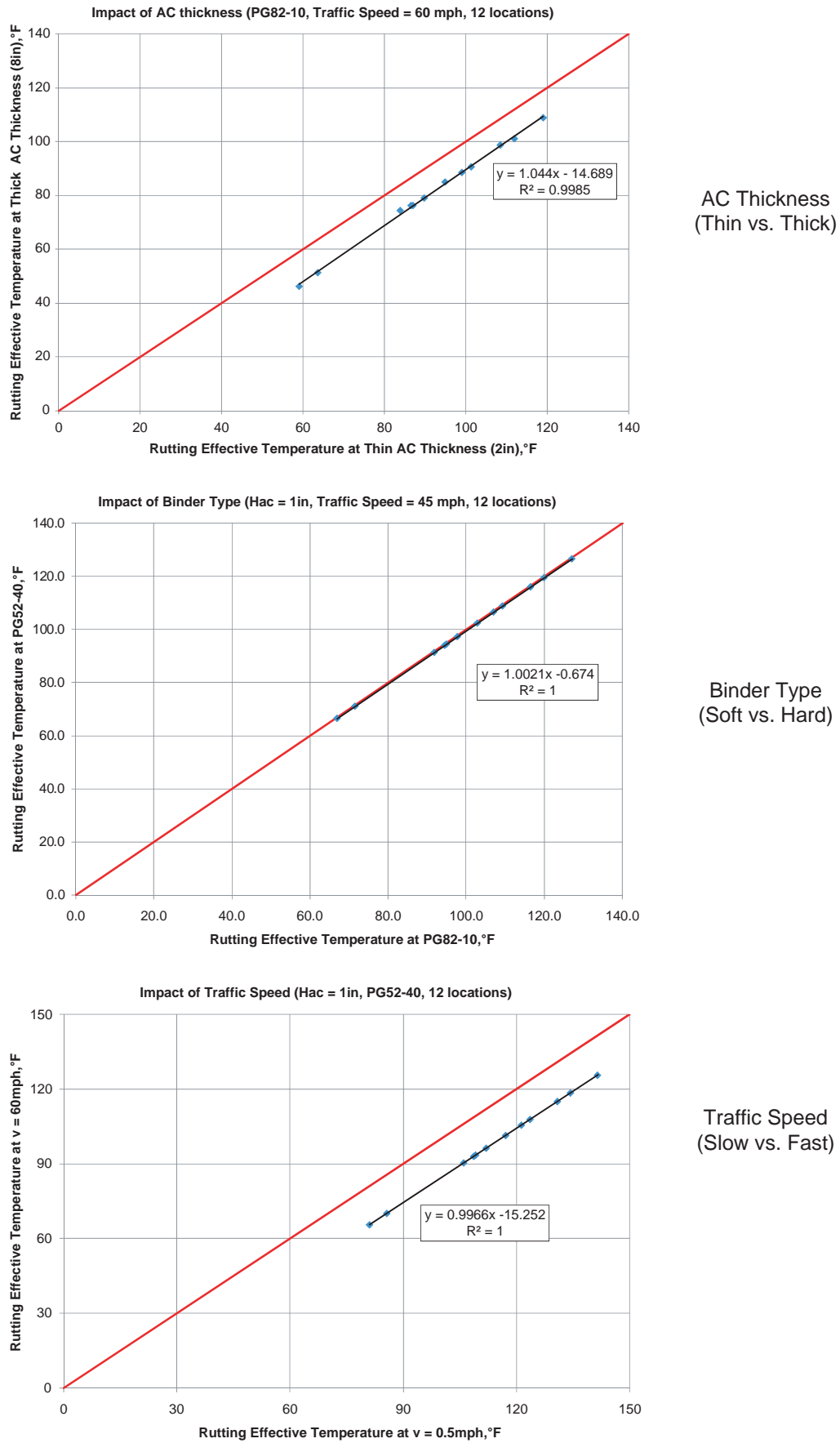


Figure 11. Sensitivity of rutting effective temperature to variables.

analysis. It was found that the AC thickness and traffic speed influence the effective temperature, while binder type does not, likely because the rutting T_{eff} is directly related to depth (z) and frequency (i.e., load pulse) as shown in Equation 15.

2.2.1.2 Fatigue Cracking Effective Temperature

Initial Effective Temperature Model. The initial form of the T_{eff} model for fatigue cracking was also a research product of SHRP Project A-001 (11). LTPP GPS sections were used to obtain varying levels of monthly based fatigue cracking from the Superpave fatigue cracking model. The approach used was to compute average monthly fatigue cracking and attempt to find a corresponding single temperature that resulted in the equivalent amount of the average fatigue cracking. The initially suggested form of the T_{eff} equation was:

$$T_{eff} (\text{°C}) = 0.8(MAPT) - 2.7 \quad (16)$$

where

T_{eff} = the effective test temperature in °C for fatigue cracking

MAPT = the mean annual pavement temperature in °C calculated at one-third of the depth of the pavement layer from climatic data for its geographic location.

The model intuitively seemed insufficient to represent environmental locations as a T_{eff} for fatigue cracking because pavement temperature is the only variable employed in the equation. In addition, the model took into account neither traffic loading as a frequency variable nor thickness of the AC layer. As previously described for the rutting T_{eff} model, the MEPDG contains various environmental terms such as rain-fall, wind speed, etc.

Therefore, for simplicity, the fatigue cracking T_{eff} model was initially developed with a similar form to that of the rutting T_{eff} model, incorporating the environmental terms and loading frequency as variables.

It should be noted that the T_{eff} modeling effort for fatigue cracking was initiated in 2005 using MEPDG Version 7.0. When Version 1.0 was released, the 2005 version of the T_{eff} model was recalibrated to obtain new coefficients. The following sections discuss the development of the T_{eff} model associated with MEPDG Version 1.0.

Revised Effective Temperature Model. A major task in NCHRP Project 9-22 was the development of closed-form regression equations predicting the amounts of distress for an HMA pavement system that were as close as practically possible to those amounts predicted by the MEPDG. The approach for developing the CFS was to run the MEPDG with a large matrix of significant variables. Using the huge database devel-

oped, the next step was to develop an accurate non-linear regression model. The final closed-form fatigue equation to predict the allowable number of traffic repetitions to fatigue failure is presented as follows (5):

$$\begin{aligned} \log N_f = & 6.3014 - \{[(b_1 \log(h_{ac})^2 + b_2 \log(h_{ac}) + b_3) \log(E^*) \\ & + b_4 \log(h_{ac})^2 + b_5 \log(h_{ac}) + b_6] \log(Ecf)^2 \\ & + [b_7 \log(E^*)^2 + b_8 \log(E^*) + b_9] \log(Ecf) \\ & + [b_{10} \log(h_{ac})^2 + b_{11} \log(h_{ac}) + b_{12}] \log(VFB)^2 \\ & + [b_{13} \log(h_{ac})^2 + b_{14} \log(h_{ac}) + b_{15}] \log(VFB) \\ & + b_{16} \log(E^*)^2 + [b_{17} (h_{ac})^2 + b_{18} (h_{ac}) \\ & + b_{19}] \log(E^*) + b_{20}\} \end{aligned} \quad (17)$$

where

N_f = allowable number of traffic repetition to fatigue failure

h_{ac} = AC thickness (inches)

E^* = dynamic modulus (psi)

Ecf = composite foundation modulus (ksi)

VFB = voids filled with bitumen (%)

$b_1 \sim b_{20}$ = regression coefficients

Equation 17 implicitly contains T_{eff} as a variable because the dynamic modulus in Equation 17 is calculated from a dynamic modulus master curve at the fatigue cracking effective temperature. The form of the potential T_{eff} model is based on an assumption that the model would at least be a function of the same variables as the rutting T_{eff} model, i.e., frequency of loading and the environmental terms. It also should be noted that the frequency of loading becomes a variable in both the T_{eff} model and Equation 17 because the equation contains AC thickness and the frequency is a function of the thickness.

Thus, a simultaneous optimization scheme was utilized to determine the 20 regression coefficients in Equation 17 as well as coefficients in a possible fatigue cracking T_{eff} model. Several modeling approaches were investigated and the final form of the model was found as follows:

$$\begin{aligned} T_{eff} = & -13.995 - 2.332(Freq)^{0.5} + 1.006(MAAT) \\ & + 0.876(\sigma_{MMAT}) - 1.186(Wind) \\ & + 0.549(Sunshine) + 0.071(Rain) \end{aligned} \quad (18)$$

It is noted that the fatigue cracking T_{eff} model differs from that for rutting because there is no term in z and the frequency appears as a square root. Also, since the experimental matrix to develop the fatigue cracking T_{eff} model was based upon three environmental locations, Grand Forks, ND (cold), Oklahoma

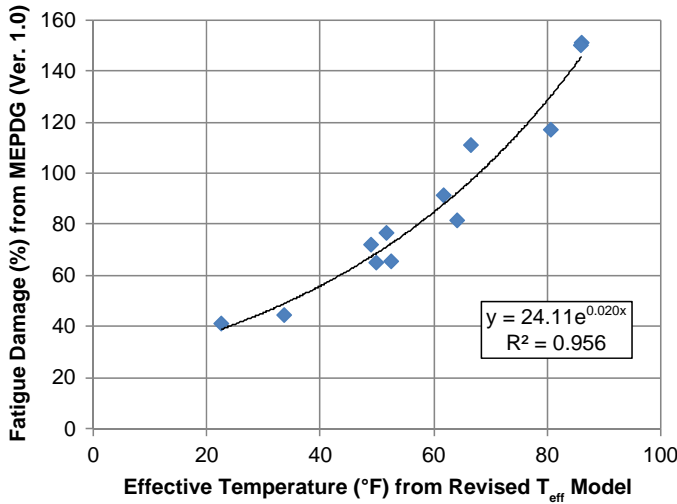


Figure 12. Relationship between fatigue cracking T_{eff} (2008 Revised Model) and fatigue damage (MEPDG Version 1.0).

City, OK (intermediate), and Key West, FL (hot), it was necessary to validate the T_{eff} model in other locations.

The 12 sites utilized for the rutting T_{eff} model were applied to the fatigue cracking T_{eff} model for a typical pavement system. Figure 12 shows the relationship between fatigue cracking T_{eff} and fatigue damage; fatigue damage has a reasonable increasing trend with the increase in T_{eff} .

Sensitivity of the Fatigue Cracking Effective Temperature.

A sensitivity study for the fatigue cracking T_{eff} similar to that for the rutting T_{eff} was performed. The study results showed an analogous trend to the results for the rutting T_{eff} as shown in Figure 13; the fatigue T_{eff} is not influenced by binder type, while it is affected by AC thickness and traffic speed.

It should be noted that the fatigue T_{eff} increases with the increase of AC thickness. This is because of the assumption that as the depth increases, the load frequency will decrease. This, in turn, will result in the use of a higher effective temperature for the effective conditions.

2.2.1.3 Comparison of Effective Temperature between Rutting and Fatigue

The effective temperatures for AC rutting and fatigue cracking for the 12 environmental (geographical) locations were calculated to look for any relationship between the two temperatures. It was observed, as shown in Figure 14, that the effective temperature for the fatigue distress is much lower (by 20–40°F) than for rutting. The temperature difference is reduced as the AC thickness increases. This observation agrees with the findings described in Deacon et al. (14).

2.2.2 Determination of Dynamic Modulus (E^*)

2.2.2.1 Background on E^*

For linear viscoelastic materials such as asphalt mixtures, the stress-strain relationship under continuous sinusoidal loading is defined by a complex number called the complex modulus E^* (15,16). This parameter has a real and an imaginary part that defines the elastic and viscous behavior of the linear viscoelastic material. E^* and its real and imaginary parts are defined as:

$$E^* = E' + iE'' \tag{19a}$$

$$E' = (\sigma_o / \epsilon_o) \times \cos \phi \tag{19b}$$

$$E'' = (\sigma_o / \epsilon_o) \times \sin \phi \tag{19c}$$

where

E' = storage or elastic modulus component of the complex modulus

E'' = loss (viscous) modulus component of the complex modulus

i = imaginary number

σ_o = peak dynamic stress amplitude

ϵ_o = peak recoverable strain

ϕ = phase lag or angle (degrees)

The loss tangent ($\tan \phi$) is the ratio of the energy lost to the energy stored in a cyclic deformation and is equal to

$$\tan \phi = E'' / E' \tag{19d}$$

The absolute value of the complex modulus $|E^*|$ is defined as the dynamic modulus.⁴ Mathematically, the dynamic modulus is defined as

$$|E^*| = \sigma_o / \epsilon_o \tag{20}$$

In current practice, dynamic modulus testing of asphalt materials is generally conducted on unconfined cylindrical specimens having a height to diameter ratio equal to 1.5 and uses a uniaxially applied sinusoidal (haversine) stress pattern (16). Under such conditions, the sinusoidal stress at any given time t , is given as

$$\sigma_t = \sigma_o \sin(\omega t) \tag{21}$$

where

ω = angular frequency in radian per second

t = time (sec)

⁴For simplicity, $|E^*|$ is expressed as E^* throughout this report.

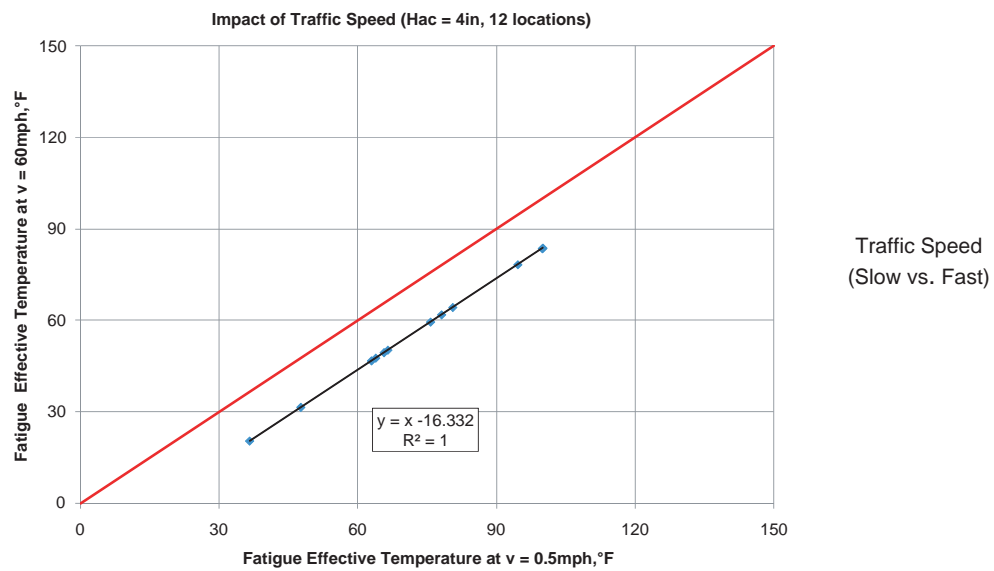
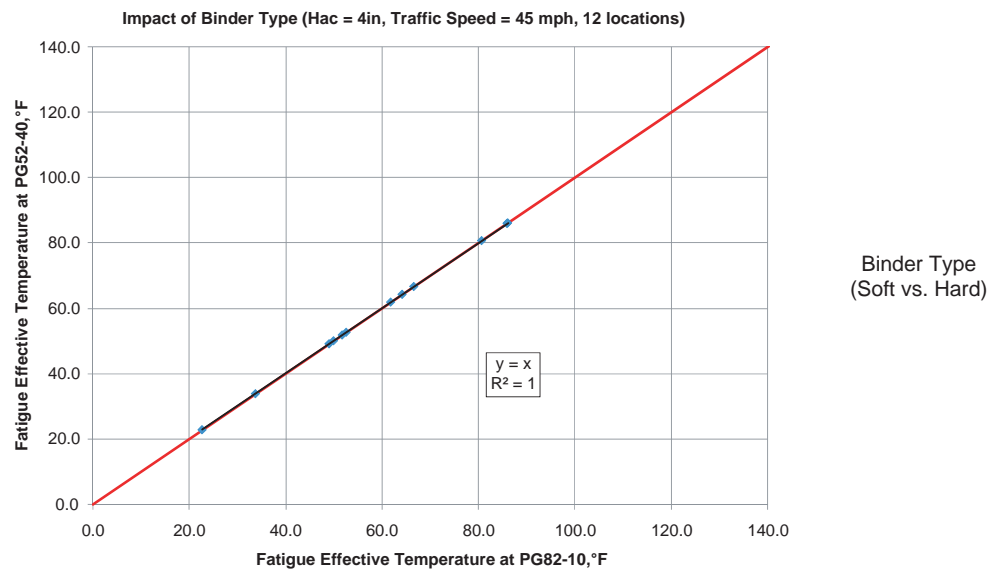
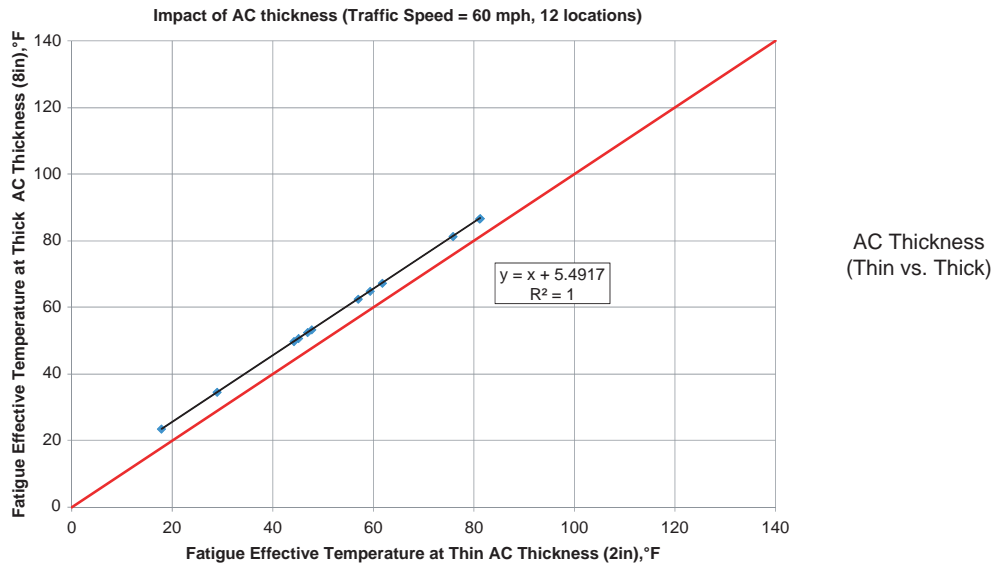


Figure 13. Sensitiveness of fatigue effective temperature on variables.

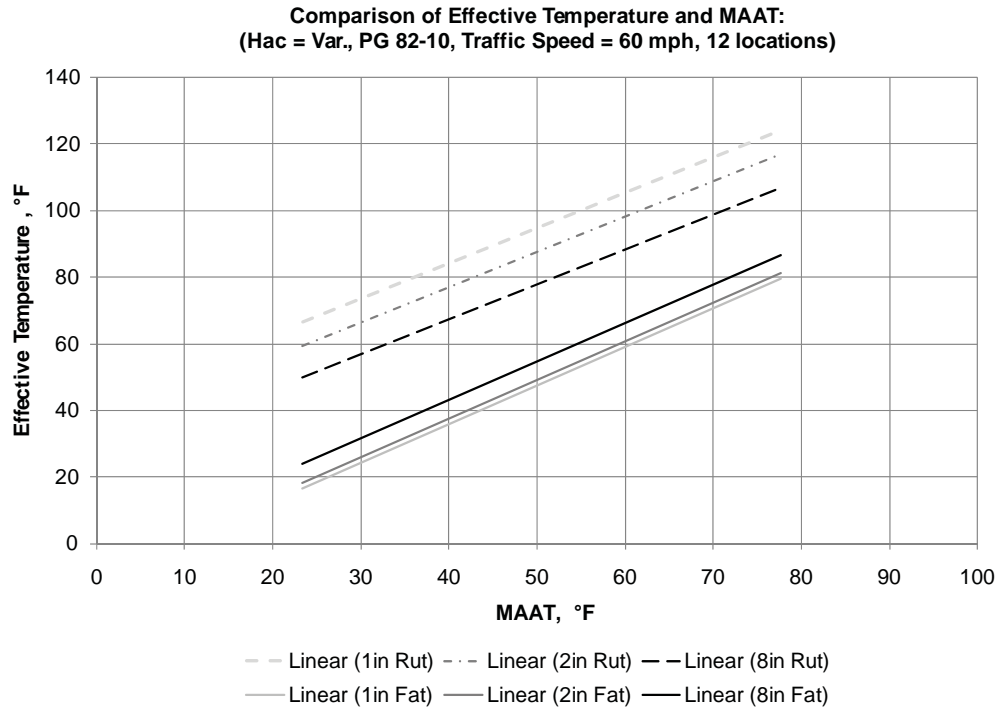


Figure 14. Comparison of the effective temperatures for rutting and fatigue cracking.

The subsequent dynamic strain at any given time is given by

$$\phi = (ti/tp) \times (360) \tag{23}$$

$$\epsilon_t = \epsilon_o \sin(\omega t - \phi) \tag{22}$$

where

ti = time lag between a cycle of stress and strain (sec)

tp = time for a stress cycle (sec)

The phase angle (ϕ) is simply the angle at which ϵ_o lags σ_o and is an indicator of the viscous (or elastic) properties of the material being evaluated. Mathematically this is expressed as

For a pure elastic material, $\phi = 0$ and for a pure viscous material, $\phi = 90^\circ$ (16). Figure 15 shows the relationship

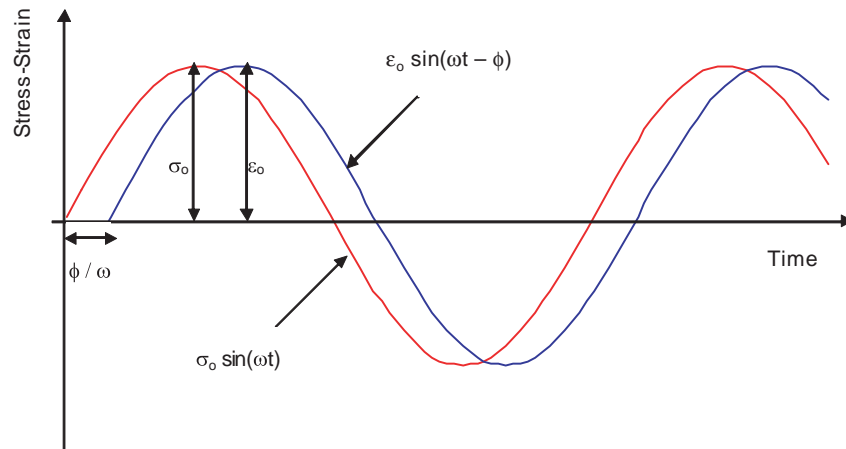


Figure 15. Asphalt mixture stress-strain responses under sinusoidal load.

between the stress and strain of an asphalt mixture under any given sinusoidal load.

The dynamic modulus (stiffness) response of an asphalt mixture is known to be dependent on variables like temperature, rate of loading, binder aging, confinement level, and mixture characteristics such as binder stiffness, aggregate gradation, binder content, and air voids (12). To account for the effect of temperature and rate of loading, master curves are constructed, using as a reference any arbitrary temperature value. Normally this value is set to be at 70°F. Using this E^* master curve, analysis and comparisons between several mixtures and conditions can be made, as well as calculation of the E^* value at temperatures and frequencies different from those used in the laboratory testing.

2.2.2.2 Constructing a Dynamic Modulus Master Curve

The E^* master curve is best defined mathematically with a sigmoidal function as follows:

$$\log(E^*) = \delta + \frac{\alpha}{1 + e^{\beta + \gamma(\log t_r)}} \quad (24)$$

where

E^* = dynamic modulus

t_r = time of loading at the reference temperature (reduced time)

δ = minimum value of E^*

$\alpha + \delta$ = maximum value of E^*

β and γ = parameters describing the shape of the sigmoidal function

The fitting parameters α and δ depend on aggregate gradation and the binder and air voids contents. The parameters β and γ depend on characteristics of the asphalt binder and the magnitude of α and δ . The sigmoidal function describes the time dependency of the modulus at the reference temperature.

The shift factors, represented in their general form in Equation 25, describe the time-temperature dependency of the modulus (12).

$$t_r = \frac{t}{a(T)} \text{ or } \log(t_r) = \log(t) - \log[a(T)] \quad (25)$$

where

t_r = time of loading at the reference temperature (reduced time)

t = time of loading at the given temperature of interest

$a(T)$ = shift factor as a function of temperature

T = temperature of interest

Thus, using Equation 25, the time of loading at the reference temperature can be calculated for any time of loading at any temperature. Then, the appropriate modulus can be calculated from Equation 24 using this time of loading at the reference temperature.

The shift factor as a function of temperature, $a(T)$, is theoretically defined by a linear relationship. However, historical analysis of data has clearly shown that a second order polynomial fit is more accurate. That is why the $a(T)$ relationship is commonly described by a quadratic equation as shown below:

$$\log a(T) = aT^2 + bT + c \quad (26)$$

where

T = temperature of interest

a, b, c = regression coefficients

If the relationship for a given mix follows a linear trend, the quadratic fit will converge to a linear one by zeroing its quadratic regressor a .

2.2.2.3 Witczak Dynamic Modulus Predictive Equation

This research is principally about the relationship of E^* and the selected pavement distresses. Obviously, for implementation purposes, this relationship must be as simple as possible. To perform a complete dynamic modulus test (master curve) requires a lot of time. Therefore any modification that will significantly reduce the time, especially when E^* is expected to be used as a simple measure of performance or a QA tool, is highly desirable.

Historically, predictive equations have been used to calculate E^* based on volumetric mix properties. The most common E^* equations are the Shell Oil equation (17), and the WPE (1). The WPE has been incorporated in the methodology of the MEPDG, as the E^* input for the lower order (Level 3) analysis, in contrast to the direct laboratory evaluation of E^* needed for the high order, Level 1 analysis (12).

Over the past 35 years, the WPE has become one of the most rational and comprehensive forms of predictive models available in the literature. Shook and Kallas (15) developed the initial set of equations in 1969. Witczak and colleagues at the University of Maryland took the initial Shook-Kallas E^* results and continuously updated the database and further refined the equation. A 1996 update by Fonseca and Witczak (18) utilized a database of 1,430 points from 149 conventional asphalt mixes. In 1999, Witczak et al. (1) added 56 additional mixes, 34 of which used modified binders. This increased the database to 2,750 points. The 2,750 dynamic modulus measurements represent 205 different asphalt mixtures tested

Table 8. Summary statistics for the Witczak dynamic modulus equation.

Statistic	Value
Goodness of fit	R ² = 0.96 Se/Sy = 0.24
Data points	2,750
Temperature range	0 to 130 °F
Loading rates	0.1 to 25 Hz
Mixtures	205 Total - 171 With unmodified asphalt binders 34 With modified binders
Binders	23 Total - 9 Unmodified - 14 Modified
Aggregates	39
Compaction methods	Kneading and gyratory
Specimen sizes	Cylindrical 4 in by 8 in or 2.75 in by 5.5 in

over the last 30 years in the laboratories of the Asphalt Institute, the University of Maryland, and the FHA.

Table 8 presents summary statistics for the current Witczak dynamic modulus equation. The following is the latest published version of the WPE:

$$\begin{aligned} \log E^* = & -1.249937 + 0.029232 p_{200} - 0.001767 (p_{200})^2 \\ & - 0.002841 p_4 - 0.058097 V_a - 0.8022 \frac{V_{beff}}{(V_{beff} + V_a)} \\ & 3.87197 - 0.0021 p_4 + 0.003958 p_{38} \\ & + \frac{-0.000017 (p_{38})^2 + 0.00547 p_{34}}{1 + e^{(-0.603313 - 0.31335 \log(f) - 0.393532 \log(\eta))}} \end{aligned} \quad (27)$$

where

- E* = asphalt mix dynamic modulus, in 10⁵ psi
- η = bitumen viscosity in 10⁶ poise (at any temperature, degree of aging)
- f = load frequency in Hz
- V_a = % air voids in the mix, by volume
- V_{beff} = % effective bitumen content, by volume
- p₃₄ = cumulative % retained on the 3/4" sieve, by total aggregate weight
- p₃₈ = cumulative % retained on the 3/8" sieve, by total aggregate weight
- p₄ = cumulative % retained on the No. 4 sieve, by total aggregate weight
- p₂₀₀ = % passing the No. 200 sieve, by total aggregate weight

2.2.3 Determination of Creep Compliance

For thermal cracking analysis with the MEPDG, the creep compliance and tensile strength of the HMA material, measured in accordance with AASHTO T 322, "Determining the Creep Compliance and Strength of Hot Mix Asphalt (HMA) Using the Indirect Tensile Test Device" are required. The creep compliance of the HMA mixture is given by the following equation:

$$D(t) = D_1 * t^m \quad (28)$$

where

- D(t) = creep compliance, psi
- t = time of loading, sec
- D₁, m = fracture coefficients

Based on the existing form of the predictive models for the creep compliance parameters, a set of new equations was developed for the three test temperatures, 0, -10, and -20°C for MEPDG Version 0.9. Temperature, as an independent variable, was removed from the equations, and a separate model was optimized individually for each test temperature. The best correlations found for the D₁ fracture parameter were:

$$\begin{aligned} \log(D_1)_{-20^\circ\text{C}} = & -11.9254 + 1.52206 * \log(V_a) + 4.49876 \\ & * \log(VFA) - 3.8132 * \log(A_{RTFO}) \end{aligned} \quad (29a)$$

$$\begin{aligned} \log(D_1)_{-10^\circ\text{C}} = & -10.7656 + 1.51960 * \log(V_a) + 3.49983 \\ & * \log(VFA) - 2.9987 * \log(A_{RTFO}) \end{aligned} \quad (29b)$$

$$\begin{aligned} \log(D_1)_{0^\circ\text{C}} = & -9.80627 + 1.50845 * \log(V_a) + 2.9900 \\ & * \log(VFA) - 2.90157 * \log(A_{RTFO}) \end{aligned} \quad (29c)$$

where

- V_a = air voids (%)
- VFA = void filled with asphalt (%) = $\frac{V_{beff}}{V_{beff} + V_a} \times 100$
- A_{RTFO} = intercept of binder viscosity-temperature relationship for the RTFO condition

For the m parameter, in addition to splitting the existing equation into separate models for every test temperature and removing temperature from the equation, another modification was made. In order to correct the problem of decreasing m values with increasing binder content, the VFA variable,

which caused the decrease of m values in the previous model, was also removed from the equation. The slope of the creep compliance was found to be a function of air voids content and asphalt binder penetration value at 77°F. The best relationships found were:

$$m_{-20^{\circ}\text{C}} = -1.75987 + 1.78187 * V_a^{0.0203} + 0.00089 * Pen_{77}^{0.9687} \quad (30a)$$

$$m_{-10^{\circ}\text{C}} = -1.82690 + 1.94218 * V_a^{0.0160} + 0.00098 * Pen_{77}^{0.96857} \quad (30b)$$

$$m_{0^{\circ}\text{C}} = -2.41043 + 2.59093 * V_a^{0.01547} + 0.00199 * Pen_{77}^{0.97247} \quad (30c)$$

where Pen_{77} is Penetration at 77°F = $10^{290.5013 - \sqrt{\frac{81177.288 + 257.0694}{*10(A + 2.72973 * VTS)}}$

The thermal fracture parameters D_1 and m were plotted in the creep compliance equation. Figure 16 shows the measured versus predicted creep compliance grouped accordingly to the test temperature. A total of 939 data points was used to obtain the above correlations with 313 points used at every temperature. A significant decrease in the bias for all temperatures was observed when compared to the MEPDG Version 0.7 MEPDG predictive equations.

Figure 17 presents the measured versus predicted creep compliance with all data combined into single plot for com-

parison with the existing MEPDG Version 0.9 model. With an R^2 of 0.80 and Se/Sy of 0.45, similar to the earlier MEPDG model, but with much lower bias, the regressions were considered to be acceptable.

Summary of results for creep compliance predictive equations (Level 3) are provided in Appendix C.

2.2.4 Frequency-Depth Relationship

For asphalt mixtures, two important factors that affect material behavior are temperature and the rate of loading (frequency). In the MEPDG, the primary material behavior for asphalt mixtures is defined by the dynamic modulus, E^* , test. The prediction of temperature is accomplished by the Enhanced Integrated Climatic Model (EICM) (12). However, the time (frequency) of loading, at any depth within the AC layer, is a function of the traffic type (axle configuration), speed of the vehicle, and the pavement structure (thickness of AC layers and critical depths) (12). This section describes the relationships between these factors that ultimately define the behavior of the asphalt mixture (i.e., its E^* value) and the construction of the E^* database required for the development of the E^* -performance criteria.

2.2.4.1 Loading Frequency

One of the keys to accurately characterizing an asphalt material is a process that can accurately estimate the effective

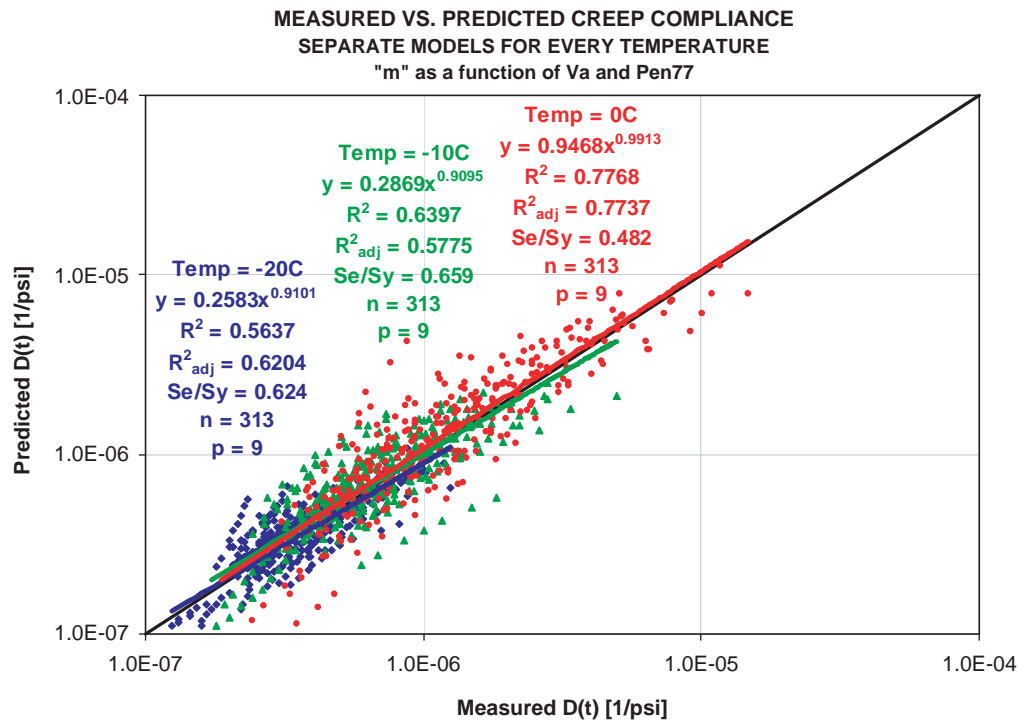


Figure 16. Measured versus Level 3 predicted creep compliance at three test temperatures—new predictive equations (MEPDG Version 0.9).

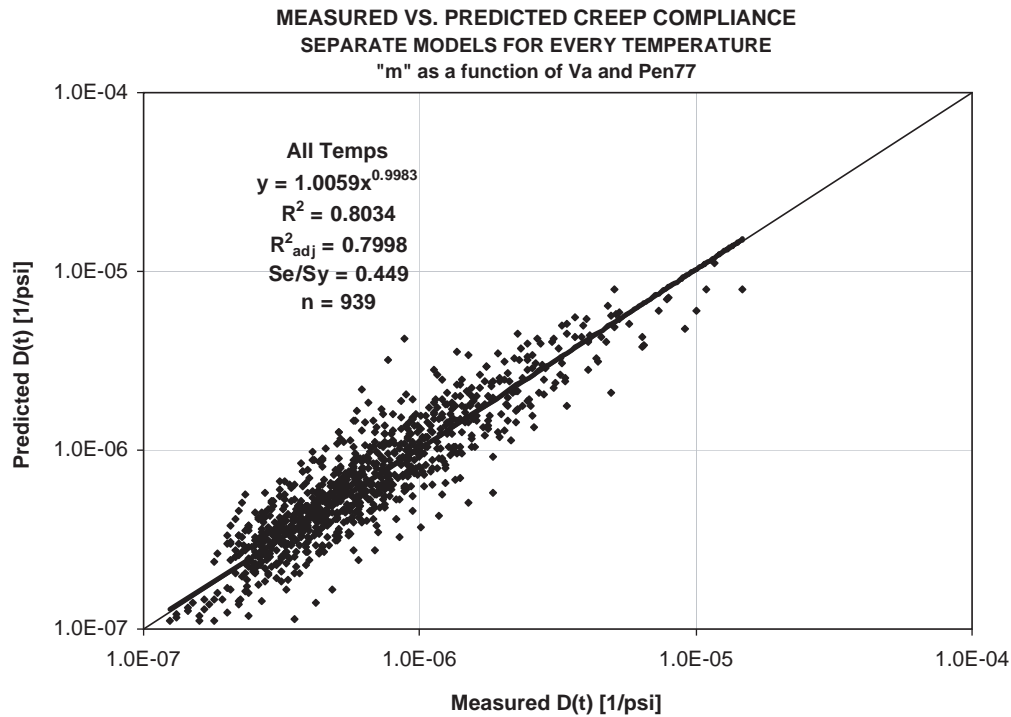


Figure 17. Measured versus Level 3 predicted creep compliance for all temperatures—new predictive equations (MEPDG Version 0.9).

loading time at any point within the asphalt layer. This process is graphically illustrated in Figure 18. When considering the stress at a point “A” within the pavement system, a wheel load at a considerable distance from point “A” will have no effect and the stress at A is zero (12). As the load starts to move towards “A,” the stress increases and becomes maximum when the load is directly above “A.” The MEPDG methodology assumes that the normal stress pulses due to load are sinusoidal or haversine, with duration dependent on the vehicle speed and the depth of point “A” below the pavement surface. Equation 31 shows the

relationship assumed to relate the time of load, vehicle speed, and the effective length of the stress pulse.

$$t = \frac{L_{eff}}{17.6v_s} \tag{31}$$

where

- t = time of load (seconds)
- L_{eff} = effective length (inches)
- v_s = velocity (mph)

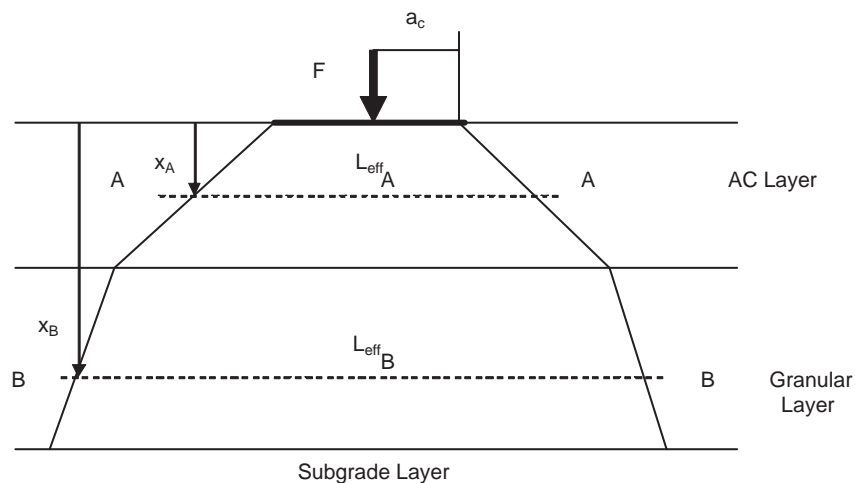


Figure 18. Effective length concept within pavement system.

The effective length of the stress pulse (at a given point) is defined as the length of the sinusoidal (haversine) stress pulse and is dependent upon the layer properties, climatic (temperature) conditions, and the loading configuration (axle spacing and tire radius of contact) (12). Thus, if L_{eff} and vehicle velocity are known, the time of loading (stress pulse time) can be calculated at any depth within the pavement system. The following relationship is used to convert this time of loading t to frequency of loading f

$$f = \frac{1}{t} \quad (32)$$

The frequency is expressed in cycles per second or Hz and not, as it is sometimes incorrectly written, with the time (t) multiplied by 2π .

2.2.4.2 Effective Length and Depth Calculation

The effective length is the length that defines the extent of the stress pulse at a specified depth within the pavement system. Figure 18 shows a typical three-layer pavement structure (surface, base, and subgrade) loaded with a uniform contact pressure at the surface, which in turn produces stresses in the underlying layers. The sloped lines show the schematic distribution of the stress zone with depth. The angle of the slope varies with the quality (stiffness) of the material, resulting in wider stress distributions for stiffer mixes. Thus, the stress distribution is wider for the stiffer asphalt layer than for the softer unbound layers.

Line AA shows the length of the stress pulse within the asphalt layer at its mid-depth, while Line BB represents the effective length of the stress pulse at the midpoint of the granular base. To quantify Lines AA and BB, it is necessary to know the stiffnesses of the layers evaluated. In order to simplify the L_{eff} analysis, the concept of equivalent thickness, established by Odemark, was used.

Odemark's method is based on the assumption that the stresses and strains below a layer depend only on the stiffness (D) of that layer. If the thickness, modulus, and Poisson's ratio of a layer are changed, but the stiffness (D value) remains unchanged, the stresses and strains below the layer also remain (relatively) unchanged (12).

In elastic layer theory, the layer stiffness, D , is defined by:

$$D = \frac{h^3 E}{1 - \nu^2} \quad (33)$$

where

- h = the layer thickness
- E = the modulus
- ν = Poisson's ratio of the layer

If a given structure is transformed as proposed in Figure 19a, then neither the stresses nor the strains (in the second layer) should be influenced, provided that the following relationship holds:

$$\frac{h_1^3 E_1}{1 - \nu_1^2} = \frac{h_e^3 E_2}{1 - \nu_2^2} \quad \text{or} \quad h_e = \sqrt[3]{\frac{E_1}{E_2} \times \frac{1 - \nu_2^2}{1 - \nu_1^2}} \quad (34a)$$

where h_e is the equivalent thickness.

To further simplify the calculations, if the layer's Poisson's ratio is assumed to be the same or very similar in magnitude, then Equation 34a can be reduced to:

$$h_e = \sqrt[3]{\frac{E_1}{E_2}} \quad (34b)$$

When the concept is expanded to a three-layer pavement system, the transformation presented in Figure 19b would be obtained. Here, the asphalt and granular base layers are transformed into layers that have an equivalent subgrade modulus and an equivalent thickness $h_e = h_{1e} + h_{2e}$.

The final step in Odemark's transformation is to estimate the stress distribution of the transformed section. Since the transformed pavement system has a modulus equal to that of the subgrade layer (i.e., Boussinesq condition) and has an equivalent thickness h_e , then for simplicity it is assumed that the typical stress distribution of the subgrade layer is at 45° degrees, as shown in Figure 19b. With the stress distribution defined, the effective length can be computed at any depth within the transformed pavement structure (12).

2.2.4.3 Effective Depth Computation using Transformed Section

In order to estimate the loading frequency necessary for calculation of the asphalt layer modulus, the calculation of the L_{eff} of the pavement layer is required. Since a transformed pavement cross section is used, it is necessary to calculate the transformed depth referred to as the effective depth (Z_{eff}). Equation 35 is used to calculate the effective depth:

$$Z_{\text{eff}} = \sum_{i=1}^{n-1} \left(h_i \sqrt[3]{\frac{E_i}{E_{SG}}} \right) + h_n \sqrt[3]{\frac{E_n}{E_{SG}}} \quad (35)$$

where h_n is the thickness of the layer of interest (layer n) at which the computation is being made.

If the mid-point of the layer of interest is desired, then Equation 36 can be rewritten as follows:

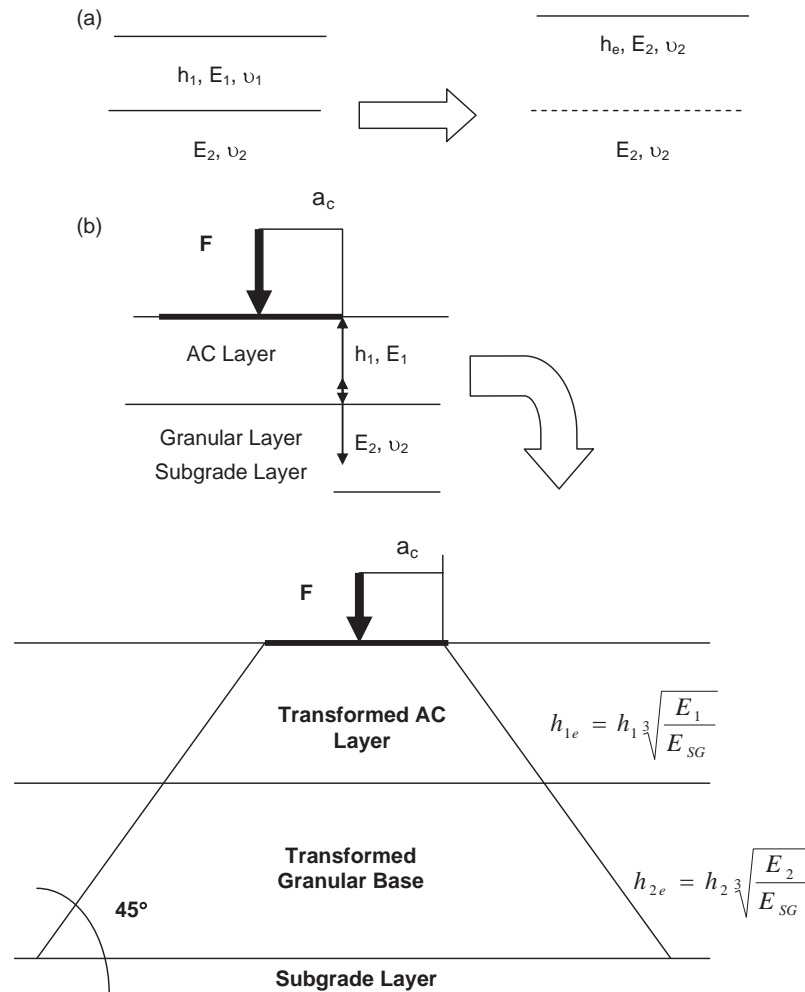


Figure 19. Odemark's transformation of a layered system: (a) two-layer system and (b) three-layer system.

$$Z_{eff} = \sum_{i=1}^{n-1} \left(h_i \sqrt[3]{\frac{E_i}{E_{SG}}} \right) + \frac{h_n}{2} \sqrt[3]{\frac{E_n}{E_{SG}}} \quad (36)$$

2.2.4.4 Computation of Effective Length

In order to be able to calculate the effective length of the stress pulse within the pavement structure, it is necessary to determine the axle configuration of the load being applied. Reference 12 provides the details for calculating the effective length of single, tandem, tridem, and quad axles. However, because the methodology presented in this report uses the 18-kip ESALs approach to characterize traffic, only the computation of effective lengths for single axles will be presented.

Figure 20 shows a typical three-layer pavement structure loaded by a wheel in a single axle system. The other wheels in the vehicle gear configuration are assumed to be so distant that they do not influence the calculations.

The first step to calculate the effective length is to transform the pavement structure into a structure that has the

modulus of the subgrade layer and an equivalent thickness, h_e . For this transformed structure, the stress zone is assumed to be distributed at a 45° angle, as observed in Figure 20.

The effective length of the stress pulse at any depth is defined by:

$$L_{eff} = 2 \times (a_c + Z_{eff}) \quad (37)$$

Knowing L_{eff} , Equation 31 can then be applied to obtain the time of loading, and Equation 32 to calculate the frequency of loading, required for the asphalt layer E^* modulus calculation.

2.2.4.5 Iteration Process for Calculation of Effective Modulus and Depth

As can be noted from Equations 31–37, one would need the depth, subgrade modulus, and modulus of the AC layer to calculate the frequency. However, the modulus, by itself, is a function of the frequency, temperature, and material properties. Also, the temperature is a function of the frequency.

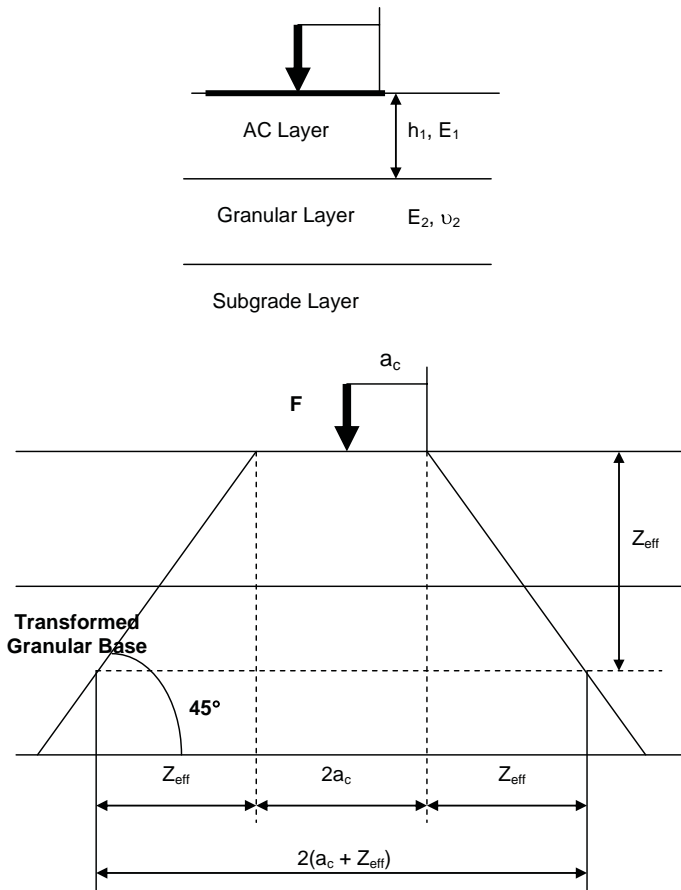


Figure 20. Transformed section.

Accordingly, an iteration process is required to calculate the frequency, temperature, and dynamic modulus. The subgrade modulus is a user input into the analysis program.

The following paragraphs show the data required, equations used, and steps followed in the iteration process to determine the effective E^* , temperature, frequency, and critical pavement depth, per layer, as used in the QRSS:

Data available:

- Traffic speed
- Effective temperature equation, T_{eff}
- WPE and volumetric mix properties
- Desired layer depth
- Unbound layer modulus
- Assumed tire pressure (120 psi), force per tire (9,000 lb), type of axle (single)

Equations used:

$$L_{EFFGUESS} = 2 * (Z_{EFFGUESS} + R_{TIRE}) \quad (38a)$$

$$R_{TIRE} = [Force / (Pressure * \pi)]^{1/2} \quad (38b)$$

where

$L_{EFFGUESS}$ = effective length based on estimated effective depth, inches

$Z_{EFFGUESS}$ = estimated effective depth, inches

R_{TIRE} = radius of tire

Force = force applied by tire, lb (assumed 9,000 lb)

Pressure = tire pressure, psi (assumed 120 psi)

$$L_{EFFCALC} = 2 * (Z_{EFFCALC} + R_{TIRE}) \quad (38c)$$

$$Z_{EFFCALC} = \sum_{(i=1 \text{ to } n-1)} \left\{ h_i * [E_i^* / M_R]^{1/3} \right\} \quad (38d)$$

where

$L_{EFFCALC}$ = effective length based on calculated effective depth, inches

$Z_{EFFCALC}$ = calculated effective depth, inches

n = number of layers including subgrade

h_i = i th layer depth, inches

E_i^* = dynamic modulus of i th layer at T_{eff} , frequency, and depth, psi

M_R = unbound layer modulus, psi

$$E_i^* = \text{calculated by WPE (based on } T_{eff} \text{ and frequency)} \quad (38e)$$

$$T_{eff} = \text{effective temperature} \quad (38f)$$

$$Freq = 17.6 * (Speed / L_{EFFGUESS}) \quad (38g)$$

where

Freq = frequency of load on asphalt layer, Hz

Speed = average traffic speed in project provided by user, mph

The iteration process is conducted by assuming a calculation depth, which in case of rutting would be the mid depth of the layer and for fatigue cracking, the bottom of the HMA layer. From this depth an initial L_{eff} is calculated and then used to calculate the effective frequency. Knowing the frequency, the effective temperature can be calculated. Then, the dynamic modulus is calculated using both the frequency and the temperature. Finally, another depth value is calculated. The new depth is compared to the initial depth; if the difference is less than or equal to 0.001 then the new value is accepted. If the difference is more than 0.001, then the new depth value is used as the initial value for a new iteration. The following is a summary of the iteration process.

Iteration Process:

- Input $Z_{EFFGUESS}$
- Calculate $L_{EFFGUESS}$

- Calculate frequency (Freq) with Equation 38e
- Calculate effective temperature (T_{eff}) based on frequency and desired depth
- Calculate E^* with T_{eff} , frequency, and mix volumetric properties for the HMA layer in consideration with WPE
- Calculate Z_{EFFCALC} (Equation 38d) with E^* , pavement depth, and M_R
- Calculate L_{EFFCALC} (Equation 38c)
- Calculate $A^2 = L_{\text{EFFCALC}} - L_{\text{EFFGUESS}}$
- Sum all values of A^2 for different layers and desired depths: ΣA^2
- Repeat all of the steps above until $\Sigma A^2 < 0.001$ (biased optimization)
- Repeat all of the steps above until $\Sigma A = 0$ (unbiased optimization, Optional Step)

In this way, E^* can be calculated at an effective temperature and frequency of loading at any desired pavement depth and at any environmental location and traffic speed. This E^* value will be correlated with MEPDG rutting predictions. The next sections will cover the methodology developed to obtain the most accurate rutting predictions for correlation with E^* .

2.3 Performance Model Development for Permanent Deformation

2.3.1 Introduction

AC rutting predictions were made with the MEPDG, which is capable of providing such predictions for a wide variety of pavement, environmental, and traffic conditions. Because the MEPDG is so comprehensive and takes into account many variables, a preliminary study was conducted to identify those variables that are significant to the AC rutting distress.

2.3.2 Selection of Variables Affecting Rutting

The MEPDG takes into account many structural design scenarios: full depth pavements (asphalt layer on top of subgrade soil), three-layer structures (asphalt layer, granular base, subgrade soil), pavements with treated bases, etc. In addition, it can consider new flexible pavement designs, as well as rehabilitation design scenarios (asphalt over asphalt, asphalt over PCC, etc.).

The series of sensitivity analyses conducted by El-Basyouny (13) determined that the subgrade soil characteristics had a minimal effect on the MEPDG rutting predictions. Therefore, for this study, it was assumed that the combination of unbound layers placed below the asphalt layer(s) was not important.

Because of this finding, it was decided to use a full-depth pavement problem, which consisted of one type of asphalt layer on top of a subgrade soil.

This two-layer problem made the preliminary analysis simpler, although it still required the input of a significant amount of variables shown by category in the following list:

General Data (4 variables)

- Design life
- Base/subgrade construction month
- Pavement construction
- Traffic opening date

Analysis Parameters (8 variables)

- Initial IRI
- Limit and reliability of terminal IRI
- AC surface-down cracking
- AC bottom-up cracking
- AC thermal cracking
- Chemically stabilized layer fatigue cracking
- Rutting—total pavement
- Rutting—AC only

Traffic Characterization (22 variables)

- Initial two-way Annual Average Daily Truck Traffic (AADTT)
- Number of lanes in design direction
- Percent of trucks in design direction
- Percent of trucks in design lane
- Operational speed (mph)
- Vehicle class distribution (Class 4 to Class 13)
- Monthly adjustment factors per vehicle class per month
- Traffic hourly distribution
- Traffic growth function
- Traffic growth factors
- Axle load distribution factors
- Axle types
- Mean wheel location
- Traffic wander standard deviation
- Design lane width
- Number of axles per truck
- Average axle width
- Dual tire spacing
- Axle spacing
- Tire pressure
- Average axle spacing
- Percent of trucks

Environmental Conditions (4 variables)

- Latitude
- Longitude
- Elevation
- Depth of groundwater table

Structure (25 variables)

- General characteristics
 - Interface
- Drainage surface
 - Surface short wave absorptivity
 - Drainage path length
 - Pavement cross slope
- Asphalt layers (Level 3)
 - Asphalt thickness
 - Aggregate gradation: retained $\frac{3}{4}$
 - Aggregate gradation: retained $\frac{3}{8}$
 - Aggregate gradation: retained No. 4
 - Aggregate gradation: passing No. 200
 - Asphalt binder (performance, viscosity, or penetration grade)
 - Effective binder content
 - Air voids
 - Total unit weight
 - Reference temperature
 - Poisson's ratio
 - Thermal conductivity asphalt
 - Heat capacity asphalt
- Unbound layers (Level 3—Representative value)
 - Layer thickness
 - Poisson's ratio
 - Coefficient of lateral pressure, K_0
 - Modulus
- Thermal cracking
 - Creep compliance
 - Average tensile strength at 14°F
 - Creep test duration
 - Aggregate coefficient of thermal contraction

Thus, the input of a total of 63 variables is required for a single full-depth problem. If it is desired to know which variables are most significant, then a design of experiment should be performed based on 2^k and 2^{k-p} factorial designs. However, even for such a powerful tool, $k = 63$ variables is excessive. Therefore, several assumptions were made to reduce the number of variables in the design of the experiment.

General Data (1)

From this category, only the design life was included in the initial study. The base/subgrade construction month was not included because it is safe to assume that since the subgrade (foundation) characteristics do not affect the rutting prediction, then the date when the section was built also should not be a variable. For the pavement construction and traffic opening date, the assumption was that both of these inputs should be quite close, and thus should not provide a significant effect

on rutting predictions. Thus, from four variables, this category was reduced to one.

Analysis Parameters (0)

In this category, none of the variables are expected to affect MEPDG rutting predictions. This category is only present so the engineer can later assess if the pavement design is appropriate or not. From eight potential variables, this category was completely eliminated.

Traffic Characterization (3)

The MEPDG has the capability to comprehensively characterize the matrix of loads applied on a pavement structure. However, for simplicity and necessity, this study was conducted using the 18-kip ESAL traffic characterization method.

The MEPDG can accept an 18-kip ESAL input by canceling some traffic variables and defining others accordingly. Thus, for example, the percent of trucks in the design direction can be changed to 100% since all of them are assumed to be 18-kip trucks. In the same way, the truck configuration is set to that of a Class 5 Vehicle (100%) and 0% for the rest of vehicle classes with a single axle. For simplicity again, no growth was assumed in the analysis. Thus, three of a possible 22 variables were required from this category:

- Initial two-way AADTT (that will be transformed into annual 18-kip ESALs)
- Operational speed (mph)
- Traffic wander standard deviation

The rest of the variables were set constant, in accordance with the 18-kip ESAL configuration, or because they did not matter for flexible pavement design.

Environmental Conditions (2)

The MEPDG provides access to data from approximately 900 weather stations in the United States. Each station is characterized by latitude, longitude and elevation. Thus, from four variables, this category was shrunk to two variables: weather station and groundwater table depth.

Structure (4)

The layer interface friction variable is assumed to be 1. For drainage, the surface short wave absorptivity was left as the MEPDG default variable (0.85) and the drainage path length and pavement cross slopes were left constant because they only influence the analysis of PCC pavements.

The asphalt layers sub-category was reduced by keeping constant the total unit weight, reference temperature, Poisson’s ratio, thermal conductivity of asphalt, and heat capacity of the asphalt mixture. It was assumed that a conventional ¾ in. nominal aggregate size mix was used. Thus, the aggregate gradation values were left constant, as well as the effective binder content and air voids value. The only input variables were the asphalt stiffness (the asphalt binder type) and the asphalt layer thickness.

Similarly, for the unbound layers, the Poisson’s ratio and the coefficient of lateral pressure were not varied, leaving the modulus and the layer thickness as the only input variables being changed. The MEPDG does not accept an asphalt layer on top of a subgrade layer directly. It requires an unbound layer in between the two main layers. The thickness of this layer is varied and the modulus of both unbound layers is assumed to be equal. Finally, since the thermal cracking variables do not affect the rutting prediction, they were not considered in the analysis.

In summary, after all of these assumptions; the variables considered in the evaluation study were the following:

- Asphalt layer thickness
- Asphalt binder type (which yields the asphalt layer stiffness)
- Unbound layer thickness
- Unbound layer modulus (which becomes the unbound layer stiffness)

Thus, just 10 of 61 variables were used in the analysis to determine which ones had statistically significant impacts on the MEPDG rutting prediction.

2.3.3 Sub-Layering Scheme

2.3.3.1 Sub-layering Scheme in the MEPDG

In the MEPDG, up to three different asphalt layers can be input by the user. Thus, for example, let an asphalt pavement system have a total thickness of 5 inches. In the initial versions of the MEPDG, the user was allowed to make his or her own subdivision for thick AC layers. For example, if a 5-in thick asphalt layer was being analyzed, the user had the option of creating several different sub-layering systems, as shown in Figure 21.

The sub-layering approach used in the latest version of the MEPDG is summarized as follows:

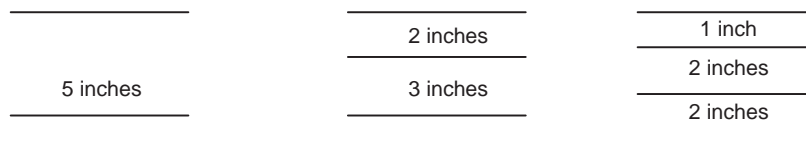


Figure 21. HMA layer sub-layering.

- HMA depths from 0 to 1 in are subdivided into two sub-layers: 0.5 and 0.5-in. (Note that no rutting is considered in the first 0.5-in. sub-layer).
- HMA depths from 1 to 4 in. are subdivided into three sub-layers: 1 in., 1 in., and 1 in.
- HMA depths from 4 to 12 in. are subdivided into two sub-layers: 4 in. and 4 in.
- HMA depths from 12 in. down are subdivided into one sub-layer representing the remaining thickness of the pavement.

This scheme is illustrated in Figure 22.

The first four inches of the pavement structure are given the most emphasis (1 in. – 1 in. – 1 in. – 1 in. subdivision) because this is the zone in which the majority of AC rutting will occur. Thus, for the example of the 5 in. structure, the MEPDG would perform the following subdivisions:

- Full (One Mix) 5 in. structure: 1 – 1 – 1 – 1 – 1
- Two Layer (Two Mixes) Structure (2 in.: 3 in.): 1 – 1 : 1 – 1 – 1
- Three Layer (Three Mixes) Structure (1 in.: 2 in.: 3 in.): 1 : 1 – 1 : 1 – 1 – 1

As can be seen, for these three AC layer structure configurations, the MEPDG subdivision is the same. However, when the runs are performed, there still may be very small deviations between the structures. A final consideration in the MEPDG sub-layering scheme is that it does not analyze layers thinner than 1 in. Thus, for example, a 3.5-in. structure would not be divided as 1-1-1-0.5 in. but as 1-1-1.5 in.

2.3.3.2 Sub-layering Scheme in this Research Study

The first option investigated in the development of the QRSS rutting methodology was to use the same sub-layering scheme as the MEPDG. This is the reason why this study was initially started with six AC layer thickness values (1 in., 2 in., 3 in., 4 in., 8 in., and 12 in.). Figure 23 shows how the Line of Maximum Rutting (LMR) would appear without a 6-inch structure for a pavement design in Phoenix, AZ, after 20 years with cumulative traffic of 10,000,000 ESALs. The LMR defines the rutting prediction values at a given environmental site, traffic level repetition, traffic speed, and asphalt material characteristics for a variety of different asphalt layer thickness values.

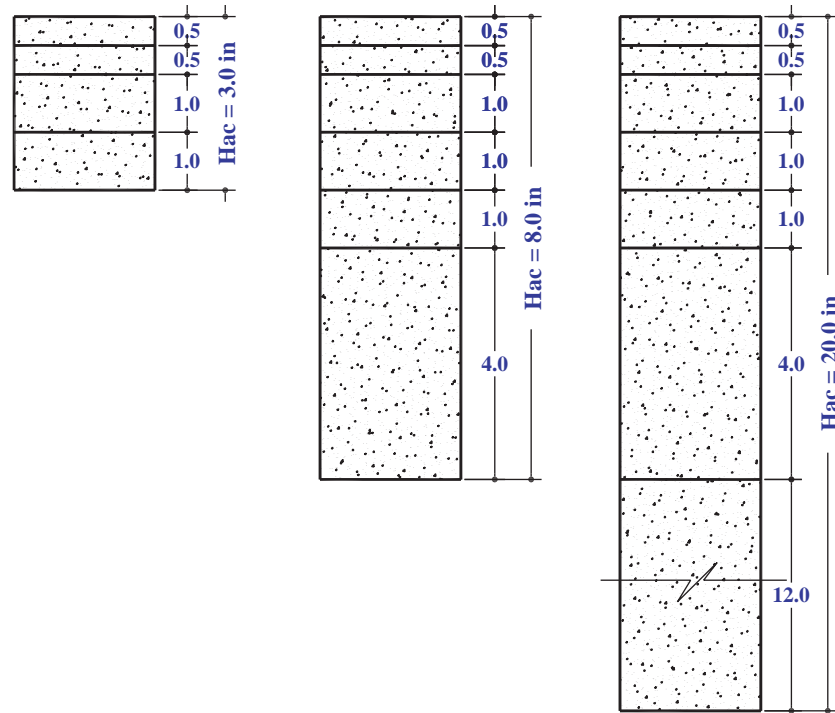


Figure 22. Examples of MEPDG AC sub-layering scheme for different asphalt layer systems.

Wide gaps are observed in Figure 23 between 4 and 8 in. and 8 and 12 in. The latter gap is considered acceptable, since at those thicknesses, the change in rutting is relatively small. However, between 4 and 8 in. the change in rutting may be substantial, leading to potential interpolation errors. As a consequence, a 6 in. AC layer was incorporated into the study and plotted against the LMR. As can be observed, the LMR without 6 in. over predicts the rutting of structures between 4 and 8 in. as observed by the dashed lines in Figure 23. Therefore, it

was decided to include MEPDG runs for a 6 in. structure to the database. This addition yielded the following sub-layering scheme:

- HMA depths from 0 to 1 in. are subdivided into two sub-layers: 0.5 and 0.5 in. (Note that no rutting is considered in the first 0.5 in. sub-layer).
- HMA depths from 1 in. to 4 in. are subdivided into three sub-layers: 1 in., 1 in., and 1 in.

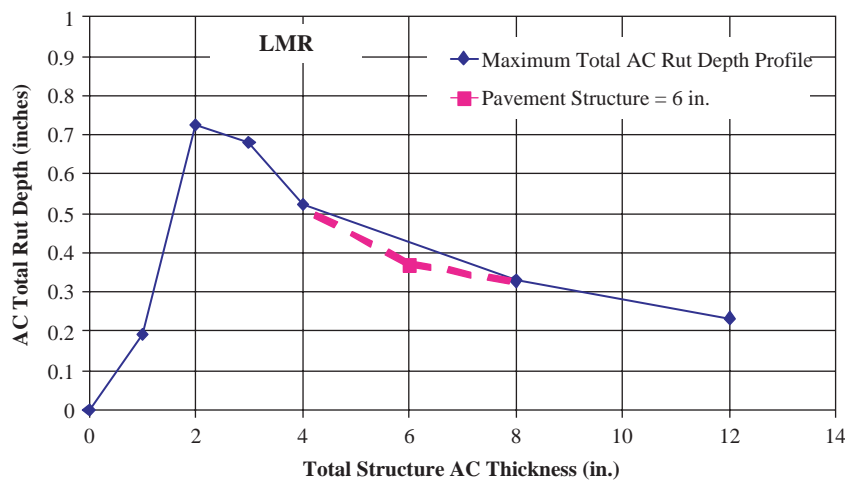


Figure 23. Effect of adding a 6-In. pavement structure in interpolation database (example: Phoenix, AZ—temperature factor: 98.6°F)

- HMA depths from 4 to 8 in. are subdivided into two sub-layers: 2 in. and 2 in.
- HMA depths from 8 to 12 in. are subdivided into one sub-layer: 4 in.
- HMA depths below 12 in. are subdivided into one sub-layer representing the remaining thickness of the pavement.

The database also was increased from the example in Figure 23 to include thicker structures. Thus, a 20 in. structure was also run, yielding the eight thickness values (1, 2, 3, 4, 6, 8, 12, and 20 inches) used to obtain the rutting database.

2.3.4 Development of MEPDG Database

Sotil (3) conducted the initial work to develop the closed form solution for rutting, which was finished in 2005, before the final version (1.0) of the MEPDG developed under NCHRP 1-40D was available. This initial study used the MEPDG Version 0.7 developed in NCHRP Project 1-37A. Version 1.0 corrected some errors in the original version. For example, the EICM was modified and the calibration effort was adjusted for the new models. Sotil's work was then re-analyzed using Version 1.0.

In order to develop a closed form solution for the prediction of rutting using the MEPDG software, the following steps were taken:

- Simulation runs of the MEPDG were conducted at different conditions to study the effect of each condition on the rutting predictions. Initially a fractional factorial was conducted to check on the significant factors that impact the HMA rutting prediction. Then a series of in-depth simulation runs were done using the selected factors to build a rutting prediction database.
- For a given structure, the database was interpolated to obtain the predicted rutting for that structure at a predefined dynamic modulus, climatic location, and traffic condition.
- For the same given structure, the dynamic modulus of the AC layer was obtained for each of the predefined climatic locations and traffic, with E^* calculated based on the effective temperature concept.
- A relationship between rutting and dynamic modulus was obtained, which can be used to predict the rutting for a given structure, climate, material property, speed, and traffic level.

2.3.4.1 Rutting Database Formation

The first step in developing the rutting CFS was calculation of the rutting prediction database. The database was prepared in two steps: (1) an initial simulation to detect the significant factors and (2) a full simulation using the selected significant variables.

Initial Factorial Simulation Runs. As already noted, of the total of 63 variables included in the MEPDG for flexible pavement design, only 10 were eventually selected to determine their statistical significance. These variables and their levels were as follows:

- Environmental condition (hot: Phoenix, AZ, and cold: Grand Forks, ND)
- Pavement service life (5 years and 15 years)
- Number of traffic repetitions (10^5 and 10^6 18-kip ESALs during service life)
- Average traffic speed (0.5 mph and 60 mph)
- Traffic wander (4 in. and 10 in.)
- Asphalt thickness (2 in. and 10 in.)
- Asphalt layer stiffness (conventional dense graded mix with PG 52-40 and PG 82-10 binder types)
- Unbound layer thickness (4 in. and 12 in.)
- Unbound layer stiffness (5 ksi and 30 ksi)
- Groundwater table (5 ft and 15 ft)

A fractional factorial of runs using these 10 variables at two levels was used, with a total of 32 runs. From the 2^{10-5} fractional factorial design, it was concluded that the main factors affecting rutting, as shown in Figure 24, were the following:

- Environmental conditions
- Number of traffic repetitions
- Average traffic speed
- Asphalt layer stiffness
- Asphalt layer thickness

It is important to note that rutting within the AC layer is not a function of any of the other pavement layers in the structure, but rather of mix quality, AC layer thickness, traffic, and the environment at the design location.

Simulation Runs to Build Database. After the initial study was finished, a detailed simulation was conducted to build the rutting prediction database. These runs used only the significant variables. A matrix of runs was conducted to create the database. All runs had the same base, subbase, and subgrade layer thickness and properties and a design life of 20 years. The matrix of runs was then based on the following levels of the variables previously defined as significant.

- 8 different HMA layer thicknesses (1, 2, 3, 4, 6, 8, 12, and 20 in.)
- 12 climatic locations, as shown in Table 9
- 8 asphalt mixture properties
- 4 traffic speeds, 0.5, 15, 45, and 60 mph
- 4 traffic levels, 10^5 , 10^6 , 10^7 , and 10^8 ESALs

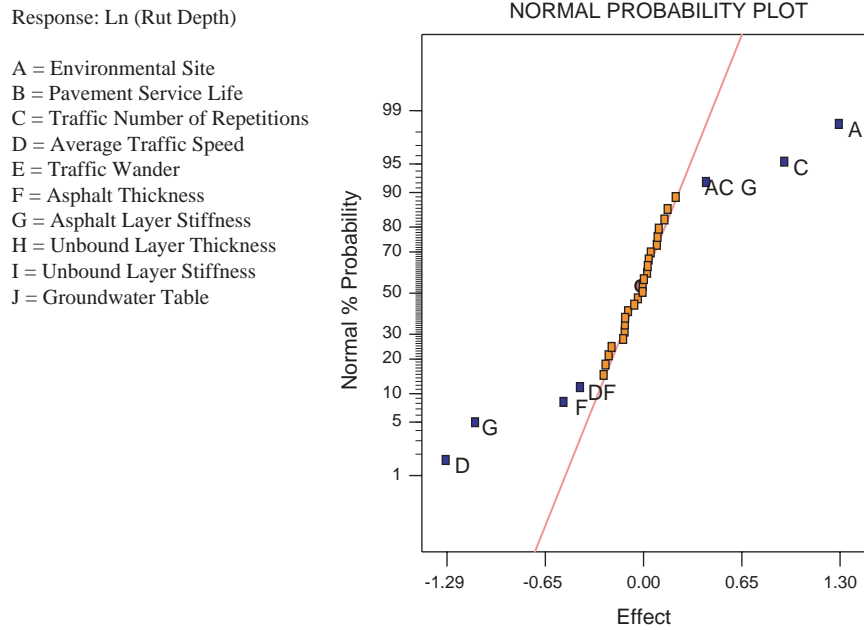


Figure 24. Significance of variables affecting rutting predictions results from 2^{10-5} fractional factorial design of experiments.

This matrix of runs yielded a total of $8 \times 12 \times 8 \times 4 \times 4 = 12,288$ MEPDG runs. Knowing that each run would take 20 minutes, the complete simulation would have taken about 6 months of computation. Consequently, a series of mini-studies were undertaken to reduce the number of runs. The following sections provide details on the results of these mini-studies for each of the five variables used in the simulation.

Climatic Locations. The environmental condition was the factor that most affected the MEPDG rutting prediction. It was therefore decided to cover a wide range of climatic conditions. Twelve environmental sites were randomly selected, with

regions as cold as Kotzebue, AK, with a MAAT of 21.9°F to regions as hot as Phoenix, AZ, and Key West, FL, with MAATs of 74.9 and 77.9°F, respectively. Table 9 summarizes the 12 environmental sites selected with their respective MAAT, Mean Annual Average Wind speed (Wind Speed), Mean Annual Sunshine Percentage (Sunshine), Cumulative Annual Precipitation (Rainfall), and Mean Monthly Air Temperature Standard Deviation (σ_{MMAT}).

The climatic variables are mandatory to calculate the effective temperature (T_{eff}) for each site. The effective temperature negates the necessity to conduct cumulative incremental damage calculations through a change in annual environmental

Table 9. Summary of 12 selected environmental sites.

Location	MAAT (°F)	Wind Speed (mph)	Sunshine (%)	Rainfall (inches)	σ_{MMAT} (°F)
Kotzebue, Alaska	21.9	9.6	40.6	8.9	23.04
Homer, Alaska	38.5	5.5	30.0	23.9	13.28
Grand Forks, ND	41.7	8.9	53.4	19.7	23.94
Great Falls, Montana	45.9	9.8	58.4	11.1	20.25
Chicago, Illinois	51.4	8.1	36.6	30.8	18.34
Hartford, Connecticut	51.5	6.8	52.6	42.0	19.91
Indianapolis, Indiana	54.1	8.3	38.8	38.3	19.22
Oklahoma City, OK	61.1	9.7	49.9	33.5	18.96
Jackson, Mississippi	64.9	4.6	68.8	50.1	16.43
Houston, Texas	69.0	5.5	39.4	51.8	14.76
Phoenix, Arizona	74.9	5.0	62.3	6.7	17.48
Key West, Florida	77.9	8.0	72.7	40.3	6.82

conditions. Thus, T_{eff} saves a significant amount of computational time. The effective temperature equation for rutting is shown in Equation 15.

HMA Mixture Properties. Eight different mixtures were initially planned for use in the simulation runs. The different types of mixtures evaluated were based on a conventional dense graded mix of 7% air voids (AV), 10% binder content (V_{beff}), and 3/4 in. nominal maximum aggregate size (NMAS). The stiffness values were calculated from the WPE given in Equation 27. The following eight PG binders were used in this analysis:

PG52-34	PG52-40	PG58-22
PG58-34	PG64-22	PG70-10
PG76-16	PG82-10	

The WPE requires the frequency of the applied load. The frequency is calculated using Equation 20 as a function of the vehicle speed and the effective length (L_{EFF}) at the mid depth of an AC layer (12, 13). (Some researchers have suggested the MEPDG methodology for computing frequency is erroneous because it doesn't take into account the delayed viscoelastic response of the moving wheel load. However, the MEPDG methodology is based upon linear elasticity and the current methods of computing the loading frequency are completely

consistent with the linear elastic pavement response utilized in the MEPDG.)

Using the effective temperature and frequency values corresponding to the project, E^* values were calculated and then related to the predicted MEPDG rutting. A highly correlated power function was found to accurately define the relationship between E^* and the rutting predicted by the MEPDG over a wide range of conditions. Figure 25 shows an example of the E^* -rut depth relationship. The equation is as follows:

$$R_D = a(E^*)^b \tag{39}$$

where

- R_D = rut depth (inches)
- E^* = effective dynamic modulus

It is clear from Figure 25 that the power model form appears to apply to all mixtures. Because of this, it was concluded that two rather than eight mixtures could be used. Accordingly, only a stiff binder (PG 82-10) and a soft binder (PG 52-40) were used to calculate the power model relating rut depth and E^* .

Traffic Speed. Since traffic speed (time of loading) is another important factor affecting rutting, it was necessary to develop an approach that was applicable to a wide range of

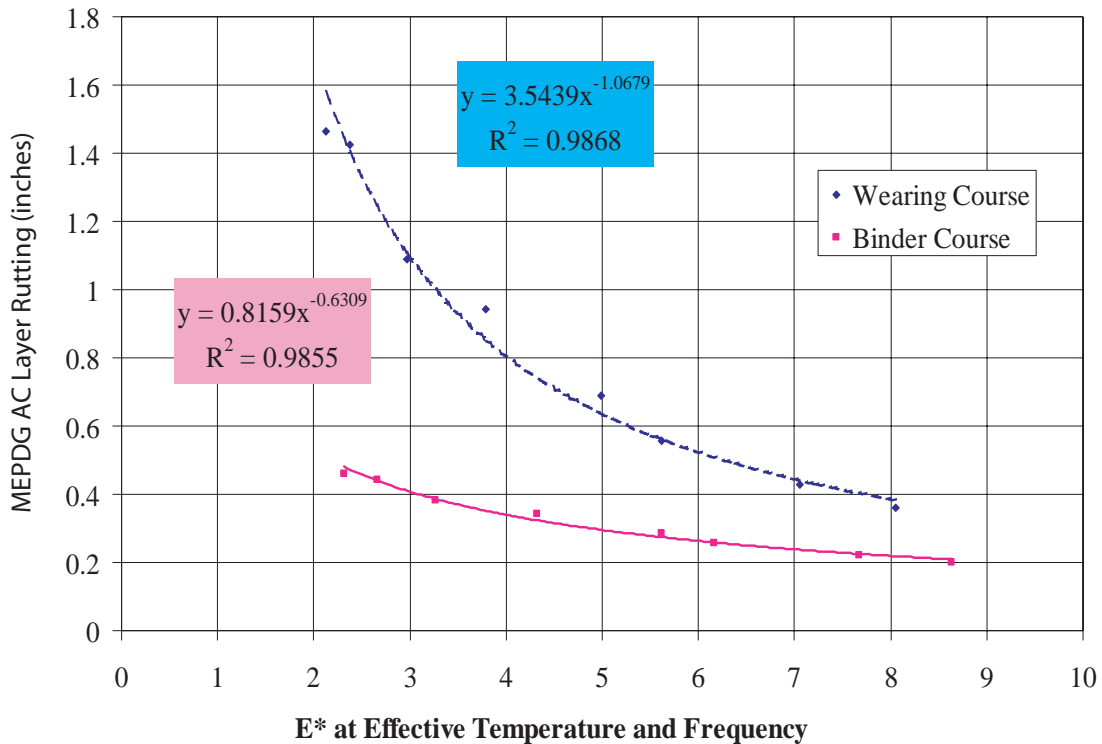


Figure 25. Typical relationships of E^* and rutting relationships at effective temperature, frequency and selected layer depth.

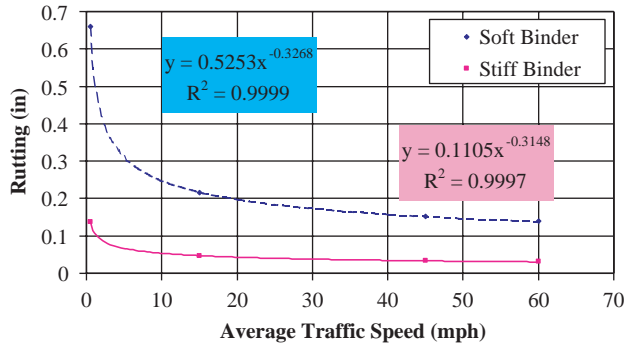


Figure 26. Typical rutting versus traffic speed power relationship.

traffic speeds. Another mini-study developed a relationship between traffic speed and rutting. Four traffic speeds were used in order to cover a wide range of functional roads:

- 0.5 mph: intersections, parking lots, traffic jams
- 15 mph: local roads, school zones
- 45 mph: collector and arterial city roads
- 60 mph: city freeways and interstate highways

As expected, a strong power relationship was found between rutting and speed. A typical example is shown in Figure 26.

Rutting is significantly increased at creep speed conditions (0.5 mph). This relationship is conceptually identical to that found in the AASHTO Road Test (19).

The correlation of these power functions is quite high at any combination of environmental site, binder type, and layer within a specific structure condition.

Table 10 shows an example of the data for Locations 1 and 2 for a 20" AC structure. It was concluded that the rutting at any given speed could be calculated using the following equation:

$$RUT_{X-SP} = M * Speed^N \tag{40}$$

where

Speed = average traffic speed, mph

RUT_{X-SP} = rutting prediction at X number of traffic repetitions and Speed average traffic speed

M, N = regression coefficients dependent on the environmental site, binder type, and AC layer thickness within given pavement structure.

This finding on the traffic speed did not reduce the number of simulation runs, but it did reduce the potential size of the database. It also provided a general model to calculate rutting at different speeds other than the ones used in the simulations.

Table 10. Summary of data used for the calculation of Equation 40.

Total AC Thickness = 20 inches									
Location ID***	PG Binder Type	Traffic Speed	Layer Thick 1 inch	Layer Thick 1 inch	Layer Thick 1 inch	Layer Thick 1 inch	Layer Thick 2 inches	Layer Thick 2 inches	Layer Thick 12 inches
1	52-40	0.5	0.0197	0.0603	0.0385	0.0164	0.007	0.0008	0
1	52-40	15	0.0074	0.0241	0.0156	0.0067	0.0029	0.0003	0
1	52-40	45	0.0056	0.0185	0.012	0.0052	0.0022	0.0002	0
1	52-40	60	0.0052	0.0173	0.0113	0.0048	0.0021	0.0002	0
		M	-0.2793	-0.2620	-0.2578	-0.2564	-0.2543	-0.2971	0
		N	0.0161	0.0500	0.0320	0.0137	0.0058	0.0007	0
		R ²	0.9994	0.9994	0.9993	0.9995	0.9994	0.9965	N/A
1	82-10	0.5	0.0045	0.0133	0.0084	0.0036	0.0015	0.0002	0
1	82-10	15	0.0023	0.0073	0.0047	0.002	0.0008	0.0001	0
1	82-10	45	0.0019	0.0062	0.004	0.0017	0.0007	0.0001	0
1	82-10	60	0.0018	0.006	0.0039	0.0016	0.0007	0.0001	0
		M	-0.1918	-0.1682	-0.1627	-0.1685	-0.1648	-0.1518	0
		N	0.0039	0.0118	0.0075	0.0032	0.0013	0.0002	0
		R ²	0.9994	0.9982	0.9979	0.9994	0.9879	0.9261	N/A
2	52-40	0.5	0.0205	0.0754	0.0534	0.0244	0.0114	0.0014	0
2	52-40	15	0.0079	0.0304	0.0217	0.0099	0.0046	0.0006	0
2	52-40	45	0.0061	0.0235	0.0168	0.0076	0.0036	0.0004	0
2	52-40	60	0.0057	0.022	0.0157	0.0072	0.0033	0.0004	0
		M	-0.2689	-0.2586	-0.2567	-0.2573	-0.2582	-0.2679	0
		N	0.0169	0.0626	0.0444	0.0203	0.0095	0.0012	0
		R ²	0.9988	0.9993	0.9993	0.9992	0.9992	0.9936	N/A
2	82-10	0.5	0.0068	0.0226	0.015	0.0066	0.003	0.0004	0
2	82-10	15	0.0034	0.0119	0.0079	0.0035	0.0016	0.0002	0
2	82-10	45	0.0028	0.01	0.0067	0.0029	0.0013	0.0002	0
2	82-10	60	0.0027	0.0096	0.0064	0.0028	0.0013	0.0002	0
		M	-0.1953	-0.1803	-0.1790	-0.1810	-0.1798	-0.1518	0
		N	0.0059	0.0198	0.0132	0.0058	0.0026	0.0003	0
		R ²	0.9984	0.9985	0.9981	0.9991	0.9967	0.9261	N/A

Traffic Levels. The traffic mix for the rutting prediction had to be converted in ESALs to simplify the analysis. However, a new calibration factor, other than the national calibration factor obtained using general traffic, was obtained to correct for this conversion. The traffic repetition effect was studied in more detail and it was found that rutting can be mathematically related to traffic repetitions by the following equation:

$$RUT_X = RUT_{ST} * 10^{0.479244 * (\log X - \log ST)} \tag{41}$$

where

RUT_X = rutting prediction at X number of traffic repetitions (inches)

RUT_{ST} = rutting prediction at standard ST number of traffic repetitions (inches)

This somewhat surprising conclusion implied that that was no need to run the simulation at different traffic volumes as one traffic volume will be enough to represent any other. Consequently, one traffic level of $N = 10^7$ was used in the study to represent all traffic levels.

Conclusion of Simulation Runs. From the previous discussion, it was concluded that 12 climatic locations, nine structures, four speeds, one traffic level, and two AC mixtures were enough to form the rutting prediction database. This

combination yields a total of $12 * 9 * 4 * 1 * 2 = 864$ runs, which was carried out. The database is presented in Appendix A. Note that the number of data points is 3,562, because the database contains the sublayer rut depths of each structure.

Rutting Model Update for the MEPDG 1.0 Version.

Since version 1.0 of the MEPDG used an upgraded climatic database, it was crucial to ensure that the distress prediction models currently implemented in the spreadsheet solutions as well as the in the ultimate QRSS were valid.

A comparison study between MEPDG Versions 0.7 and 1.0 was performed. This found that there was a quite noticeable discrepancy between the two versions as shown in Figure 27, which called into question the validity of the rutting database. To resolve this question, the 864 MEPDG simulation runs were rerun with the same matrix conditions to develop a rutting prediction database derived from MEPDG Version 1.0.

Rutting Interpolation. The second step of the rutting CFS development was to estimate the rutting for any given structure using the predefined 12 climatic locations, two AC mixtures, speed, and traffic level. This interpolation is done for each sublayer in the pavement structure. (If the thickness of the AC layer was similar to that in the database no interpolation was required.)

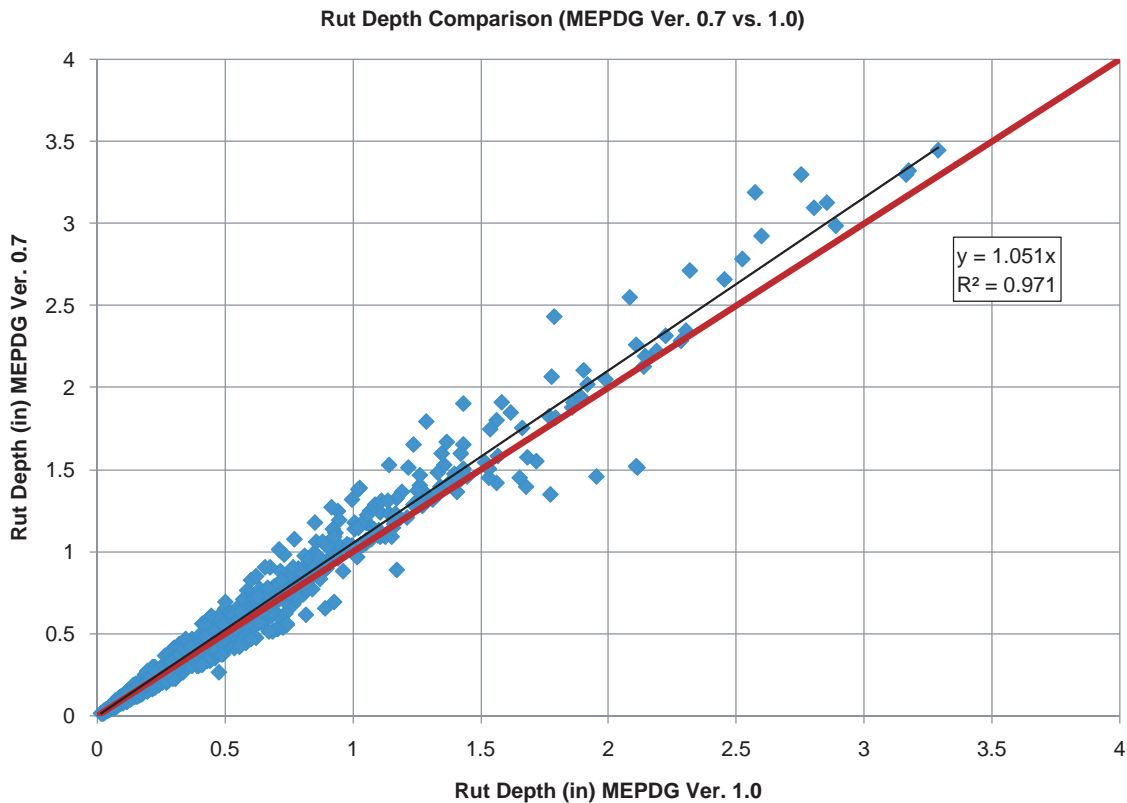


Figure 27. Rut depth comparison between MEPDG Ver. 0.7 and 1.0.

The database is first reduced to two structures: one thinner than the given structure and one thicker. For example, if the required structure is 4.5 in., then 4 in. and 6 in. structures are used.

Then, the rutting is calculated for the given traffic speed using Equation 40. Similarly, using Equation 41, the rutting is obtained from the database for the given traffic level.

The next step is to interpolate between the different structures to obtain the rutting prediction for the given structure. Linear interpolation is used for this process. Table 11 shows a sample of the calculation sheet for the rutting interpolation. The last point (corresponding to the total AC rutting for the 4.5 in.) is interpolated between the total AC rutting values of the 4 in. and 6 in. structures.

Hence, the nine variables and levels of the database are reduced to one structure at one speed and traffic level, which reduces the database from 864 to 24 points (12 climatic locations and two AC mixtures) for each sublayer of the pavement structure.

Dynamic Modulus, Effective Temperature, and Frequency Calculation. The first two steps of the process focus on the rutting estimation. The third step of the rutting CFS development requires the computation of E^* at the effective temperature (T_{eff}) and frequency (Freq) associated with the rutting predictions. The database was obtained using two AC mixtures (soft and stiff binder) for the 12 environmental sites given in Table 9. The database was also formulated using the traffic speed for the specific project to calculate the loading frequency at the mid-depth of each sublayer.

In order to compute the effective loading frequency, the WPE and frequency are used in an iteration process to calculate the E^* values. The output of this iteration process will yield an E^* , T_{eff} and Freq value for each sublayer, binder type, and climatic location. Similar to the reduced rutting database, the total number of E^* values will be $12 \times 2 = 24$ for each sublayer. The same iteration process is used to obtain the E^* , T_{eff} , and Freq of the specific structure using the actual material properties.

E^* and AC Rut Relationship. The last step required is to determine the final relationship between the E^* and AC rutting. This process is done in two steps. First, the database is reduced to the actual climate of the specific project, then the rutting is found for the actual mixture for each sublayer.

The database reduction, from the 24-database to a 2-database for each sublayer, is performed by creating relationships for each binder type and sublayer between the 12 effective temperatures and the 12 corresponding rutting predictions. The resulting relationships follow a power function trend, as shown in Figure 28. If the project effective temperature is known, then the corresponding rutting prediction at the given binder type and sublayer is easily found, as also shown in Figure 28. As explained in the previous step, the T_{eff} for the given structure is obtained using the iteration process.

Finally, the rutting database is reduced to two rutting values and two E^* values for each of the two binders for each sublayer. Using these two points, a power relationship is then obtained between E^* and the AC rut depth for each sublayer as shown in Figure 29. It should be recalled from previous

Table 11. Calculation sheet for database interpolation with respect to total AC thickness.

Traffic Repetitions (ESALs)	Climatic Site	PG Binder	Traffic Speed (mph)	Database Pavement Thickness (inch)	0 to "n" AC Layer Cumulative Rutting, inch						
					1	2	2.75	3	4	6	
1,000,000	Chicago, IL	52-40	35	1	0.0568						
				2	0.0043	0.2233					
				2.75	0.0018	0.1698	0.2972				
				3	0.0010	0.0913	0.2036	0.2411			
				4	0.0034	0.0636	0.1236	0.1436	0.2065		
				6	0.0105	0.0664	0.1037	0.1162	0.1411	0.1646	
				8	0.0147	0.0710	0.1031	0.1138	0.1341	0.1460	
				12	0.0127	0.0733	0.0745	0.0816	0.0946	0.1007	
				20	0.0102	0.0768	0.0659	0.0723	0.0838	0.0891	
				User-Specified Total AC Thickness				4.5	Final Interpolation Results		
				Cumulative	0.0052	0.0643	0.1186	0.1368	0.1905	0.1960	
				Individual	0.0052	0.0591	0.0544	0.0181	0.0541	0.0051	
AC Sub-Layer Range					0-1	1-2	2-2.75	2.75-3	3-4	4-4.5	

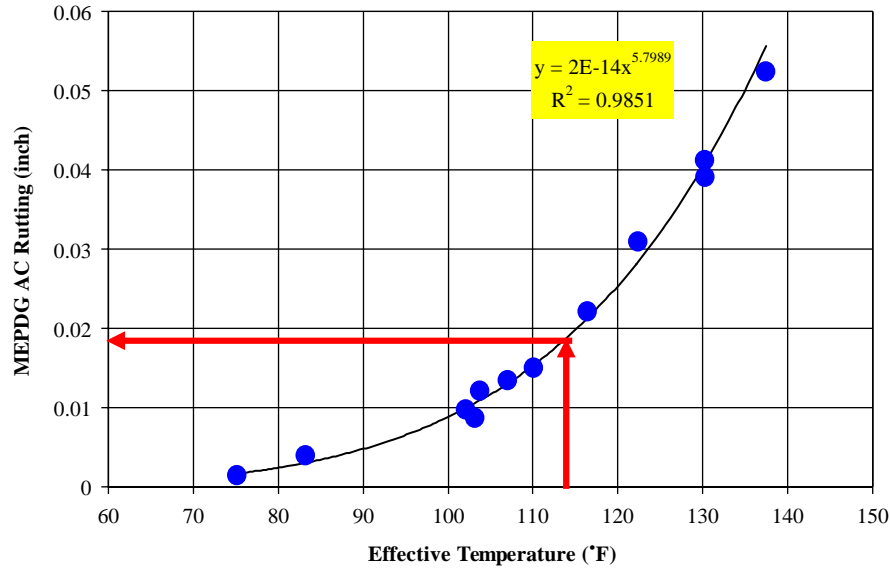


Figure 28. Typical rut depth versus effective temperature relationship (2 plots like these = 2 binder types for each sub-layer).

discussions that these two points are accurate enough to create the E*-AC rut relationship shown in Figure 25.

From the E*-AC rut power model, and using the actual E* for each sublayer, the sublayer rut depths can be summed to obtain an estimate of the total AC rut depth in a given pavement structure.

Overall Prediction Accuracy. To validate this rutting prediction process, an independent set of 3,457 MEPDG Ver-

sion 1.0 AC rutting data points were calculated and compared to the rutting database predictions. These 3,457 runs were composed of different structures, climatic locations, AC mixtures, traffic levels, traffic speeds, and design lives.

Figure 30 compares the MEPDG-predicted rut depth with that predicted by the CFS. Figure 30 shows an excellent correlation (regression coefficient $R^2 = 0.996$) between the rutting CFS predictions and the MEPDG predictions and the narrow scatter.

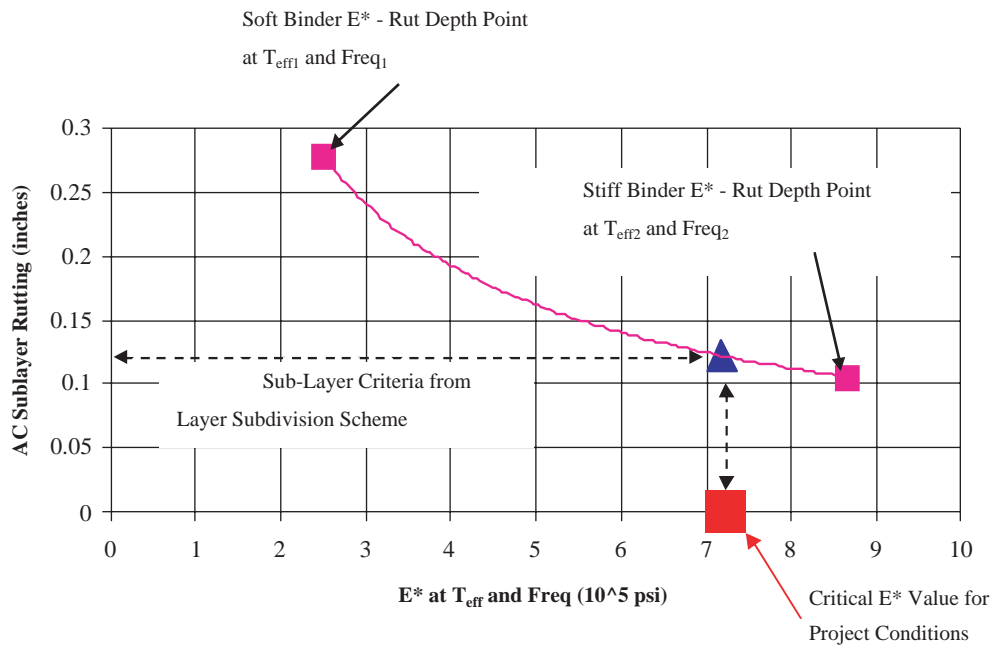


Figure 29. Typical AC sub-layer E* versus rut depth universal relationship at environmental, traffic and structural design conditions.

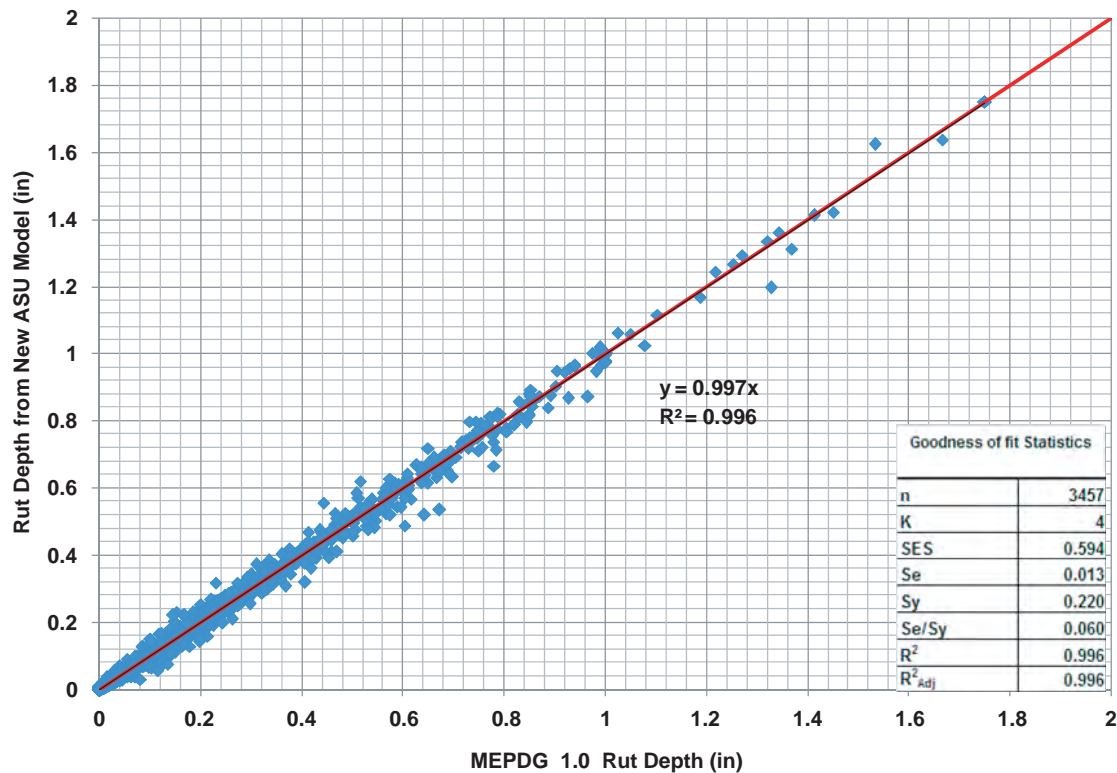


Figure 30. Comparison between rutting CFS and MEPDG 1.0 AC rut depth.

2.4 Performance Model Development for Fatigue Cracking

2.4.1 Introduction

MEPDG Version 1.0 was run through a large number of simulations using various combinations of inputs believed to be the most significant variables for classical bottom-up alligator fatigue cracking to develop an accurate closed form solution for the prediction of fatigue damage and fatigue cracking distress. Four major studies were completed for the development of the fatigue cracking prediction methodology:

- Development of a predictive methodology to estimate the composite foundation modulus from the actual layered pavement system below the AC layer;
- Development of relationships between major variables and fatigue damage;
- Development of a bottom-up fatigue damage and cracking model in a two-layer system; and
- Validation of the overall prediction process.

The methodology is then used in a probabilistic approach that utilizes the mean and standard deviation of the variables used in the fatigue cracking prediction. Thus, the mean and standard deviation of alligator fatigue cracking (FC) distribution is used as the basis for the stochastic QRSS analysis for HMA construction QA.

2.4.2 Fatigue Distress Variables

2.4.2.1 Pavement Structure

The pavement structure that was selected for the simulation runs consists of one AC layer (with variable thickness) over a foundation layer characterized by a composite modulus. This composite foundation represents different materials and pavement cross sections that may be encountered in practice.

2.4.2.2 Composite Foundation Modulus (E_{cf})

The proposed fatigue damage model was developed based upon a two-layer pavement system in which the foundation is assumed to be a combined layer representing all layers below the AC layer. Since pavement systems with three or more layers are generally the rule rather than the exception, the need for converting the multi-layer moduli below the AC layer into what is called a composite foundation modulus (E_{cf}) was necessary in order to apply the fatigue prediction model to the widest range of possible pavement layer systems.

The fundamental theoretical concept underlying the E_{cf} is that the maximum tensile strain must occur at the bottom of the AC layer in both the two- and multi-layer system. In addition, the methodology should provide a solution that yields a modulus in a two-layer system equal to E_{cf} . In order to find the value of E_{cf} that yields the same maximum strain that occurs in the multi-layer system, calculation of the tensile strains in

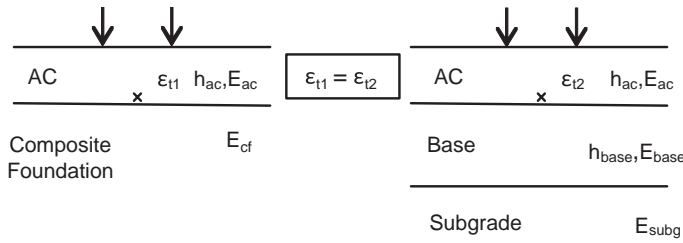


Figure 31. Equivalent tensile strain concept in two- and three-layer pavement systems.

the multi-layer system is critical. Figure 31 illustrates the concept of equivalent tensile strain analysis.

Development of a comprehensive database to be used in the transformation of a three-layer into a two-layer system required consideration of many combinations of layer conditions across the ranges of probable moduli and thicknesses for each layer. The selection of typical pavement layer moduli and thicknesses in the three-layer system was based upon common ranges normally encountered in practice. Table 12 summarizes

the factors, levels, and values used in this study. Based on this matrix, a total of 5,184 simulations were completed for a three-layer system with JULEA, a linear elastic analysis computer program developed by Dr. Jacob Uzan at the Technion University in Israel. JULEA was later enhanced by the U.S. Army Corps of Engineers to permit the determination of the complete state of stress, strain, and displacements at any computational point in a layered pavement system.

In order to capture the maximum tensile strain at the bottom of the AC layer, the tensile strain was determined at the 10 different locations that the MEPDG uses in the tensile strain calculations (12). The 18-kip standard axle load properties were used for the calculations. The E_{cf} values were then estimated by using the relationships between E_{cf} and tensile strain in the two-layer system. To find the relationship, a further 168 runs of JULEA were carried out for the two-layer system as summarized in Table 13.

These analyses found that the tensile strain and the E_{cf} have a three-order polynomial relationship in the logarithmic scale. Figure 32 shows the relationship for the example of a two-layer

Table 12. Summary of parameters used in the three-layer system analysis.

Parameter	Values	Levels
Tire load (dual tire)	4.5 kips each	1
Tire pressure	120 psi	1
AC layer		
Thickness (h_{ac})	1; 2; 4; 6; 8; 20 in.	6
Modulus (E_{ac})	50; 300; 1,000; 4,000 ksi	4
Poisson's ratio	0.35	1
Base layer		
Thickness (h_{base})	4; 8; 12; 20 in.	4
Modulus (E_{base})	15; 50; 100; 200; 350; 500; 600; 750; 1,000 ksi	9
Poisson's ratio	0.35	1
Subgrade layer		
Modulus (E_{subg})	3; 8; 15; 20; 50; 200 ksi	6
Poisson's ratio	0.35	1
Total matrix size		5,184

Table 13. Summary of parameters used in the two-layer system analysis.

Parameter	Values	Levels
Tire load (dual tire)	4.5 kips each	1
Tire pressure	120 psi	1
AC layer		
Thickness (h_{ac})	1; 2; 4; 6; 8; 20 in.	6
Modulus (E_{ac})	50; 300; 1,000; 4,000 ksi	4
Poisson's ratio	0.35	1
Subgrade layer		
Modulus (E_{subg})	3; 8; 25; 75; 250; 1,000; 4,000 ksi	7
Poisson's ratio	0.35	1
Total matrix size		168

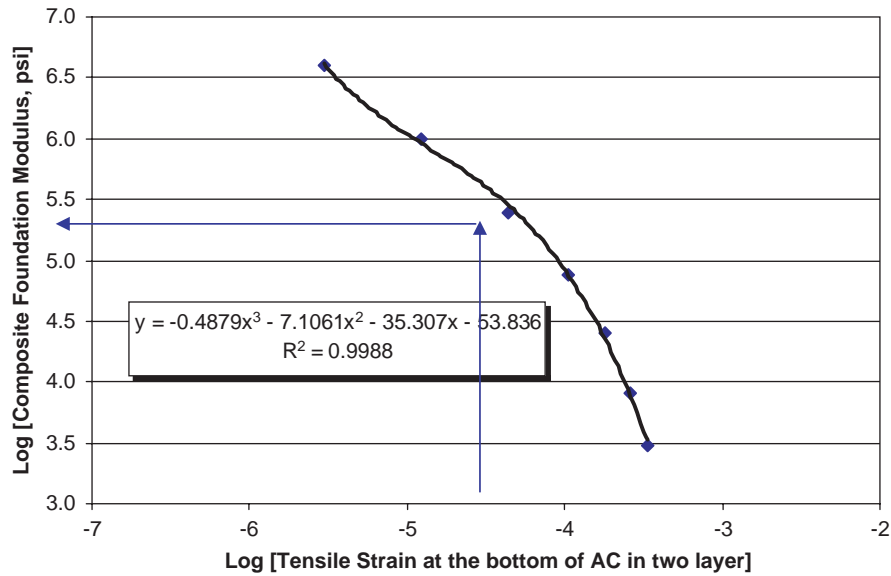


Figure 32. Relationship between tensile strain and E_{cf} ($h_{ac} = 8$ in. and $E_{ac} = 300$ ksi).

system where the AC layer has a thickness of 8 in. and a modulus of 300 ksi. Similar plots were developed to estimate E_{cf} for various AC layer conditions. All estimated E_{cf} values were tabulated according to the five parameters that were used in the analysis matrix: AC thickness, AC modulus, base thickness, base modulus, and subgrade modulus. This tabulation was then used to find the composite foundation modulus needed to convert a three-layer pavement system into a two-layer system. If the actual E_{cf} has a value somewhere between the values used in the analysis, the E_{cf} could be obtained through simple interpolation.

A similar method is required to convert a pavement system having an AC layer, base, subbase, and subgrade (i.e. 4-layer pavement system) to a 3-layer system having an AC layer, combined base layer, and subgrade. The fundamental basis of this conversion is similar to that used to find the composite foundation modulus. The concept is that the same maximum tensile strain at the bottom of the AC layer must occur in both the 3-layer and 4-layer systems. A graphical illustration of this concept is shown in Figure 33.

As discussed previously in Section 2.2.4.2, a common, widely known method to combine two layers into one layer

is through the use of Odemark’s transformation. This transformation is based on the theory of elasticity with the assumption that any stresses and strains occurring below a layer are dependent only upon the stiffness of that layer (21). This simple concept makes it possible to have either an equivalent thickness or an equivalent modulus as a combined characteristic of the separate base-subbase layers. A general equation of Odemark’s transformation is given by Equation 42 (21):

$$\frac{h_1^3 E_1}{1 - \nu_1^2} = \frac{h_c^3 E_2}{1 - \nu_2^2} \tag{42}$$

where

h_1 = thickness of upper layer

E_1 and E_2 = moduli of upper and lower layer

h_c = thickness of combined layer

ν_1 and ν_2 = Poisson’s ratio of upper and lower layer

Three different case studies of Odemark’s method were investigated in order to choose the most accurate procedure for transforming the base and subbase layers to one combined layer. Those cases are conceptually illustrated in Figure 34.

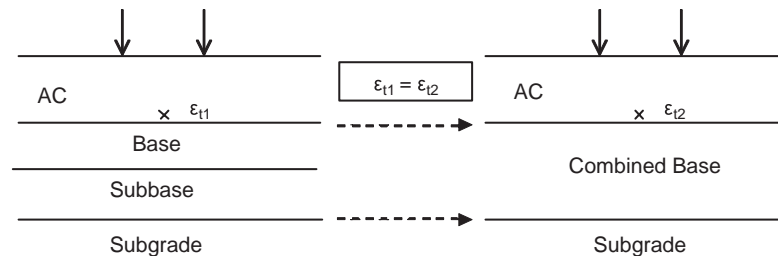
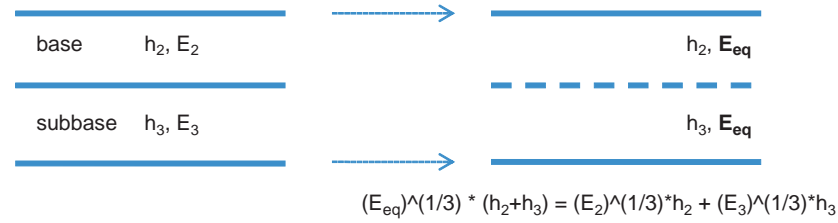
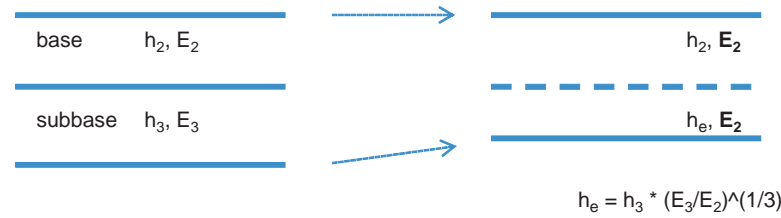


Figure 33. Four-layer and converted three-layer system.

Case 1: Use of E_{eq} (equivalent base modulus)



Case 2: Use of E_2 (base modulus)



Case 3: Use of E_3 (subbase modulus)

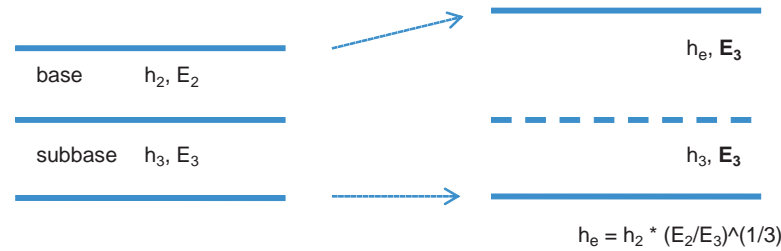


Figure 34. Application cases of Odemark’s method for transformation of base and subbase layers to a combined base layer.

In Case 1, the conversion uses the sum of the base and subbase thicknesses as a combined layer thickness and the moduli of each layer are changed into an equivalent modulus. In Case 2, the base modulus is used as a combined layer modulus and only the subbase thickness is changed. In Case 3, the subbase modulus is used as a combined modulus and only the base thickness is changed. The relevant equations for the three cases are as follows:

$$(h_2 + h_3) \sqrt[3]{E_{eq}} = (h_2) \sqrt[3]{E_2} + (h_3) \sqrt[3]{E_3} \quad : \text{ for Case 1} \quad (43a)$$

$$h_e = (h_3) \sqrt[3]{E_3/E_2} \quad : \text{ for Case 2} \quad (43b)$$

$$h_e = (h_2) \sqrt[3]{E_2/E_3} \quad : \text{ for Case 3} \quad (43c)$$

where

- h_2 and h_3 = base and subbase thickness
- h_e = equivalent thickness
- E_{eq} = equivalent modulus for a combined base
- E_2 and E_3 = base and subbase modulus

A study to find the best (i.e., most accurate) case of the three was performed by comparing the maximum tensile strain of a 4-layer system with that of transformed 3-layer system for each case. The tensile strain computations were carried out with the elastic layer program, JULEA. The JULEA simulation matrix is presented in Table 14.

This study found that the tensile strains between the 4-layer system and converted 3-layer system are very close to each other when using Case 2. Figure 35 clearly shows

Table 14. Matrix for the JULEA simulation.

Thickness (in.)	AC	4
	Base	6, 12
	Subbase	6, 12
Modulus (ksi)	AC	100
	Base	30, 100
	Subbase	15, 50
	Subgrade	3, 10, 20
Total number of simulations: $(1*2*2*1*2*2*3) * 3$ cases = 144 JULEA runs		

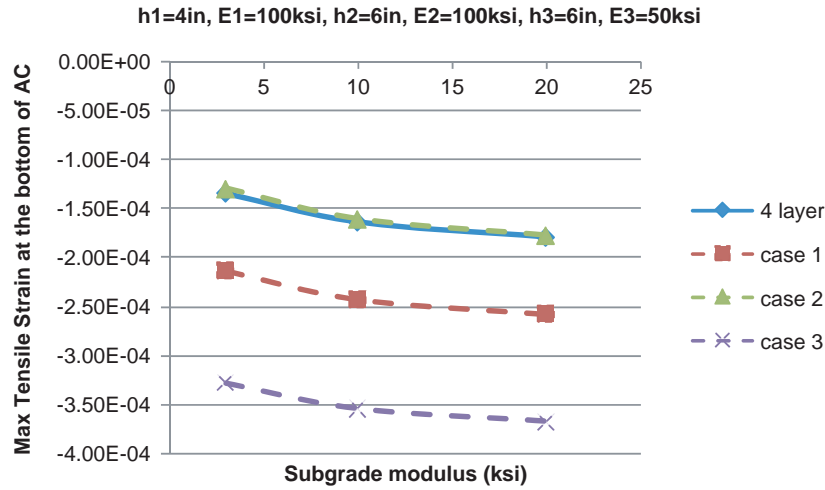


Figure 35. Example: tensile strains computed by using different cases.

that the tensile strains of a 4-layer system nearly overlap those of a converted 3-layer system. On the other hand, the strains computed from Cases 1 and 3 are grossly different from those of the 4-layer system as shown in the figure.

Figure 36 compares all tensile strains computed between the 4-layer system and the converted 3-layer system. The tensile strains of the converted 3-layer system using Case 2 show an excellent estimation of the 4-layer system. Thus, the conversion method using Case 2 for transformation of a 4-layer system into a 3-layer system was chosen and incorporated in the fatigue cracking spreadsheet solution.

2.4.2.3 Design Parameters

Seven factors believed to significantly affect the fatigue-related distress were considered for the MEPDG computer simulations.

Table 15 shows the full factorial of the conducted simulations. The database is given in Appendix B. It also summarizes the levels used for each factor. The following subsections explain the levels chosen for each variable.

Environmental Sites. Three different climatic locations were selected for the MEPDG simulation runs. These loca-

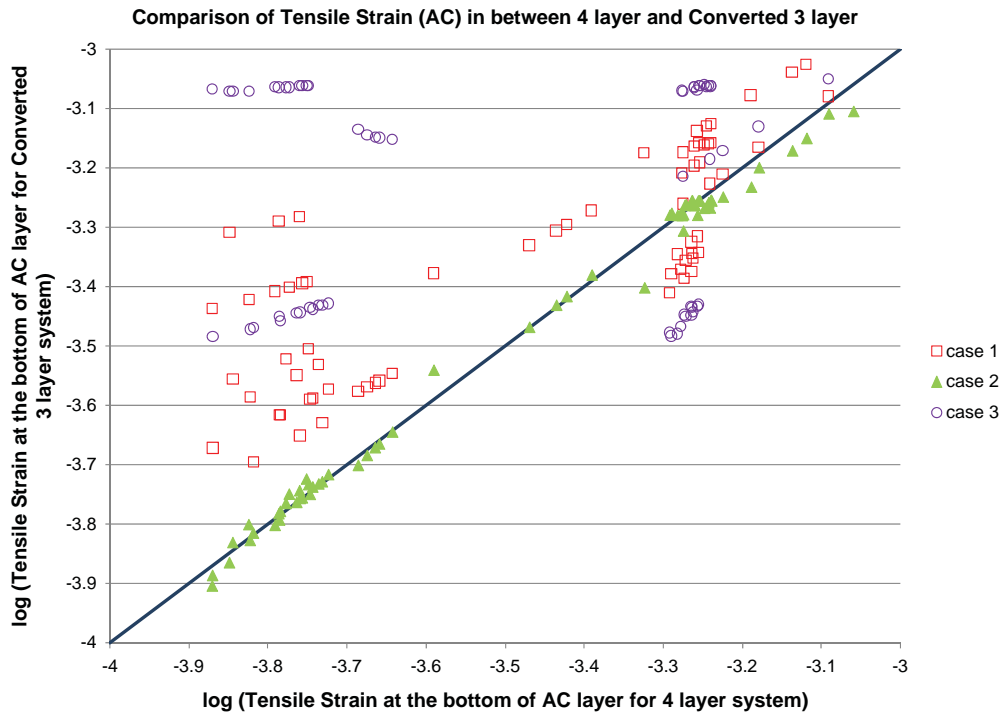


Figure 36. Comparison of tensile strain at the bottom of AC layer in between 4-layer and converted 3-layer system.

Table 15. Matrix of fatigue distress MEPDG simulation runs.

Factor	Value	Number of values
1. Environmental Sites	Grand Forks, North Dakota Oklahoma City, Oklahoma Key West, Florida	3
2. Design Life, years	20	1
3. Design Traffic, ESALs	2×10^6	1
4. AC Thickness, in.	1, 2, 3, 4, 6, 8, and 20	7
5. Vehicle Speed, mph	0.5, 15, 45, and 60	4
6. E*/AC :	Aggregate gradation (¾" Nominal Aggregate Size (Retained ¾" = 0%, Retained 3/8" = 26.8%, Retained No.4 = 46.41%, Passing No.200 = 8.28%))	1
	PG grades (PG 82-10, PG 64-22, and PG 52-40)	3
	V _a (air voids) and V _b (binder content): (V _a = 4, V _b = 16), (V _a = 8, V _b = 12), and (V _a = 12, V _b = 8)	3
7. E _{cf} (Composite Foundation Modulus), ksi	3, 8, 25, 75, 250, and 1,000	6

Total number of runs performed = 4,536 runs (1,512 per site)

tions were chosen to cover a broad range of temperature conditions as follows:

- Cold: (Grand Forks, ND), MAAT = 41.6°F
- Moderate: (Oklahoma City, OK), MAAT = 60.7°F
- Hot: (Key West, FL), MAAT = 77.8°F

Design Life. A design life of 20 years was selected for the MEPDG simulation.

Design Traffic. All simulation runs were performed using the classical 18-kip ESAL approach. The number of traffic repetitions used in the analyses was set at 2×10^6 ESALs in 20 years.

Vehicle speed. Four traffic speeds, ranging from creep speed to highway speed, were used in the study. These speeds are as follows:

- 0.5 mph: intersections, parking lots, traffic jams
- 15 mph: local roads, school zones
- 45 mph: collector and arterial city roads
- 60 mph: city freeways and interstate highways

AC Layer Thickness. Seven different AC layer thickness values were used to cover the wide range of thicknesses found in practice. These AC thicknesses were selected to ensure that the extreme fatigue conditions (controlled strain and controlled stress) would be assessed in the study.

Asphalt Mix Characteristics. Three levels of asphalt binder performance grade (PG) were selected: PG 82-10, PG

64-22, and PG 52-40. These grades ranged from a very soft binder (PG 52-40) typically used in a cold climatic region through a very stiff one (PG 82-10) used in a hot region. Additionally, three levels of Voids Filled with Bitumen (VFB) and one aggregate gradation were used. The combination of these mix characteristic levels provided values of E_{eff}^* ranging from approximately 30 ksi to 3,000 ksi depending on AC layer thickness and vehicle speed.

2.4.3 Database Analysis and Results

This section discusses the analyses and results of the 4,536 computer simulation runs performed for this study. All the simulation runs were performed at 2×10^6 ESALs. In addition, the analyses were performed to yield the percentage of alligator (bottom-up) fatigue damage rather than cracking. Fatigue damage is defined as the ratio of the predicted number of traffic repetitions to the allowable number of load repetitions (to some failure level) as shown in Equation 44.

$$D = \sum_{i=1}^T \frac{n_i}{N_{fi}} \quad (44)$$

where

D = damage

T = total number of computational periods

n_i = actual traffic for period i

N_{fi} = allowable failure repetitions under conditions prevailing in period

The allowable number of repetitions to failure (N_f) is calculated in the MEPDG methodology using the following set of equations:

$$N_f = 0.007566 * C * \beta_{f1} * k'_1 \left(\frac{1}{\epsilon_t} \right)^{3.291 * \beta_{f2}} \left(\frac{1}{E} \right)^{0.854 * \beta_{f3}} \quad (45)$$

$$k'_1 = \frac{1}{0.000398 + \frac{0.003602}{1 + e^{(11.02 - 3.49 * hac)}}} \quad (46)$$

$$C = 10^M \quad (47)$$

$$M = 4.84 \left(\frac{V_b}{V_a + V_b} - 0.69 \right) \quad (48)$$

where

ϵ_t = tensile strain at the critical location

E = stiffness of the material, psi

$\beta_{f1}, \beta_{f2}, \beta_{f3}$ = national calibration parameters (1.0, 1.2, and 1.5, respectively)

hac = thickness of the asphalt layer, in

V_b = effective binder content (%)

V_a = air voids (%)

In the calibrated version of the MEPDG, if the AC layer thickness is known, damage is transformed into fatigue cracking by Equation 49.

$$F.C. = \left(\frac{6,000}{1 + e^{(C_1 * C'_1 + C_2 * C'_2 * \log_{10}(D))}} \right) * \left(\frac{1}{60} \right) \quad (49)$$

where

$C_1 = C_2 = 1.0$

$C'_1 = -2 * C'_2$

$C'_2 = -2.40874 - 39.748 * (1 + hac)^{-2.856}$

$F.C.$ = fatigue cracking (% of lane area)

D = damage in percentage

2.4.3.1 Relationship between Fatigue Damage and Major Variables

In this section, the relationship between fatigue damage obtained from the multiple MEPDG simulation runs with the major variables is described. This sensitivity study reveals the impact of each variable on the fatigue damage.

Design Traffic (ESALs). A mini-study was initially performed prior to the Table 15 matrix analysis to validate the hypothesis that damage and traffic repetitions were directly correlated. A total of 34 MEPDG simulation runs were performed using different AC thicknesses, traffic speeds, pavement design life values, binder performance grades, effective binder contents, air voids, and composite foundation moduli. The results revealed a direct relationship between the number of traffic repetitions and damage, if all the other variables are held constant. This relationship can be expressed as follows:

$$D_i = D_j * (Tr_i / Tr_j) \quad (50)$$

where

D_i = percent damage predicted at traffic repetitions Tr_i

D_j = percent damage predicted at traffic repetitions Tr_j

Environmental Location. The environmental location was found to be one of the most significant factors affecting the development of alligator FC. In order to implement the environmental location in a regression model to predict the alligator fatigue damage, each location was expressed by a climatic factor.

Table 16 summarizes the environmental characteristics for the three climatic locations used in this analysis as well as the calculated climatic factors. Figure 37 depicts the effect of changing the climatic location on the development of the alligator fatigue damage.

Composite Foundation Modulus (E_{cf}). Analysis of the simulation results showed that a very significant variable affecting fatigue performance was E_{cf} . As this variable increased the

Table 16. Climatic characteristics for the locations used in the analysis.

Climatic Location	MAAT, °F	σ_{MMAT} , °F	Wind, mph	Sunshine, %	Rainfall, in	T'_i
Grand Forks, ND	40.37	21.86	8.93	52.26	19.95	79.23
Oklahoma City, OK	60.50	15.80	9.68	49.36	31.78	92.53
Key West, FL	77.76	5.63	8.42	72.92	39.84	115.97

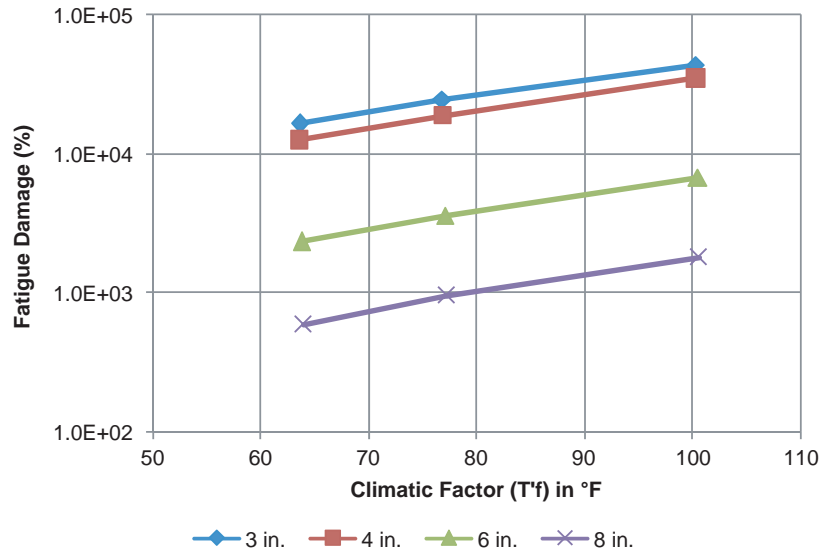


Figure 37. Influence of the climatic factor upon alligator fatigue damage (PG 52-40, VFB = 0.4, v = 0.5 mph, 20 years, 2*10⁶ ESALs, and E_{cf} = 3,000 psi).

alligator fatigue damage decreased. Furthermore, the relationship between the fatigue damage and composite foundation modulus could be fit with a second degree polynomial function in log space.

Figure 38 presents an example plot for the relationship between the E_{cf} and fatigue damage. This figure clearly shows the excellent accuracy of these relationships, as indicated by the R² values on these plots. Furthermore, the coefficient of determination (R²) for all the 756 polynomial relationships representing the whole database (4,536 computer simulation runs) was always higher than 0.99 indicating excellent model predictions.

The general model relating damage (D) to E_{cf} can be expressed by the following:

$$\log D = a_1 \log(E_{cf})^2 + a_2 \log(E_{cf}) + a_3 \quad (51)$$

where

- D = % bottom-up alligator fatigue damage
- E_{cf} = composite foundation modulus, ksi
- a₁, a₂, and a₃ = regression constants depending on AC thickness, performance grade, traffic speed, VFB, and environmental location.

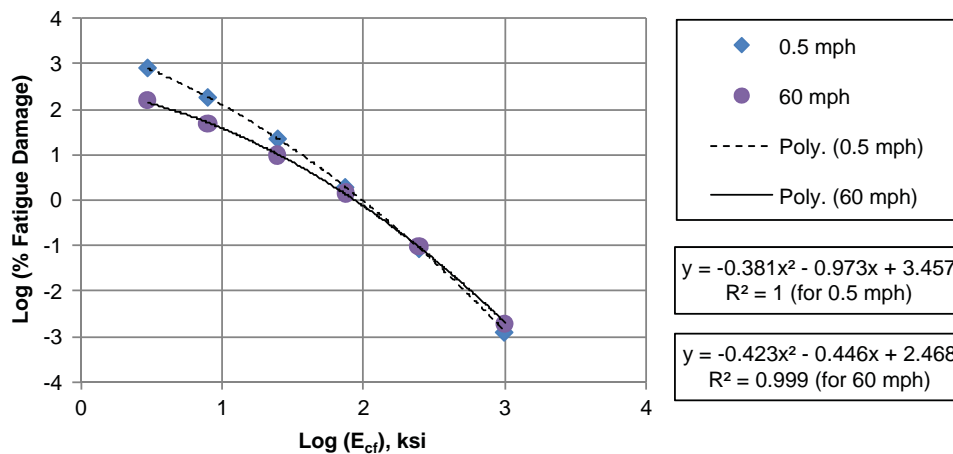


Figure 38. Relationship between damage and composite foundation modulus (h_{ac} = 4 in., PG 64-22, V_a = 8%, V_{beff} = 12%, Oklahoma).

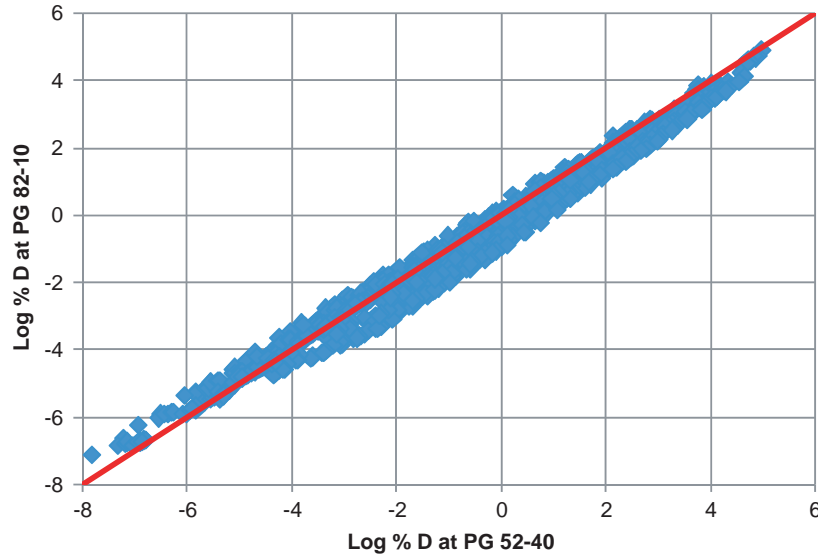


Figure 39. Relationship between damage predicted using a PG 52-40 versus PG 82-10, 4,536 data points.

Binder Grade. Figure 39 shows the scatter around the equality line for log(D) predicted using a PG 52-40 binder (very soft) versus log(D) corresponding to a PG 82-10 (very stiff) binder. This figure implies that the binder stiffness (very soft versus very stiff) has some impact on the development of the alligator FC and should be considered as a variable in the final alligator FC model.

VFB. VFB was found to significantly affect the development of alligator fatigue damage, as shown in Figure 40.

Traffic Speed. Figure 41 depicts the typical influence of the traffic speed upon alligator fatigue damage. This figure shows a significant change in the alligator fatigue damage with the change of traffic speed. There is a dramatic decrease in the

alligator fatigue damage as the vehicle speed increases from creep (0.5 mph) to slow speed (15 mph), but the effect of the speed change above 15 mph on fatigue damage is less remarkable. A linear relationship was found between fatigue damage and traffic speed in log-log space. This relationship can be expressed as follows:

$$D = a(v)^b \tag{52}$$

where

- D = % alligator fatigue damage
- v = traffic speed, mph
- a, b = regression coefficients

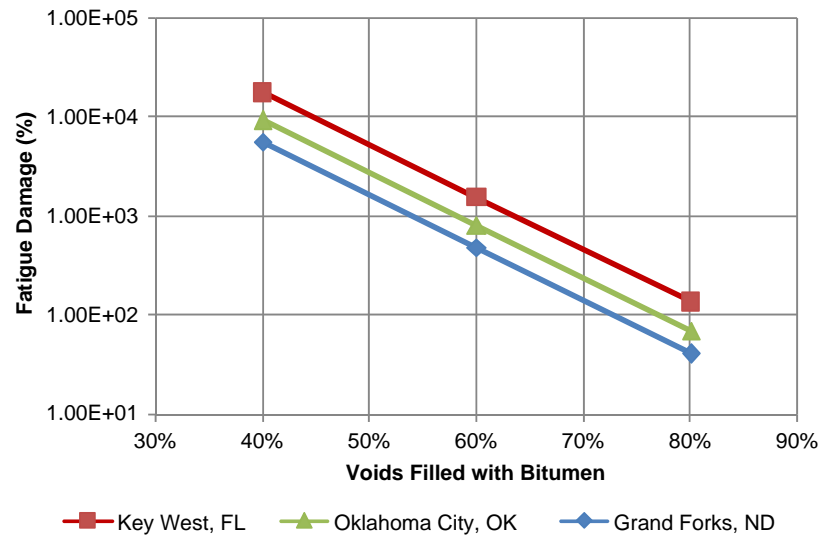


Figure 40. Influence of VFB upon alligator fatigue damage ($h_{ac} = 4$ in., PG 64-22, speed = 0.5 mph, and $E_{cf} = 3,000$ psi).

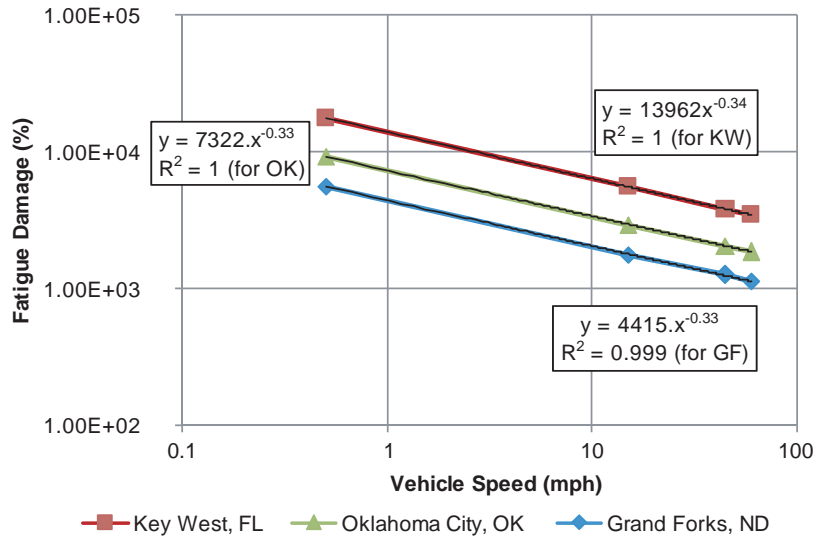


Figure 41. Influence of speed upon alligator fatigue damage ($h_{ac} = 4$ in., PG 64-22, VFB = 0.4, and $E_{cf} = 3,000$ psi).

The regression coefficients a and b were found to vary with the AC layer thickness, AC mix characteristics, binder performance grade, composite foundation moduli, and environmental location.

AC Thickness. AC Thickness is one of the most important factors affecting alligator fatigue damage. Figure 42 shows how the effect of AC layer thickness upon fatigue damage is related to the composite foundation modulus. A significant reduction in fatigue damage occurs with increasing AC layer thickness, especially for thicknesses greater than 3 to 4 in. AC layer thicknesses below 3 to 4 in. show a quite complicated trend in damage reduction. In this range, depending on

foundation stiffness, the fatigue damage either decreases or increases or both with increasing AC thickness. This result led to a decision to develop the fatigue damage model with two different sets of coefficients: one for an AC layer thickness less than three inches and the other for thicknesses greater than three inches. More details are provided in the next section.

2.4.3.2 Fatigue Damage Predictive Model Development

A comprehensive analysis of the output data from the MEPDG Version 1.0 showed that several key variables must be considered in the development of the final fatigue damage

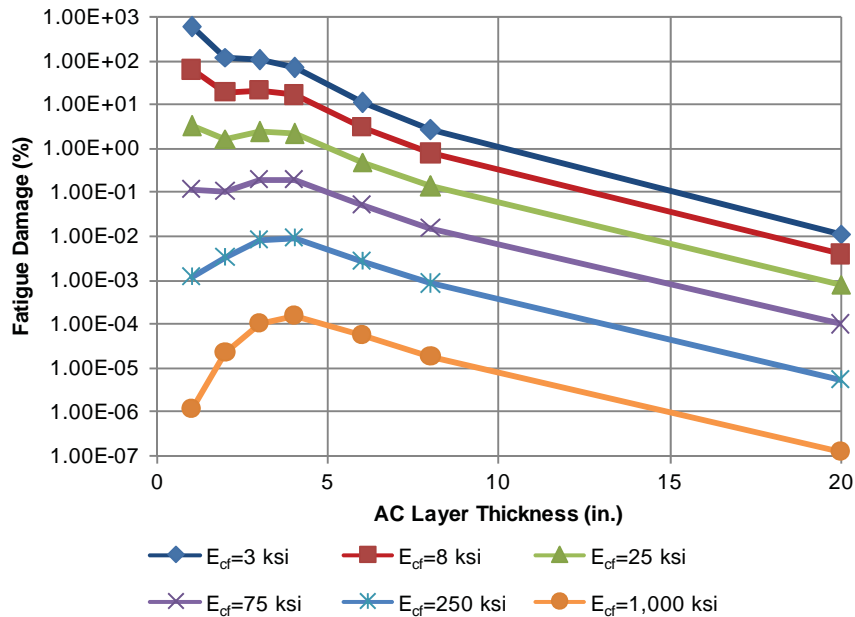


Figure 42. Influence of the AC thickness upon damage, (VFB = 0.8, PG 64-22, Speed = 0.5 mph, and Oklahoma City).

model. These variables were found to be: traffic speed, ESAL, VFB, climatic factor ($T'f$), composite foundation modulus (E_{cf}), AC thickness, and binder stiffness. The AC modulus itself is heavily dependent upon VFB, traffic speed (frequency of loading), binder viscosity, and climate (temperature). Thus fatigue damage can be related to the AC modulus.

Based on the 4,536 MEPDG Version 1.0 simulation runs, a general comprehensive model to predict fatigue damage as a function of the effective AC modulus, AC thickness, VFB, and E_{cf} was developed. The E_{eff}^* itself depends upon the aggregate gradation of the AC mixture, VFB, traffic speed (effective loading frequency), and binder viscosity at the effective temperature as shown in Equation 53.

$$\log N_f = 8.3014 - \left\{ \left[\left(b_1 \log(h_{ac})^2 + b_2 \log(h_{ac}) + b_3 \right) \log(E^*) + b_4 \log(h_{ac})^2 + b_5 \log(h_{ac}) + b_6 \right] \log(E_{cf})^2 + \left[b_7 \log(E^*)^2 + b_8 \log(E^*) + b_9 \right] \log(E_{cf}) + \left[b_{10} \log(h_{ac})^2 + b_{11} \log(h_{ac}) + b_{12} \right] \log(VFB)^2 + \left[b_{13} \log(h_{ac})^2 + b_{14} \log(h_{ac}) + b_{15} \right] \log(VFB) + b_{16} \log(E^*)^2 + \left[b_{17} (h_{ac})^2 + b_{18} (h_{ac}) + b_{19} \right] \log(E^*) + b_{20} \right\} \quad (53)$$

where

- N_f = allowable number of repetitions to fatigue failure
- h_{ac} = AC thickness, inch
- b_1 to b_{20} = regression coefficients

Nonlinear optimization was performed simultaneously on Equations 53 and the fatigue effective temperature (T_{eff}) model to determine the regression coefficients for the T_{eff} model as well as the general fatigue damage model. Once N_f is determined, the fatigue damage at the ESALs of interest can then be calculated using Equation 50. In addition, fatigue cracking can be calculated from the predicted damage using the MEPDG transfer function shown in Equation 49.

As mentioned previously, two different sets of coefficients were developed and the selection of either coefficient set is determined by AC thickness of a pavement structure of concern. In general, fatigue damage is reduced as either AC thickness or sub AC layer (i.e., composite foundation) stiffness increases. However, if a pavement structure has a thin AC layer along with a very strong composite foundation, little or no tensile strain will be induced at the bottom of the pavement structure by loading; indeed, compressive strain may be induced in the pavement and the predicted fatigue damage would be zero or close to zero. In this situation, as the AC thickness increases, tensile strain (i.e., fatigue damage) will increase up to a certain point and then begin to decrease. The sensitivity analysis placed this transition thickness at approximately 3~4 inches. There-

fore, the final model that was developed takes the form of Equation 53 with the two sets of coefficients presented in Table 17.

The presence of two sets of coefficients for the model leads to a discontinuity for a 3 in. AC layer because two fatigue damage values are predicted. Figure 43 shows how the predicted FC from the model using less than 3 in. coefficient set (“thin” model in the figure) differs from that using the greater than 3 in. coefficient set (“thick” model in the figure). This problem is of concern in a probabilistic analysis where the standard deviation of the AC thickness is taken into account.

To mitigate the discontinuity, a transition range of AC thickness was established. When the AC layer is between 2.5 and 3.5 inches, fatigue cracking is calculated by the following equation:

$$\text{Fatigue cracking} = \alpha (\text{Fatigue Cracking predicted by "Thick" Model}) + (1 - \alpha) * (\text{Fatigue Cracking predicted by "Thin" Model}) \quad (54)$$

where

$$\alpha = -2.5 + h_{ac}$$

When the AC thickness is less than 2.5 in. or greater than 3.5 in. (i.e., $\alpha = 0$ and 1), Equation 54 simply becomes the original “Thin” and “Thick” models, respectively.

Figure 44 compares the fatigue damage predicted using the general model developed in this study and the damage predicted using the MEPDG for the 4,536 computer simulation

Table 17. Regression coefficients for fatigue damage prediction model.

Regression Coefficients	$h_{ac} \leq 3$ in. (Thin Model)	$h_{ac} \geq 3$ in (Thick Model)
b1	-0.0095	0.0645
b2	-0.0756	-0.0144
b3	0.0438	0.0416
b4	-0.5414	-0.6003
b5	1.4319	0.7046
b6	-1.0252	-1.0276
b7	-0.0208	-0.0218
b8	0.7040	0.6280
b9	-4.1171	-3.2499
b10	-4.1659	28.9186
b11	-3.0733	-51.9588
b12	-6.4418	12.7671
b13	-1.5883	15.8844
b14	-2.8014	-28.6128
b15	-9.2885	0.9160
b16	-0.1177	-0.1792
b17	0.0681	0.0024
b18	-0.3789	-0.1009
b19	0.8989	1.2623
b20	2.9330	1.4613

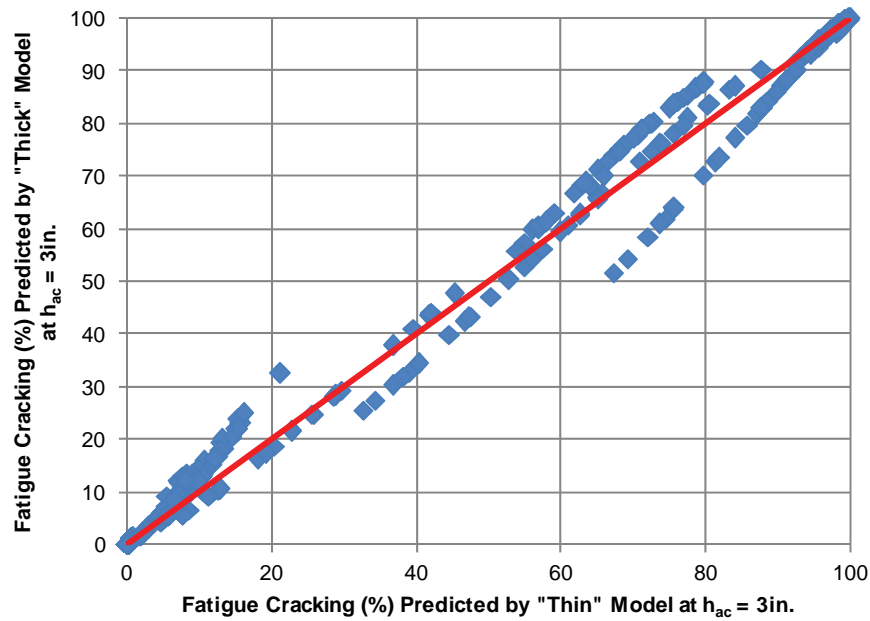


Figure 43. Comparison of predicted fatigue damage at $h_{ac} = 3$ in. between “Thin” and “Thick” models.

runs. The model show excellent prediction accuracy with $Se/Sy = 0.045$ and an adjusted R^2 of 0.998 in the logarithmic scale.

2.4.3.3 Validation of the Developed FC Prediction Methodology

At this point, a process to predict FC using the predictive models developed here was established. The process included the transformation of any multi-layer system into a two-layer

system, calculation of the effective AC modulus, and finally the prediction of the load-associated FC based on the effective modulus. The next step was to validate the process by comparing outputs obtained from the MEPDG and the developed prediction methodology for a three-layer pavement system.

One thousand simulations were run with both the MEPDG and the developed methodology to validate the process. The simulations embraced conditions that may be potentially encountered in the field. The following parameters were varied:

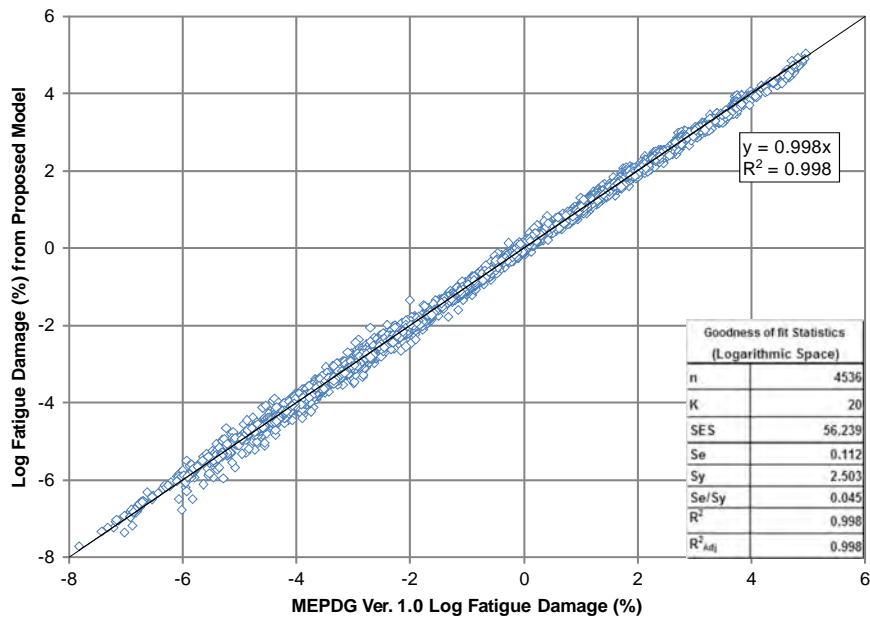


Figure 44. Fatigue damage predicted using MEPDG versus fatigue damage predicted using the proposed model.

binder performance grade, V_a and V_b , AC thickness, AC modulus, traffic speed, base thickness, base modulus, subgrade modulus and environmental location. All simulation runs were performed at traffic repetitions of two million ESALs. Table 18 summarizes the number of simulations associated with each variable used in the validation study.

Figure 45 compares percentage fatigue damage predicted from both models. Data points represent results from various combinations of environmental and physical road conditions; variables contain not only particular values used in the damage predictive model and the layer transformation but also other values between the initially considered ones. In fact more than 70% of the simulation matrix used for the validation process of the developed alligator fatigue cracking methodology contains levels for each variable considered in the developed models that are different from the levels initially used in the development of the predictive methodology. For example, the fatigue damage model was developed based upon three different climatic locations while 10 climatic locations distributed all over the United States were used for the validation process.

Figure 45 shows a very good agreement between the percentage alligator fatigue damage predicted using the devel-

oped methodology and the MEPDG. The adjusted R^2 is 0.87 and the Se/Sy is 0.354 in arithmetic scale.

2.4.3.4 Overall Prediction Accuracy

To check the overall prediction accuracy of the developed methodology, the database used to develop the effective temperature, effective AC modulus, and the general fatigue damage predictive model were combined with the database used for the validation. Because all the MEPDG simulations were run at only one traffic repetition of two million ESALs, the damage values at various traffic levels of 5, 10, and 50 million ESALs were calculated to ensure the developed model's overall prediction accuracy.

FC predicted from the proposed fatigue model at the four traffic levels was compared to that from the MEPDG as shown in Figure 46. The FC is rationally predicted by the proposed model in most cases. Some scattering of data was observed for very thin AC thicknesses (less than 2.0 in.) because the damage-to-cracking transfer function is sensitive to AC thickness and becomes more sensitive with the decrease in AC thickness. Excluding the thin sections eliminates the scattering as shown in Figure 47. Therefore, it is

Table 18. Summary of the MEPDG simulation runs used for the validation of the alligator FC spread sheet solution.

PG Grade	# of Runs	V_a (%), V_b (%)	# of Runs	AC Thickness (in.)	# of Runs	Environmental Location	# of Runs
52-40	80	4,16	120	1	70	Chicago, IL	100
58-28	350	6,14	420	1.5	40	Great Falls, MT	100
64-22	110	8,12	120	2	70	Homer, AK	100
76-16	340	10,10	270	2.5	70	Houston, TX	100
82-10	120	12,8	70	3	100	Indianapolis, IN	100
				3.5	100	Jackson, MS	100
				4	190	Oklahoma City, OK	100
				5	100	Phoenix(Deer), AZ	100
				5.5	30	Seattle, WA	100
				6	100	Washington, DC	100
				7	100		
				8	30		
Total	1000	Total	1000	Total	1000	Total	1000
Traffic Speed (mph)	# of Runs	Base Thickness (in.)	# of Runs	Base Modulus (ksi)	# of Runs	Subgrade Modulus (ksi)	# of Runs
0.5	140	4	160	15	240	3	160
45	310	5	560	30	560	5	320
55	310	6	130	40	80	8	150
65	240	8	150	50	70	10	340
				80	50	30	30
						Total	1000
						AC Modulus (ksi)	# of Runs
						< 500	179
						> 500	821
Total	1000	Total	1000	Total	1000	Total	1000

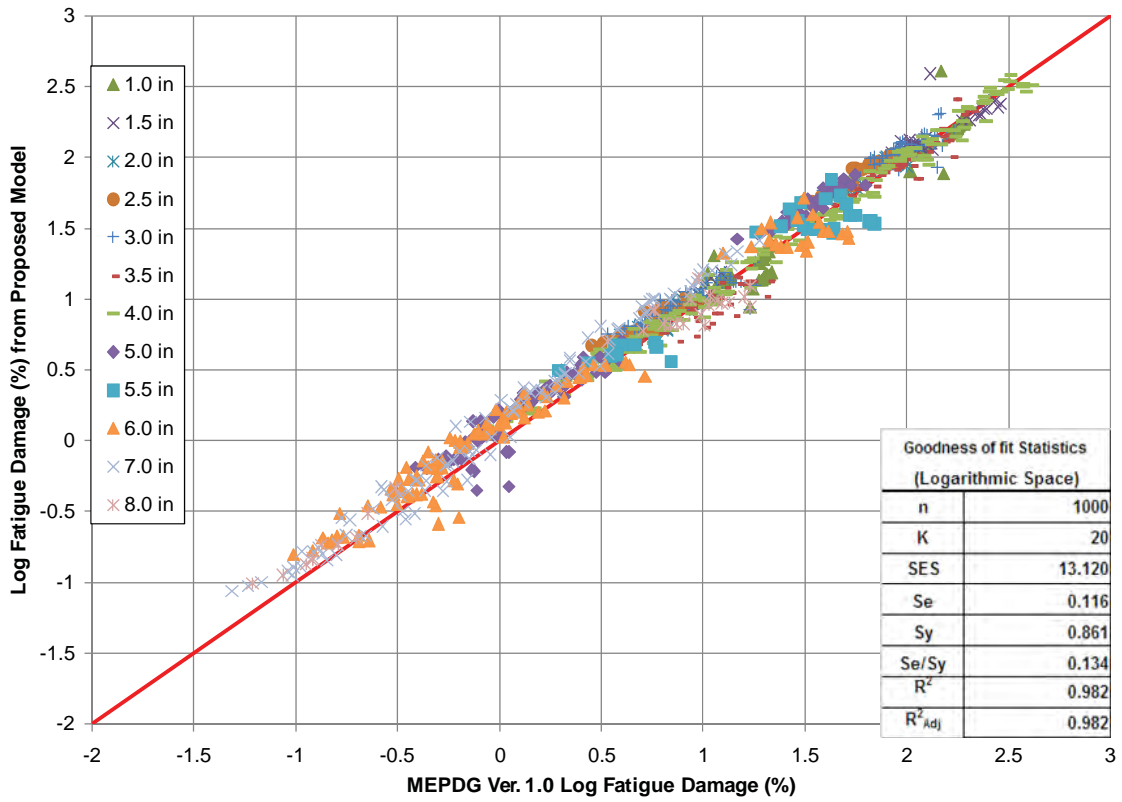


Figure 45. Comparison of %fatigue damage predicted from MEPDG and the developed predictive process (all AC thicknesses).

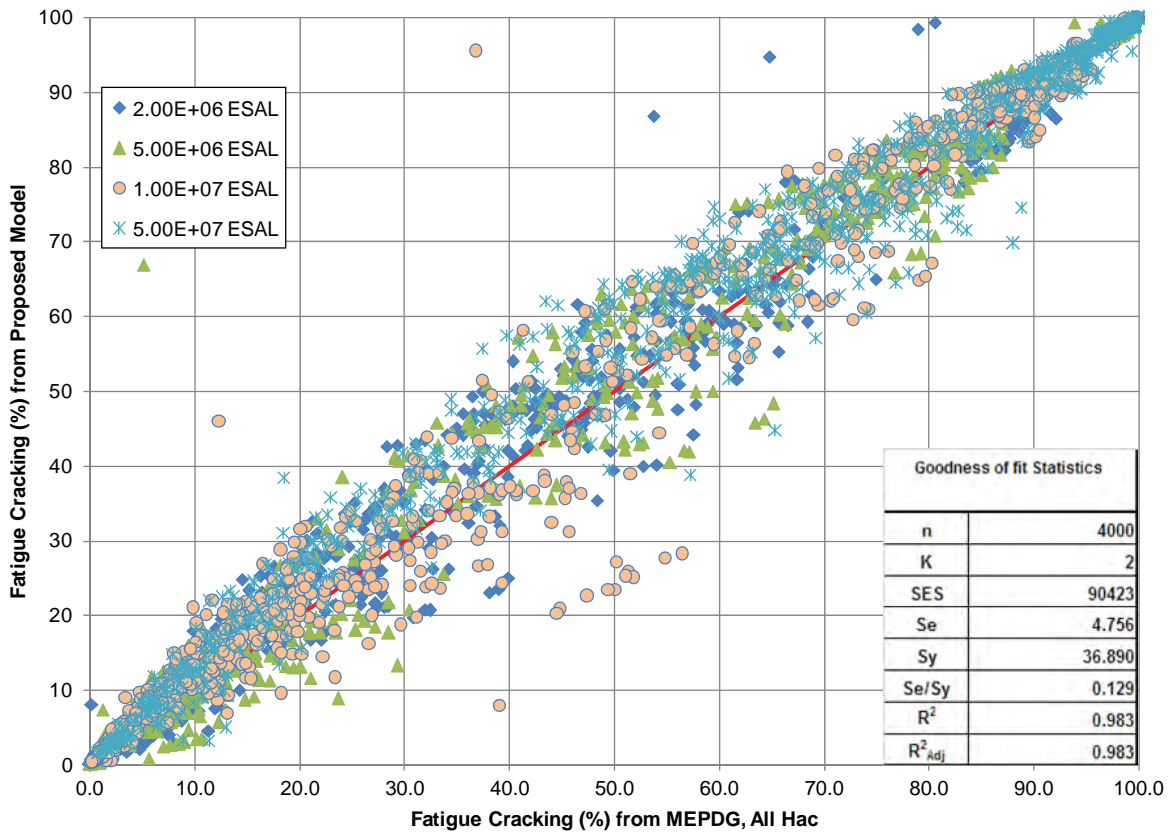


Figure 46. Comparison of FC at various traffic levels between MEPDG and proposed model (all AC thicknesses).

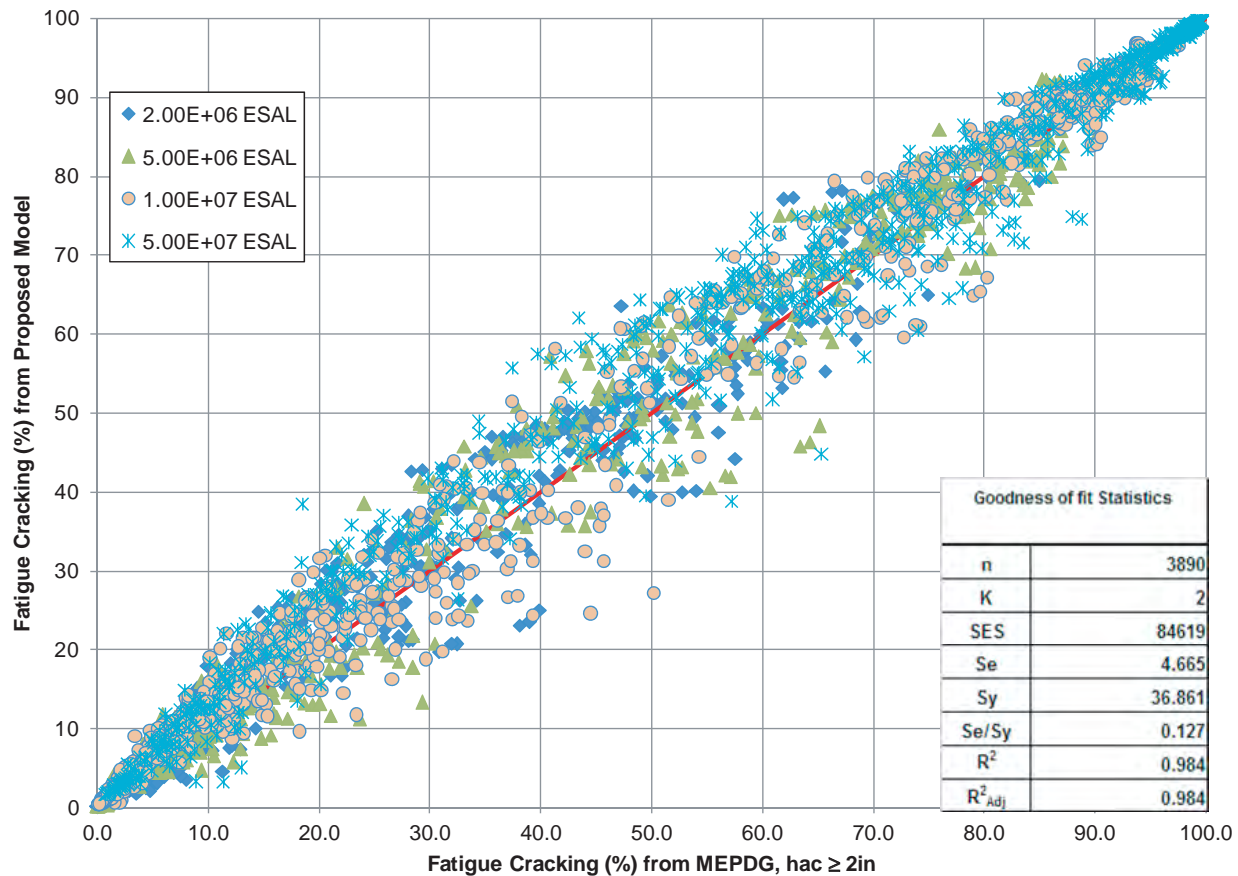


Figure 47. Comparison of FC at various traffic levels between MEPDG and proposed model (AC thickness ≥ 2 in.).

obvious that the model is most accurate for AC thicknesses equal to or greater than two inches.

Figure 48 illustrates the sensitivity of the fatigue cracking to the predicted fatigue damage. Due to the sharp slope in the log fatigue damage range of interest, a small change of fatigue damage can cause a large change in FC; it is also observed that the range of interest is narrowed down as AC thickness decreases.

2.5 Performance Model Development for Thermal Cracking

2.5.1 Introduction

Much effort was expended on development of a potential closed form solution of the AC thermal cracking distress. While this solution was envisioned to be the most direct and simplest of the three distresses considered, the reverse was actually found to be true. Significant difficulties were encountered in trying to formulate a closed form solution. In addition, NCHRP Project 1-40 discovered a coding error in the MEPDG software that required re-running nearly 3,000 thermal fracture simulation runs that were being used in the attempt to develop the closed form solution.

2.5.2 Sensitivity Study

A preliminary sensitivity study was conducted with the corrected database for the thermal cracking model recalibration of the MEPDG. The study included 40 test sites at both MEPDG analysis levels 1 and 3. The following summarizes the findings of this study:

- Using the result of the creep tests, creep compliance master curve parameters D_0 , D_1 , and m -value were computed. The parameters were correlated with mix properties: air voids (V_a), effective binder contents (V_{beff}), voids filled with asphalt (VFA), and Pen_{77} . The correlations were poor. Therefore, it was decided to directly generate the master curve rather than to rely on correlations for each temperature.
- The relation between the master curve parameters and observed thermal cracking was studied; m , the slope of the master curve, was found to be slightly correlated with the observed thermal cracking.
- Pen_{77} and A_i of the asphalt binder were also found to be slightly correlated with the observed thermal cracking.
- The minimum air and surface temperature were found to be weakly correlated with the observed thermal cracking.

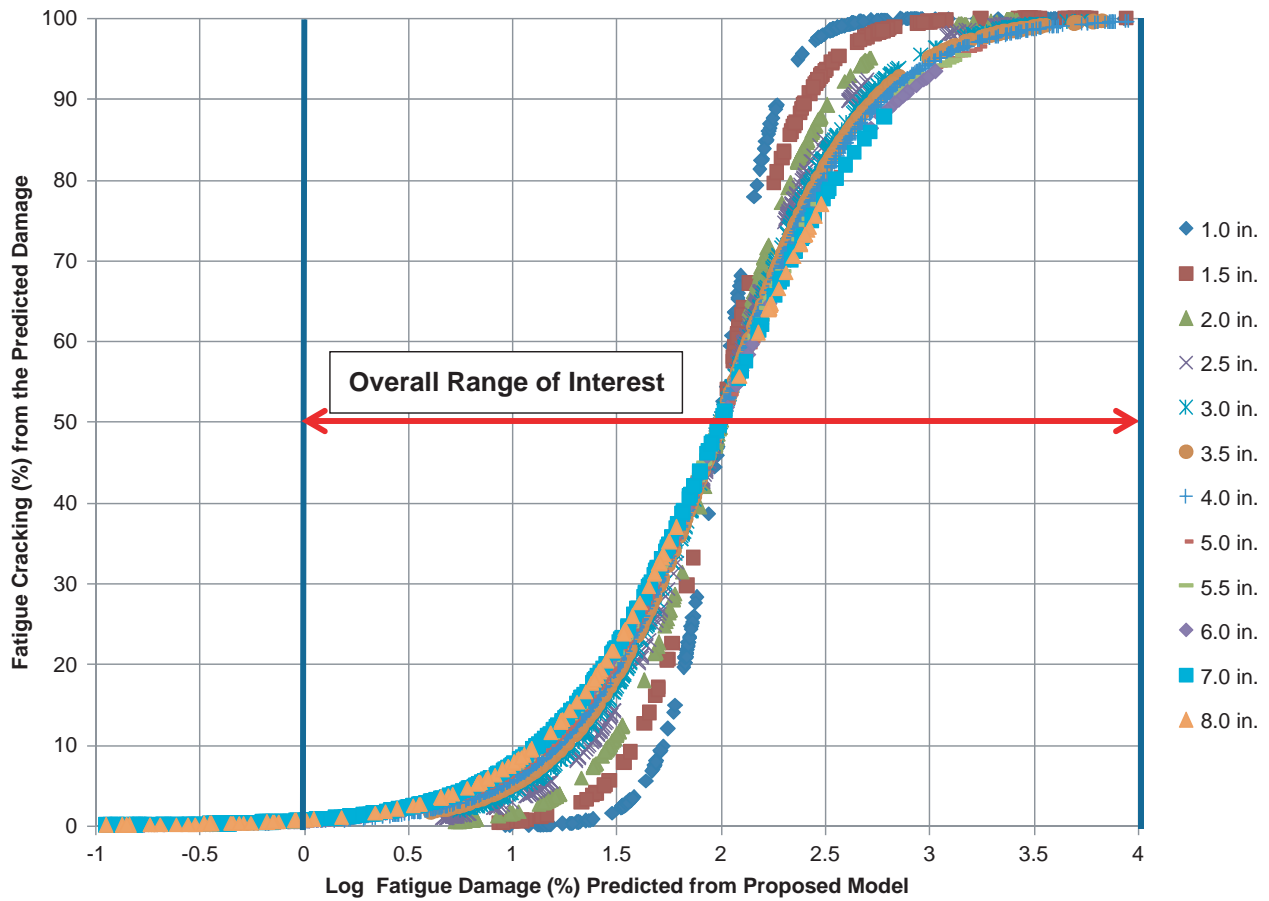


Figure 48. Relationship between log fatigue damage and fatigue cracking at various AC thicknesses.

Therefore, some provisional conclusions of the thermal cracking analysis were:

- Thermal cracking is influenced by a combination of climatic, mix, and binder properties.
- Approaches with either non-linear or linear regression may not be rational and a different (more accurate) methodology may need to be established.
- Development of a simple mechanistic-based fracture model is necessary.

2.5.3 Mechanistic-Based Fracture Model Process

The development of the new preliminary model more closely followed the actual mechanistic-based fracture process. It was based upon:

- Use of the minimum air temperature during the design life in a climatic file generated in the MEPDG from which the minimum pavement surface temperature (MPST) and the temperature gradient (ΔT) can be computed.
- Use of creep compliance to develop a master curve.

- Use of power model parameters: D_0 , D_1 , and m , and shift factors: a_1 and a_2 , to define the master curve.
- Computation of the relaxation modulus (E) as $E=1/D$, where D is the compliance at the MPST for time = 1 hour (the unit of the temperature gradient is $^{\circ}F/hour$)
- Computation of a “stress” value using:

$$\sigma = E\alpha\Delta T \tag{55}$$

where

- E = relaxation modulus ($1/D$)
- D = creep compliance at the MPST
- α = thermal contraction coefficient (0.000013 in $1/^{\circ}C$)

- Computation of the stress to strength ratio:

$$S = \sigma/S_t \tag{56}$$

where

- S_t = tensile strength at $-10^{\circ}C$
- $S_t = 4976.34 - 42.49(V_a) - 2.73(V_a)^2 - 80.61(VFA) + 0.465(VFA)^2 + 174.35 \log(Pen_{77}) - 1217.54 \log(A_{RTFO})$

where

V_a = air void (%)

VFA = voids filled with asphalt ($V_{\text{beff}}/(V_{\text{beff}}+V_a)$)

V_{beff} = effective binder contents (%)

A_{RTFO} = intercept of binder viscosity-temperature relationship for the RTFO condition

- Computation of n , A , and K for the Paris law and ΔC , the increment of thermal cracking:

$$n = 0.8(1 + 1/m) \quad (57)$$

$$A = (1.5^{n+1}) * 10^{(4.389 - 2.52 \log(10000 * S_t * n * 0.00689^2))} \quad (58)$$

$$\Delta K = \{b_1(0.00689\sigma) + b_2\} * \{0.45 + 1.99(25.4 * C_0)^{0.56}\} \quad (59)$$

$$\Delta C = A(\Delta K)^n \quad (60)$$

where

1.5^{n+1} = calibration factor for the level 3 analysis

S_t = tensile strength (psi)

b_1 and b_2 = calibration coefficients

C_0 = initial cracking (0.1 inch)

- Correlation of ΔC with the thermal cracking obtained from the MEPDG thermal cracking model (12)

To recapitulate, a preliminary sensitivity study conducted with the MEPDG revealed that it would be very difficult to develop accurate closed form thermal fracture cracking using probabilistic approaches, including linear and non-linear regression methods. As a consequence, attention was given to the development of a mechanistic-based method. This implied that the method would follow the same fundamental theory that is currently used as a thermal fracture subroutine in the MEPDG, since the thermal fracture analysis is entirely developed on a mechanistic basis.

The project team thoroughly evaluated each step of the subroutines of the two major execution files (master.exe and tmodel.exe) in the thermal fracture part of the MEPDG. The project team was able to develop a mechanical-based solution that produced estimates of thermal cracking closely matching predictions of thermal cracking made with the MEPDG. The comparison of the two sets of predictions at the end of the pavement design life had an R^2 value in excess of 0.99.

The final developed solution was provisionally coded in FORTRAN. The user must create an input file containing several critical variables in a particular format. The variables include: design life, AC thickness, and mixture properties (effective binder content, air void content, and binder type).

The input data also includes a pavement temperature data file for the project location. Then, the user runs the program named "program.exe" that quickly yields the predicted thermal cracking at the end of the design period.

The following sections will not focus upon the theoretical background of the thermal cracking development, as this is already available in the literature as well as the MEPDG documentation (12, 20). Instead, the discussion will explain the input, analysis, and output, present an overall design flow-chart for thermal cracking solutions, and compare the results with those obtained with the MEPDG.

2.5.4 Input

The input is composed of four parts: pavement structure, design period, climate, and AC mix properties. All these inputs are also required for the rutting and fatigue cracking solutions. However, unlike the rutting and fatigue cracking methodologies, thermal cracking requires hourly temperatures, with depth, within a given pavement. In the final integrated QRSS, the three major distresses share a single input screen.

Based on the user's choice of the distress of interest, the QRSS asks the user to input the relevant information required for that distress. If the user's choice is to consider all three distresses, then the program will show a common input screen with all relevant information required to perform the analysis. The following bullets explain the five main inputs required to perform the thermal cracking analysis:

- Pavement structure: Unlike fatigue cracking, only the AC layer mix properties and thickness affect the initiation and propagation of thermal cracking. The effect of the foundation layers such as base, subbase, and subgrade are negligible. Thus, the only input value regarding pavement structure is the thickness of AC layer in inches. If the AC layers have differing layer mix types, the total AC thickness is still considered as the input AC thickness. This assumption is the same as that made by the developers of the Superpave mix analysis system that incorporated the thermal cracking prediction model that is the basis for that in the MEPDG
- Design period: The program will produce estimates of thermal cracking development at the end of every month during a design life.
- Climate: Since the AC pavement is extremely sensitive to temperature, climatic information for the project location is one of the most critical factors in the analysis of thermal cracking. The program requires a specific pavement temperature data file as an input. The temperature file can be created either by (1) running the Enhanced Integrated Climatic Model (EICM) which, in the installation of the MEPDG, exists as the executable file "im.exe" in the sub-

routine files (specifically C:\DG2002\bin), or (2) running the MEPDG itself.

- AC mix properties: Along with the climatic information for the specific project location, the volumetric properties for the AC mix are critical information. The user inputs for the AC mix are: the intercept and slope, A and VTS, of the RTFO-conditioned binder's viscosity-temperature relationship; in-situ air voids (%); and effective binder content (%). If multiple AC layers are used, it is very important to recognize that only the properties of the top AC layer will be used for the thermal cracking analysis, because these govern the initiation of thermal cracking.
- Date of analysis: Since the development of thermal cracking begins at the end date of pavement construction, the thermal cracking program uses the inputted date as the starting point of the analysis.

2.5.5 Analysis

When data input is complete, the program conducts the analysis and produces predictions of thermal cracking for the desired period. As previously mentioned, these analytical processes are based on the same mechanistic concepts used to develop the thermal cracking predictions in the MEPDG. Thus, the fundamental background of the thermal cracking prediction is already well documented and available in the literature. The step by step solution for the thermal cracking module is as follows:

- VFA and penetration at 77°F (Pen_{77}) are computed by the following equations:

$$VFA(\%) = \frac{V_{beff}}{V_{beff} + V_a} \times 100 \quad (61)$$

$$Pen_{77} = 10^{290.513 - \sqrt{91177.288 + 257.0694 + 10^{(A+2.72973VTS)}}} \quad (62)$$

where

V_a = air voids (%)

V_{beff} = effective binder content (%)

A = A_{RTFO} = intercept of binder viscosity-temperature relationship for the RTFO condition

VTS = slope of binder viscosity-temperature relationship for the RTFO condition

- Creep compliance parameters D_1 and m-value are computed at the three standard testing temperatures in AASHTO T 322: -20, -10, and 0°C:

$$\log(D_1)_{-20^\circ C} = -11.9254 + 1.52206 * \log(V_a) + 4.49876 * \log(VFA) - 3.8132 * \log(A_{RTFO}) \quad (63a)$$

$$\log(D_1)_{-10^\circ C} = -10.7656 + 1.51960 * \log(V_a) + 3.49983 * \log(VFA) - 2.9987 * \log(A_{RTFO}) \quad (63b)$$

$$\log(D_1)_{0^\circ C} = -9.80627 + 1.50845 * \log(V_a) + 2.9900 * \log(VFA) - 2.90157 * \log(A_{RTFO}) \quad (63c)$$

$$m_{-20^\circ C} = -1.75987 + 1.78187 * V_a^{0.0203} + 0.00089 * Pen_{77}^{0.9687} \quad (64a)$$

$$m_{-10^\circ C} = -1.82690 + 1.94218 * V_a^{0.0160} + 0.00098 * Pen_{77}^{0.96857} \quad (64b)$$

$$m_{0^\circ C} = -2.41043 + 2.59093 * V_a^{0.01547} + 0.00199 * Pen_{77}^{0.97247} \quad (64c)$$

- Three individual creep compliance curves are drawn with the calculated D_1 and m-values and each curve is fitted to a second order polynomial function.
- The creep compliance master curve (CCMC) is then constructed by shifting the curves at -10 and 0°C through an optimization process.
- The CCMC is fitted to both a Power model and a Prony series.
- The CCMC fitted to the Prony series is converted to the relaxation modulus master curve by a numerical conversion process.
- The hourly-based thermal stresses within the AC layer are calculated from the pavement temperature and the relaxation modulus at the surface and then at every two inches in depth to the bottom of the layer (i.e., for 3 in. AC layer, they are 0, 2, and 3 in.; for 8.5 in., 0, 2, 4, 6, 8, and 8.5 in.)
- The maximum and minimum stresses for a 48-hour period are calculated. Specifically, the minimum stress is found at times between 7 and 22 hours; while the maximum stress is found between 19 and 34 hours.
- Maximum and minimum stress intensity factors (K) are calculated by the following equations:

$$\Delta K = \sigma(0.45 + 1.99C^{0.56}) \quad (65)$$

where

σ = stress during one cycle

C = initial cracking (zero)

$$\Delta K = K_{max} - K_{min} \quad (66)$$

where

K_{max} = stress is maximum

K_{min} = stress is minimum

2.5.6 Output

After all computations in the analysis are completed, the increment of crack depth (ΔC) is simply calculated by Paris' law:

$$\Delta C = A(\Delta K)^n \tag{67}$$

where

- ΔC = change in the crack depth due to a cooling cycle
- ΔK = change in the stress intensity factor due to a cooling cycle

A, n = fracture parameters for the asphalt mixture

A probabilistic model is then used to predict the amount of thermal cracking from the crack depth. The MEPDG defines thermal cracking as “a function of the probability that the crack depth is equal to or greater than the thickness of the total asphalt layers”; and uses the following equation (12):

$$C_f = \beta_1 * N\left(\frac{\log C/D}{\sigma}\right) \tag{68}$$

where

- C_f = observed amount of thermal cracking in ft/500ft
- β_1 = regression coefficient determined through field calibration (=353.5)
- $N()$ = standard normal distribution evaluated at ()
- σ = standard deviation of the log of the depth of cracks in the pavement (=0.769)

- C = cracking depth
- D = thickness of AC layer

2.5.7 Results

The thermal cracking program developed in this project was validated by comparing the thermal cracking output from the program with that from MEPDG Version 1.0 for a wide range of environmental and physical conditions for the pavement. Ten environmental locations were originally selected to characterize climate. In order to have a more reliable validation, the database was expanded by adding 12 more locations and then excluding five warm to hot locations, resulting in 17 sites.

Table 19 shows all the environmental locations employed with their geographical information. Therefore, the final matrix employed in the analysis included: 17 geographically diverse locations (cold to warm); five AC thicknesses (thin to thick); five binder types (soft to hard); and eight combinations of mix volumetric properties. The design life used in this validation study was 20 years, yielding a total of 3,400 MEPDG simulation runs (17 sites * 5 AC thicknesses * 5 PG * 8 volumetric = 3,400 runs).

Figure 49 compares the thermal cracking predicted from the MEPDG with that predicted by the program developed in this project. Each data point in the plot is a predicted thermal cracking amount after 20 years for a certain condition. The plot indicates the predicted thermal cracking obtained from both methods is nearly identical, with an R² value greater than 0.999 and an Se/Sy of 0.006. Nonetheless, a few data points are slightly distant from the equality line.

Table 19. Environmental locations used in the analysis.

Location		Latitude	Longitude	EI. (ft)
Alpena, MI	Phelps CO RGNL Airport	45.04	-83.35	686
Barrow, AK	W Post-W Rogers MEML Airport	71.17	-156.46	38
Billings, MT	Billings Logan INTL Airport	45.49	-108.32	3,582
Bismarck, ND	Bismarck Municipal Airport	46.46	-100.45	1,654
Caribou, ME	Caribou Municipal Airport	46.52	-68.02	630
Chicago, IL	O'Hare INTL Airport	41.59	-87.55	658
Dallas, TX	Dallas/Ft. Worth INTL Airport	32.54	-97.02	562
Fargo, ND	Hector INTL Airport	46.56	-96.49	911
Grand Forks, ND	Grand Forks INTL Airport	47.57	-97.11	842
Great Falls, MT	Great Falls INTL Airport	47.28	-111.23	3,673
Green Bay, WI	Austin Straubel INTL Airport	44.31	-88.07	685
Hartford, CT	Hartford-Brainard Airport	41.44	-72.39	18
Homer, AK	Homer Airport	59.39	-151.29	78
Memphis, TN	Memphis INTL Airport	35.04	-89.59	286
Rochester, NY	Rochester INTL Airport	43.07	-77.41	588
Santa Fe, NM	Santa Fe Municipal Airport	35.37	-106.05	6,335
Spokane, WA	Spokane INTL Airport	47.37	-117.32	2,384

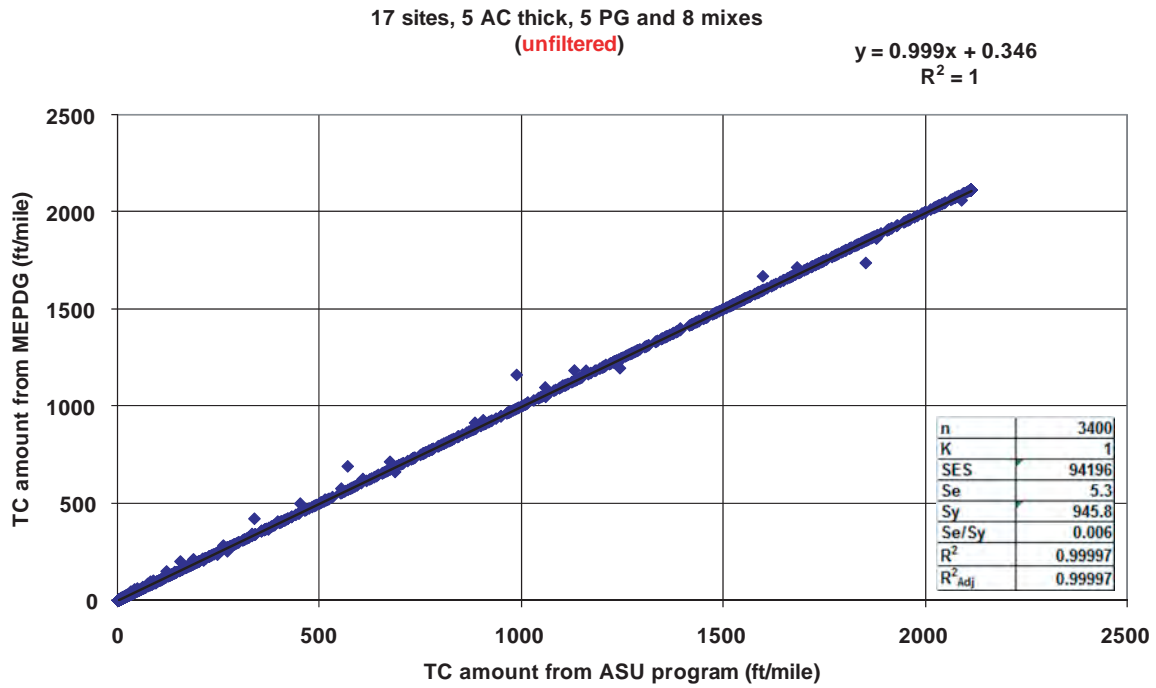


Figure 49. Comparison of thermal cracking amount between MEPDG and ASU program (unfiltered).

It was hypothesized that these small differences could be explained as follows. As mentioned earlier, in developing the thermal cracking program, the project team tried to replicate the process used in the MEPDG. The team compared each analysis step between the two methods and found out that several significant discrepancies occurred in the power model parameters D_1 , D_0 , and m -value.

Since 40 different mixes (5 binder * 8 combinations of volumetric) were investigated in the analysis, the same number of power models were produced. Of those mixes, five yielded parameters in the MEPDG that were different from those computed from the project program. Careful checking of the parameters by a manual calculation using an Excel spreadsheet was conducted and the team concluded that the MEPDG,

specifically the “tcmol.exe” code, occasionally produces incorrect parameters. The comparison of the inconsistent parameters is presented in Table 20. Figure 50 shows the comparison of those parameters computed from (1) the MEPDG, (2) the program developed in this project, and (3) the Excel spreadsheet. Most notably, the project program and the manual method using Excel produce very close parameters, while the MEPDG does not.

After filtering the five cases yielding the incorrect power model parameters, the comparison plot was re-drawn and is presented in Figure 50. The scattered data points in Figure 49 termed “unfiltered” disappeared as shown in the “filtered” plot. In addition, the R^2 value and Se/Sy became slightly better.

Table 20. Comparison of the power model parameters.

Mix Type (PG-V _b -V _a)	MEPDG			ASU program			Excel spreadsheet		
	D ₀	D ₁	m	D ₀	D ₁	m	D ₀	D ₁	m
5240-8-10	1.91E-07	1.15E-08	0.696	2.56E-07	8.51E-09	0.726	2.55E-07	8.51E-09	0.726
5834-8-3	2.61E-07	1.51E-08	0.593	2.38E-07	1.92E-08	0.566	2.38E-07	1.92E-08	0.566
5834-12-3	2.30E-08	2.30E-08	0.636	3.47E-07	3.18E-08	0.595	3.47E-07	3.18E-08	0.595
5834-12-8	2.81E-08	2.81E-08	0.610	4.99E-07	3.67E-08	0.581	4.99E-07	3.67E-08	0.581
5834-16-4	3.54E-08	3.54E-08	0.643	5.46E-07	4.89E-08	0.602	5.46E-07	4.89E-08	0.602

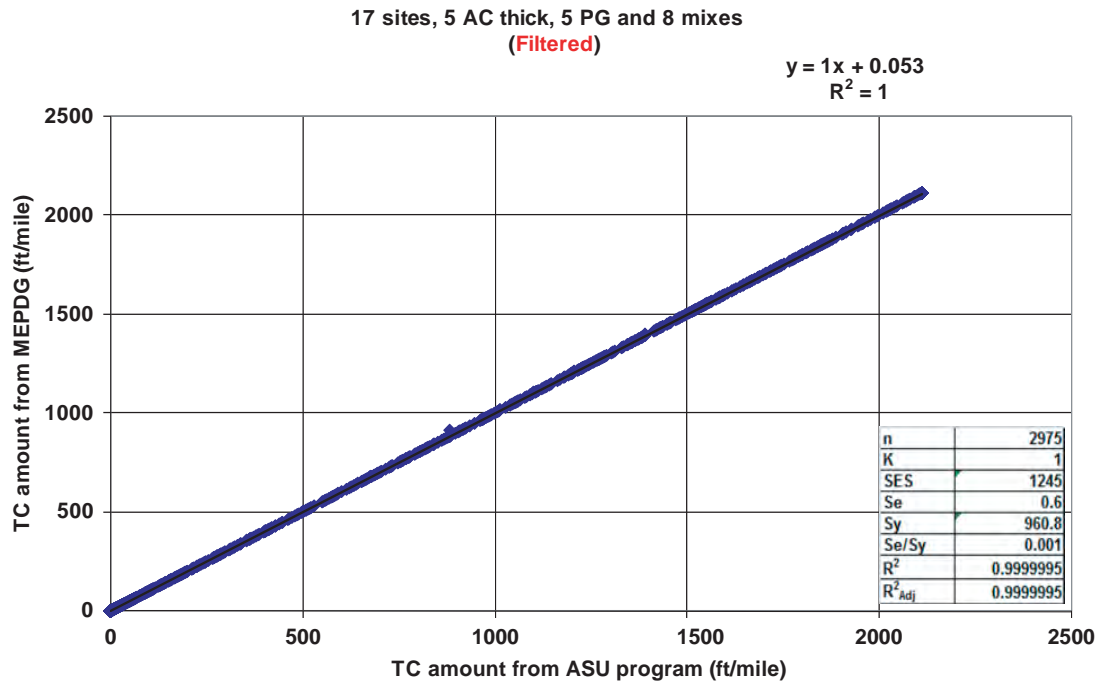


Figure 50. Comparison of thermal cracking amount between MEPDG and ASU program (filtered).

CHAPTER 3

Development of the Quality Related Specification and Software

3.1 Introduction

The QRSS provides two analysis modes: Mode I and II. Mode I, “Performance Pay Factor Analysis,” is intended for use as a construction quality assurance tool. The user measures as-built pavement properties (AQCs such as air voids and binder content) and then uses the QRSS to calculate fundamental engineering properties (i.e., dynamic modulus for the analysis of FC and AC rutting; and creep compliance for the analysis of thermal fracture), convert them into predictions of the magnitude of potential distresses, compare these predictions with those obtained from the job mix formula (the as-designed mix), determine the pay factors, and decide whether the construction is subject to an incentive or disincentive. An incentive is awarded to the contractor or the contractor is penalized due to poor pavement construction based upon the pay factor system.

Mode II, “Interactive Mix and Structure Design,” is a tool for finding an appropriate mix for a specific pavement structure. Using the relationships between AQCs, fundamental engineering properties, and distress, the user has an option to change either the mix or structure, or both simultaneously, in order to achieve an integrated design of mix and structure that meets the requisite performance limits.

The QRSS inputs will vary depending on the selection of the distress type(s) of interest and the mode. For example, if Mode I is selected, additional information will be needed that includes QA data for the as-built project.

The program starts with the introduction screen followed by the selection of the mode. Then, depending on the mode selected, its analysis flow bifurcates as shown in Figure 7 (Chapter 1). Basically, the QRSS input system is divided into three parts:

- Initial Inputs (Mode I and II)—refer to Table 21
- Inputs for probabilistic analysis of the as-designed mix (Mode I)—refer to Table 22
- Inputs for the as-built mix and pavement (Mode I)—refer to Table 23

The initial inputs will include general project information, such as project ID and name, and basic design input variables, such as traffic and structure. Some input properties are commonly used for all three distresses, while some are not. For instance, design traffic speed is not required for the analysis of thermal cracking, whereas it is a critical input for the rutting and FC analyses. The required initial inputs for each distress are specified in Table 21.

Second, for the operation of pay factor analysis (Mode I), the program requires information on the as-designed mix to set a quality standard for a particular construction project. For the probabilistic analysis, (historical) standard deviations of some critical properties must be input so that frequency distribution curves for the intended distress type can be developed. Table 22 summarizes the JMF input properties.

Third, the program requires as-built mix and pavement data as inputs to develop the predicted distress distribution for the project. These inputs are summarized in Table 23.

Finally, the program requires the inputs shown in Table 24 to carry out the pay factor analysis for the distress types of interest.

3.2 Determination of Deterministic Solution

There are two steps in the quality related specification of an AC layer: (1) a deterministic analysis of a mix design, a structural design, or a combination of the two; and (2) a probabilistic analysis to assess the variability of the as-built AC.

The main aim of the deterministic analysis is to develop a relationship between the pavement distress and the dynamic modulus (E^*) or creep compliance (D) of the AC layer. These relationships are developed using the closed form solutions for each distress described in the previous chapter. These relationships can be used as mix design or structural design tools. They are also needed to conduct the probabilistic analysis.

Table 21. Critical inputs in the initial input screen.

Critical Inputs		Unit	Rutting	Fatigue Cracking	Thermal Cracking	IRI
1. Project General Input	Project ID	N/A	○	○	○	○
	Project Location	N/A	○	○	○	○
	Date of Analysis	N/A	○	○	○	○
	Operator's Name	N/A	○	○	○	○
2. Traffic	Design Life	yr.	√	√	√	○
	Design Traffic Speed	mph	√	√	○	○
	Initial ESAL	N/A	√	√	○	○
	Annual Growth Rate (r)	%	√	√	○	○
	Total ESAL	N/A	C	C	-	-
3. Pavement Structure	AC Surface Thickness	in.	√	√	√	○
	AC Binder Thickness	in.	○	○	○	○
	AC Base Thickness	in.	○	○	○	○
	Base Thickness	in.	○	√	○	○
	Base Modulus	psi	○	√	○	○
	Subbase Thickness	in.	○	√	○	○
	Subbase Modulus	psi	○	√	○	○
	Subgrade Modulus	psi	○	√	○	○
3.1. AC Material Properties for All AC Layers	Design Air Voids	%	○	○	○	○
	Asphalt Content by Weight	%	√	√	√	○
	Binder Type (Select PG, AC, Pen or A / VTS)	VAR	√	√	√	○
	Sp. Gr. of Binder	N/A	√	√	√	○
	Target In-Situ V_a	%	√	√	√	○
	Bulk Sp. Gr. of Mix (Gmb)	N/A	√	√	√	○
	Bulk Sp. Gr. of Agg. (Gsb)	N/A	√	√	√	○
	Theoretical Bulk Sp. Gr. of Mix (Gmm)	N/A	√	√	√	○
	Eff. Binder Content by Vol. (V_{beff})	%	C	C	C	-
	VMA	%	C	C	C	-
	VFA	%	C	C	C	-
	Passing 1½"	%	○	○	○	○
	Passing 1"	%	○	○	○	○
	Passing ¾"	%	√	√	○	○
	Passing ½"	%	○	○	○	○

Table 21. (Continued).

Critical Inputs		Unit	Rutting	Fatigue Cracking	Thermal Cracking	IRI
3.1. AC Material Properties for All AC Layers	Passing 3/8"	%	√	√	○	○
	Passing #4	%	√	√	○	○
	Passing #8	%	○	○	○	○
	Passing #10	%	○	○	○	○
	Passing #16	%	○	○	○	○
	Passing #30	%	○	○	○	○
	Passing #40	%	○	○	○	○
	Passing #50	%	○	○	○	○
	Passing #100	%	○	○	○	○
	Passing #200	%	√	√	○	○
4. Climatic Location	Select Specific Location or Enter Geographical Position (Lat., Long, El.)	VAR	√	√	√	√
	Mean Annual Average Temperature	°F	C	C	-	-
	Mean Monthly Air Temperature	°F	C	C	-	-
	Temperature St. Dev.					
	Mean Annual Wind Speed	mph	C	C	-	-
	Mean Annual Sunshine	%	C	C	-	-
	Annual Cumulative Rainfall Depth	in.	C	C	-	-
	Pavement Temperature with Depth	°F	-	-	C	-
5. Design limit (Performance Criteria)	AC Rutting	in.	√	-	-	-
	Fatigue Cracking	%	-	√	-	-
	Thermal Cracking	ft/mile	-	-	√	-
	IRI	in/mile	-	-	-	√
6. Mix Design	SPT Recom. Freq.	Hz	√	√	-	-
	SPT Recom. Temp.	°F	C	C	-	-
○	Information Not Required					
C	Information Computed from other inputs					
√	Information needed as input					

Table 22. Critical inputs for probabilistic analysis of job mix formula (as-designed).

Critical Inputs	Unit	Rutting		Fatigue .C.		Thermal C.	
		Mean	S.D.	Mean	S.D.	Mean	S.D.
Total AC Thickness	in.	-	-	T	H.V.	T	H.V.
Target In-Situ Air Voids	%	T	H.V.	T	H.V.	T	H.V.
Effective Binder Content by Vol.	%	C	C	C	C	C	C
Cum. Retained 3/4	%	T	H.V.	T	H.V.	-	-
Cum. Retained 3/8	%	T	H.V.	T	H.V.	-	-
Cum. Retained #4	%	T	H.V.	T	H.V.	-	-
Passing #200	%	T	H.V.	T	H.V.	-	-
Gmm	N/A	T	H.V.	T	H.V.	T	H.V.
Gmb	N/A	T	H.V.	T	H.V.	T	H.V.
Gsb	N/A	T	H.V.	T	H.V.	T	H.V.
Asphalt Content by Weight	%	T	H.V.	T	H.V.	T	H.V.
Ai	N/A	T	-	T	-	T	C
VTSi	N/A	T	-	T	-	T	C
Effective Temperature	°F	C	-	C	-	-	-
Effective Frequency	Hz	C	-	C	-	-	-

Legend

-	Information Not Required
C/T	Information Computed from other inputs / Transported from the initial input screen
H.V.	historically known value or the user can input (Default value is provided)

3.2.1 Mix Design

The main purpose of the mix design option (Mode II) is to provide a tool to select the appropriate mix properties for a project. A second purpose is to provide a tool for evaluating interactions between the mix and structural designs. The design acceptance is based on the calculated dynamic modulus and creep compliance of the HMA mixture and the predicted distresses. The predicted distresses are then compared with limiting values (criteria). If the criteria are not met, the design (structural or mix) is modified and the process is repeated until satisfactory results are obtained.

The mix design option requires inputs that quantify the mix and structural design. These include, for example, the volumetric properties and gradation of the HMA mixture, the thickness of the AC layer, and the thickness and modulus of the unbound layers. Also, the limiting values (criteria) are set in accordance with agency policy.

The process of the mix design analysis for rutting and FC is to predict the HMA dynamic modulus using the WPE, as explained in Chapter 2 “Determination of Dynamic Modulus E^* .” The E^* is calculated at a certain frequency and temperature that are referred to as the effective temperature and frequency, as also explained in Chapter 2. The dynamic modulus predicted at the effective temperature and frequency is called effective modulus.

The effective temperatures for rutting and FC are obtained from the climatic conditions at the project site, explained in Chapter 2. The effective frequency is a function of depth, traffic speed, and layer modulus, while the effective modulus is a function of the temperature and the frequency. Accordingly, an iteration process is required to determine the effective modulus, by assuming an initial value of the frequency to calculate the temperature and modulus, then iterating to converge the difference between the assumed and predicted effective modulus.

Table 23. Critical inputs for as-built pavement property for each distress.

Critical Inputs		Unit	Rutting	Fatigue Cracking	Thermal Cracking	IRI
1. Project General Input	Mix Design Type (Gyratory or Marshall)	N/A	○	○	○	○
	Lot Definition (Constant Tonnage or Daily Production)	N/A	√	√	√	√
	Number of Lot	N/A	√	√	√	○
	Date of Each Lot	N/A	√	√	√	○
2. General Statistical Analysis Input (For Gradation, Binder, and E*)	Number of Sample	1 to 10	√	√	√	-
	Hist. Std. Dev.	Var	T or D	T or D	T or D	-
	Reliability	%	○	○	○	-
	Significance Interval	N/A	○	○	○	-
	Target Value	Var	T or D	T or D	T or D	-
3. Gradation	Passing 1 ½"	%	○	○	○	-
	Passing 1"	%	○	○	○	-
	Passing ¾"	%	√	√	○	-
	Passing ½"	%	○	○	○	-
	Passing 3/8"	%	√	√	○	-
	Passing #4	%	√	√	○	-
	Passing #8	%	○	○	○	-
	Passing #10	%	○	○	○	-
	Passing #16	%	○	○	○	-
	Passing #30	%	○	○	○	-
	Passing #40	%	○	○	○	-
	Passing #50	%	○	○	○	-
	Passing #100	%	○	○	○	-
Passing #200	%	√	√	○	-	
4. In-situ Volumetric	Asphalt Content	%	√	√	√	-
	Rice Sp. Gr. (Gmm)	N/A	√	√	√	-
	Bulk Density	lb/in ³	√	√	√	-
	Air Voids	%	√	√	√	-
	AC Thickness	in	○	○	○	-
	Sp. Gr. of Binder (Gsb)	N/A	√	√	√	-
5. Binder	PG or AC or Pen	N/A	√	√	√	-

Table 23. (Continued).

Critical Inputs		Unit	Rutting	Fatigue Cracking	Thermal Cracking	IRI
6. E*	Air Voids	%	√	√	-	-
	Eff. Binder Content	%	√	√	-	-
	Cum. Retained 3/4"	%	√	√	-	-
	Cum. Retained 3/8"	%	√	√	-	-
	Cum. Retained #4	%	√	√	-	-
	Passing #200	%	√	√	-	-
7. IRI	Number of Lane	1 to 12	-	-	-	√
	Unit Mileage	N/A	-	-	-	√
	Average IRI	in/mile	-	-	-	√

Legend

O / -	Information Not Required
T or D	Information Computed from other inputs/ Transported from the initial input screen
√	Historically known value or the user can input (default value is provided)

The effective modulus, effective temperature, and effective frequency are obtained for each sublayer of the pavement HMA layers. Then the rutting and FC distresses are predicted from the CFS models. A relationship is obtained between the predicted distress and the effective modulus. This relationship is only valid for the specified traffic, structure, climate, and material properties.

The predicted rutting is reported as the summation of the sublayer rutting, while, the predicted E* is the modulus of the critical sublayer (most rutting). For FC, the E* used in the subroutine corresponds to the E* for the bottom HMA layer. Finally, the thermal cracking subroutine is run using the properties of the surface layer. The predicted distresses are then compared to the limiting values (criteria). If the pre-

Table 24. Critical inputs pay factors.

Critical Inputs		Unit	Rutting	Fatigue Cracking	Thermal Cracking	IRI
1. Pay Adjustment Factor (Rutting, Fatigue, IRI)	Max. Bonus	%	√	√	√	√
	Max. Penalty	%	√	√	√	√
	Max. PLD	yr.	√	√	√	√
	Min PLD	yr.	√	√	√	√
	PLD for no Bonus	yr.	√	√	√	√
	PLD for no Penalty	yr.	√	√	√	√
	PLD for Remove and Replace	yr.	√	√	√	√
	Traffic Type	N/A	-	-	-	√

Legend

O	Information Not Required
C	Information Computed from other inputs
√	Information needed as input

dicted values are less than or equal to the criteria, the mix and structural designs are accepted. If the predictions are greater than the criteria, adjustments are needed to lower the predicted distresses or increase the effective modulus or structure. The proposed adjustments can be either in the form of modifying the mixture properties or modifying the pavement structure. Another round of comparison is then conducted until the predictions meet the criteria set by the agency.

The following sections discuss the use of the relationship between dynamic modulus and rutting and FC distress.

3.2.2 E* Testing Temperature and Frequency

The effective temperature and frequency are calculated values from the QRSS analysis module. Often, the required loading frequency is not practical to use in actual testing⁵ to measure E*.

Most testing machines used to measure E* values have limits on the frequency and temperature used to perform the test. For example, the testing frequency on many types of loading systems generally should not exceed 25 Hz, while the value predicted from the QRSS analysis might exceed this value. Accordingly, the frequency needs to be adjusted to a suitable frequency that can be applied by the dynamic testing machine. The user is given an option to input the frequency that will be used to perform the E* test. Changing the frequency will lead to correcting the corresponding temperature while keeping the modulus constant. The following equation is used to solve for the temperature from the user inputted frequency.

$$\log(T) = \frac{\log \left[\frac{\log \left(\frac{1}{f} \right) + c \log(\eta_{tr}) - \frac{\ln \left(\frac{\alpha}{\log E^* - \delta} - 1 \right) - \beta}{\gamma}}{c} \right] - A}{VTS} \quad (69)$$

where

T = temperature in degrees Rankine (°F + 459.7)

E* = dynamic modulus

f = loading frequency (Hz)

$\alpha, \beta, \gamma, \delta, c$ = regression coefficients

η_{tr} = viscosity at reference temperature, centipoise

A, VTS = viscosity – temperature susceptibility coefficients

⁵AASHTO TP 62, Determining Dynamic Modulus of Hot Mix Asphalt (HMA), and AASHTO TP 79, Determining the Dynamic Modulus and Flow Number for Hot Mix asphalt (HMA) Using the Asphalt Mixture Performance Tester (AMPT).

The modulus E* used in Equation 69 will be the effective modulus predicted from the mix design analysis, i.e., there will be no change in the modulus value. What will change is the temperature and frequency at which the E* testing will be conducted.

3.2.3 Dynamic Modulus-Distress Relationship for Rutting

A primary goal of developing performance tests in NCHRP Project 9-19 was to provide the engineer with tools to determine if the mix being designed with the Superpave volumetric approach was appropriate to withstand the unique project conditions according to the design limit (the Rutting Failure Criterion, RFC) specified by the engineer. This process is implemented in Mode II of the QRSS; a schematic example is presented in Figure 51.

Having a defined, constant E* versus rutting relationship (and an RFC-E*_{ALLOW} relationship) for the project traffic, environmental, and project structure conditions, the user of Mode II has the opportunity of assessing the mix E*. If it is found to be unsatisfactory, the design may be changed until the mix meets the criteria.

The user can test mixes which will fall in the Rejection Region (square in Figure 51) or Acceptance Region (triangle in Figure 51) and, based on these tests, define the appropriate mix for the project. Critical in this approach is the availability of a methodology that can determine the effective temperature and frequency of the as-designed mix associated with the design input conditions.

Similarly, the pavement structure can be modified. A structural modification will provide a new distress relationship as demonstrated in Figure 51 by the dotted lines. The new relationship can then be compared to the criteria and a decision to accept or reject the new structure can be made. *However, it is imperative for the user to understand that structural (thickness) changes will likely have a minimal effect upon the HMA rutting criteria. From a practical standpoint, if HMA rutting criteria cannot be met, the most significant way to meet the criteria is to enhance the quality of the HMA mix.*

3.2.4 Dynamic Modulus-Distress Relationship for FC

The relationship between dynamic modulus and FC shows two different patterns depending upon AC layer thickness. For a pavement having a thick (generally greater than 3 in. to 4 in.) AC layer, the fatigue distress increases with the decrease of the layer stiffness (E*) to a certain point as shown in Figure 52.

On the other hand, a pavement system having a thin AC layer shows the opposite behavior. Since the thin AC layer gets brittle and is prone to the development of higher tensile strains with an increase of AC layer stiffness, FC will obviously increase as depicted in Figure 53.

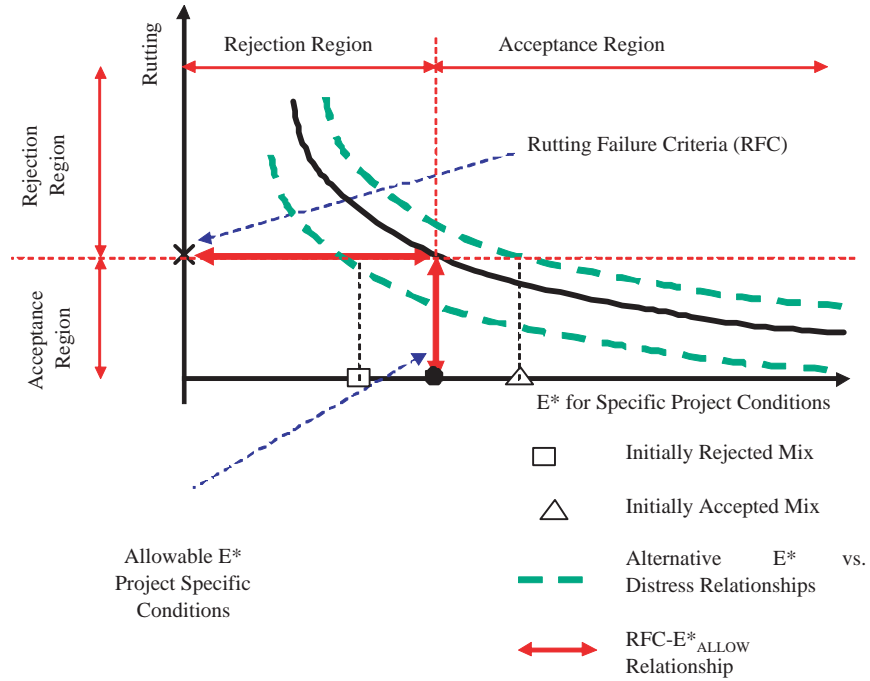


Figure 51. Schematic of rutting- E^* relationship for a given climatic, traffic, and AC layer structural characteristics.

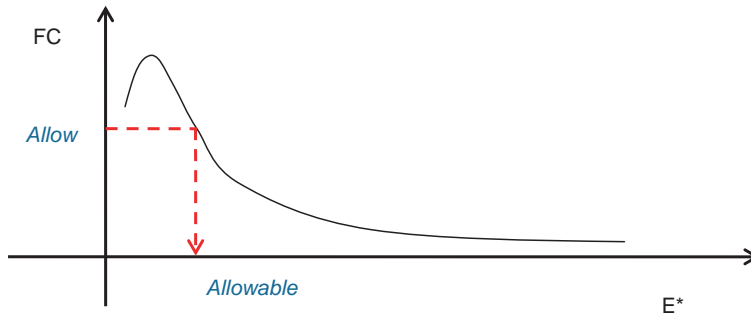


Figure 52. FC- E^* relationship for thick HMA layers.

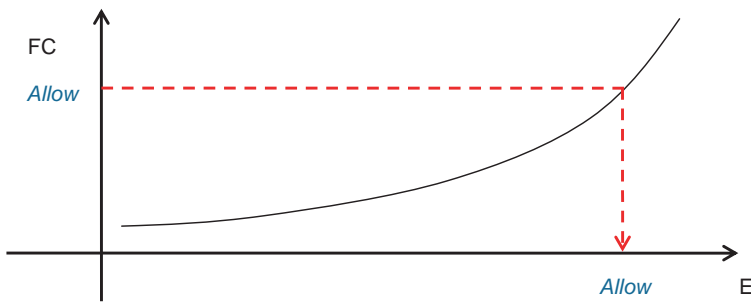


Figure 53. FC- E^* relationship for thin HMA layers.

3.3 Determination of a Probabilistic Solution

The QRSS uses probabilistic analysis to study the variability of different properties of HMA. The output of the probabilistic analysis will be the mean and the standard deviation of the dynamic modulus (E^*) or creep compliance (D), which in turn is used to predict the pavement distress as explained in Chapter 2. In the following sections, different aspects of the QRSS probabilistic solutions are explained.

3.3.1 Analysis of Variance for Significance of Regression

3.3.1.1 Regression Model Analysis of Variance

Analysis of variance (ANOVA) (22,23) is a statistical tool for determining the degree of correlation or significance between measured (observed) values and the predicted responses obtained from equations or models (regressions). For simplicity, the use of ANOVA for the Significance of Regression will be briefly explained through the use of the following.

Let

$$\hat{y} = f(x_1, x_2, x_3, \dots, x_k) + e \quad (70)$$

be a regression model on the observed or measured values “ y ” based on “ k ” regressors $x_1, x_2, x_3, \dots, x_k$, and with “ $p=k+1$ ” regression coefficients. Of interest is whether the predicted \hat{y} value correlates appropriately to the observed data y , or in other words, whether the error between the measured (y_i) and the predicted values (\hat{y}_i), e_i , is significant or insignificant. In order to determine this, several parameters must be calculated from the data. The first parameter that can be obtained is the residual sum of squares (SS_{RES}), as follows:

$$SS_{RES} = \sum_{i=1}^n e_i^2 = \sum_{i=1}^n (y_i - \hat{y}_i)^2 \quad (71)$$

The next parameter obtained is the total sum of squares (SS_T):

$$SS_T = \sum_{i=1}^n (y_i - \bar{y})^2 \quad (72)$$

Where, \bar{y} is the average of the measured or observed y_i values. Once these parameters are known, the regression or model sum of squares (SS_R) can be calculated as follows:

$$SS_R = SS_T - SS_{RES} \quad (73)$$

Every sum of squares is associated with a determined number of degrees of freedom (d.f.). Thus, for the SS_T , there are “ $n-1$ ” d.f.; for the SS_{RES} there are “ $n-p = n-k-1$ ” d.f.; and for

the SS_R there are “ k ” d.f. Dividing the sum of squares by their degrees of freedom, the regression mean squares (MS_R) and residual mean squares (MS_{RES}) can be calculated as follows:

$$MS_R = \frac{SS_R}{k} \quad (74)$$

$$MS_{RES} = \frac{SS_{RES}}{n-k-1} = \frac{SS_{RES}}{n-p} \quad (75)$$

The significance of regression can then be tested using the F statistic “ F_0 ,” calculated as follows:

$$F_0 = \frac{SS_R/k}{SS_{RES}/(n-k-1)} = \frac{MS_R}{MS_{RES}} \quad (76)$$

This F_0 value follows a statistical $F_{k,n-k-1}$ distribution. This statistic is a measure of whether the proposed regression is significant; however, the statistic does not measure the goodness of the correlation. To do that, two other parameters are widely used. The coefficient of multiple determinations (R^2) is calculated from

$$R^2 = \frac{SS_R}{SS_T} = 1 - \frac{SS_{RES}}{SS_T} \quad (77)$$

The Adjusted R^2 (R^2_{adj}) is calculated from

$$R^2_{adj} = 1 - \frac{SS_{RES}/(n-p)}{SS_T/(n-1)} \quad (78)$$

which can be rewritten as follows:

$$R^2_{adj} = 1 - \frac{(n-1)}{(n-p)} \times \left(\frac{Se}{Sy} \right)^2 \quad (79)$$

where

Se = standard error of estimate = $\sqrt{SS_{RES}}$

Sy = standard deviation of the criterion variable = $\sqrt{SS_T}$

For linear models, R^2 and R^2_{adj} are measures of model accuracy. However, it is important to recognize that for evaluation of non-linear models, neither R^2 nor R^2_{adj} are good measures of model accuracy since they depend on a linear separation of the variables. Instead, the standard error ratio or relative accuracy, Se/Sy , is used to assess the accuracy of non-linear models.

3.3.1.2 QA Data Statistical Analysis and ANOVA

Different data analysis options are provided in the QRSS to analyze QA data, including ANOVA and other statistical analysis and charts. These analysis options are provided to aid

LOT #	Date	Sample1	Sample2	Sample3	Sample4
1	7/17/2000	92.0	94.0	96.0	97.0
2	7/18/2000	93.0	93.0	96.0	96.0
3	7/20/2000	95.0	95.0	95.0	98.0
4	7/21/2000	93.0	95.0	94.0	93.0
5	7/22/2000	93.0	92.0	96.0	96.0
6	7/24/2000	97.0	92.0	92.0	93.0
7	7/25/2000	98.0	96.0	91.0	96.0
8	7/26/2000	97.0	94.0	95.0	94.0
9	7/27/2000	93.0	95.0	96.0	94.0
10	7/28/2000	95.0	95.0	96.0	97.0

Figure 54. Example of QA statistical analysis.

in checking the quality of construction on a daily basis and make quick decisions to correct for errors.

The QA data is collected for every lot (or day's production). Data may be collected on two to 10 samples per lot. In addition to the number of samples, the historical standard deviation, reliability level, and target value are needed. Figure 54 shows an example of the QRSS input data.

The historical standard deviation and the reliability level are used to calculate the significance interval (+R and -R) as shown in the following equation:

$$+R = \text{InvNorm}(\text{Rel}) * \sqrt{\frac{\text{Stdev}^2}{\text{Num}}} \quad (80a)$$

$$-R = -\text{InvNorm}(\text{Rel}) * \sqrt{\frac{\text{Stdev}^2}{\text{Num}}} \quad (80b)$$

where

InvNorm = inverse of standard normal cumulative distribution

Rel = reliability (%)

Stdev = standard deviation

Num = number of samples

For each lot, the following statistical parameters are calculated, as shown in Figure 55:

- mean = $\bar{X} = \sum \frac{X}{\text{Num}}$
- standard deviation = $\sigma = \sqrt{\frac{\sum (X - \bar{X})^2}{\text{Num}}}$
- coefficient of variation = $\frac{\sigma}{\bar{X}} * 100$
- range = maximum - minimum
- Lower control limit (LCL) = mean of the ranges of all lots * D_1 (Table 25)
- Upper control limit (UCL) = mean of the ranges of all lots * D_2 (Table 25)
- target value (TV) = design value or overall average of all lots
- lower limit (LL) = TV - R
- upper limit (UL) = TV + R

LOT #	Average	Sample Variance	Coeff. of Variation (%)	Range	LCL	UCL	LL	TV	UL
1	94.8	4.9	2.34	5.0	0.0	9.2	91.0	92.0	93.0
2	94.5	3.0	1.83	3.0	0.0	9.2	91.0	92.0	93.0
3	95.8	2.3	1.57	3.0	0.0	9.2	91.0	92.0	93.0
4	93.8	0.9	1.02	2.0	0.0	9.2	91.0	92.0	93.0
5	94.3	4.3	2.19	4.0	0.0	9.2	91.0	92.0	93.0
6	93.5	5.7	2.55	5.0	0.0	9.2	91.0	92.0	93.0
7	95.3	8.9	3.13	7.0	0.0	9.2	91.0	92.0	93.0
8	95.0	2.0	1.49	3.0	0.0	9.2	91.0	92.0	93.0

Figure 55. Example of QA statistical analysis.

A second critical statistical analysis is the ANOVA, as shown in Figure 56. ANOVA is conducted on a given variable for samples obtained by lot (treatment). The overall average, pooled variance, and pooled coefficient of variation are calculated. At the same time, an ANOVA and F-test are conducted to check the significance of differences between lots and samples. Finally, hypothesis testing is done at different significance levels of 5% and 1% on the average values of the lots to determine whether they are the same or different. A control chart is generated to clearly present the results of the statistical analysis, as shown in Figure 57.

3.3.2 Monte Carlo Simulation

Monte Carlo simulation determines the variance of the function $f(x_1, x_2, \dots, x_k)$ by generating random values for the different variables using their individual probability distributions. Hundreds or thousands of simulations may be required to calculate the variance of the function f . As a consequence, this simulation technique requires significant computational power.

The simulation starts with the input of the characterization parameters for the probability distribution of each stochastic variable. For example, if the variables follow a normal distribution,

then the mean and variance of the distribution would be necessary.

The next step is to generate a random value for all the stochastic variables, input them in the function $f(x_1, x_2, \dots, x_k)$, and record a value f_1 for Simulation Number (SN-) 1. The process is repeated for SN-2, The value f_2 is recorded, and the average and variance between f_1 and f_2 is obtained. With SN-3, the value f_3 is recorded and the average and variance is calculated based on three values ($f_1, f_2,$ and f_3). The process is repeated “n” times. For SN-(n+1), the variance should not differ significantly from the variance calculated with SN-(n) based on f_1, f_2, \dots, f_n . Plots of convergence are obtained like the one in Figure 58 to help determine when to stop the simulation.

As can be seen, the Monte Carlo simulation is a powerful tool, especially when the predictive function is a closed form equation. In this case, thousands of simulations can be easily performed within a matter of seconds in a spreadsheet. However, Monte Carlo simulation may require a significant number of runs, and it may become impractical or computationally challenging, when a large number of variables are involved in the Function f .

3.3.3 Rosenblueth Method

A major difference between the thermal cracking module and the rutting and FC modules in the QRSS deals with the method of determining the variability of the distress prediction. For rutting and FC, the Monte Carlo simulation described in the previous section is used.

On the other hand, if the prediction model is not a closed form equation, as is the case with the thermal cracking analysis in the QRSS, the number of the Monte Carlo simulations and the corresponding simulation time become problematic. Using Monte Carlo simulation, the thermal cracking program required approximately 1 to 5 seconds per simulation, depending on computer capacity and analysis conditions. Thus, if

Table 25. Control limits multiplier.

Number of Sample	LCL Factor, D_1	UCL Factor, D_2
2	0	3.267
3	0	2.574
4	0	2.282
5	0	2.114
6	0	2.004
7	0.076	1.924
8	0.136	1.864
9	0.184	1.816
10	0.223	1.777

Summary of Pooled Variance

Total Average of All Samples	94.3
Total Average Range of All Lots	4.0
Pooled Sample Variance, S	4.1
Sample Coefficient of Variation CV	2.2
Pooled Lot Variance	0.7
Lot Coefficient of Variation	0.9

Analysis of Variance

Source	Sum of Squares	Deg. of Freedom	Mean Square	F	Critical F @ $\alpha = 0.05$	Critical F @ $\alpha = 0.01$
Lot	196.3	29	6.8	1.63	1.59	1.93
Sample	373.3	90	4.1			
Total	569.6	119				

ANOVA Variance Estimates

Lot Variance Estimate	0.7
Sample Variance Estimate	4.1

Final Decision

Hypothesis	95%	99%
Lot	No	Yes

Project Variance

Variance at $\alpha = 0.05$	σ_s^2	4.1
	σ_i^2	0.66
Variance at $\alpha = 0.01$	σ_s^2	4.8
	σ_i^2	N/A

Figure 56. Example of QA/QC ANOVA.

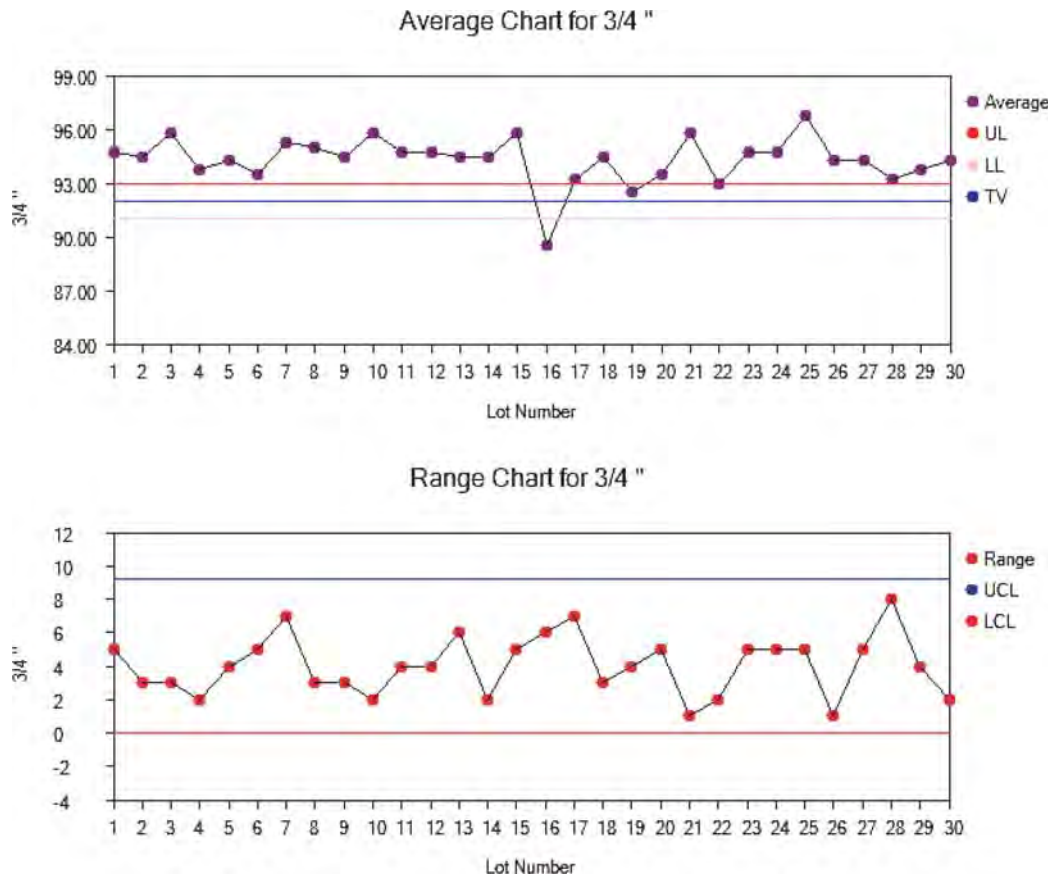


Figure 57. Example of QA/QC control charts.

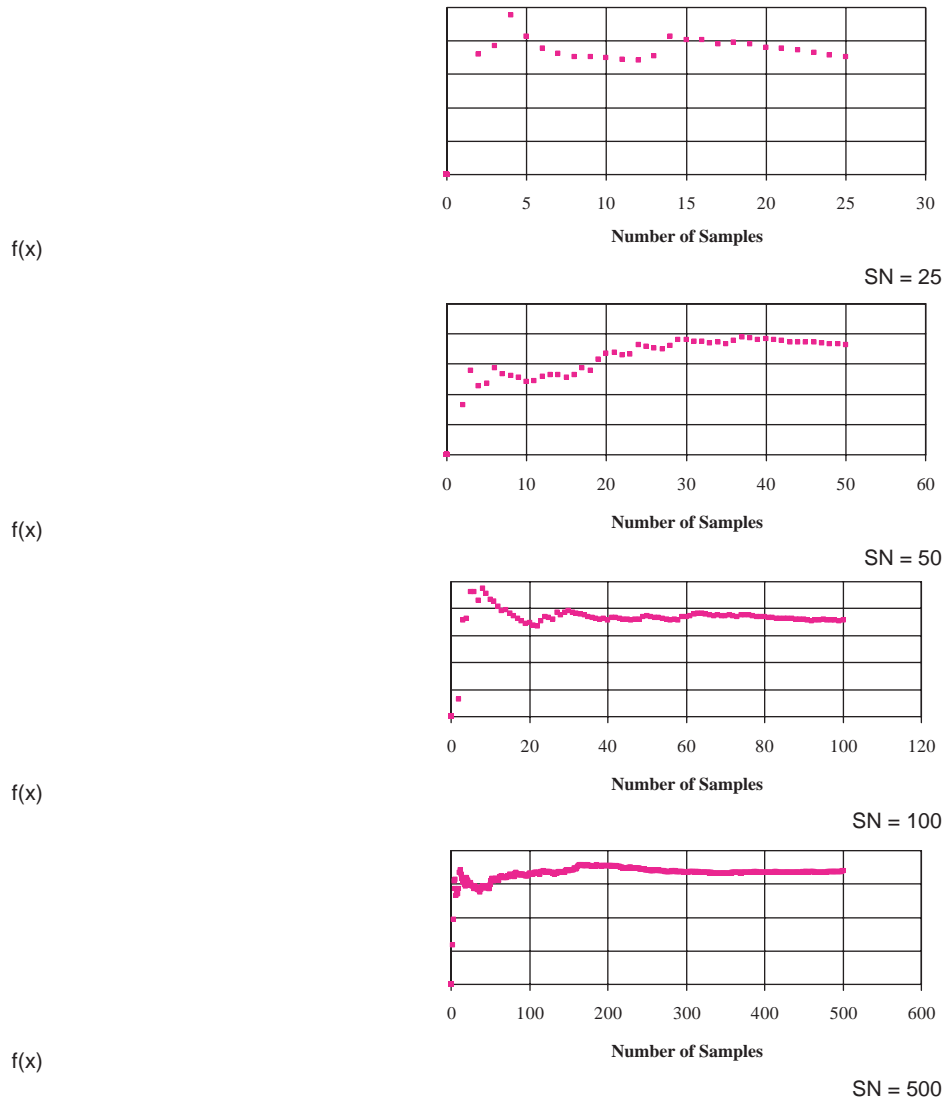


Figure 58. Example of convergence of variance for a Function f under the Monte Carlo simulation for different number of samples/simulations.

1,000 simulations were run, the analysis would require at least 16 minutes, and possibly as long as 83 minutes, which seemed impractical.

For this reason, the project team chose to use the Rosenblueth point-estimate method for the thermal cracking simulation. The main advantage of the Rosenblueth method is that it can significantly reduce the number of simulations needed. For the 2-point Rosenblueth with five variables, only 32 simulations ($2^5=32$) are needed. For the 3-point Rosenblueth in the same case, the number increases to 243 ($3^5=243$). Weighing both computation time and statistical accuracy, the decision was made to the 2-point Rosenblueth method for the probabilistic analysis of the thermal cracking.

In the 2-point Rosenblueth method, the variance of the given function, $y=f(x_1, x_2, \dots)$, can be simply calculated by the following equation.

$$V[y] = E[y^2] - (E[y])^2 \quad (81)$$

where

$V[y]$ = variance of the given function, y

$E[y^2]$ = expectation of y^2

$E[y]$ = expectation of y

The expectations of y and y^2 can be computed as:

$$E[y^m] = (1/2)(y_+^m + y_-^m) \quad (82)$$

for one variable, $y=f(x_1)$ and

$$E[y^m] = (1/2)^2 (y_{++}^m + y_{+-}^m + y_{-+}^m + y_{--}^m) \quad (83)$$

for two variables, $y=f(x_1, x_2)$

where

m = index (superscript) for y and y^2

y_+^m = y evaluated for x_1 plus one standard deviation of x_1

y_-^m = y evaluated for x_1 minus one standard deviation of x_1

y_{++}^m = y evaluated for x_1 plus one standard deviation of x_1 and x_2 plus one standard deviation of x_2

y_{+-}^m = y evaluated for x_1 plus one standard deviation of x_1 and x_2 minus one standard deviation of x_2

y_{--}^m = y evaluated for x_1 minus one standard deviation of x_1 and x_2 minus one standard deviation of x_2

y_{-+}^m = y evaluated for x_1 minus one standard deviation of x_1 and x_2 , plus one standard deviation of x_2

Since the thermal cracking prediction analysis includes five variables (viz., V_a , V_{beff} , AC thickness, A_i , and VTS_i), the proce-

dures shown in Equations 81-83 is expanded for a five-variable function [i.e., $y = f(x_1, x_2, x_3, x_4, x_5)$] by adding appropriate y^m terms. The total number of y^m terms is thus $2^5 = 32$. It should be noted that this number is reduced by a half (to 16) due to the correlation between A_i and VTS_i which will be explained later in this chapter.

The following examples illustrate the Rosenblueth method. An as-designed (JMF) mix is selected. The pavement structure and mix conditions along with assumed standard deviations are shown in Table 26. Based upon the information given, the thermal cracking prediction program estimates thermal cracking 16 (2^4) times. Averages and standard deviations of the thermal cracking (TC) as well as the service life (SL) are computed and the results are shown in Table 27. These statistics are then employed to develop the corresponding beta distributions.

Table 26. Input conditions for as-designed JMF mix.

Variable	Average	Standard Deviation	CV (%)
AC Thickness (in.)	4.0	0.801	20.0
Target In-Situ V_a (%)	7.5	0.685	9.1
Effective V_b (%)	9.0	0.198	2.2
A_{RTFO}	10.015	0.033	0.33
VTS_{RTFO}	-3.315	0.012	0.35
Location: Chicago, IL			
Design Life: 20 years			

Table 27. Rosenblueth table and results for as-designed JMF mix.

Rosenblueth Table							Output			
Run#	Term	h_{ac}	V_a	V_{beff}	A	VTS	TC	TC^2	SL*	SL^2
1	++++-	4.801	8.185	9.183	10.048	-3.327	479	229345	20	403
2	+++++	4.801	8.185	9.183	9.982	-3.303	302	91023	20	403
3	+++--	4.801	8.185	8.788	10.048	-3.327	677	457923	19	342
4	+++++	4.801	8.185	8.788	9.982	-3.303	479	229441	20	403
5	+++-	4.801	6.815	9.183	10.048	-3.327	216	46742	21	424
6	++-+	4.801	6.815	9.183	9.982	-3.303	157	24680	23	506
7	+--+	4.801	6.815	8.788	10.048	-3.327	417	174139	20	403
8	+---+	4.801	6.815	8.788	9.982	-3.303	229	52487	21	424
9	-+++	3.199	8.185	9.183	10.048	-3.327	787	619212	19	342
10	-++++	3.199	8.185	9.183	9.982	-3.303	482	232131	20	403
11	-++-	3.199	8.185	8.788	10.048	-3.327	999	998800	17	272
12	-+++	3.199	8.185	8.788	9.982	-3.303	797	635209	19	342
13	-+--	3.199	6.815	9.183	10.048	-3.327	358	128307	20	403
14	-+--+	3.199	6.815	9.183	9.982	-3.303	269	72146	21	424
15	-+--	3.199	6.815	8.788	10.048	-3.327	630	396396	19	342
16	-+--+	3.199	6.815	8.788	9.982	-3.303	377	142431	20	403
Sum							7654	4.5E+6	315	6242
Mean							478		19.7	
Standard Deviation							233		1.6	

*SL = Service Life

where

$$\begin{aligned} \text{Mean of TC} = E[y] &= \left(\frac{1}{2^n}\right) \sum_{i=1}^{2^n} y_i = \left(\frac{1}{2^4}\right) \sum_{i=1}^{2^4} \text{TC}_i = 7,654 / 16 \\ &= 478 \text{ ft/mile} \end{aligned}$$

$$\begin{aligned} \text{Variance of TC} = E[y^2] - (E[y])^2 &= \left(\frac{1}{2^4}\right) \sum_{i=1}^{2^4} \text{TC}_i^2 - (478)^2 \\ &= 54,667 \end{aligned}$$

$$\text{Standard deviation of TC} = (54667)^{0.5} = 233 \text{ ft/mile}$$

$$\begin{aligned} \text{Mean of SL} = E[y] &= \left(\frac{1}{2^n}\right) \sum_{i=1}^{2^n} y_i = \left(\frac{1}{2^4}\right) \sum_{i=1}^{2^4} \text{SL}_i = 315 / 16 \\ &= 19.69 \text{ years} \end{aligned}$$

$$\begin{aligned} \text{Variance of SL} = E[y^2] - (E[y])^2 &= \left(\frac{1}{2^4}\right) \sum_{i=1}^{2^4} \text{SL}_i^2 - (19.69)^2 \\ &= 2.527 \end{aligned}$$

$$\text{Standard deviation of SL} = (2.527)^{0.5} = 1.6 \text{ years}$$

3.3.4 Historical Variance of Variables

To simulate actual construction practice, a literature review of the historical pooled standard deviation of key mixture parameters was completed as well as a statistical analysis of Arizona Department of Transportation (ADOT) QA data.

A total of 20 ADOT projects were used for this study. Various statistical analyses were conducted on the AC mix QA parameters including mix gradation, % AC, %V_a (gyratory), maximum theoretical specific gravity (G_{mm}), bulk specific gravity (G_{mb}) from field cores, and in-place air voids from field cores.

The statistical variability of these key QA parameters for the ADOT projects were evaluated along with those derived from several studies in the literature. The list of literature sources of statistical variability that were reviewed include:

- ADOT (2005) (24)
- Klemunes—FHWA Study (1995) (25)
- FHWA recommendations (1995) (26)
- Epps et al. ADOT Report (1/2") (1989) (27)
- Epps et al. ADOT Report (3/4") (1989) (27)
- Witzczak and Yoder—(1975)—From BPR 1964/1969 Summary Reports (28)

Table 28 summarizes the key parameters used in the probabilistic analysis of the as-designed mix. The average pooled standard deviations shown in the table for each parameter were incorporated into the QRSS.

A comparative analysis was conducted of the data available from the various literature sources. In the analysis, the pooled standard deviation values calculated by various reference sources for each parameter were compared. This analysis showed that the variability of several key QA parameters for

the ADOT projects was high compared to the average values in Table 28. Figures 59 and 60 are example plots for two of the ADOT projects showing the high variability of the change in G_{mm} with a change in AC percentage. For a typical HMA mix G_{mm} should decrease linearly as percentage of AC increases. Thus the scatter shown in Figures 59 and 60 is highly suggestive of variability among plant-produced samples that is much greater than that found in the literature.

It should be noted that statistically "true" confidence intervals on the variance of any variable are correctly accomplished only by a "chi-square" distribution. The assumption of using a normal probability distribution to ascertain upper and lower confidence intervals on variance is erroneous. The data show an increase in the standard deviation with an increase in the probability for all QA parameters studied.

The pooled standard deviation based on the chi-square distribution as a function of probability for key parameters is calculated using the following relationship:

$$P_R = \left\{ \lambda_{1-\alpha/2; N-k}^2 \leq \lambda^2 \leq \lambda_{\alpha/2; N-k}^2 \right\} = 1 - \alpha \quad (84)$$

where

N = total number of samples
k = number of sites (projects)

$$P_R \left\{ s \sqrt{\frac{N-k}{\lambda_{\alpha/2; N-k}^2}} \leq \sigma \leq s \sqrt{\frac{N-k}{\lambda_{1-\alpha/2; N-k}^2}} \right\} = 1 - \alpha \quad (85)$$

$$\text{Lower Limit} = s \sqrt{\frac{N-k}{\lambda_{\alpha/2; N-k}^2}} \quad (86)$$

$$\text{Upper Limit} = s \sqrt{\frac{N-k}{\lambda_{1-\alpha/2; N-k}^2}} \quad (87)$$

3.3.5 Use of Beta Distribution

One objective of the probabilistic procedure is to report the distribution of the predicted distress along with its statistics such as mean and variance. Many phenomena that occur in nature as well as industry are known to follow the normal distribution in which data is symmetrical about the center (i.e., the average) of the data. The width of the distribution is determined by the statistical variance. The larger the standard deviation, the wider the normally distributed curve. Thus, the normal distribution is simple and convenient to interpret.

However, a major drawback of the normal distribution is that it sometimes yields a curve with data falling within the negative region or going beyond a specified maximum value. For thermal cracking (as well as FC), the irrational normal curve is most likely to occur when the mean value of thermal

Table 28. Historical pooled standard deviation of the input parameters required for the QA/QC program.

Parameter	Pooled Std Dev S_p					Avg. Pooled Std Dev
	ASU	Klemunes	Epps-1/2"	Epps-3/4"	Y & W	
	2005	1995	1989	1989	1975	
1 1/2"						
1"	0.863	0.797				0.830
3/4"	2.046	1.591				1.819
1/2"	3.675	2.459			3.22	3.118
3/8"	3.691	2.903	2.37	2.62	3.91	3.099
1/4"	3.368					3.368
#4	3.13	3.146			3.72	3.332
#8	1.906	2.67	2.5	2.38		2.364
#10	1.72	2.4				2.060
#16	1.28	2.093				1.687
#20		2.103				2.103
#30	0.954	3.6				2.277
#40	0.875	1.88	1.29	1.16	1.53	1.347
#50	0.729	1.117				0.923
#80		1.615				1.615
#100	0.574	0.798				0.686
#200	0.378	0.917	0.41	0.42		0.531
AC%-Ign Oven	0.221					0.221
AC%-Nuclear		0.265				0.265
AC%-Extraction		0.254	0.24	0.21	0.25	0.239
Va%-Marshall		0.774			1.19	0.982
VMA%-Marshall		0.604				0.604
VFB%-Marshall		4.974				4.974
Stability(Adj)-Marshall		279.89	321	257	283	285.223
Flow-Marshall		1.257			1.29	1.274
Va%-Gyratory	0.685					0.685
Gmm-Max. Theor Grav	0.0109					0.011
Gmb-Marshall	1.486	1.4325				1.459
Gmb-Gyratory						
Gmb-Field Cores			1.92	2.03		1.975
Va%-in situ (Field Cores)	0.962		1.41	1.258		1.210
AC Thickness-1					0.39	0.390
AC Thickness-2					0.48	0.480

cracking is close to either the minimum (i.e., 0 ft/mile) or maximum (i.e., 2,112 ft/mile) with a relatively large variance. As a more specific example, if the average of predicted thermal cracks is 2,000 ft/mile and the standard deviation is 300 ft/mile, then approximately 35% of the predicted TC will fall beyond the maximum thermal cracking, which is unacceptable. A conceptual plot for the thermal cracking normal distribution is presented in Figure 61. In another case, the pre-

dicted thermal cracking using the normal distribution falls in the negative region, which is irrational.

For this reason and to satisfy the condition in which the minimum and maximum thermal cracking values predicted are within a pre-determined range (i.e., from 0 to 2,112 ft/mile), a beta distribution was fitted to the predicted thermal cracking. The beta distribution is useful for data sets having minimum and maximum values because the distribution is fitted within

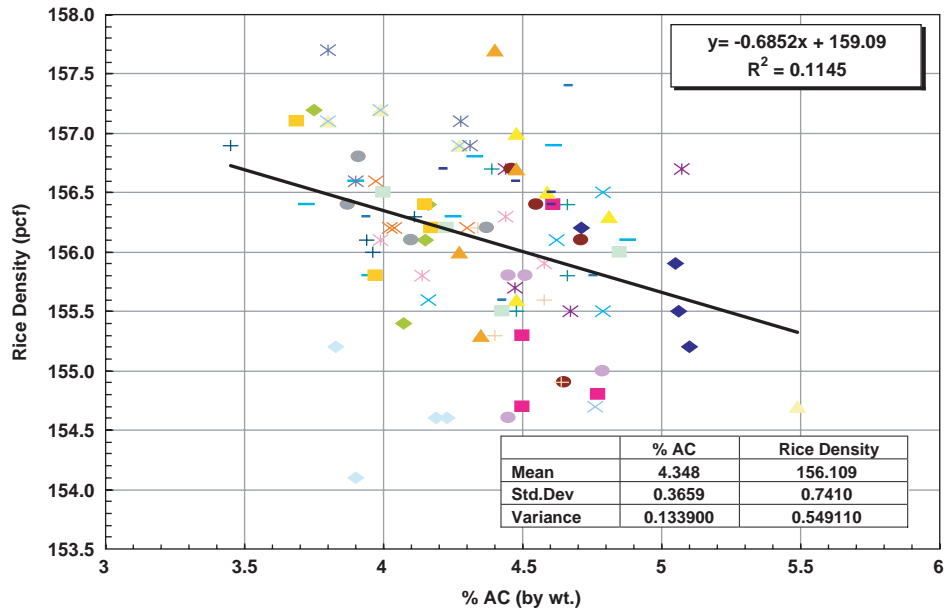


Figure 59. Rice density versus % AC for signal section road project.

them. Thus, the example described above and shown in Figure 61 is replaced by the beta distribution illustrated in Figure 62, where all predicted thermal cracking is distributed within the restricted (minimum and maximum) values.

The beta frequency distribution density function is presented in the following equation:

$$f(x) = \frac{(x-a)^{\alpha-1} (b-x)^{\beta-1}}{B(\alpha, \beta)(b-a)^{\alpha+\beta-1}} \text{ for } a < x < b, \alpha > 0 \text{ and } \beta > 0 \quad (88)$$

where

$$\alpha = \rho_0 \left(\frac{\rho_0(1-\rho_0)}{\rho_1} - 1 \right)$$

$$\beta = (1-\rho_0) \left(\frac{\rho_0(1-\rho_0)}{\rho_1} - 1 \right)$$

$$\rho_0 = \frac{\mu - a}{b - a}$$

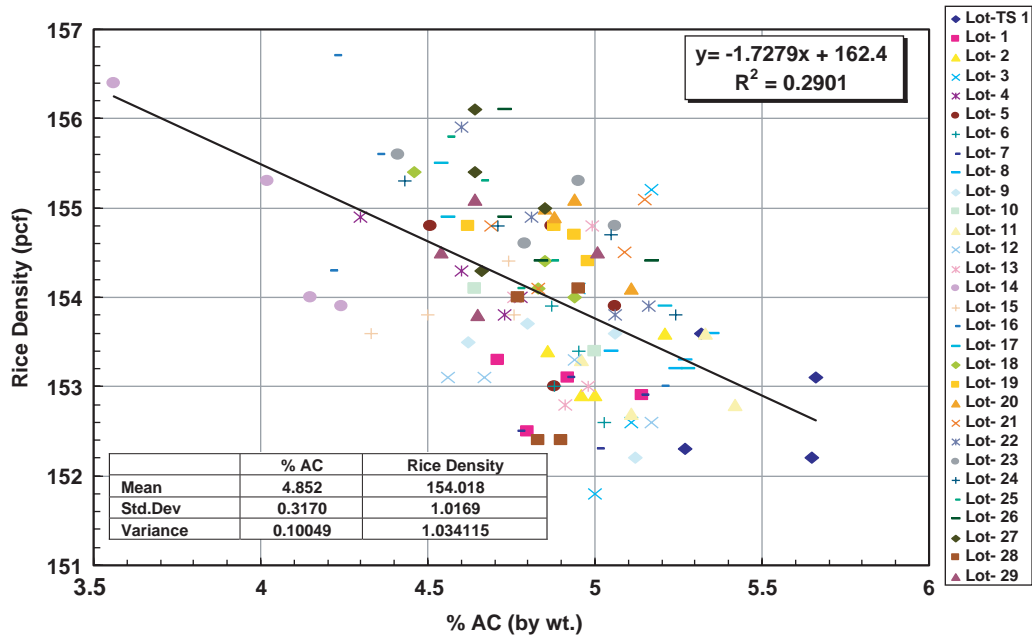


Figure 60. Rice density versus % AC for signal section road project.

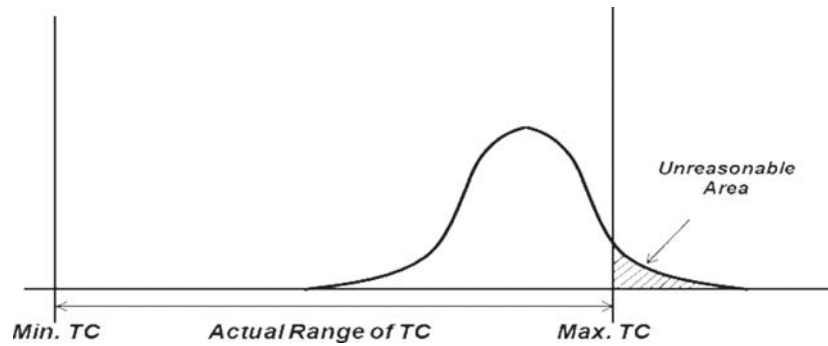


Figure 61. Conceptual plot for the TC "normal" distribution.

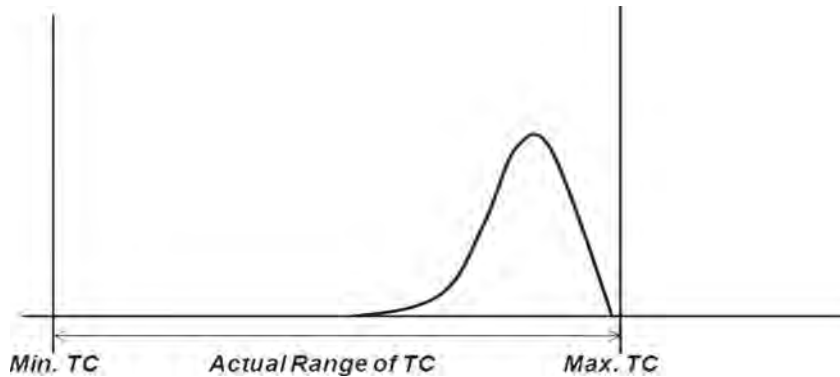


Figure 62. Conceptual plot for the TC "beta" distribution.

$$\rho_1 = \frac{\sigma^2}{(b-a)^2}$$

$$B(\alpha, \beta) = \int_0^1 t^{\alpha-1} (1-t)^{\beta-1} dt$$

3.4 Application of Stochastic Methods in Performance Prediction

This section covers the use of probabilistic solutions in the QRSS. Rutting and FC use the Monte Carlo simulation, while TC uses the Rosenblueth point-estimate method. The probabilistic performance prediction is done twice in Mode I of the QRSS, first with the job mix formula (the as-designed mix) and second with the field QA lot data (the as-built mix).

3.4.1 Application of Stochastic Methods to Dynamic Modulus

To calculate the standard deviation of E^* ($\sigma-E^*$) that would simulate the variability of the HMA, the Monte Carlo simulation is applied to the WPE (presented in Chapter 2).

When the probabilistic analysis is conducted for the JMF (as-designed mix), the QRSS will use the average or mean design

values for the air voids content (V_a), asphalt content (AC%), maximum theoretical specific gravity (G_{mm}), bulk specific gravity of the aggregate (G_{sb}), specific gravity of the binder (G_b), binder type, and aggregate gradation of the mixture in question as well as the combination of temperature and frequency at which it is desired to predict E^* with the WPE. In addition to the mean design value, the historical standard deviations are used to simulate typical construction variability.

When the probabilistic analysis is conducted for the as-built mix, the mean and standard deviation of the mix obtained for each lot or day's production is used to predict E^* with the WPE.

Each variable in the WPE is treated as a random number following a normal probability distribution with the mean equal to the design value and the standard deviation set as default or as varied by the user. The following paragraphs describe how the variability is treated for each specific variable used by the program. The temperature component is incorporated in the viscosity without any variability and it is calculated from the environmental factors at the pavement location. The frequency, f , is calculated from the traffic speed.

Binder Viscosity

The user can enter the performance grade of the asphalt binder used in the project. With this information, the pro-

gram identifies the A and VTS parameters associated with the binder at a short-term aging level (i.e., at mix laydown). Alternatively, a viscosity or penetration grade may be entered. The values of the A and VTS parameters used in the QRSS are similar to those used in the MEPDG (12).

Binder Hardening Ratio

The hardening ratio (HR) is defined as the ratio of the log-log RTFO viscosity to the log-log original (tank) viscosity, as shown in Equation 89. This ratio is used to assess the short-term aging of the binder that occurs during mix production and laydown.

The HR is used in the Monte Carlo simulation to assess the variability of the binder during mixing. The HR mean and standard deviation is used to vary the binder viscosity by back-calculating the original viscosity from the RTFO viscosity, applying the random variation to the HR, and then calculating the RTFO viscosity.

The HR mean and variance used were obtained from the Global Aging Model developed by Mirza and Witczak (29, 30). Their model is based on the results of 740 tests on five different binder grades over a range of temperatures. The overall reported mean and standard deviation values were 1.0492 and 0.0387, respectively.

$$HR = \frac{\log \log \eta_{\text{Mix-LaydownCondition}}}{\log \log \eta_{\text{OriginalCondition}}} \tag{89}$$

Modification to the HR. The overall HR mean and variance developed by Mirza and Witczak, which is used to predict the dynamic modulus of the AC mixture, commonly yields a coefficient of variation (CV) for the dynamic modulus around 40%. This computed CV is much greater than the value obtained in practice.

The data base was reexamined to determine whether it was possible to reduce the variability of the HR. The review confirmed that the overall mean and overall variance reported by Mirza and Witczak was for the entire database, including different binders and temperatures, which might have led to the high variance value of the HR.

The database was eventually reduced to 709 test results after eliminating tests having incomplete data. This revised database included data for five different binder grades. The viscosity grades selected to characterize the consistency for all data entries are listed in Table 29 while Appendix D presents the entire HR database. The overall mean of the HR from the revised database was 1.0487 and the standard deviation was 0.0376, values almost identical to those presented by Mirza (30).

The HR data were then analyzed by two different methods: (1) by binder grade and (2) by temperature for all binder grades.

Table 29. Viscosity grades.

Viscosity "Grade"	Viscosity Range
V1	100 - 350p
V2	350 - 700p
V3	700 - 1400p
V4	1400 - 2800p
V5	2800 - 5200p

HR Data Analysis by Binder Grade. Table 30 lists the mean and standard deviation of each binder grade at different temperatures. Figures 63 and 64 plot the HR mean and standard deviation, respectively, as a function of the temperature.

Figure 63 shows that the mean HR value as a function of temperature (°F) can be expressed for all binders by:

$$HR_{\text{mean}} = 0.0004(Temp) + 0.9981 \tag{90a}$$

$$R^2 = 0.9514$$

No regular trend by viscosity grade is observed in the data.

Similarly, from Figure 64, the standard deviation of the HR as a function of temperature (in °F) can be expressed for all binders by

$$HR_{\text{STDEV}} = 0.0002(Temp) - 0.0033 \tag{90b}$$

$$R^2 = 0.8005$$

Table 30. Mean and standard deviation of HR.

binder	Temp	Mean	Stdev	Count
V1	41.0	1.0036	0.0019	2
	77.0	1.0312	0.0159	39
	140.0	1.0451	0.0315	4
	275.0	1.1114	0.0731	4
V2	41.0	1.0064	0.0051	3
	59.8	1.0162	0.0057	4
	77.0	1.0367	0.0152	85
	140.0	1.0619	0.0361	19
V3	275.0	1.0989	0.0510	17
	59.8	1.0182	0.0081	8
	77.0	1.0324	0.0169	80
	96.2	1.0228	0.0086	9
V4	140.0	1.0553	0.0305	50
	275.0	1.0911	0.0484	40
	39.2	1.0153	0.0049	4
	60.0	1.0210	0.0038	7
V5	77.0	1.0332	0.0142	100
	95.0	1.0204	0.0092	6
	140.0	1.0620	0.0316	73
	275.0	1.1023	0.0474	60
	39.2	1.0137	0.0046	5
	59.0	1.0200	0.0066	11
Total	77.0	1.0275	0.0112	35
	96.0	1.0397	0.0050	11
	140.0	1.0523	0.0240	21
	275.0	1.0957	0.0266	12
Total				709

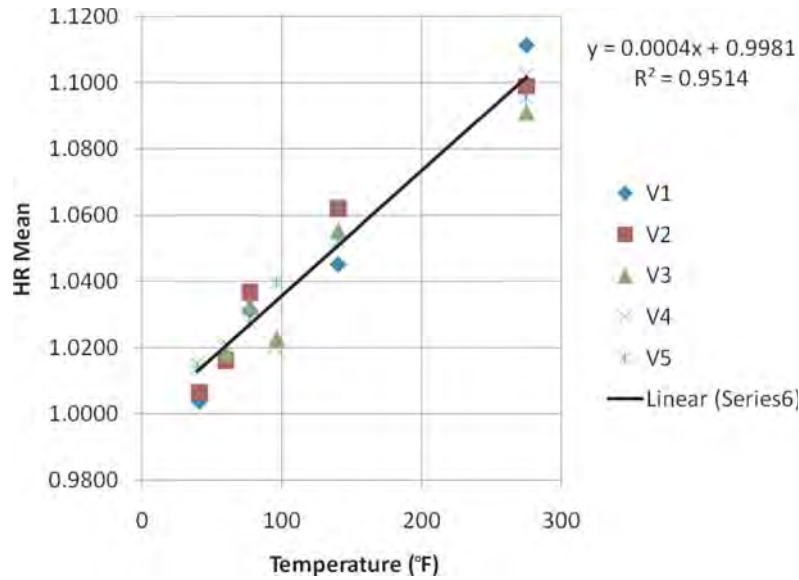


Figure 63. HR mean by binder type versus temperature.

At high temperatures, variability of the standard deviation is very high, leading to a similar problem as described above for the analysis based on the database taken as a whole.

Figures 63 and 64 also illustrate the reason for the abnormally high standard deviation of the HR value currently used in the QRSS algorithm. It appears that the value of the HR standard deviation recommended in the Mirza and Witczak report represented the standard deviation of the entire HR database (i.e., a composite HR standard deviation of the overall temperature range). Thus, this value is comparable to the Sy param-

eter across the temperature ranges evaluated by Mirza. These values ranged from near 40°F to as high as 275°F (the standard temperature for measurement of kinematic viscosity).

However, if the analysis is carried out for the effective temperature calculated for a specific AC layer and environmental condition, the most likely HR standard deviation from Figure 64 could be significantly different than Mirza and Witczak’s original value of 0.0387. For rutting, the maximum worldwide effective temperature is approximately 120°F, yielding a maximum HR standard deviation of 0.0207 from Figure 64. For a common effective temperature of 80°F, Figure 64 yields an HR

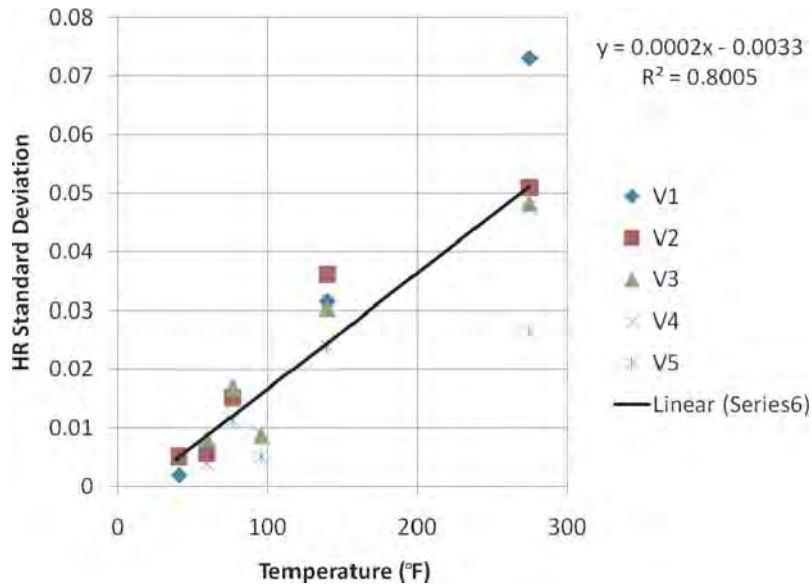


Figure 64. HR standard deviation by binder type versus temperature.

standard deviation of 0.0127, which would yield an E* CV of 12–15%.

HR Data Analysis by Temperature. The other method used to analyze the HR data was to sort the data only by temperature, including all binder grades at a given temperature. Table 31 shows the mean and standard deviation of the HR for each temperature as well as the number of data points and coefficient of variation.

Table 31. Mean and standard deviation of HR by temperature.

Temperature (°F)	Mean	Stdev	Count	CV (%)
39.8	1.0132	0.0100	15	0.9873
59.6	1.0193	0.0063	30	0.6175
77	1.0331	0.0152	339	1.4725
96	1.0289	0.0116	27	1.1286
140	1.0583	0.0309	167	2.9203
275	1.0982	0.0471	133	4.2888

Figures 65 and 66 show the resulting mean and standard deviation of the HR, sorted by temperature, irrespective of the binder grade. The correlation of the HR mean value to temperature is shown in Equation 91a.

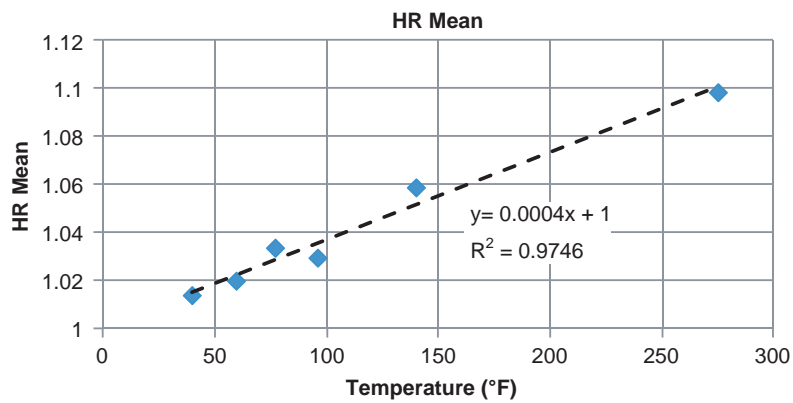


Figure 65. HR mean versus temperature.

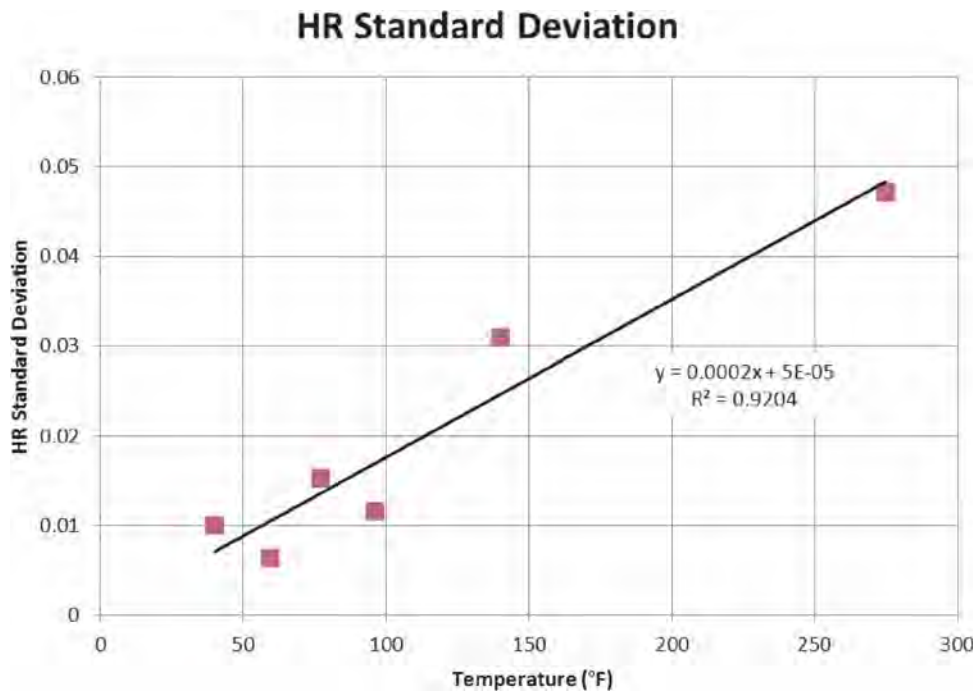


Figure 66. HR standard deviation versus temperature.

$$HR_{mean} = 0.0004(Temp) + 1.0 \quad (91a)$$

$$R^2 = 0.9746$$

The correlation of the HR standard deviation to temperature is shown in Equation 91b.

$$HR_{STDEV} = 0.0002(Temp) + 5e-5 \quad (91b)$$

$$R^2 = 0.9204$$

Final HR Recommendation. Two methods were used to analyze the HR data. The first method subdivided the data by binder grade and then found the mean and standard deviation of the HR for each temperature within each binder grade. In the second method, the mean and standard deviation of the HR, for all binder grades, were calculated by temperature.

The second method was found to be more rational. This approach gave good correlation coefficients and was more precise than the earlier methods of analysis used by the project team. Also, at high temperatures the HR variation between binder grades is large (partially due to the number of data points for each binder grade); this variability was reduced by combining all binder grade data at the same temperature.

Comparing the regression models obtained for the HR mean from both methods of analysis, it is observed that they are close, with no significance difference. However, the HR standard deviation model is improved by using all temperatures within a given binder grade.

In summary, the final recommended models for the HR mean and standard deviation selected for the QRSS were those obtained as a function of temperature regardless of binder grade and shown in Equations 91a and 91b.

Air Void Content

The as-designed mean value is used, with the historic standard deviation (σ) set to 0.774%.

Aggregate Gradation

The mean values for the four gradations incorporated in the WPE (cumulative % retained $\frac{3}{8}$ in., cumulative % retained $\frac{3}{4}$ in., cumulative % retained No. 4, and % passing No. 200 sieve) are used. The associated historic standard deviations are as follows (31):

Cumulative % Retained on $\frac{3}{4}$ in. = 1.591

Cumulative % Retained on $\frac{3}{8}$ in. = 2.903

Cumulative % Retained on #4 = 3.146

% Passing #200 = 0.917

Effective Binder Content (V_{beff})

The effective binder content is not entered by the user but is calculated from six variables: air voids (AV), asphalt content by total weight of mix (AC%), theoretical maximum specific gravity (G_{mm}), bulk specific gravity of the aggregate (G_{sb}), specific gravity of the asphalt binder (G_b), and effective specific gravity of the aggregate (G_{se}). The procedure to find V_{beff} is as follows.

The G_b value is set to 1.025 with no associated standard deviation. The values of AV, AC%, G_{mm} , and G_{sb} are then entered with their associated standard deviations set to (3):

$$AV\% = 0.774$$

$$AC\% = 0.267$$

$$G_{sb}^6 = 0.015$$

$$G_{mm} = 0.013$$

G_{se} is then calculated with Equation 92:

$$G_{se} = \left(\frac{100 - \%AC}{\frac{100}{G_{mm}} - \frac{\%AC}{G_b}} \right) \quad (92)$$

Then, after solving equation 92 for G_{mm} , a randomized G_{mm} (G_{mm1}) can be recalculated using the calculated G_{se} , the fixed G_b , and a normal random value of %AC where μ = design value and σ = 0.267. Next, a final G_{mm} value (G_{mm2}) is obtained using a value under a normal probability distribution with μ = G_{mm1} and σ = 0.013. Finally, using random values of AV, %AC, and G_{mm2} , a totally random value of V_{beff} is calculated with Equation 93 and used as direct input in the WPE for each simulation run.

$$V_{beff} = (100 - V_a) \frac{(100 G_{sb} - 100 G_{mm} + G_{mm} AC(\%))}{(100 G_{sb})} \quad (93)$$

Number of Random Repetitions

The user can select the number of random simulation runs to use, up to a limit of 1,000 repetitions. As a practical matter, it was found that after approximately 300 repetitions, the standard deviation of E^* ($\sigma-E^*$) remains relatively constant. Nevertheless, in the QRSS the default number of repetitions is set at 1,000 repetitions.

3.4.2 E^* Variability Calculation

In this section the standard deviation of E^* ($\sigma-E^*$) and CV will be calculated. As mentioned above the WPE is used to

⁶Standard deviation not found, but assumed to be close to that of the G_{mm} .

calculate E^* . The means and standard deviations of the WPE input variables run through, typically, 1,000 Monte Carlo simulations.

In each simulation and for each variable, a different random number is assumed. This random number will be multiplied by the standard deviation and then added to the mean to obtain a new value as shown in Equation 94 for the air voids V_a .

$$V_{a_{new}} = V_{a_{mean}} + \text{Random} * V_{a_{STDEV}} \quad (94)$$

The new values are used in the WPE with the effective temperature and effective frequency to calculate E^* . This process is repeated for 1,000 simulations. Then the mean and standard deviation of E^* are calculated from the 1,000 values of E^* . The coefficient of variation is then calculated from the mean and standard deviation as shown in Equation 95.

$$CV\% = \frac{STDEV}{Mean} \times 100 \quad (95)$$

3.4.3 Application of Stochastic Methods on Rutting and FC

As detailed in Chapter 2, closed form solutions were obtained to predict rutting and FC for the AC layer using E^* . Also, pavement service life is related to predicted distress as explained later in this chapter. Accordingly, if the value of E^* for a certain pavement structure, environmental location, and material is known, then major distresses and pavement service life can be predicted.

In order to calculate the variability in the rutting and FC, the E^* variability is used. For each of the 1,000 Monte Carlo simulations, the calculated E^* is used to calculate pavement distress (rutting and FC) and pavement service life.

From the 1,000 calculated values of the predicted distress and pavement service life, a mean, standard deviation, and CV are calculated that represent the variability in the distress prediction based on the variability in the HMA.

3.4.4 Application of Stochastic Methods to Thermal Cracking

The Rosenblueth point-estimate method is a powerful statistical method for determining the probability distribution of a function, $f(x)$, which has multiple variables. The method uses linear combinations of adequately selected point estimates around any desired value, x , and by using approximations for the point estimates, the first moments of $f(x)$ (i.e., the average and standard deviation) can be found. A review of this method can be found in the referenced papers (8, 9).

The original plan was to use the 3-point Rosenblueth method in the QRSS thermal cracking module for the sto-

chastic analysis. This would require running the thermal cracking model $3^5 = 243$ times (3-points and 5 variables) to calculate the average and standard deviation of both thermal cracking and pavement service life. However, due to the long running time for the 3-point method (approximately 10 minutes), two alternative methods, component analysis and the 2-point Rosenblueth method, were considered.

Component analysis was originally proposed by Harr as an alternative to the Rosenblueth point-estimate method to reduce the number of estimated points (9). This method considers correlations between given variables and is able to dramatically reduce the required number of simulations from 2^n to $2n$ where n is the number of variables in the dependent function, $f(x)$. The power of this method is especially emphasized when the number of independent variables is large. For example, if a function of $f(x)$ has 10 variables, the 2-point Rosenblueth method requires run $2^{10} = 1,024$ runs while the component analysis needs only $2 * 10 = 20$ runs.

The second alternative considered was the generalized 2-point Rosenblueth method with consideration of the correlation of random variables. Equation 96, as an example, shows the expectation of $y = f(x_1, x_2, x_3)$ without the use of the correlation coefficient (ρ), while Equation 97 shows the expectation of the same function including correlation (ρ_{xxx}) terms.

$$E[y^m] = \left(\begin{matrix} y_{+++}^m + y_{++-}^m + y_{+-+}^m + y_{+--}^m \\ + y_{-++}^m + y_{-+-}^m + y_{-+-}^m + y_{---}^m \end{matrix} \right) / 2^n \quad (96)$$

where

$E[y^m]$ = expectation of a function, y

n = number of variables

m = index for y

$$y_{+++}^m = f(x_1 + \sigma_{x1}, x_2 + \sigma_{x2}, x_3 + \sigma_{x3})$$

$$y_{++-}^m = f(x_1 + \sigma_{x1}, x_2 + \sigma_{x2}, x_3 - \sigma_{x3})$$

...

(The signs are in the same order for the rest of terms)

$$E[y^m] = p_{+++} y_{+++}^m + p_{++-} y_{++-}^m + \dots + p_{---} y_{---}^m \quad (97)$$

where

$$p_{+++} = p_{---} = (1 + \rho_{12} + \rho_{23} + \rho_{31}) / 2^n$$

$$p_{++-} = p_{--+} = (1 + \rho_{12} - \rho_{23} - \rho_{31}) / 2^n$$

$$p_{+-+} = p_{-+-} = (1 - \rho_{12} - \rho_{23} + \rho_{31}) / 2^n$$

$$p_{+--} = p_{--+} = (1 - \rho_{12} + \rho_{23} - \rho_{31}) / 2^n$$

Notice that if there is no correlation between the variables (i.e., all $\rho_{ij} = 0$, $i \neq j$), Equation 97 collapses to Equation 96 because all p terms are going to be $1/(2^n)$.

Evaluation of possible correlations among the five variables used in the QRSS thermal cracking model (air voids, effective binder content, AC thickness, and the asphalt binder

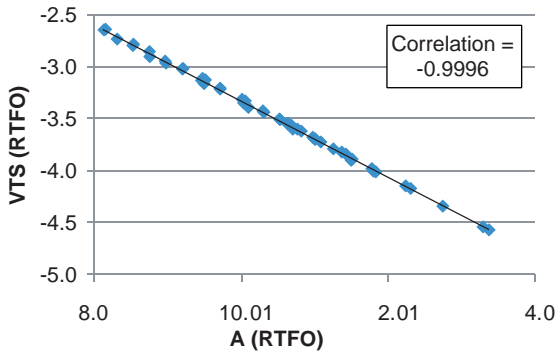


Figure 67. Correlation plot between A and VTS at RTFO condition.

parameters A and VTS) found that a high-level correlation existed in the binder RTFO condition between A and VTS as shown in Figure 67.

For the QRSS thermal cracking model, the assumption was made that only A and VTS are fully correlated ($\rho_{A,VTS} = -1$) and that the other variables are completely independent of each other. Consequently, half the p terms in Equation 97 became zero and the number of y^m terms is reduced by half to $2^5/2 = 16$.

In reality, the difference in the number of simulations for the two methods, $2 \times 5 = 10$ for the component analysis and $2^5/2 = 16$ for the Rosenblueth 2-point method, is not significant. Therefore, the decision was made to use the generalized Rosenblueth 2-point method with correlation coefficients in the QRSS TC module. This choice drastically reduces the analysis time compared to that required for the original 243 simulations.

3.4.4.1 Standard Deviation of Asphalt Binder Characteristics (A and VTS)

In the probabilistic analysis of TC prediction, it is essential to know the variance of each significant variable. For an as-designed (JMF) mix, these variances come from the historic

database, while for the as-built mix they come from the lot or daily production samples collected at the project site. The TC prediction methodology utilizes five variables as major factors: AC thickness, air voids, effective binder content, and the binder characteristic parameters A and VTS under the short-term aged condition (i.e., the RTFO condition). This section discusses how the standard deviation of these binder parameters, A and VTS, are determined.

The MEPDG-recommended default RTFO condition A and VTS values vary by the binder grading system used: PG, penetration grade, or viscosity grade. Once the binder and its grade are selected for the HMA mix, the default RTFO A and VTS values are retrieved from a database in the MEPDG program. These default A and VTS values are then used as average values in the probabilistic analysis.

In order to determine the standard deviation of the A and VTS values, it was necessary to make several assumptions:

- The variability of the A and VTS values follows a normal distribution.
- Adjacent binder grades having identical rutting temperature have the same standard deviation (e.g., the standard deviations for PG 52-22, PG 52-16, and PG 52-10 are the same).
- The normal distributions of adjacent PGs do not overlap within a range of 3σ .

Based on these assumptions, the standard deviation of A and VTS for a certain binder grade can be calculated by dividing the absolute difference of the adjacent A and VTS values by 12. The divisor is 12 because the performance grading system defines A and VTS at six degree intervals, so the difference in degrees between the adjacent performance grades is 12 (e.g., difference between PG xx-22 and PG xx-10 when PG xx-16 is the binder grade of interest).

As an example, Figure 68 depicts the computation of the standard deviation of a PG 52-16 binder with adjacent low-temperature binder grades of PG 52-22 and PG 52-10. Their A and VTS values at the RTFO condition are the MEPDG

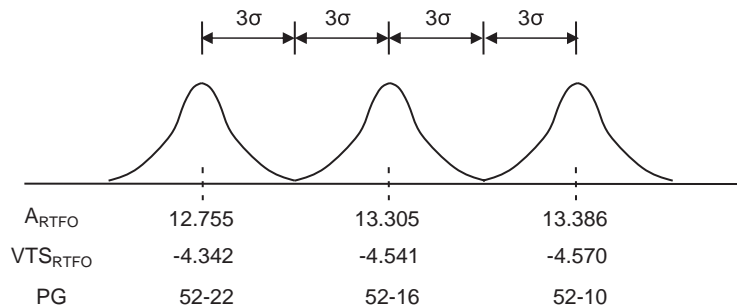


Figure 68. Example: concept of standard deviation of the A and VTS values.

default values. The standard deviations are then easily calculated as follows:

- Standard deviation of A for PG 52-16: $|(13.386 - 12.755)| / 12 = 0.05258$
- Standard deviation of VTS for PG 52-16: $|(-4.570 + 4.342)| / 12 = 0.019$

If only one adjacent binder grade exists, such as for PG xx-10 or PG xx-46, the computation considers two distributions (i.e., the grade of interest and the single adjacent grade) and the A and VTS values should be divided by six, not 12.

3.5 Determination of Service Life and the Predicted Life Difference (PLD)

3.5.1 Conversion of Distress to Service Life for Rutting Distress

Predicted service life is a key QRSS output that is obtained from the probabilistic analysis of the rutting closed form solution. The service life computation for rutting is based upon the relationship between the predicted rutting performance and the design traffic repetitions (ESALs) during the specified design life, as shown in Figure 69.

The as-designed mix will produce a specific design rut depth corresponding to the design traffic repetitions while a variable mix quality that depends upon variable volumetric properties will be obtained from each Monte Carlo simulation. These simulated mixes will have different stiffnesses and correspondingly different service lives. If the quality of a

simulated mix is better than that of the as-designed mix, the simulated mix will have less rutting and longer predicted life. The service life can then be estimated from the difference between the rut depths of the simulated mix and the as-designed mix.

Sotil found a strong relationship between predicted rutting and the number of traffic repetitions from the MEPDG simulations (3). The predicted rutting will increase almost exactly three-fold for a 10-fold increase in ESALs. As an example, if the predicted rutting is 0.006 inch at 10^5 ESALs, the rutting at 10^6 ESALs would be 0.018 inch which is exactly three times. This relationship is applicable to any pavement system having the same structure (AC thickness), climatic location, and binder type. It can be simply described by the following equation:

$$\left(\frac{RUT_i}{RUT_j}\right) = \left(\frac{ESAL_i}{ESAL_j}\right)^{0.479244} \tag{98}$$

where RUT_i and RUT_j are Rut depth at traffic repetitions of $ESAL_i$ and $ESAL_j$, respectively.

Using this relationship a rutting value can be predicted at any traffic level when a rutting value is known for any given corresponding traffic level. This strong relationship is not surprising because it is derived from the rutting model implemented in the MEPDG. Note that the last term (N term) of that model (equation 99) contains the same exponent value as that in the right-hand side of Equation 98 and that $(10)^{0.479244} \approx 3$.

$$(\epsilon_p / \epsilon_r) = k_1 10^{-3.4488} T^{1.5606} N^{0.479244} \tag{99}$$

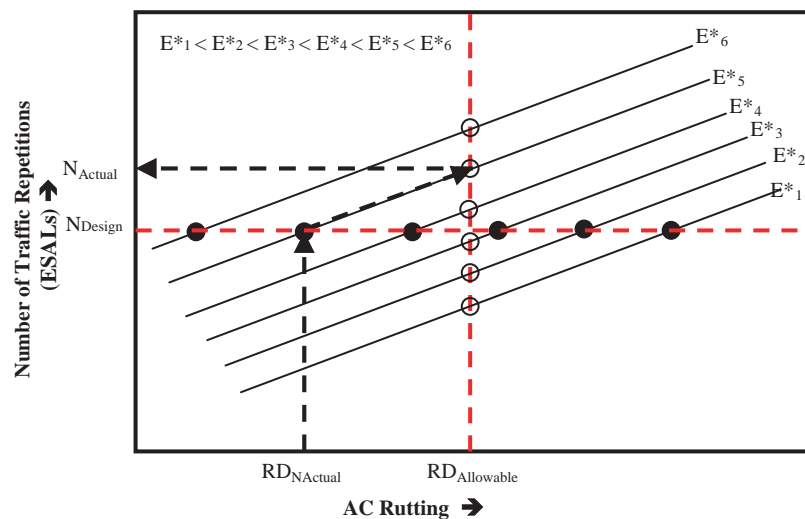


Figure 69. Methodology used for the calculating the actual traffic repetitions.

where

- ϵ_p = accumulated plastic strain after N traffic repetitions
- ϵ_r = accumulated elastic strain
- N = number of traffic repetitions
- T = pavement temperature at specified depth
- k_1 = a parameter as a function of asphalt thickness

The elastic strains are calculated from Equation 100.

$$\epsilon_r = \frac{1}{E} * (\sigma_z - \nu * (\sigma_x + \sigma_y)) \quad (100)$$

where

- E = modulus
- σ_x σ_y σ_z = stresses in x, y, z directions
- ν = Poisson's ratio

The permanent strain can be converted into rutting with the following equation:

$$RUT = \epsilon_p * h_{ac} = k_1 * T^{k_2} * ESAL^{0.479244} * \epsilon_r * h_{ac} \quad (101)$$

where

- h_{ac} = thickness of AC layer

For two mixes, specifically the as-designed mix and the simulated mix, the rut depth ratio can be calculated as

$$\begin{aligned} \frac{RUT_i}{RUT_j} &= \left(\frac{k_1 * T^{k_2} * ESAL_i^{0.479244} * \epsilon_{ri} * h_{ac}}{k_1 * T^{k_2} * ESAL_j^{0.479244} * \epsilon_{rj} * h_{ac}} \right) \\ &= \left(\frac{ESAL_i^{0.479244} * \epsilon_{ri}}{ESAL_j^{0.479244} * \epsilon_{rj}} \right) \end{aligned} \quad (102)$$

where

RUT_i and RUT_j = Rut depth at traffic repetitions of $ESAL_i$ and $ESAL_j$, respectively

Assuming that the stress states at the same location and for the same structure do not differ, Equation 102 can be simplified to:

$$\frac{RUT_i}{RUT_j} = \left(\frac{ESAL_i^{0.479244} * E_j}{ESAL_j^{0.479244} * E_i} \right) \quad (103)$$

And then rearranged to:

$$\left(\frac{ESAL_i}{ESAL_j} \right) = \left(\frac{RUT_i}{RUT_j} * \frac{E_i}{E_j} \right)^{1/0.479244} \quad (104)$$

In converting the predicted rutting to the service life, it is important to understand that the traffic repetition (ESAL) is

calculated as a function of several components such as initial ESAL ($ESAL_0$), traffic growth rate (r), and design life (Y), as shown in Equation 105:

$$ESAL = \frac{(ESAL_0)(365)}{\ln(1+r)} \left[(1+r)^Y - 1 \right] \quad (105)$$

where

- $ESAL_0$ = year one, initial daily ESALs on the day traffic is opened
- r = growth rate (rate of traffic increase per year)
- Y = design life in years

Taking the ratio of two ESALs, knowing that Y will be the only variable, gives:

$$\left(\frac{ESAL_i}{ESAL_j} \right) = \frac{\left[(1+r)^{Y_i} - 1 \right]}{\left[(1+r)^{Y_j} - 1 \right]} \quad (106)$$

Then solving for the design life (Y_i)

$$Y_i = \frac{\log \left(\left(\frac{ESAL_i}{ESAL_j} \right) \left((1+r)^{Y_j} - 1 \right) + 1 \right)}{\log(1+r)} \quad (107)$$

And substituting Equation 104 in Equation 107 yields

$$Y_i = \frac{\log \left(\left(\frac{RUT_i}{RUT_j} * \frac{E_i}{E_j} \right)^{1/0.479244} \left((1+r)^{Y_j} - 1 \right) + 1 \right)}{\log(1+r)} \quad (108)$$

Now if the simulated mix is the i th mix and the design mix is the D mix:

$$Y_i = \frac{\log \left(\left(\frac{RUT_i}{RUT_D} * \frac{E_i}{E_D} \right)^{1/0.479244} \left((1+r)^{Y_D} - 1 \right) + 1 \right)}{\log(1+r)} \quad (109)$$

Note that the Y_i value is for one simulation out of the hundreds of Monte Carlo simulations run in the QRSS analysis and that the rut depth predicted for each Monte Carlo simulation can be transformed into a corresponding service life. Then, the average, standard deviation, and frequency distribution of the simulated service lives can be easily computed.

The analysis presented here is applicable to both the as-designed and as-built mixes. For the as-built mix analysis, however, the average rutting of the as-designed mix becomes the rutting criterion (RUT_D) in Equation 109 and each RUT_i

is obtained from the Monte Carlo simulation of the as-built mix for each lot.

3.5.2 Conversion of Distress to Service Life for FC Distress

The prediction of a fatigue distress service life for an HMA mix is shown in Figure 70. In the figure, the as-designed or standard mix has a predicted 30% fatigue damage at the end of the 20-year design life. Analogous to the discussion for rutting in the previous section, each Monte Carlo simulation carried out by the QRSS yields a variable mix quality and a different service life that depend upon variable volumetric properties. If the quality of a simulated mix is worse than the as-designed mix (MCS₁ in the figure), the simulated mix would accumulate the same damage as that of the design mix before the end of the design life. This will result in the predicted service life less than 20 years (SL₁ in the figure).

On the other hand, if the simulated mix quality is better than that of the design mix, it will take a longer time to reach the same damage as the design mix, i.e., the predicted service life for this simulated mix will be longer than the 20-year design life (MCS₂ and SL₂ in the figure).

Fatigue damage, *D*, is defined as the ratio of the actual number of traffic repetitions, *n_i*, to the allowable number of load repetitions, *N_f*. It can be simply represented as follows:

$$\%D = \frac{n_i}{N_f} \times 100 \quad (110)$$

where

- %D = percent fatigue damage
- n_i* = actual traffic repetitions
- N_f* = allowable traffic repetitions

The expected fatigue damage is computed for each run of the Monte Carlo simulation. Each individual fatigue damage value predicted by the Monte Carlo simulation will be different due to the variability of the volumetric and structural factors such as AC thickness, air voids, binder content, gradation, and so forth.

To predict the service life for each simulated run, it is important to understand that, in Equation 110, the *N_f* term uniquely represents the capacity of a simulated mix and is calculated by the following equations:

For *h_{ac}* ≤ 3 in. (*thin model*)

$$\begin{aligned} \log N_f = 8.3014 - \left\{ \left[-0.0095 \log(h_{ac})^2 - 0.0756 \log(h_{ac}) \right. \right. \\ + 0.0438 \log(E_{eff}^*) - 0.5414 \log(h_{ac})^2 \\ + 1.4319 \log(h_{ac}) - 1.0252 \left. \right] \log(E_{cf})^2 \\ + \left[-0.0208 \log(E_{eff}^*) + 0.7040 \log(E_{eff}^*) \right. \\ - 4.1171 \left. \right] \log(E_{cf}) + \left[-4.1659 \log(h_{ac})^2 \right. \\ - 3.0733 \log(h_{ac}) - 6.4418 \left. \right] \log(VFB)^2 \\ + \left[-1.5883 \log(h_{ac})^2 - 2.8014 \log(h_{ac}) \right. \\ - 9.2885 \left. \right] \log(VFB) - 0.1177 \log(E_{eff}^*)^2 \\ + \left[0.0681(h_{ac})^2 - 0.3789(h_{ac}) \right. \\ + 0.8989 \left. \right] \log(E_{eff}^*) + 2.9330 \left. \right\} \quad (111a) \end{aligned}$$

For *h_{ac}* ≥ 3 in. (*thick model*)

$$\begin{aligned} \log N_f = 8.3014 - \left\{ \left[0.0645 \log(h_{ac})^2 - 0.0144 \log(h_{ac}) \right. \right. \\ + 0.0416 \log(E_{eff}^*) - 0.6003 \log(h_{ac})^2 \\ + 0.7046 \log(h_{ac}) - 1.0276 \left. \right] \log(E_{cf})^2 \end{aligned}$$

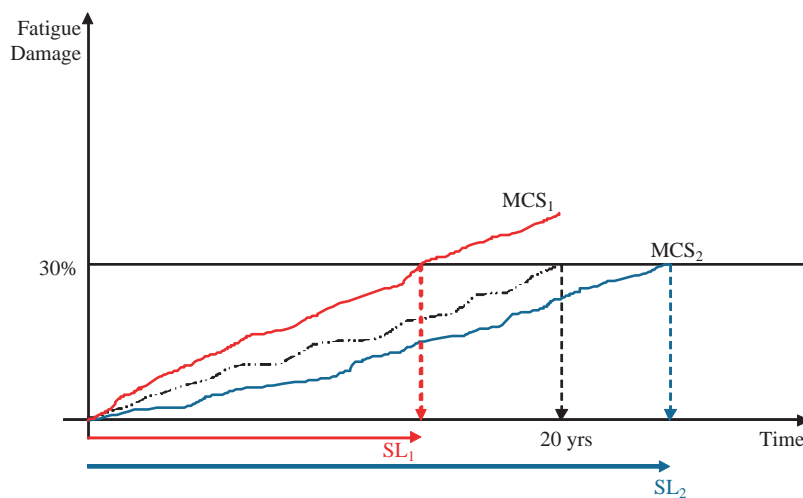


Figure 70. Example of predicting service life for FC.

$$\begin{aligned}
& + [-0.0218 \log(E_{eff}^*)^2 + 0.6280 \log(E_{eff}^*) \\
& - 3.2499] \log(E_f) + [28.9186 \log(h_{ac})^2 \\
& - 51.9588 \log(h_{ac}) + 12.7671] \log(VFB)^2 \\
& + [15.8844 \log(h_{ac})^2 - 28.6128 \log(h_{ac}) \\
& + 0.9160] \log(VFB) - 0.1792 \log(E_{eff}^*)^2 \\
& + [0.0024(h_{ac})^2 - 0.1009(h_{ac}) \\
& + 1.2623] \log(E_{eff}^*) + 1.4613 \} \quad (111b)
\end{aligned}$$

where

N_f = number of traffic repetitions to failure
 h_{ac} = AC thickness in inches
 E_{cf} = composite foundation modulus in psi
 VFB = voids filled with bitumen, $V_{beff}/(V_{beff} + V_a)$

In Equation 110, the %D value is that for the as-designed mix (e.g., 30% in the figure). In order to determine how long a simulated mix will take to reach the same damage as the as-designed mix, Equation 110 is rearranged as follows:

$$n_i = \frac{(N_{fi})(\%D)}{100} \quad (112)$$

where

n_i = actual traffic repetition to cause %D
 %D = damage criterion determined for the as-designed mix
 N_{fi} = actual failure traffic repetitions for an i th simulated mix

In calculating the actual traffic repetition (n_i), it should be noted that the initial traffic ($ESAL_0$) and traffic growth (r) over time are constants, but the time (service life) varies. Therefore, if the design period (e.g., 20 years in the figure) is held constant, actual traffic repetition will remain the same; and if the simulated mix is better than the as-designed mix, the damage will be less than the %D value.

If the left side of Equation 112 is replaced by the typical equation to calculate a total ESAL, which is a function of an initial ESAL, traffic growth rate, and time period in years, Equation 112 becomes:

$$\frac{ESAL_0(365)}{\ln(1+r)} \left((1+r)^{Y_i} - 1 \right) = \frac{(N_{fi})(\%D)}{100} \quad (113)$$

where

$ESAL_0$ = year one, initial daily ESALs on the day traffic is opened
 r = growth rate (rate of traffic increase per year)
 Y_i = years to equal fatigue damage for the i th simulated mix

By rearranging Equation 113 in terms of Y_i , the predicted service life for each simulated run is obtained:

$$Y_i = \frac{\log \left(\frac{(N_{fi})(\%D) \ln(1+r)}{ESAL_0(365)(100)} + 1 \right)}{\log(1+r)} \quad (114)$$

where %D is the fatigue damage criterion determined for the as-designed mix.

Equation 114 can again be rearranged by substituting the right-hand side of equation 110 for %D:

$$Y_i = \frac{\log \left(\frac{\left(\frac{N_{fi}}{N_{fc}} \right) (n_i) \ln(1+r)}{ESAL_0(365)} + 1 \right)}{\log(1+r)} \quad (115)$$

In Equation 115, n_i is the number of the anticipated traffic repetitions determined from the initial ESAL ($ESAL_0$), traffic growth rate (r), and design period, as shown in the following equation:

$$n_i = \frac{ESAL_0(365)}{\ln(1+r)} \left((1+r)^{Y_c} - 1 \right) \quad (116)$$

Therefore, Equation 115 can be simplified by substituting the right-hand side of Equation 116 for n_i :

$$Y_i = \frac{\log \left(\frac{N_{fi}}{N_{fc}} \left((1+r)^{Y_c} - 1 \right) + 1 \right)}{\log(1+r)} \quad (117)$$

Once the predicted service life is calculated for each simulated run, the average, standard deviation, and frequency distribution of the service life are calculated.

In Equation 117, if the log of the term N_{fi}/N_{fc} is taken, it becomes $\log(N_{fi}) - \log(N_{fc})$ and expresses the difference between the predicted number of traffic repetitions to failure presented in Equation 111 for two different mixes. Equation 111 can then be used to expand the log term:

$$\begin{aligned}
\log(N_{fi}) - \log(N_{fc}) = & \alpha_1 \left(\log \frac{E_i^*}{E_c^*} \right) (\log E_{cf})^2 + \left(a_8 \log \frac{E_i^{*2}}{E_c^{*2}} + a_9 \log \frac{E_i^*}{E_c^*} \right) \log E_{cf} \\
& + \alpha_2 \left(\log \frac{VFB_i^2}{VFB_c^2} \right) + \alpha_3 \left(\log \frac{VFB_i}{VFB_c} \right) + a_{17} \left(\log \frac{E_i^{*2}}{E_c^{*2}} \right) \\
& + \alpha_4 \left(\log \frac{E_i^*}{E_c^*} \right) \quad (118)
\end{aligned}$$

where

$$\begin{aligned}
\alpha_1 &= a_2 \log h_{ac}^2 + a_3 \log h_{ac} + a_4 \\
\alpha_2 &= a_{11} \log h_{ac}^2 + a_{12} \log h_{ac} + a_{13} \\
\alpha_3 &= a_{14} \log h_{ac}^2 + a_{15} \log h_{ac} + a_{16} \\
\alpha_4 &= a_{18} h_{ac}^2 + a_{19} h_{ac} + a_{20} \\
a_2 &= -0.0095 \text{ for thin model or } 0.0645 \text{ for thick model} \\
a_3 &= -0.0756 \text{ for thin model or } -0.0144 \text{ for thick model} \\
a_4 &= 0.0438 \text{ for thin model or } 0.0416 \text{ for thick model} \\
a_{11} &= 4.1659 \text{ for thin model or } 28.9186 \text{ for thick model} \\
a_{12} &= -3.0733 \text{ for thin model or } -51.9588 \text{ for thick model} \\
a_{13} &= -6.4418 \text{ for thin model or } 12.7671 \text{ for thick model} \\
a_{14} &= -1.5883 \text{ for thin model or } 15.8844 \text{ for thick model} \\
a_{15} &= -2.8014 \text{ for thin model or } -28.6128 \text{ for thick model} \\
a_{16} &= 9.2885 \text{ for thin model or } 0.9160 \text{ for thick model} \\
a_{17} &= -0.1177 \text{ for thin model or } -0.1792 \text{ for thick model} \\
a_{18} &= 0.0681 \text{ for thin model or } 0.0024 \text{ for thick model} \\
a_{19} &= -0.3789 \text{ for thin model or } -0.1099 \text{ for thick model} \\
a_{20} &= 0.8989 \text{ for thin model or } 1.2623 \text{ for thick model}
\end{aligned}$$

The right-hand side of Equation 118 can be rearranged in terms of E^* :

$$\begin{aligned}
&(a_{17} + a_8 \log E_{cf}) \left(\log \frac{E_i^{*2}}{E_c^{*2}} \right) \\
&+ \left(\alpha_1 (\log E_{cf})^2 + a_9 \log E_{cf} + \alpha_4 \right) \left(\log \frac{E_i^*}{E_c^*} \right) \\
&+ \alpha_2 \left(\log \frac{VFB_i^2}{VFB_c^2} \right) + \alpha_3 \left(\log \frac{VFB_i}{VFB_c} \right) \quad (119a)
\end{aligned}$$

or

$$\beta_1 \left(\log \frac{E_i^{*2}}{E_c^{*2}} \right) + \beta_2 \left(\log \frac{E_i^*}{E_c^*} \right) + \beta_3 \quad (119b)$$

where

$$\begin{aligned}
\beta_1 &= a_{17} + a_8 \log E_{cf} \\
\beta_2 &= \alpha_1 (\log E_{cf})^2 + a_9 \log E_{cf} + \alpha_4 \\
\beta_3 &= \alpha_2 \left(\log \frac{VFB_i^2}{VFB_c^2} \right) + \alpha_3 \left(\log \frac{VFB_i}{VFB_c} \right)
\end{aligned}$$

Substituting the expression 119b in Equation 117 yields the final service life Y_i for the i th simulated mix in terms of the dynamic moduli and VFB for the simulated mix and the as-designed mix:

$$Y_i = \frac{\log \left(\left\{ 10^{\left(\beta_1 \left(\log \frac{E_i^{*2}}{E_c^{*2}} \right) + \beta_2 \left(\log \frac{E_i^*}{E_c^*} \right) + \beta_3 \right) \right\}}{\left\{ (1+r)^{Y_c} - 1 \right\} + 1} \right)}{\log(1+r)} \quad (120)$$

Thus, the predicted service life is mainly affected by the difference of the dynamic moduli; the composite foundation modulus (E_{cf}) is constant for the two mixes and a single total thickness of AC (h_{ac}) is used regardless of the number of AC layers.

In the QRSS, Equation 117 is applied for the calculation of service life for a multi-layer pavement system.

3.5.3 Conversion of Distress to Service Life for Thermal Cracking Distress

The conversion of TC distress to service life is relatively simple and straightforward to understand as compared to the two other distress types. In order to effectively describe the conversion, an example is presented and explained.

Figure 71 shows the development of TC for three mixes, viz., “mix design,” “bad mix,” and “good mix.” The curve labeled “mix design” in Figure 71 traces the TC over the design life for an as-designed mix without variability. After the design life of 20 years, the TC is approximately 110 ft/mile. Since the as-designed mix should be the criterion for this particular TC analysis, the other TC predictions developed from the Rosenblueth method will be compared with the criterion to determine their relative service life.

The TC of the “bad mix” in the figure reaches 110 ft/mile of TC amount before the design life. This implies that the mix does not satisfy the criterion and, as shown in the figure, the TC of the “bad mix” reaches almost 400 ft/mile at the 20-year design life, indicative of its relatively poor quality. The predicted service life of this “bad mix” is determined at the point where its TC reaches the criterion if 110 ft/mile, or 11.3 years after the pavement construction.

If, however, a mix is good compared to the as-designed mix, its TC will develop at a slower rate over time than the as-designed mix, its TC would be less than that of the as-designed mix at the design life, and it will provide a longer service life than the as-designed mix. The QRSS TC program computes the point when the given mix reaches the TC criterion and this time is the probable service life of the mix. For extremely good mixes, which may never reach the TC criterion, the maximum probable service life is set to 50 years for computation of the frequency distributions.

Using the data set populated by the Rosenblueth method, the average and standard deviation of the service life is calculated.

3.5.4 Comparison Between the As-Designed (JMF) Mix and the As-Built Mix Data

The QRSS probabilistic approach uses the mean and standard deviation of all the WPE variables to predict E^* from the mixture QA data. These E^* values are then used to predict the

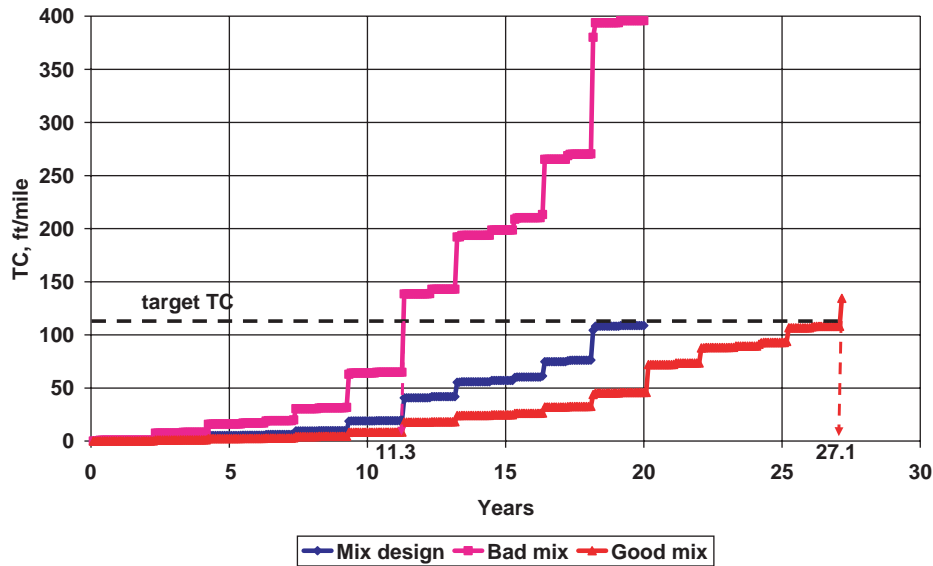


Figure 71. Example: TC development profile with time.

rutting and FC distresses, from which the mean and standard deviation of the distress frequency distributions can be found. In reliability analysis, a frequency distribution of this type is termed a Demand Function. Figure 72 is an example of the frequency distribution of the AC rut depth (R_d) from the Monte Carlo simulation. Knowing distribution type as well as the mean and standard deviation, the cumulative frequency distribution of the AC rut depth can be developed as shown in Figure 73.

The QRSS also uses Monte Carlo simulation analysis to calculate the mean and variance for the probable E* (and pavement distress) for the as-designed mix. As discussed earlier, this probabilistic solution is based upon a set of historical variance values for all the parameters used in the calculation of E*. The mean and variance of the AC rut depth for the as-designed mix is then calculated using the same methodology as for the project QA data.

The project team initially considered a provisional methodology for calculating what was termed the Quality Index (QI) variable to judge the adequacy of AC mixtures based on the difference in the area between the cumulative frequency distribution curve of the as-designed mix (termed the Capacity Function in reliability analysis) and that of the as-built mix (the Demand Function). This Quality Index could then be used to determine the penalty or bonus. However, after further study, a decision was made to use the PLD to determine the Penalty/Bonus for a given distress type. This methodology is explained in Figures 74 and 75.

A project-dependent methodology to calculate the actual service life based on the predicted rutting for both as-designed and as-built mixtures was developed and is incorporated in the QRSS AC rutting routine. The program allows the user to calculate the predicted life difference (PLD) using the following method:

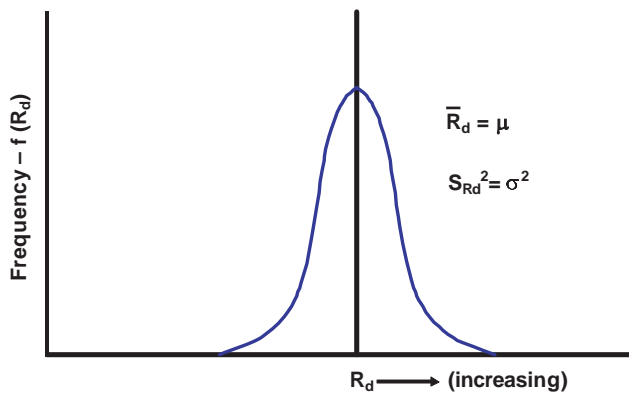


Figure 72. Frequency distribution of AC rut depth.

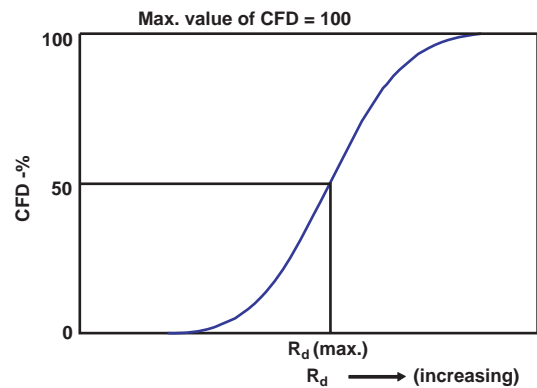


Figure 73. Cumulative frequency distribution of AC rut depth.

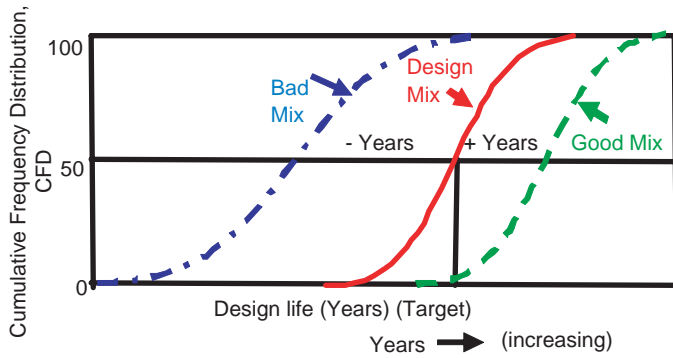


Figure 74. Cumulative frequency distribution of the service life.

$$PLD_j = (\text{As-Built Mix Life} - \text{As-Designed Mix Life})$$

The PLD_j is calculated as the average difference between the cumulative frequency distribution curves for the as-built mix life and as-designed mix life. This is shown in Figure 74.

3.6 Pay Adjustment Factor and Payment (Penalty/Bonus) Computation

3.6.1 Three Distresses

The purpose of a Performance Related Specification (PRS) like the QRS is to promote the construction of a quality pavement by measuring and evaluating characteristics directly related to its performance. The pavement performance is then predicted using key variables such as asphalt content and air voids, depending on the distress types of interest. The quality of the as-built mix is converted into its predicted service life and is then compared with the as-designed mix. The

predicted life difference between the two mixes becomes the basis of the payment system.

The concept behind the payment system is that the contractor’s compensation is based on the expected performance difference, i.e., the PLD between as-designed and as-built mixes. The Penalty/Bonus payment system implemented in the QRSS was modified and enhanced over the course of the project to obtain a rational, realistic formula. The QRSS payment system started with the following equation:

$$Total\ P/B = \frac{\sum(n_i)(P/B)_i}{N_t} \tag{121}$$

where

- Total P/B = total penalty/bonus (%)
- n_i = tonnage of each lot
- $(P/B)_i$ = penalty/bonus (%) of each lot
- N_t = total tonnage (ton)

The total Penalty/Bonus in Equation 121 represents the weighted average Penalty/Bonus of all lots in a given project by tonnage. Note that the percent Penalty/Bonus of each lot is obtained by an agency-defined relationship between PLD and Penalty/Bonus. An example of a possible relationship for the three major distresses is presented in Figure 76. The figure clearly shows that the contractor is compensated based upon the quality of a product (e.g., when the PLD is positive, Penalty/Bonus factor will be more than 100%).

The total Penalty/Bonus (%) is then used to calculate the actual Penalty/Bonus in dollars for a given project. Equation 121 can be, therefore, revised to account for the construction cost as follows:

$$C_{PB} = \left(\frac{\sum(n_i)(P/B)_i}{N_t} - 1 \right) C_{AC} \tag{122}$$

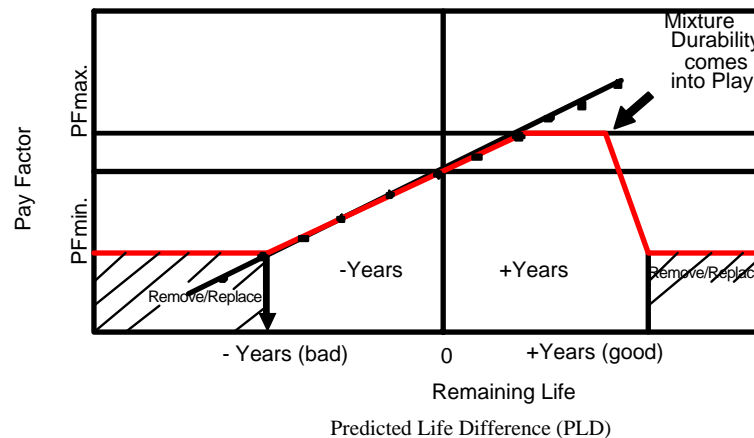


Figure 75. Determination of the pay factor based on the loss or gain in the predicted life difference.

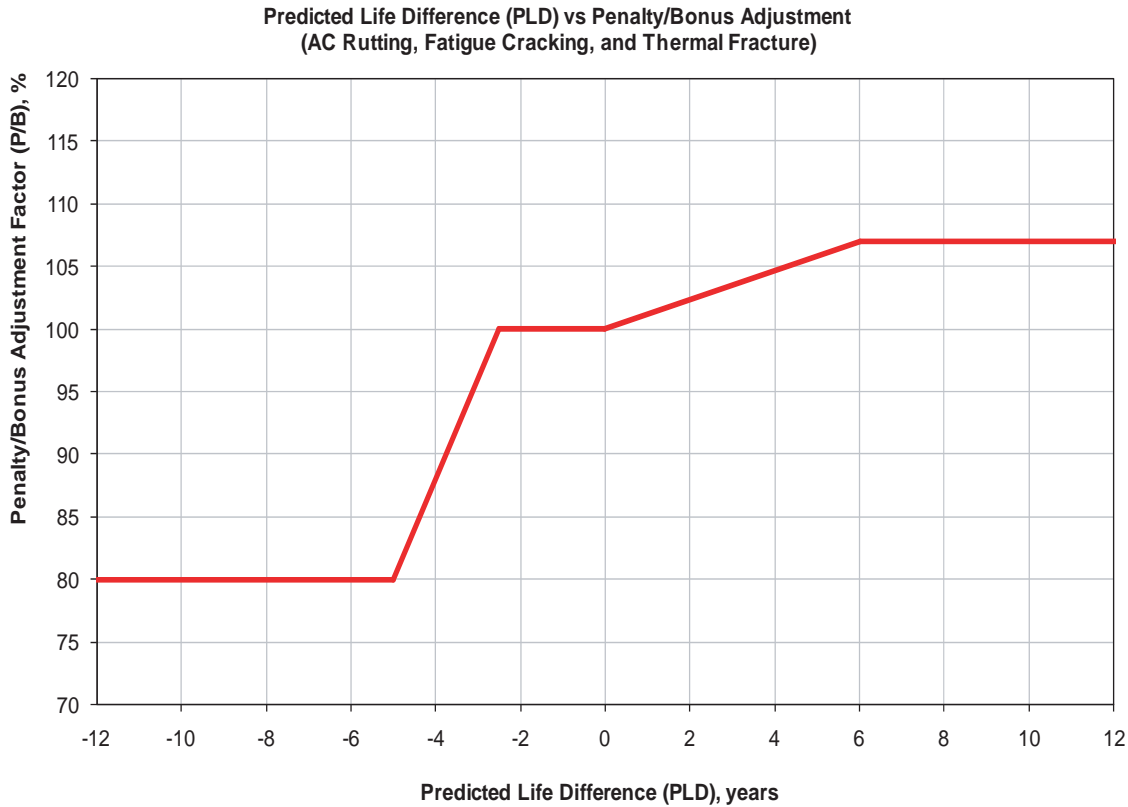


Figure 76. Sample of penalty/bonus adjustment factor (%) for major distresses.

where

C_{PB} = Final Penalty/Bonus cost for a given project
 C_{AC} = Construction Cost for AC pavement

For example, if the average Penalty/Bonus value turns out to be 107% and the asphalt pavement construction cost is \$50,000, the final Penalty/Bonus dollar amount would be \$3,500 = (1.07 - 1) * 50,000.

Since the QRSS considers three major distresses, Equation 122 can be expanded to the form of Equation 123.

$$\begin{aligned}
 C_{PB} = & \beta_r \left(\frac{\sum(n_i)(P/B)_{ri}}{N_t} - 1 \right) C_{AC} \\
 & + \beta_f \left(\frac{\sum(n_i)(P/B)_{fi}}{N_t} - 1 \right) C_{AC} \\
 & + \beta_{tf} \left(\frac{\sum(n_i)(P/B)_{tifi}}{N_t} - 1 \right) C_{AC} \quad (123)
 \end{aligned}$$

where

$(P/B)_{ri}$, $(P/B)_{fi}$, and $(P/B)_{tifi}$ = penalty/bonus factor for rutting, FC, and TF
 β_r , β_f , and β_{tf} = weighting factor (sum of all betas should be unity or 100%)

Each distress term in Equation 123 represents the Penalty/Bonus factor for that distress. The beta (β) parameters permit the agency to weigh each distress depending upon its experience or policy on the importance of the specific distress to the overall performance of its network. For example, TC is not a critical distress in the warmer portion of the United States. Therefore, in such regions, the beta parameter for TC would be set to be less than those of the other distresses. On the other hand, in the colder regions of the United States or in Canada, rutting may be of less importance compared to cracking distress in terms of evaluating HMA mix quality. In this situation, the beta value for rutting could have a reduced weight. However, whatever the relative weights assigned to the three distresses by the agency, the sum of the beta parameters must be unity or 100%.

As written, Equation 123 is valid only if for a pavement system with one AC layer. However, since pavement systems with two or three AC layers are generally the rule rather than the exception, it was essential to modify Equation 123 to define a universal Penalty/Bonus pay adjustment equation.

The critical location of each distress in a multi-AC layer depends on the type of distress considered. The critical location of FC is always a bottom AC layer because the FC dealt with in the QRSS is bottom-up alligator cracking. The critical location of TC is always the top layer, while rutting dis-

stress is considered to occur within all AC layers. Applying these definitions of distress locations, a universal equation for a three AC layer pavement system can be written as:

$$\begin{aligned}
 C_{PB} = & \beta_r \left\{ P_{r_s} \left(\frac{\sum n_k (P/B)_{rk}}{N_{t(AC_s)}} - 1 \right) C_{AC_s} \right. \\
 & + P_{r_m} \left(\frac{\sum n_l (P/B)_{rl}}{N_{t(AC_m)}} - 1 \right) C_{AC_m} \\
 & \left. + P_{r_b} \left(\frac{\sum n_m (P/B)_{rm}}{N_{t(AC_b)}} - 1 \right) C_{AC_b} \right\} \\
 & + \beta_f \left(\frac{\sum n_m (P/B)_{fm}}{N_{t(AC_b)}} - 1 \right) C_{AC_b} \\
 & + \beta_{tf} \left(\frac{\sum n_k (P/B)_{tk}}{N_{t(AC_s)}} - 1 \right) C_{AC_s} \quad (124)
 \end{aligned}$$

where

k, l, and m = lot number for surface, middle, and bottom layer

$N_{t(AC_s)}$, $N_{t(AC_m)}$, and $N_{t(AC_b)}$ = tonnage for surface, middle, and bottom layers

C_{AC_s} , C_{AC_m} , and C_{AC_b} = construction cost for surface, middle, and bottom layers

P_{r_s} , P_{r_m} , and P_{r_b} = rutting contribution factor for surface, middle, and bottom layers

Equation 124 has five terms; the first three terms are related to rutting, while the fourth and the fifth terms are related to FC and TC, respectively. The subscripts used in the equation denote each relevant AC layer.

Another factor introduced in Equation 124 is termed the layer rutting contribution factor. The rutting that occurs in a pavement due to excessive loading or poor mix design is observed on the pavement surface. In the majority of AC pavements, most of rutting occurs within the thickness of the surface AC layer and the magnitude of the rutting within each AC layer (or AC mix type) is highly variable. Because of this, layer rutting contribution factors (P_{ri}) have been introduced.

The QRSS provides default values for the layer rutting contribution factors; as with the beta parameters, the agency may change (overwrite) the default values based on its experience or policy. As with the beta parameters, the rutting contribution factors must total to unity or 100%.

3.6.2 Inclusion of IRI

The ride quality indicator (IRI) is included as an additional distress in the QRSS. Unlike rutting, FC, and TC, the QRSS does not predict the change in IRI over time and the consid-

eration of the IRI in the calculation of the penalty/bonus cost is entirely at the user's discretion. Figure 77 shows a screen shot from the alpha version of the QRSS for the selection of IRI as a desired distress.

Once the user selects the IRI, the program requires input of the actual measured average initial IRI over 0.1 miles at each milepost of the project to evaluate the smoothness of the as-built pavement surface. The fundamental concept used in the QRSS follows the traditional state DOT approach. However, the input values found in the QRSS allow each agency to tailor their own Penalty/Bonus criterion and methodology.

The QRSS adjusts the Penalty/Bonus based on the initial IRI measured at every mile post. Three different payment schedules are included to allow the user to adjust the Penalty/Bonus values as a function of traffic volume. The recommended IRI payment schedule as a function of traffic volume and IRI₀ is presented in Table 32

The following step-by-step example is presented to show how to use Table 32:

- A 0.5-mile Interstate highway having two lanes in one direction is constructed.
- An average initial IRI (in/mile) is measured for 0.1 mile at every milepost for each lane.
- Penalty/Bonus cost (\$) for each mile post is determined from Table 32.
- Table 33 presents the average initial IRI inputted in the QRSS along with the corresponding Penalty/Bonus.
- The final cost is the sum of amount of money for each lane: \$1,640 = \$2,660 – \$1,020

The QRSS uses a user-defined pay adjustment schedule plot for the determination of Penalty/Bonus for IRI rather than the tabular form shown in Table 32. This is done for programming convenience as well as for consistency of the IRI payment methodology with the other distresses. Figure 78 illustrates an example of the pay adjustment schedule for IRI in the QRSS. The pay adjustment can be altered for the three traffic volumes or for the user's preference as shown in the figure. Three schedules (the three lines in the figure) are presented for low traffic (local road), intermediate traffic (arterial road), and high traffic (interstate highway). Agencies have complete freedom to define their own set of Penalty/Bonus versus IRI₀ schedules based on experience or policy.

Figure 79 is a screen shot of the IRI₀ pay adjustment schedule coded in the QRSS. As discussed above, the program provides three sets of default values for the schedule, but the user can overwrite each cell to use values selected by the agency.

The QA part of the QRSS provides a user input table for IRI₀. Figure 80 is a screen shot of the IRI₀ user input. Once the user selects the IRI₀, the average IRI₀ at every 0.1 mile for each

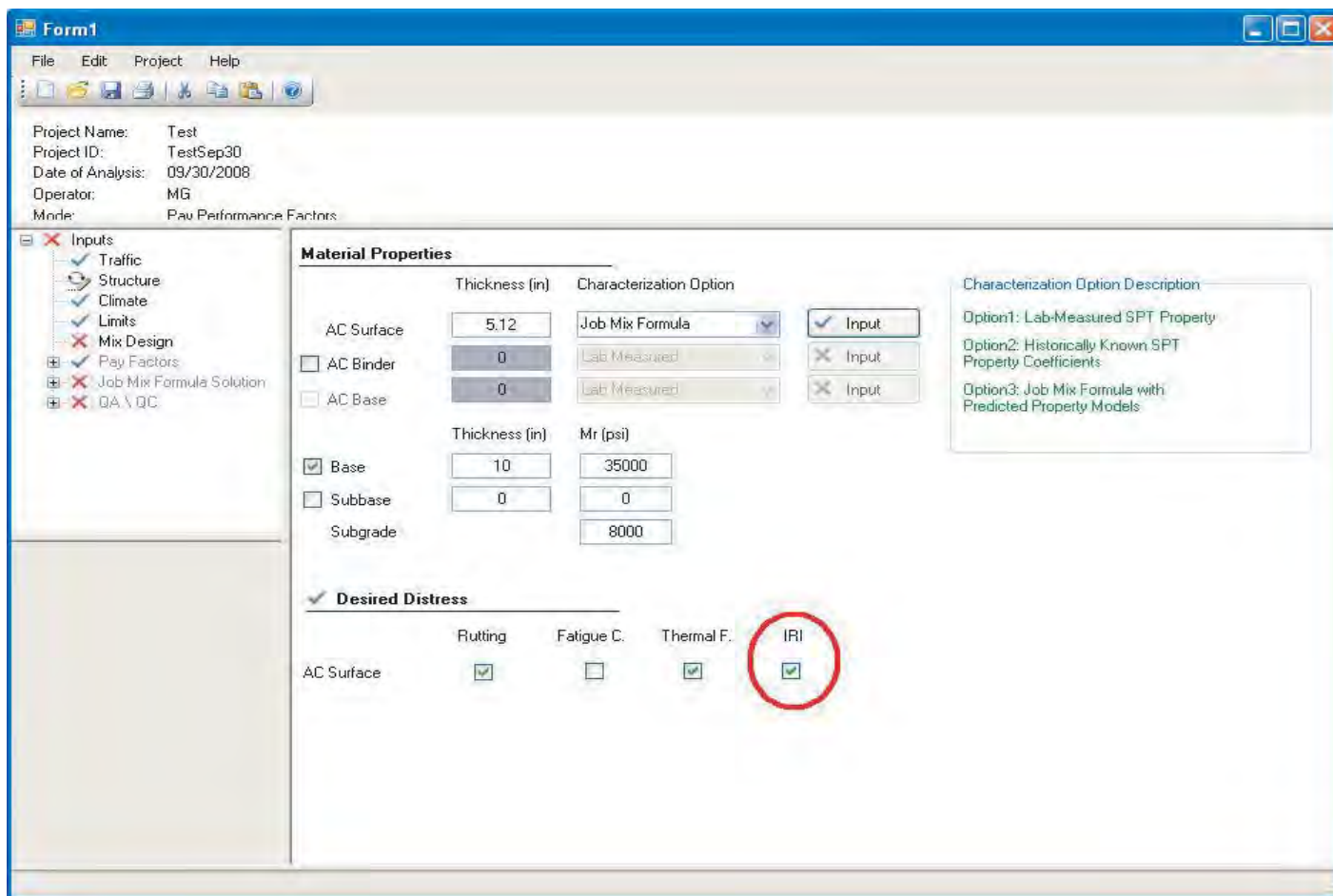


Figure 77. Screen shot for IRI selection in the QRS software.

Table 32. QRS recommended schedule for initial pavement— IRI_0 .

Average IRI for each 0.1 mile of Traffic Lane (in/mile)	Pay Adjustment (\$/0.1 mile of Traffic Lane)		
	Schedule 1 (High Traffic Volume)	Schedule 2 (Intermediate Traffic Volume)	Schedule 3 (Low Traffic Volume)
≤ 30	600	600	300
31	580	580	290
32	560	560	280
33	540	540	270
...
74	-180	0	0
75	-200	0	0
76	-220	-20	0
77	-240	-40	0
78	-260	-60	0
...

Table 33. Example of IRI_0 measured and penalty/bonus cost.

Mile Post	Unit Mileage (mile)	Lane 1		Lane 2	
		Average Initial IRI	Penalty or Bonus (\$)	Average Initial IRI	Penalty or Bonus (\$)
1	0.1	33	+540	74	-180
2	0.1	34	+520	76	-220
3	0.1	32	+560	77	-240
4	0.1	35	+500	75	-200
5	0.1	33	+540	74	-180
Sum	0.5		+2,660		-1,020

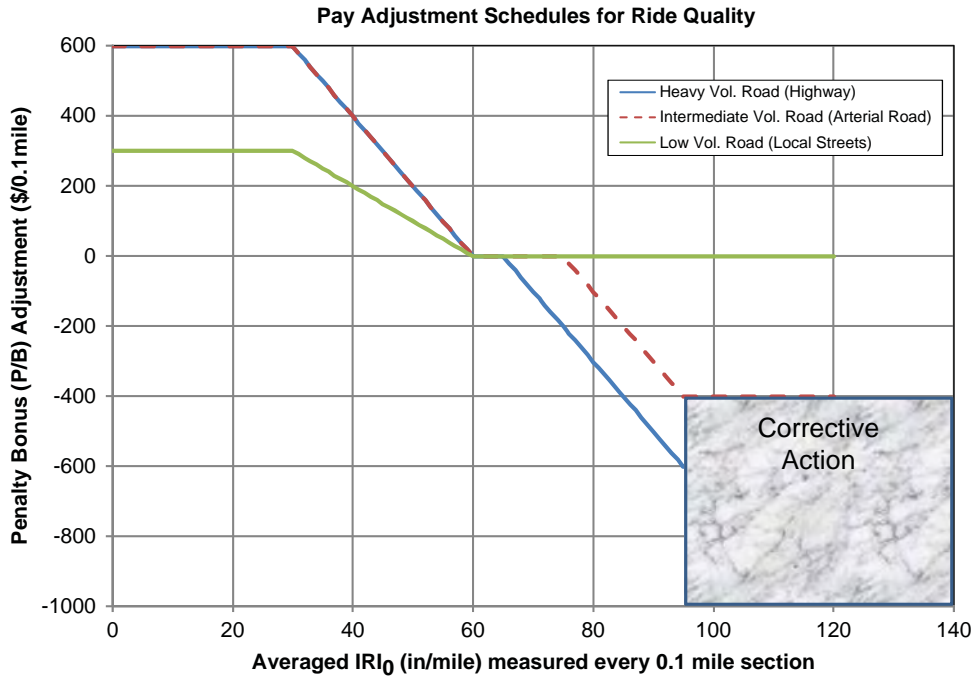


Figure 78. Pay adjustment schedule for IRI.

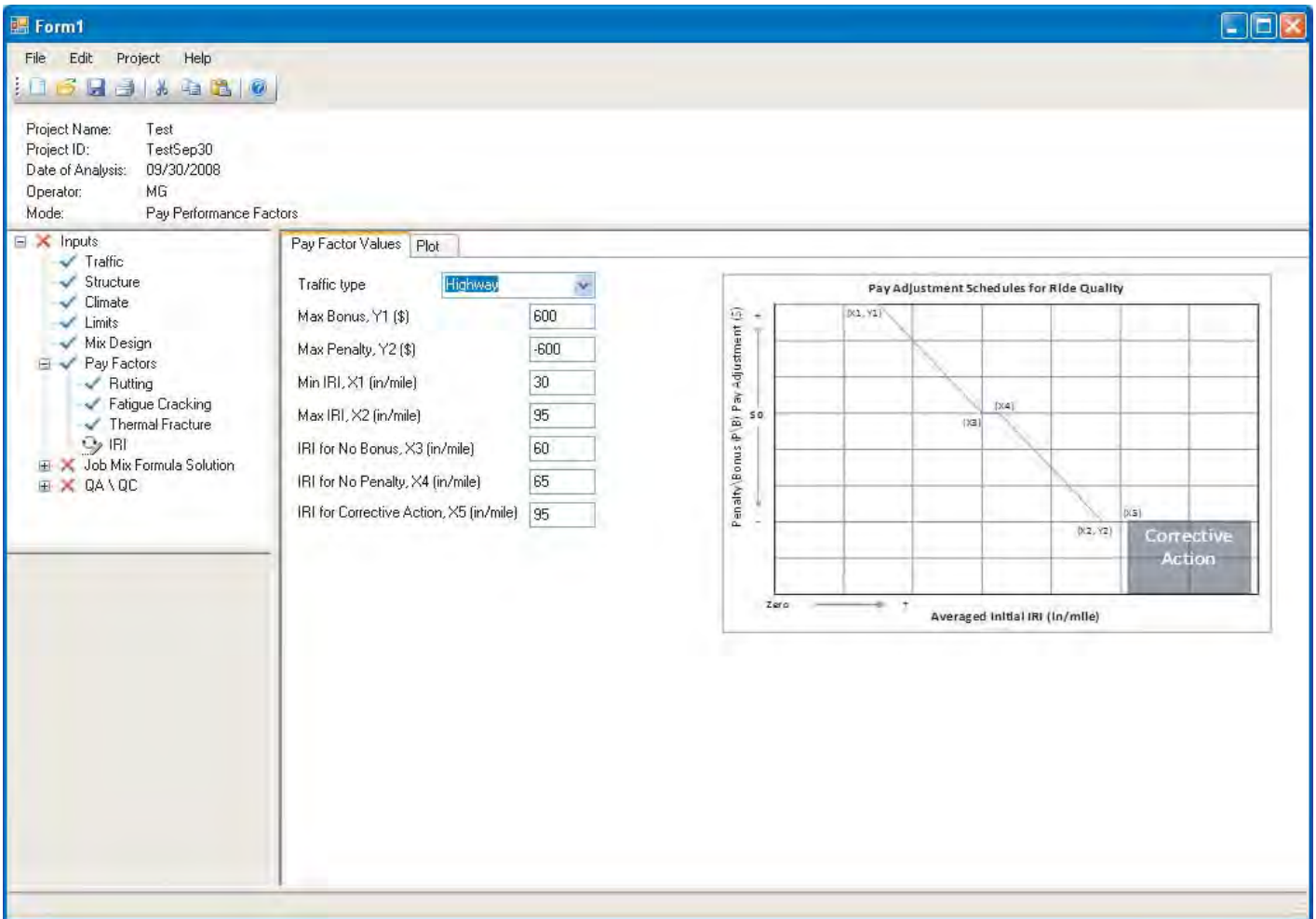


Figure 79. Screen shot of IRI₀ pay adjustment schedule input in the QRS program.

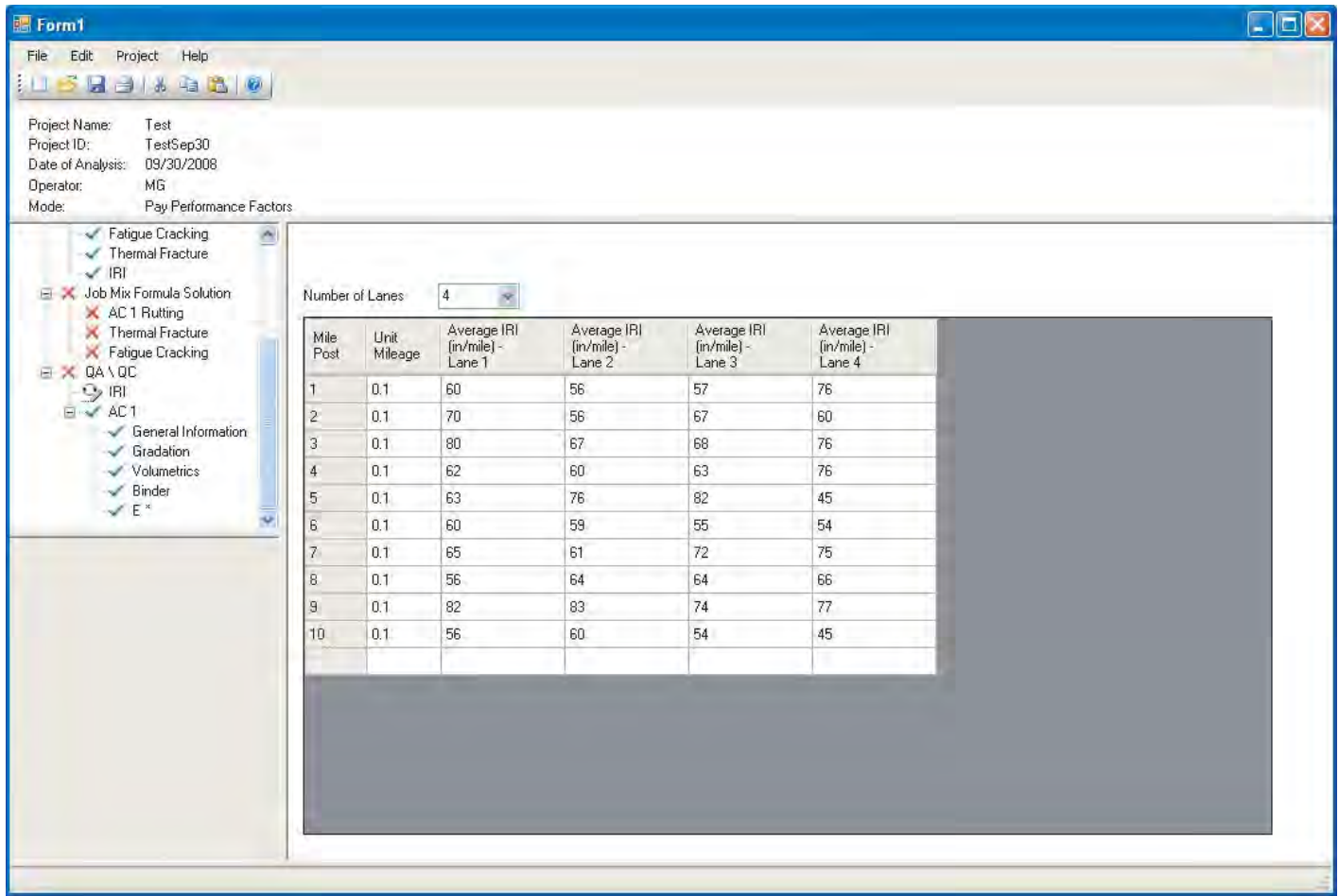


Figure 80. User Input screen for measured IRI₀.

lane is entered in the program. These IRI₀ values are then used to calculate the IRI₀ Penalty/Bonus which is included in the calculation of final Penalty/Bonus with the other distresses. The IRI₀ Penalty/Bonus cost is computed by Equation 125.

$$C_{PB} = \sum_{i=1}^L \sum_{j=1}^{Lp/0.1} (P/B)_{IRI_{ij}} \quad (125)$$

where

- L = number of total lanes
- Lp = length of project (mile)
- (P/B)_{IRI_{ij}} = penalty or bonus (\$) for IRI_{ij}
- IRI_{ij} = average IRI₀ for *i*th lane and *j*th mile post

The final Penalty/Bonus cost is the sum of the IRI₀ Penalty/Bonus cost from Equation 125 and the Penalty/Bonus cost for the three distresses (Equation 124). Equation 126 represents the final Penalty/Bonus equation that is implemented in the QRSS.

$$C_{PB} = C_{PB1} + C_{PB2} \quad (126)$$

where

- C_{PB} = Final Penalty/Bonus cost for a given project
- C_{PB1} = Penalty/Bonus cost associated with the three distresses (Equation 124)
- C_{PB2} = Penalty/Bonus cost associated with IRI₀ (Equation 125)

CHAPTER 4

QRSS General Procedure

4.1 Introduction

This chapter presents a general description of the QRSS and a series of screen shots illustrating its operation. Similar to other pavement-related analysis programs such as the MEPDG, the QRSS requires the user to enter all information needed to perform the requisite calculations. It is important to understand that the inputted data should be reasonably selected (or prepared) and correctly entered into the specified locations in accordance with the user's manual provided in Appendix E. Otherwise, the program may produce unreasonable results or unexpected errors.

The following sections describe the detailed QRSS procedures in the order of the program's operation.

4.2 Detailed Procedure

4.2.1 Mode Selection and General Information

4.2.1.1 Mode Selection

When the QRSS is opened (Figure 81), the initial screen provides two options for the user's selection: mix design and pay performance factors. As described in Chapter 3, in the mix design mode, the user can interactively verify that the volumetric properties of the as-designed mix and pavement structure are acceptable, considering the desired distress criteria. In the pay performance factors mode, the QRSS serves as a tool for quality assurance of the as-built mix and structure, with each field lot evaluated in comparison to the quality of the as-designed mix. Note that if the pay performance factors mode is selected, the QRSS first evaluates the as-designed mix and then continues on to the quality assurance and payment computation portion of the program.

4.2.1.2 General Information Input

The general project information is entered in the initial window shown in Figure 81. This information is not used for any

of the later program calculations, but it is continuously displayed in the left upper side of the program window during the program operation for the user's reference. The information includes the followings:

- Agency name
- Project ID
- Project name
- Analysis date
- Operator's name

4.2.2 User Input

4.2.2.1 Traffic Input

Calculation of the predicted rutting and FC distresses requires the expected traffic volume during the design life. These analyses utilize the total Equivalent Single Axle Load (ESAL) as a single variable representing the entire effect of traffic on the development of the distresses. The ESAL is computed from several traffic-related factors: design life (Y); year 1 daily ESAL ($ESAL_0$); and annual growth rate (r) in percent. The total ESAL is computed by the following equation:

$$ESAL = \frac{(ESAL_0)(365)}{Ln(1+r)} [(1+r)^Y - 1] \quad (127)$$

Figure 82 presents the program window for ESAL data input and calculation.

4.2.2.2 Structure and Distress Selection and Material and Volumetric Property Input

In the structure and distress selection input (Figure 83), the user enters the thickness for each designed AC layer and the unbound material layers. Up to AC three layers (AC surface, AC binder, and AC base) and three unbound material layers (granular base, subbase, and subgrade) are allowed in the structure for analysis. Resilient modulus (M_r) values must be entered

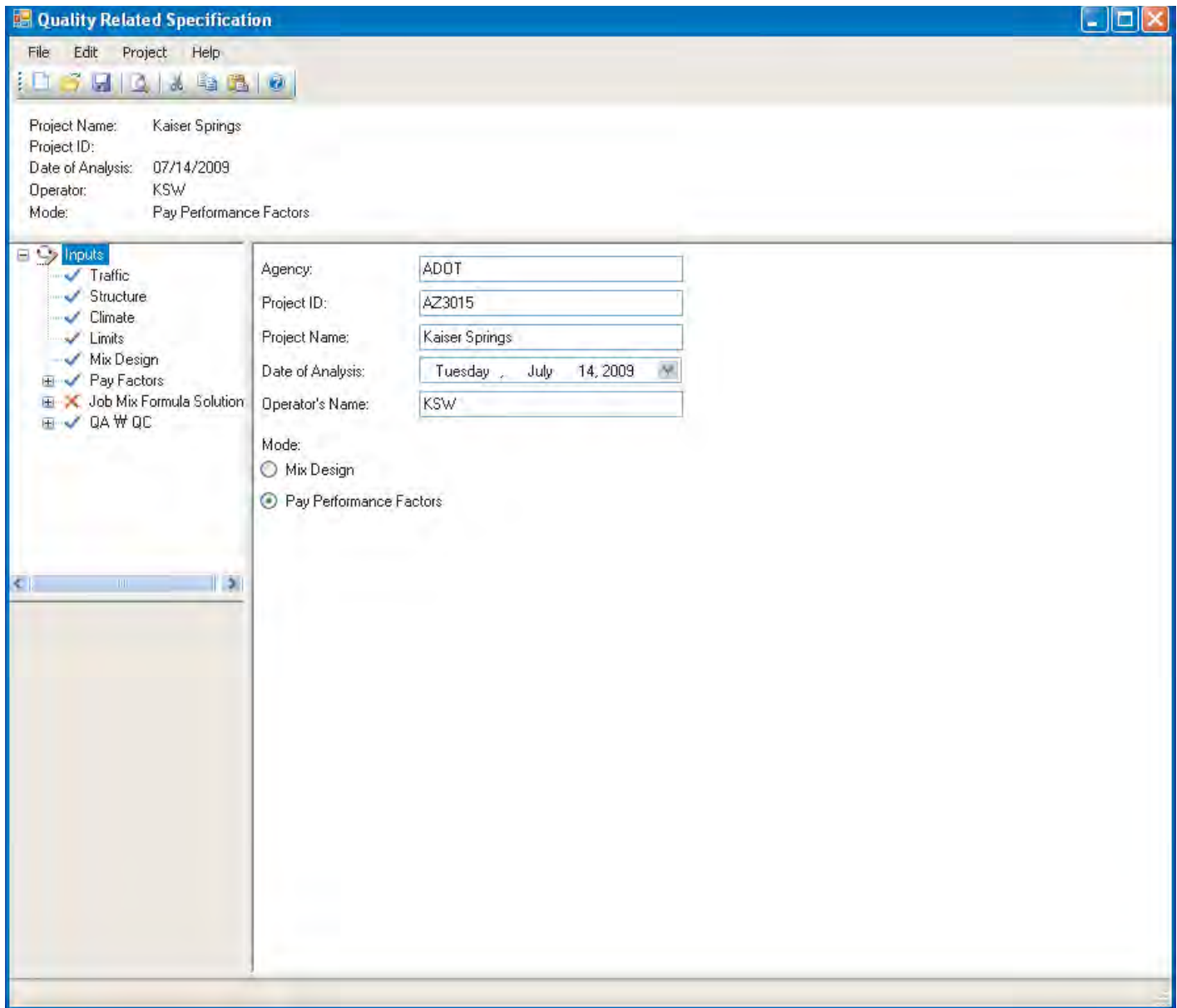


Figure 81. Initial screen of the QRSS.

for the selected unbound layers. Note that the resilient modulus is only used in the fatigue distress analysis. For the rutting analysis, it is assumed that a subgrade layer resilient modulus of 14,500 psi exists regardless of the actual properties of the sub-surface unbound layers. The thermal cracking analysis does not consider the effect of the unbound layers.

The program allows the user to select the distresses to be analyzed by interactively showing the structural AC layer system and critical distresses for each layer, as shown in Figure 83. For instance, in a three-layer AC pavement structure, the rutting analysis can be performed for one, two, or three AC layers by checking or unchecking the boxes in the Desired Distress portion of the window. The same procedure is applied for the fatigue and thermal cracking distresses.

The bottom AC layer is considered the operative layer for the fatigue distress while the surface AC layer is that for TC. IRI can also be selected for analysis in the Desired Distress portion of the window. However, IRI is only used in the final Penalty/Bonus calculation of the pay-performance analysis and is not involved in a deterministic or stochastic distress prediction.

The program next requires the user to provide the design volumetrics, binder characteristics, and target in-situ volumetrics for the as-designed mix in the material properties window shown in Figure 84. The following properties are required:

- Air voids (%)
- Asphalt content by weight (%)

The screenshot shows a software window titled "Quality Related Specification" with a menu bar (File, Edit, Project, Help) and a toolbar. The main area is divided into a left sidebar and a right main panel.

Project Information:

- Project Name: Kaiser Springs
- Project ID:
- Date of Analysis: 07/14/2009
- Operator: KSW
- Mode: Pay Performance Factors

Inputs (Left Sidebar):

- Inputs (expanded)
 - Traffic (selected)
 - Structure (checked)
 - Climate (checked)
 - Limits (checked)
 - Mix Design (checked)
 - Pay Factors (checked)
 - Job Mix Formula Solut (checked)
 - QA W QC (checked)

Main Panel Fields:

- Design Speed (mph): 65
- Design Life (yrs): 20
- Design ESALs** (Section Header)
- Year 1 Daily ESALs (Design Lane): 2,000
- Annual Growth Rate 'r' (%): 4.0
- Total ESALs: 22,169,915 (grayed-out)

Figure 82. Design ESAL calculation.

- Binder type
- G_b (binder specific gravity)
- Air voids— V_a (%)
- G_{sb} (bulk specific gravity of aggregate)
- G_{mm} (maximum theoretical specific gravity)

The air voids required to compute the target in-situ volumetrics is the specified field (in-situ) computed air voids. It is not the laboratory air voids of the as-designed mix.

Several target in-situ volumetrics are calculated from the inputted data with the following equations and entered by the program in the associated grayed-out cells in Figure 84.

$$\text{Bulk Density, } G_{mb} = \left(1 - \frac{V_a}{100}\right) G_{mm} \quad (128)$$

Effective Binder Content by Volume,

$$V_{beff} = \frac{(100 - V_a)G_{sb} - (100 - AC)G_{mb}}{G_{sb}} \quad (129)$$

$$\text{or } \%V_{beff} = \left(\frac{100 - \%V_a}{100}\right) \left(\frac{100G_{sb} - 100G_{mm} + \%AC G_{mm}}{G_{sb}}\right) \quad (130)$$

The screenshot shows the 'Quality Related Specification' software window. The title bar includes 'File', 'Edit', 'Project', and 'Help' menus. The main area is divided into a left sidebar and a main content area.

Project Information:
 Project Name: Kaiser Springs
 Project ID:
 Date of Analysis: 07/14/2009
 Operator: KSW
 Mode: Pay Performance Factors

Inputs (Left Sidebar):
 Traffic
 Structure
 Climate
 Limits
 Mix Design
 Pay Factors
 Job Mix Formula Solut
 QA QC

Material Properties (Main Content):

	Thickness (in)	Characterization Option	
AC Surface	2.00	Job Mix Formula with Predicted Property	<input checked="" type="checkbox"/> Input
<input checked="" type="checkbox"/> AC Binder	3.00	Job Mix Formula with Predicted Property	<input checked="" type="checkbox"/> Input
<input checked="" type="checkbox"/> AC Base	5.00	Job Mix Formula with Predicted Property	<input checked="" type="checkbox"/> Input

	Thickness (in)	Mr (psi)
<input checked="" type="checkbox"/> Base	10	30,000
<input type="checkbox"/> Subbase		
Subgrade		3,000

Desired Distress (Main Content):

	Rutting	Fatigue C.	Thermal F.	IRI
AC Surface	<input checked="" type="checkbox"/>		<input type="checkbox"/>	<input type="checkbox"/>
AC Binder	<input checked="" type="checkbox"/>			
AC Base	<input checked="" type="checkbox"/>	<input type="checkbox"/>		

Figure 83. Structure and distress selection.

$$\text{Voids in Mineral Aggregate, \%VMA} = V_a + V_{beff} \quad (131)$$

$$\text{Voids Filled with Asphalt, \%VFA} = \left(\frac{V_a}{V_a + V_{beff}} \right) 100 \quad (132)$$

For the aggregate gradation shown in the right half of the materials properties window, the absolute minimum requirement is entry of percent passing values for the following four sieves: $\frac{3}{8}$ in., $\frac{1}{2}$ in., #4, and #200. These are critical variables for the volumetric-based WPE. The user may also provide the percent passing data for the other sieve size shown, but it is not necessary to input all cell values shown in the window.

4.2.2.3 Climate

The climate at the project location is selected to allow the consideration of climatic effects on the distress predictions. The QRSS provides three options for the user to retrieve the climatic data. The first option is to manually enter the following climatic data, if known, into the requisite cells in the climatic location selection window in Figure 85:

- Mean Annual Air Temperature ($^{\circ}$ F)
- Mean Monthly Air Temperature Standard Deviation ($^{\circ}$ F)
- Mean Annual Wind Speed (mph), Wind

Material Properties

Design Volumetrics

Air Voids (%) 4.0

Asphalt Content by Weight (%) 4.8

Binder Characteristics

Binder Type PG70-16

Direct Input (A and VTS)

A (RTFD) 10.641

VTS (RTFD) -3.548

Gb 1.030

Target In-Situ Volumetrics

Air Voids - Va (%) 7.0

Gsb 2.650

Gmm 2.500

Bulk Density - Gmb 2.325

Asphalt Content by Weight (%) 4.8

Effective Binder Content by Volume - Vbeff (%) 9.475

VMA (%) 16.5

VFA (%) 57.5

* Sieve	% Passing
1 1/2 "	100
1 "	100
* 3/4 "	92
1/2 "	
* 3/8 "	53
* #4	34
#8	
#10	
#16	
#30	
#40	
#50	
#100	
* #200	4.1

* Required Field

OK Cancel

Figure 84. Material and volumetric property input.

- Mean Annual Sunshine (%), Sunshine
- Annual Cumulative Rainfall Depth (in), Rain

These climatic data, designated as MAAT, δ_{MMAT} , Wind, Sunshine, and Rain, respectively, are used to calculate the effective temperatures for rutting and fatigue cracking distress, with the following equations from Chapter 2:

$$T_{eff} = 14.620 - 3.361 \ln(f_{eff}) - 10.940z + 1.121(MAAT) + 1.718(\sigma_{MMAT}) - 0.431(Wind) + 0.333(Sunshine) + 0.080(Rain) \quad \text{for Rutting}$$

$$T_{eff} = -2.3316\sqrt{f_{eff}} - 13.9951 + 1.0056(MAAT) + 0.8755(\sigma_{MMAT}) - 1.1861(Wind) + 0.5489(Sunshine) + 0.0706(Rain) \quad \text{for Fatigue Cracking}$$

The second, most convenient option to obtain these key climatic data is to choose a weather station near the project location from the U.S. weather station list by clicking the “Select Station” button in Figure 85. This option is identical to the approach used in the MEPDG.

If there is no weather station near the project location, the third option is to interpolate a virtual weather station from data obtained from several adjacent weather stations. To use this option, the user enters the longitude, latitude, and elevation at the project location into the cells provided in the positioning window and clicks the approx. climate button.

For the first or second option, the selected weather station is saved by clicking the Export.icm button; for the third option, clicking the Import .icm button saves the interpolated climatic data in an .icm file. The .icm file format is the same as that used by the Enhanced Integrated Climatic Model in the MEPDG.

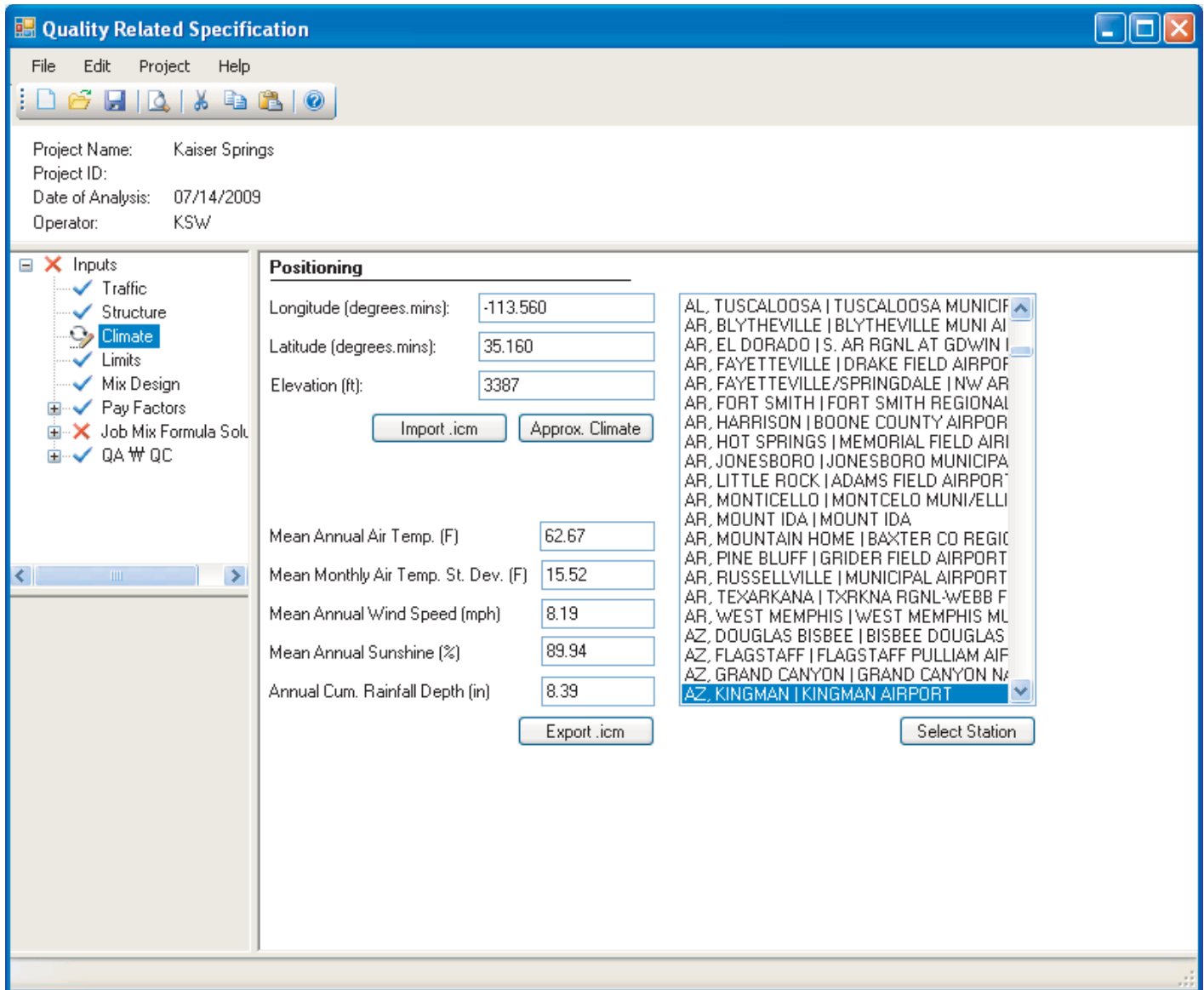


Figure 85. Climatic location selection.

While the rutting and FC distress analyses can use any of the three options, only the second and third options can be used for TC analysis since the TC analysis requires actual hourly climatic data, not summarized data, to create the pavement temperature file from the information in the icm files.

4.2.2.4 Limits

The allowable distress limits are set by the user for the mix and structural pavement design in the Average Allowable Distress Values window shown in Figure 86. The distresses deterministically predicted from the given input variables should be less than the allowable distress limits for acceptance. If one or more are not, the as-designed mix or the pavement structure or both do not comply with the specification and should

be modified to meet the requirements. The QRSS will indicate whether the combination of design mix and pavement structure is acceptable in terms of the allowable distress limits in the deterministic design solution window, as explained later in the chapter.

Since the allowable distress values are used to determine allowable values of E^*_{eff} for rutting and FC distresses, they should fall within reasonable ranges, given that they are ultimately selected by each agency on the basis of factors such as design period, environmental location, traffic volume, and available budget for maintenance. A typical allowable range for each distress suggested in the QRSS is as follows:

- Total AC Rutting: 0.2 ~ 0.35 inches
- Fatigue Cracking: 15 ~ 30%
- Thermal Cracking: 300 ~ 700 ft/mile

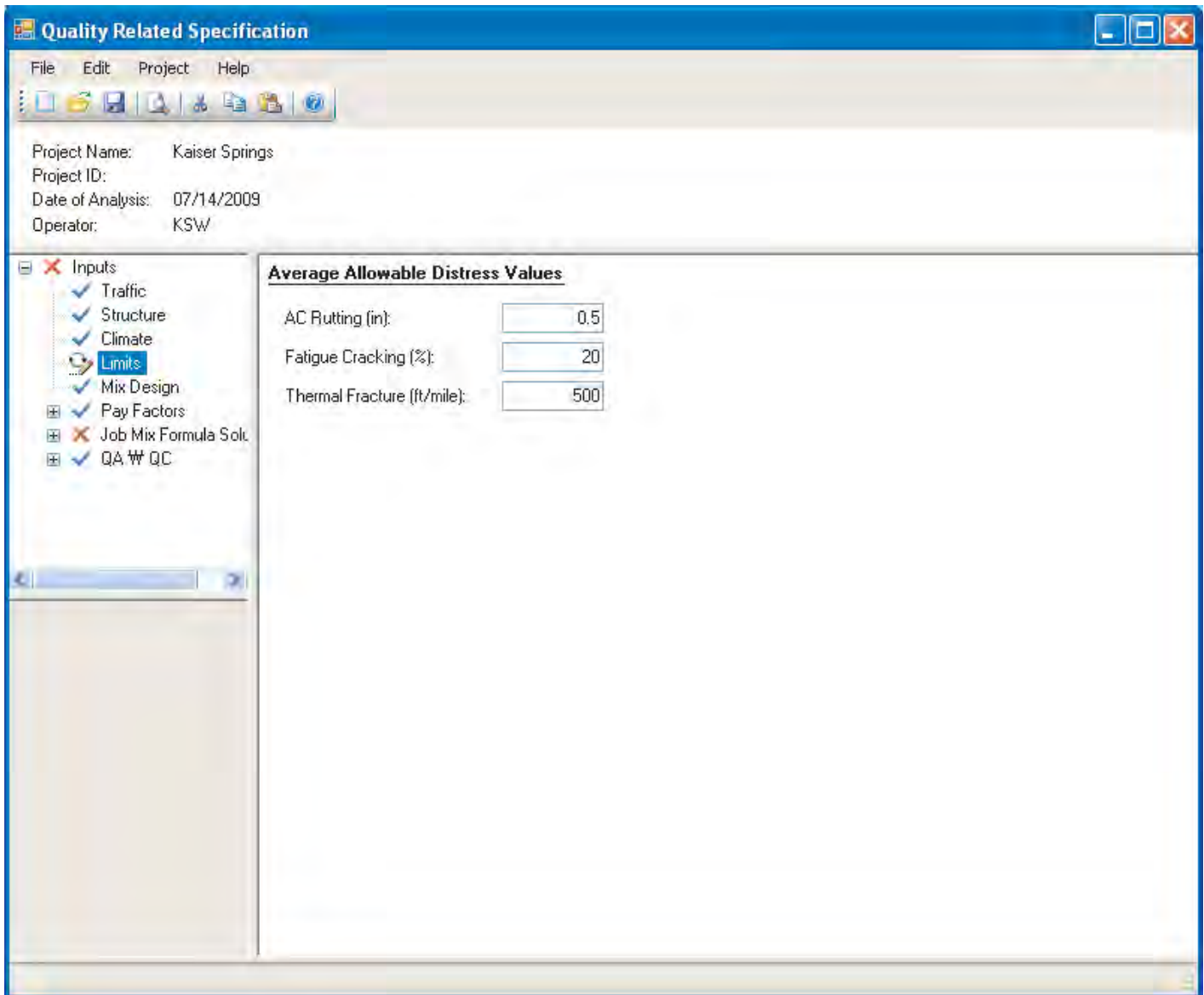


Figure 86. Allowable distress values input.

However, these values can be overridden based on the agency's experience or policy.

4.2.3 Mix Design

Once this data input portion of the program is completed, the user clicks the "Mix Design" button under the "Inputs" tree and the QRSS performs all necessary computations and displays the results for the as-designed mix. The Mix Design Output window, illustrated in Figure 87, contains the following results from the top row down:

- Layer Thickness (in): Each AC layer thickness for rutting and the total AC thickness for FC and TC. These values are those entered by the user in the Structure and Distress Selection window (Figure 83).
- Effective Frequency (Hz) and Temperature (°F): These values are computed by the QRSS based on the methodology described in Section 2.2.1. No effective temperature or frequency is needed for TC.
- Recommended Testing Frequency (Hz) and Temperature (°F): Typically, the frequency value is 25 Hz, but the user can input a different value; the corresponding test temperature is then calculated. No recommended testing frequency and temperature are needed for TC.
- Allowable Distress and Allowable Layer E* (ksi): Allowable Distress is a user-defined criterion as explained in the previous section; the corresponding layer E* is calculated by the relationship between allowable distress and E*. The distress-E* relationship was explained in Section 3.2. Only the criterion is needed for thermal cracking as the value of E* is not used in the prediction of this distress.

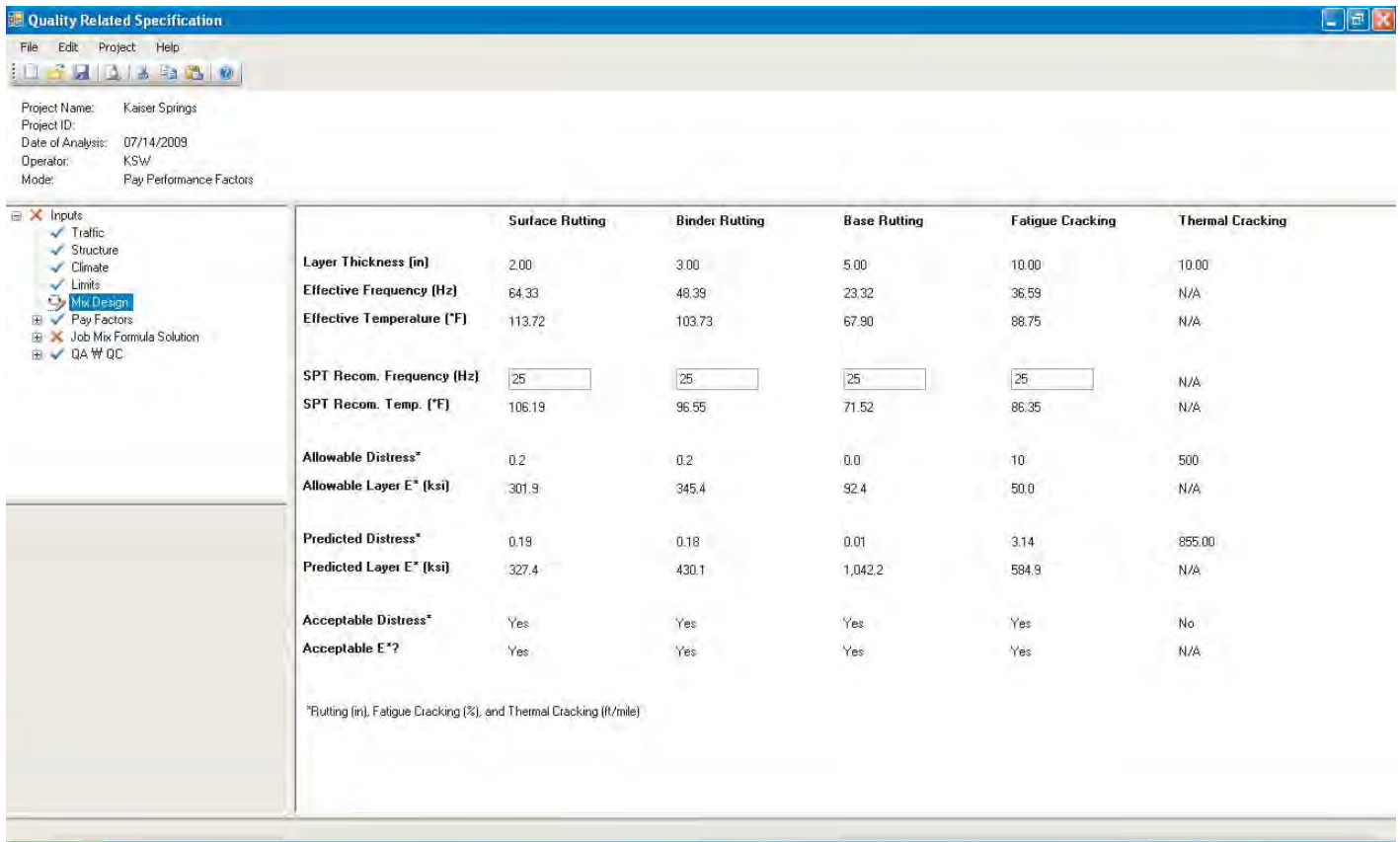


Figure 87. Mix design output.

For a multi-AC layer pavement system, the allowable rutting distress for each layer is calculated with the rutting distribution by pavement depth.

- Predicted Distress and Predicted Layer E* (ksi): Based upon the mix properties, pavement structure, climate, and traffic volume, the QRSS predicts the amount of each selected distress using the deterministic solutions described in Chapter 2. For the rutting and FC distresses, the calculation is internally completed, while the TC distress runs an external subroutine where a temperature file (Thermal.tmp) conforming to the selected climate and total AC pavement thickness is created. Figure 88 shows an example of the TC subroutine in the process of creating this temperature file. The temperature file is unique to a particular project location and AC thickness. If either one is changed, the temperature file must be recreated.
- Acceptable Distress and Acceptable E*?: These results aid the user in reaching a decision on the acceptability of the as-designed mix for the proposed project pavement structure. This decision is made based upon a comparison of the predicted distresses with those entered as specification criteria. If a predicted distress is less than the allowable distress, the program suggests that the proposed mix design can be used (Yes), and vice versa (No). Further, the differ-

ence in magnitude between the predicted and allowable E^*_{eff} helps estimate how good or bad the as-designed mix is. This comparison helps avoid a design that may be too conservative and achieve a cost-effective combination of pavement structure and mix design. Since the dynamic modulus (E^*) is not used in the thermal cracking analysis, only the Acceptable Distress cell shows a result for TC.

4.2.4 Pay Adjustment Analysis (Stochastic Analysis of the As-Designed Mix)

4.2.4.1 Pay Factors

The pay adjustment system in the QRSS is directly linked to the predicted performance of the pavement. The gain or loss in service life between the as-designed mix and the as-built mix determines the pay factor. After the acceptability of the as-designed mix and pavement structure is established, the user enters the parameters needed by the program to calculate the pay adjustment factors for the three distresses, as shown on the Pay Factors tab in the Pay Factor Values window for each distress (Figure 89):

- Max Bonus, Y1 (%)
- Max Penalty, Y2 (%)

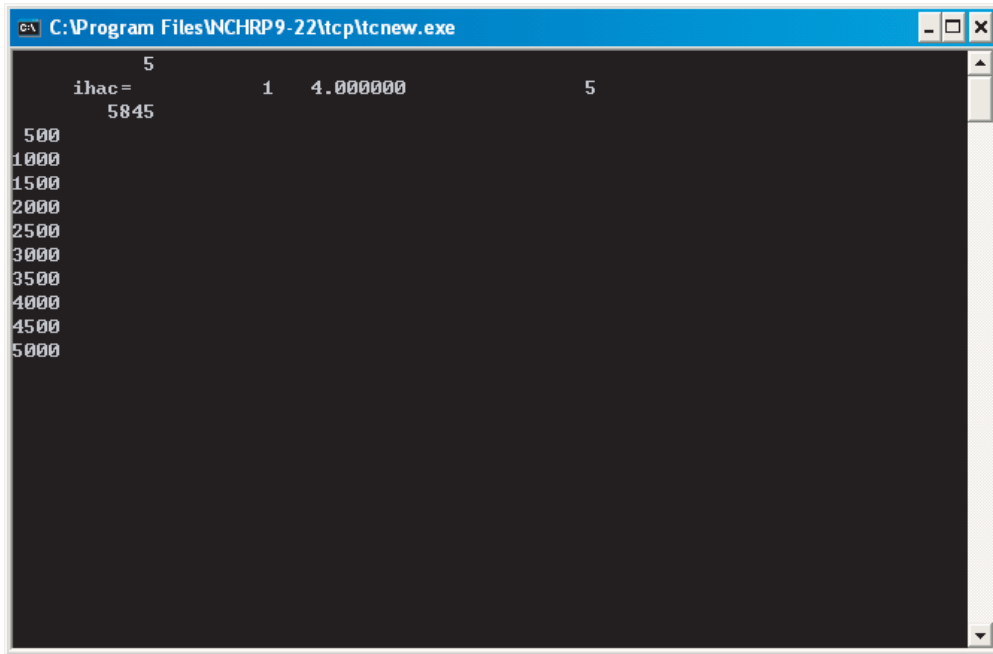


Figure 88. Creation of temperature file (Thermal.tmp) for TC analysis.

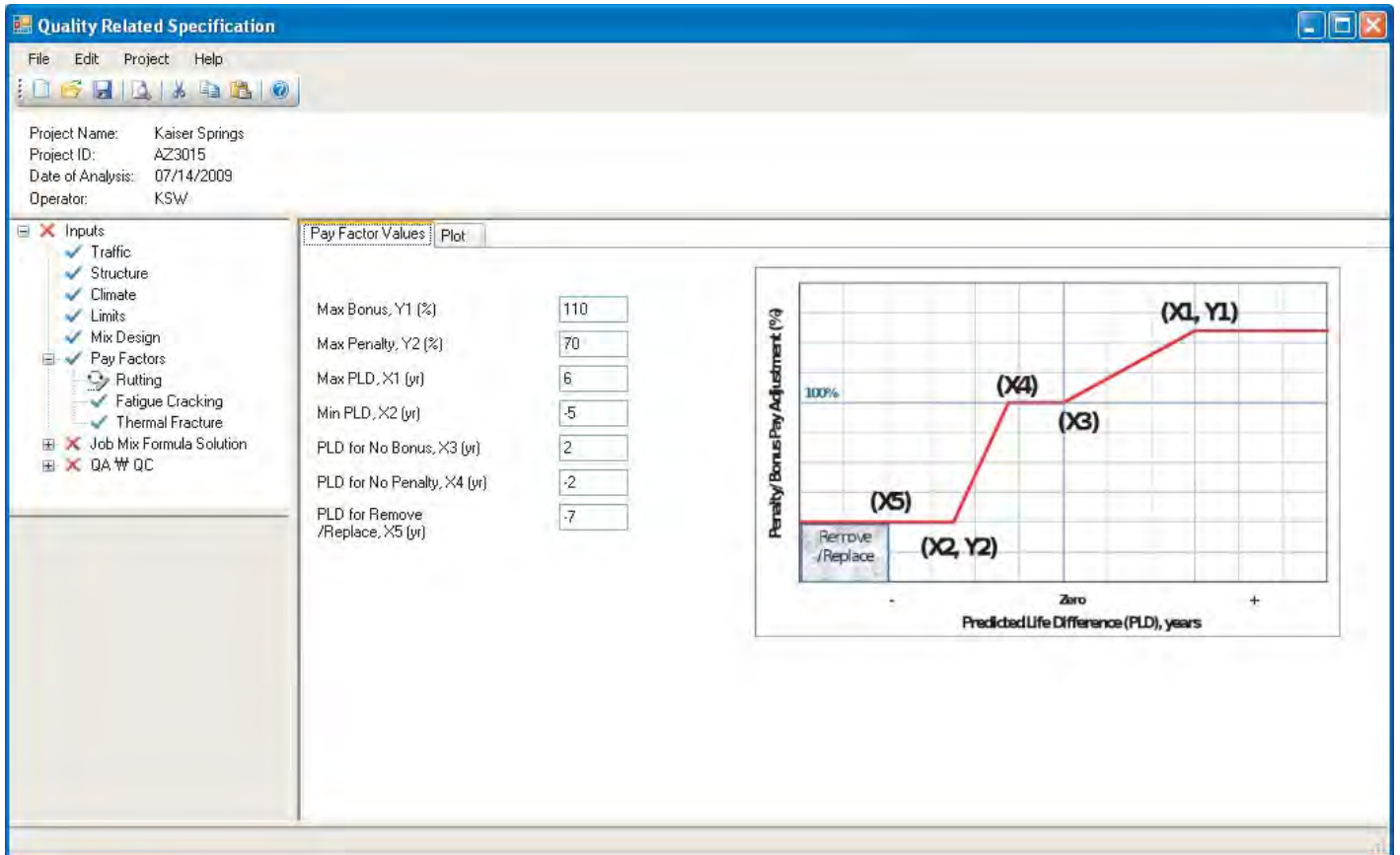


Figure 89. Pay factor values for each distress.

- Max PLD, X1 (yr)
- Min PLD, X2 (yr)
- PLD for No Bonus, X3 (yr)
- PLD for No Penalty, X4 (yr)
- PLD for Remove/Replace, X5 (yr)

The X and Y parameters define the coordinates of the slope points of the pay adjustment schedule. The QRSS provides default values for these parameters, but these may be changed by the agency. The maximum bonus may not exceed 120% and maximum penalty may not be less than 50%. Figure 90 illustrates a typical pay adjustment schedule plot for rutting as an example; the plot is obtained by selecting the plot tab in the window.

The pay adjustment schedule for IRI is defined using similar parameters. The QRSS provides default values of the parameters for the three typical roadway types: 1) local road (low speed traffic), 2) arterial road (intermediate speed traffic), and 3) highway (high speed traffic). The agency may replace the default values at its discretion. The Pay Adjustment IRI window and an example of an actual plot are shown in Figures 91 and 92, respectively.

4.2.4.2 As-Designed Mix (Job Mix Formula) Solution

Rutting: The stochastic solution for rutting of the as-designed mix utilizes Monte Carlo simulation to obtain the variance of the effective dynamic modulus, rut depth, and service life. The mean and standard deviation of the dynamic modulus are estimated from the WPE by using the frequency distribution of key design volumetric properties having means from the mix design and standard deviations from historic variance of the properties, as discussed in Chapter 3. The user may replace any of the default standard deviation values with agency-determined values. These volumetric property values and the coefficient of variation for each property are presented on the Summary tab of the window in Figure 93; the variables include:

- Total Thickness
- Layer Thickness
- Air Voids- V_a (%)
- Retained $\frac{3}{4}$
- Retained $\frac{3}{8}$
- Retained #4
- Passing #200

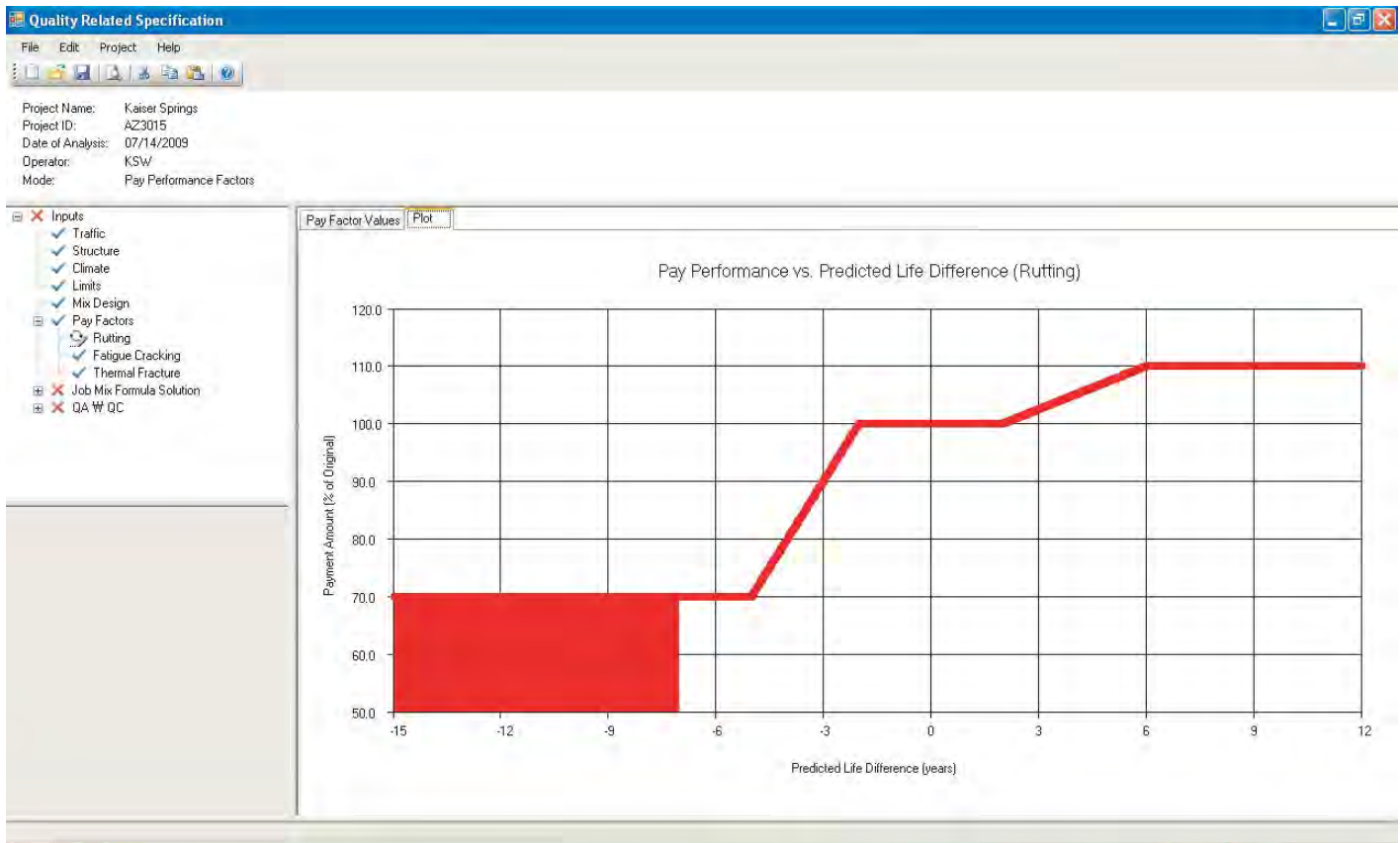


Figure 90. Pay performance versus predicted life difference (rutting).

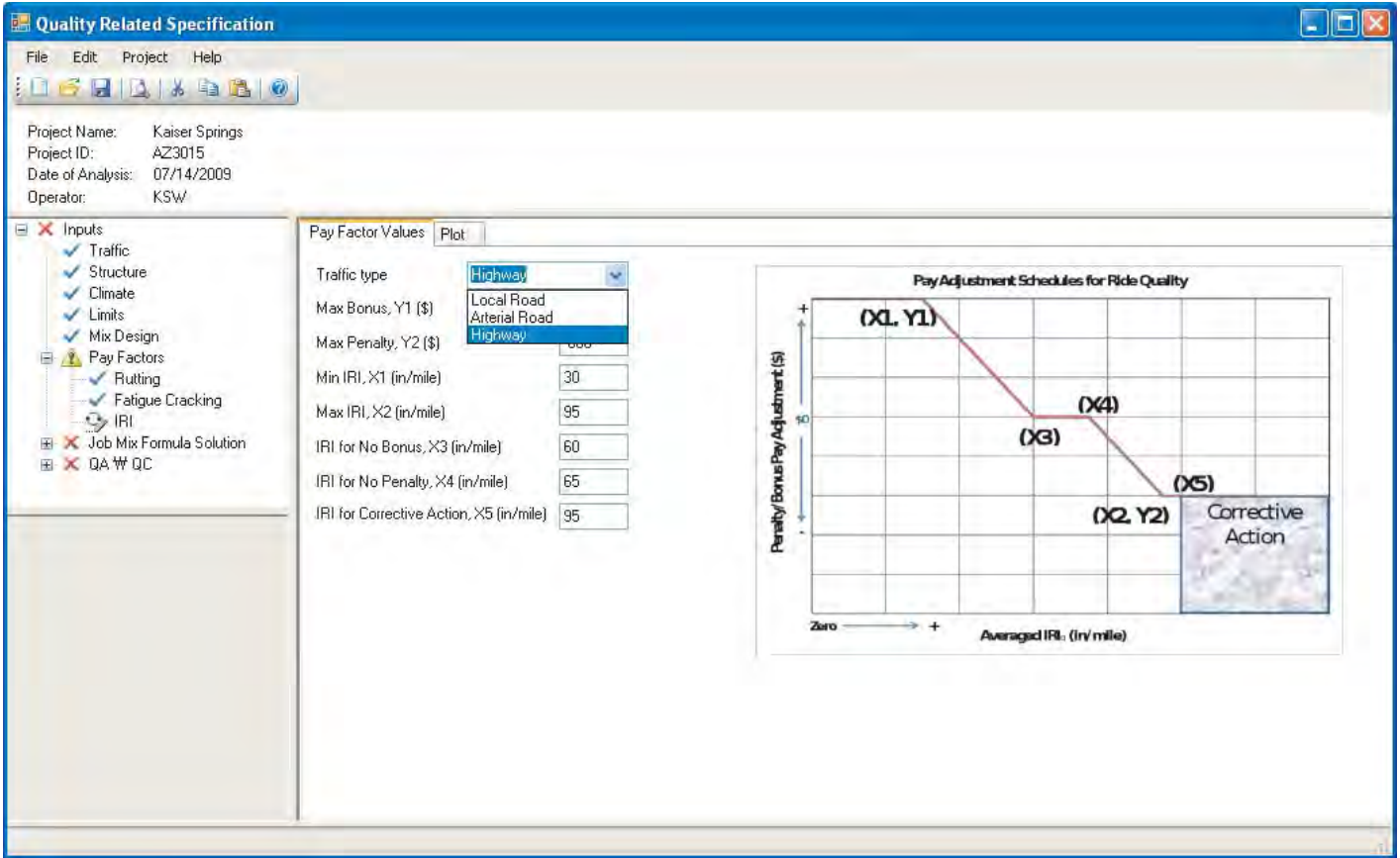


Figure 91. Pay adjustment schedules for ride quality (based on IRI).



Figure 92. Plot of pay adjustment schedule for ride quality.

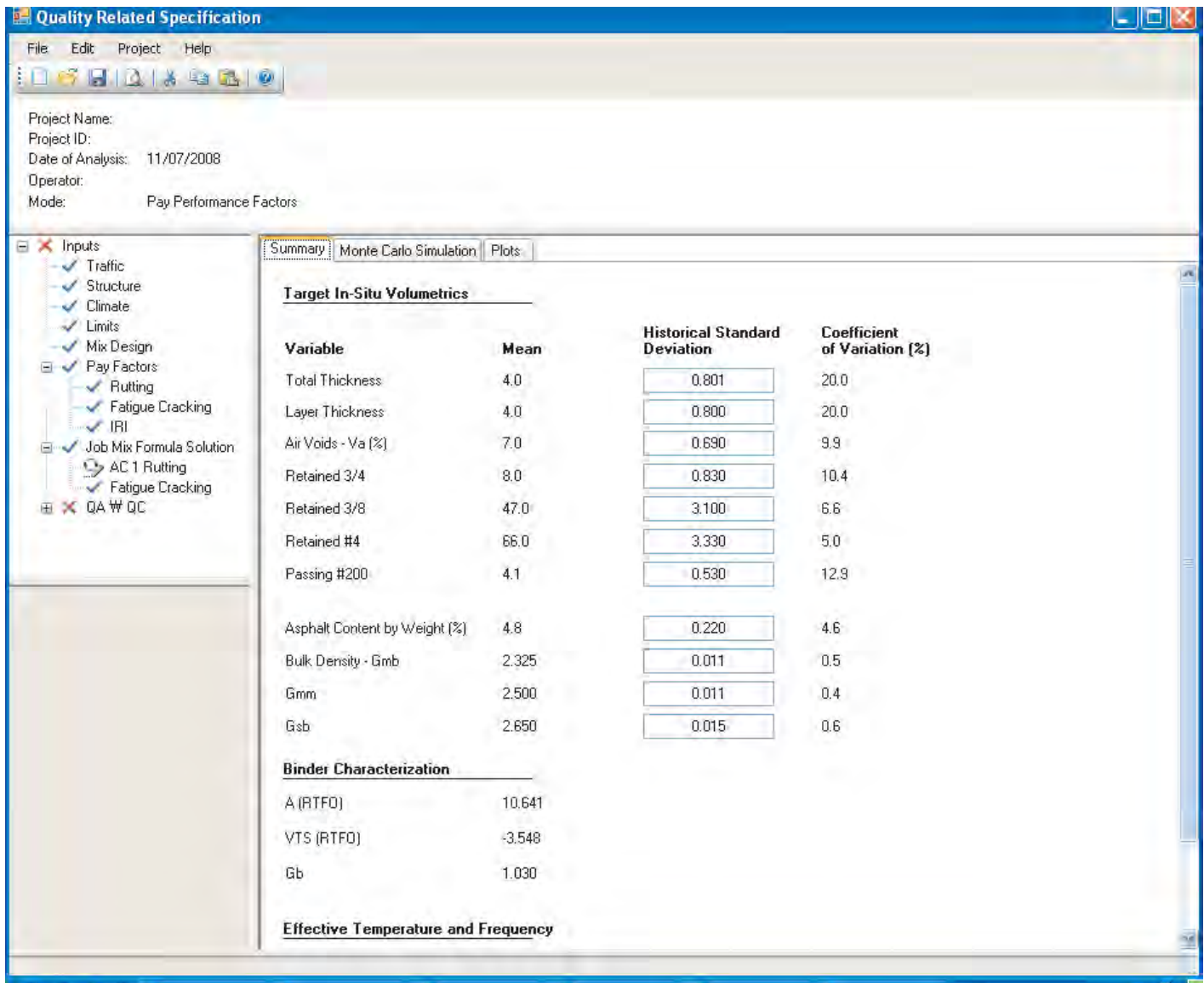


Figure 93. Target in-situ volumetrics.

- Asphalt Content by Weight (%)
- Bulk Density— G_{mb}
- G_{mm}
- G_{sb}

The predictive equation for E^* was discussed in Chapter 2 and is repeated here:

$$\begin{aligned} \log E^* = & -1.249937 + 0.029232 p_{200} - 0.001767 (p_{200})^2 \\ & - 0.002841 p_4 - 0.058097 V_a - 0.8022 \frac{V_{beff}}{(V_{beff} + V_a)} \\ & + \frac{3.87197 - 0.0021 p_4 + 0.003958 p_{38} - 0.000017 (p_{38})^2 + 0.00547 p_{34}}{1 + e^{(-0.603313 - 0.31335 \log(f) - 0.393532 \log(\eta))}} \end{aligned}$$

There are three tabs in the Job Mix Formula Solution window. The Summary tab, as explained in the previous paragraph, shows the variables. The second tab is labeled Monte Carlo Simulation (Figure 94). When the user presses the Run button, the QRSS performs the probabilistic analysis for the selected layer rut depth and produces the mean, standard deviation, and coefficient of variation of the following properties through the Monte Carlo simulation: effective dynamic modulus, rutting, service life, and effective binder content by volume. The third tab (Plot) provides a set of plots that show the development of the means, standard deviations, and coefficients of variation (Figures 95, 96, and 97, respectively) of the predicted distress, dynamic modulus, and service life as the Monte Carlo simulation proceeds.

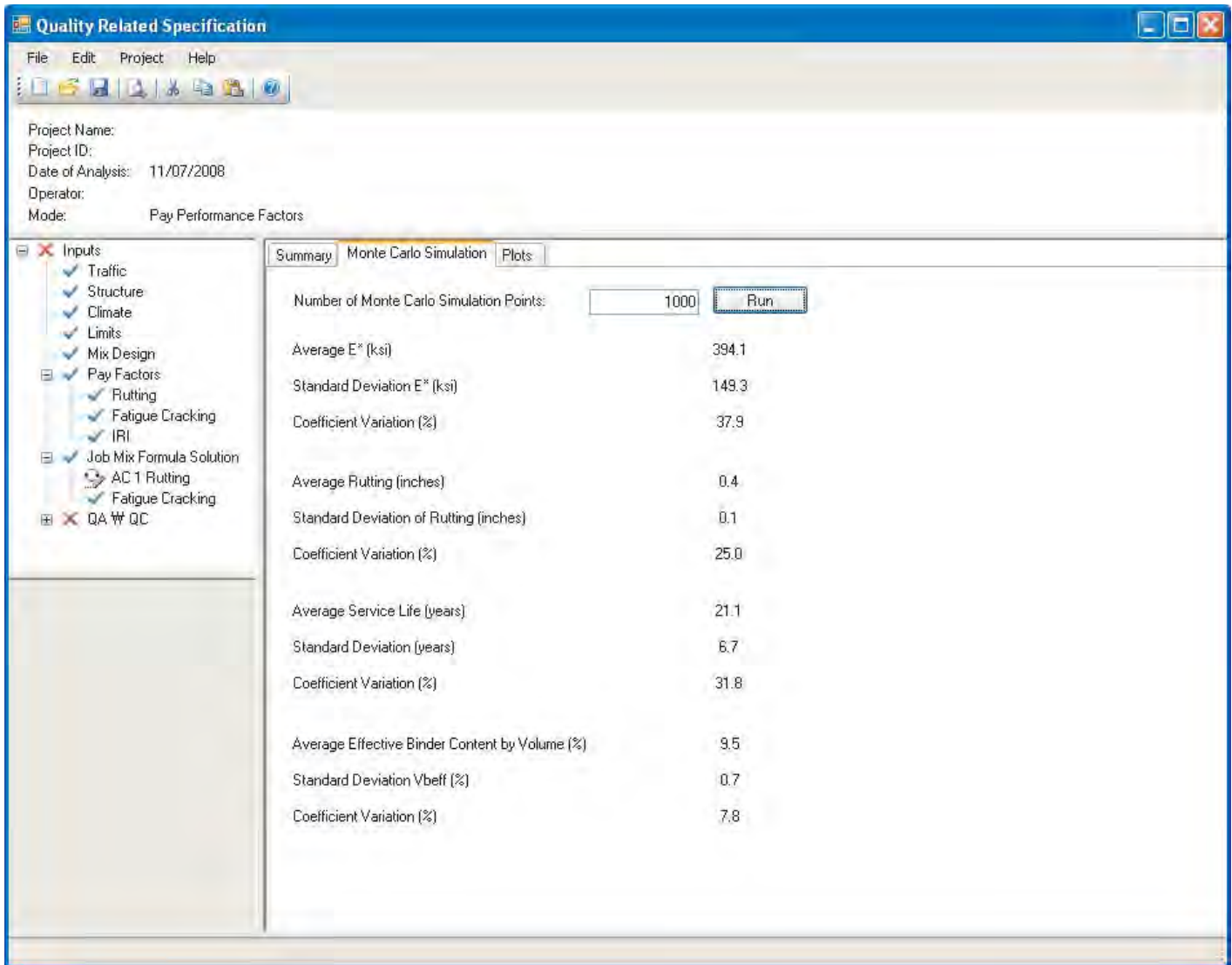


Figure 94. Monte Carlo simulation for rutting.

Fatigue Cracking: Similar to the process for rutting, the Monte Carlo simulation for fatigue cracking estimates the mean, standard deviation, and coefficient of variation of the dynamic modulus, fatigue cracking distress, and corresponding service life. The closed-form model for fatigue is used to predict the fatigue cracking; its standard deviation is obtained by using the historic standard deviation of each volumetric variable. All stochastic results are presented in the second tab (“Monte Carlo Simulation”) in the same manner as the rutting results.

The third tab (“Plots”) provides a set of plots of the Beta and cumulative Beta distributions of the predicted life and distress, as illustrated in Figures 98 and 99.

Thermal Cracking: Unlike the rutting and FC distresses, the stochastic analysis for TC in the QRS uses the Rosenblueth method to estimate the mean and standard deviation of TC

and its service life. When the user selects the “Thermal Cracking” option under the “Job Mix Formula Solution” tree, the QRS displays three tabs as it does for rutting and FC, with the exception that the second tab is labeled Rosenblueth Simulation rather than Monte Carlo Simulation, as shown in Figure 100. Clicking the RUN button on this tab creates temperature files for two thicknesses: (1) the mean minus the standard deviation of AC thickness and (2) the mean plus the standard deviation of the AC thickness, as shown in Figure 101. For example, if the total AC thickness is four inches and the standard deviation is 0.801, then the corresponding temperature files will be created for the following AC thicknesses:

$$4 + 0.801 = 4.801$$

$$4 - 0.801 = 3.199$$



Figure 95. Monte Carlo simulation plots for average rutting.



Figure 96. Monte Carlo simulation plots for standard deviation of rutting.

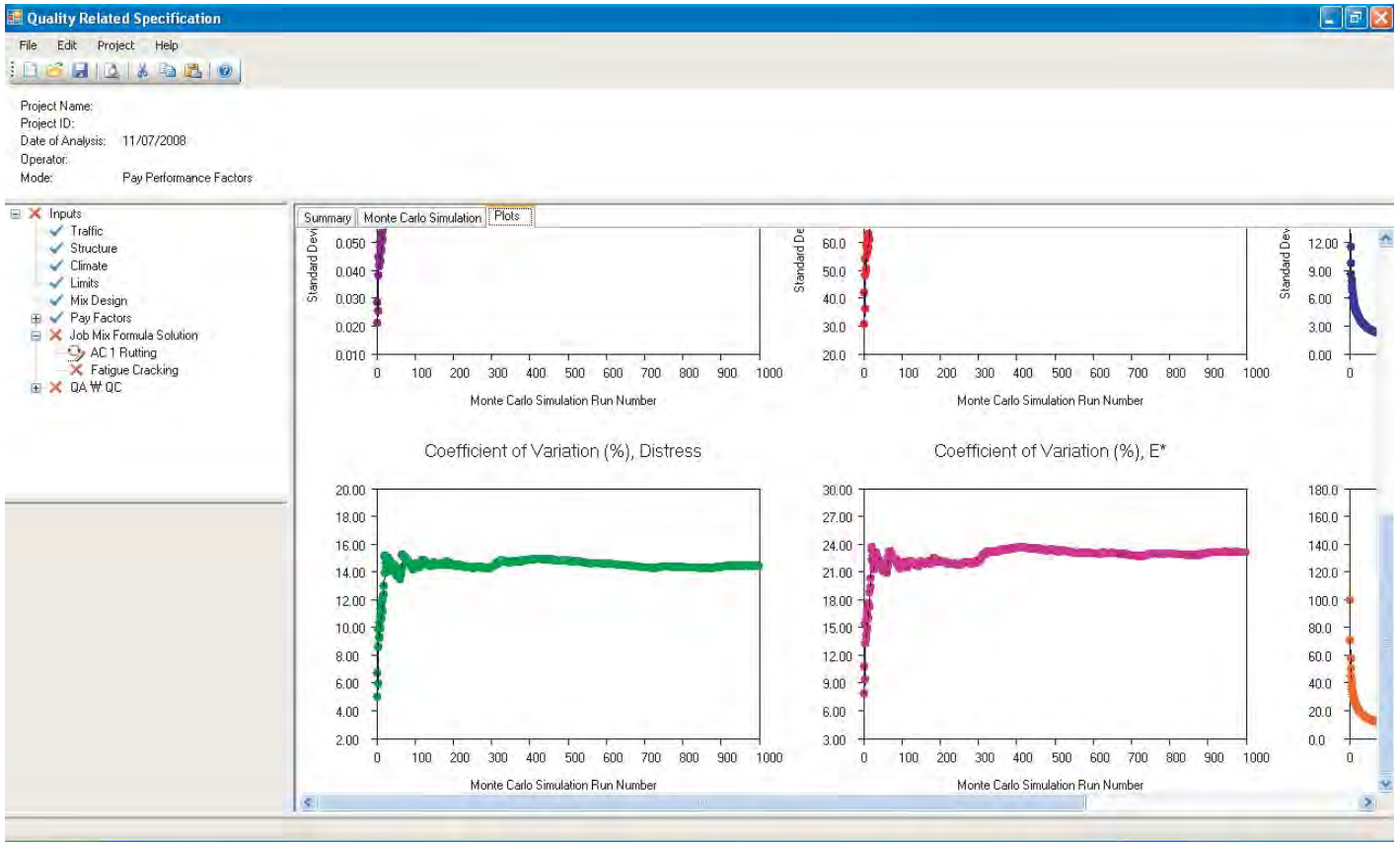


Figure 97. Monte Carlo simulation plots for coefficient of variation of rutting.

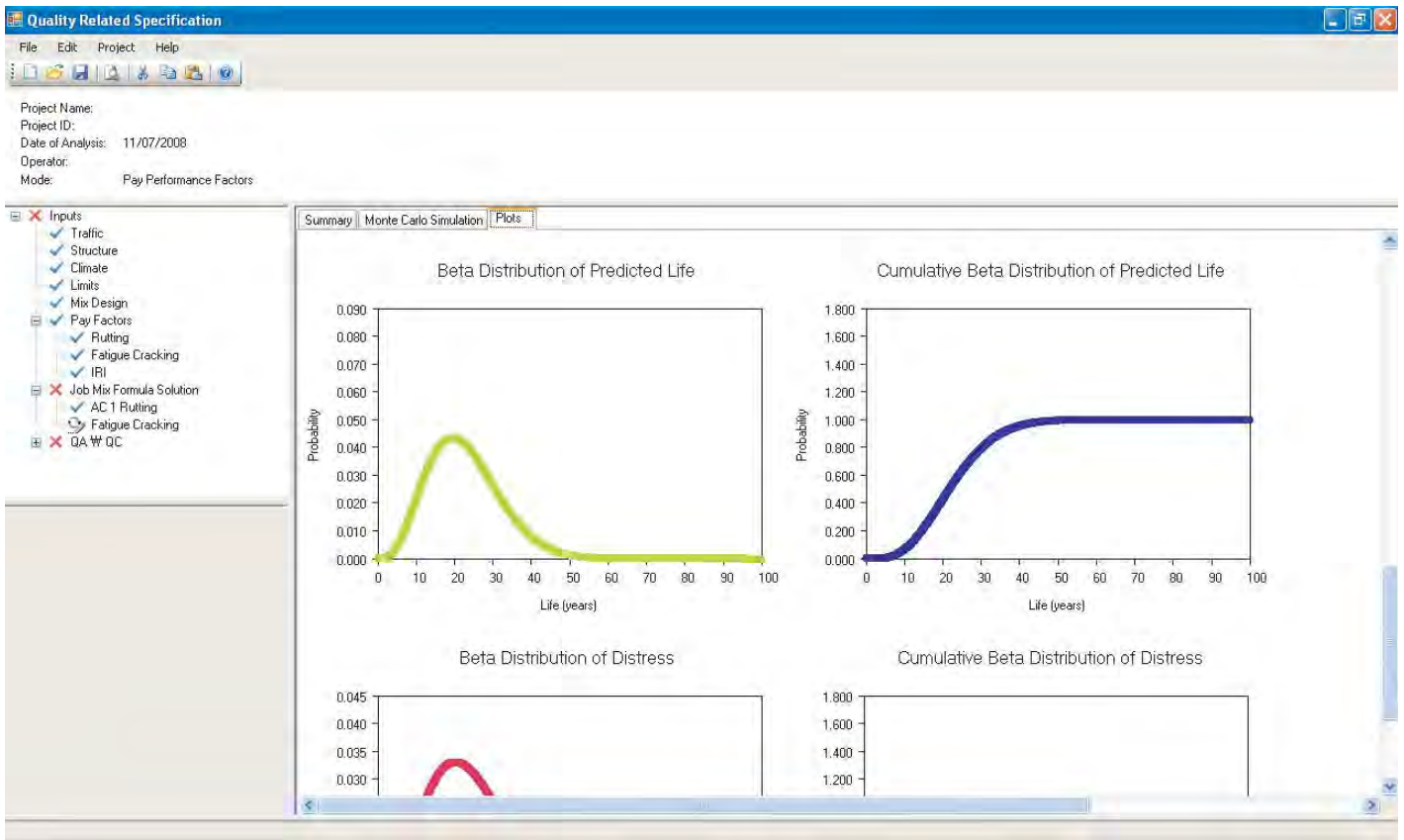


Figure 98. Beta distribution of predicted life for FC.

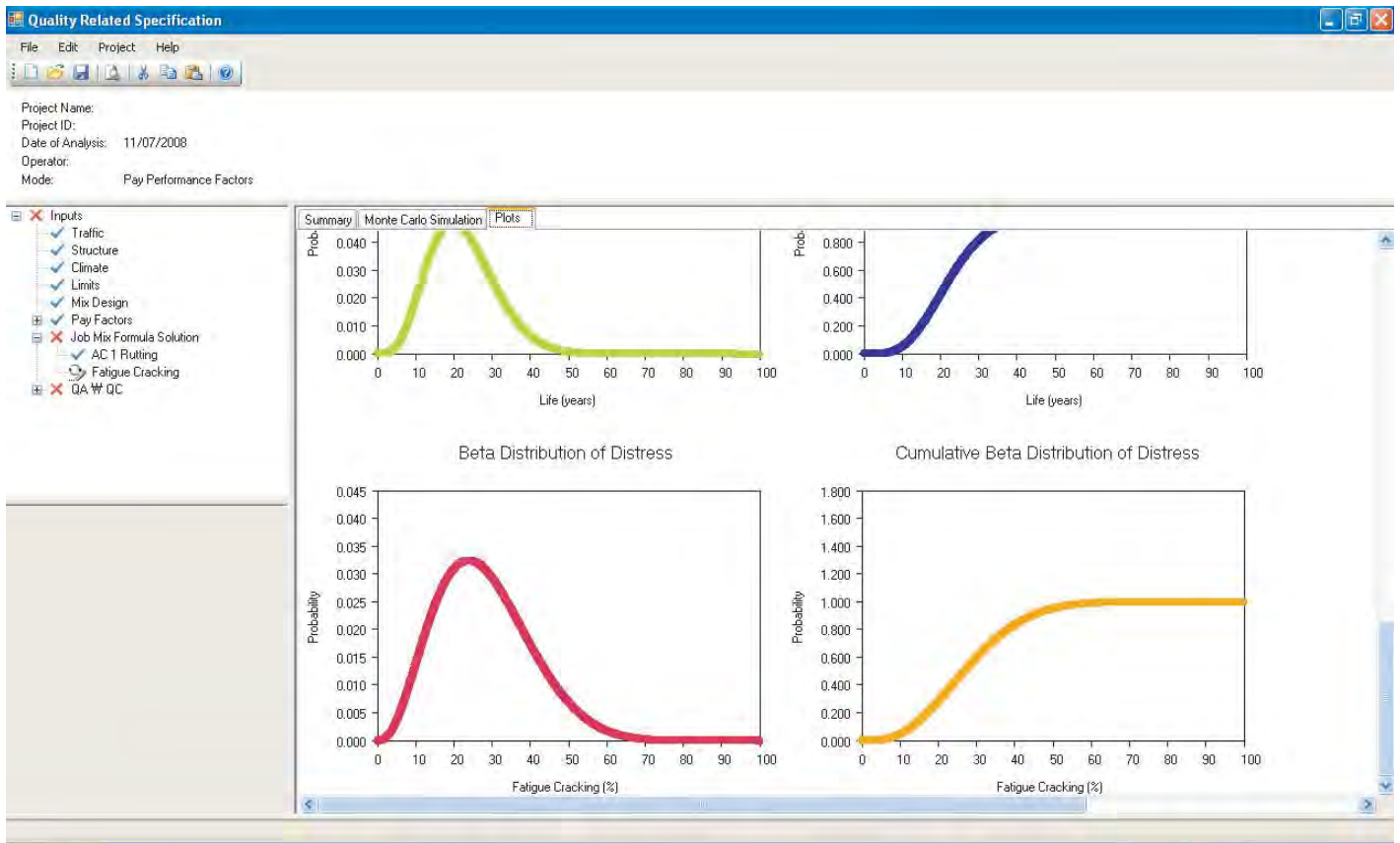


Figure 99. Beta distribution of FC distress.

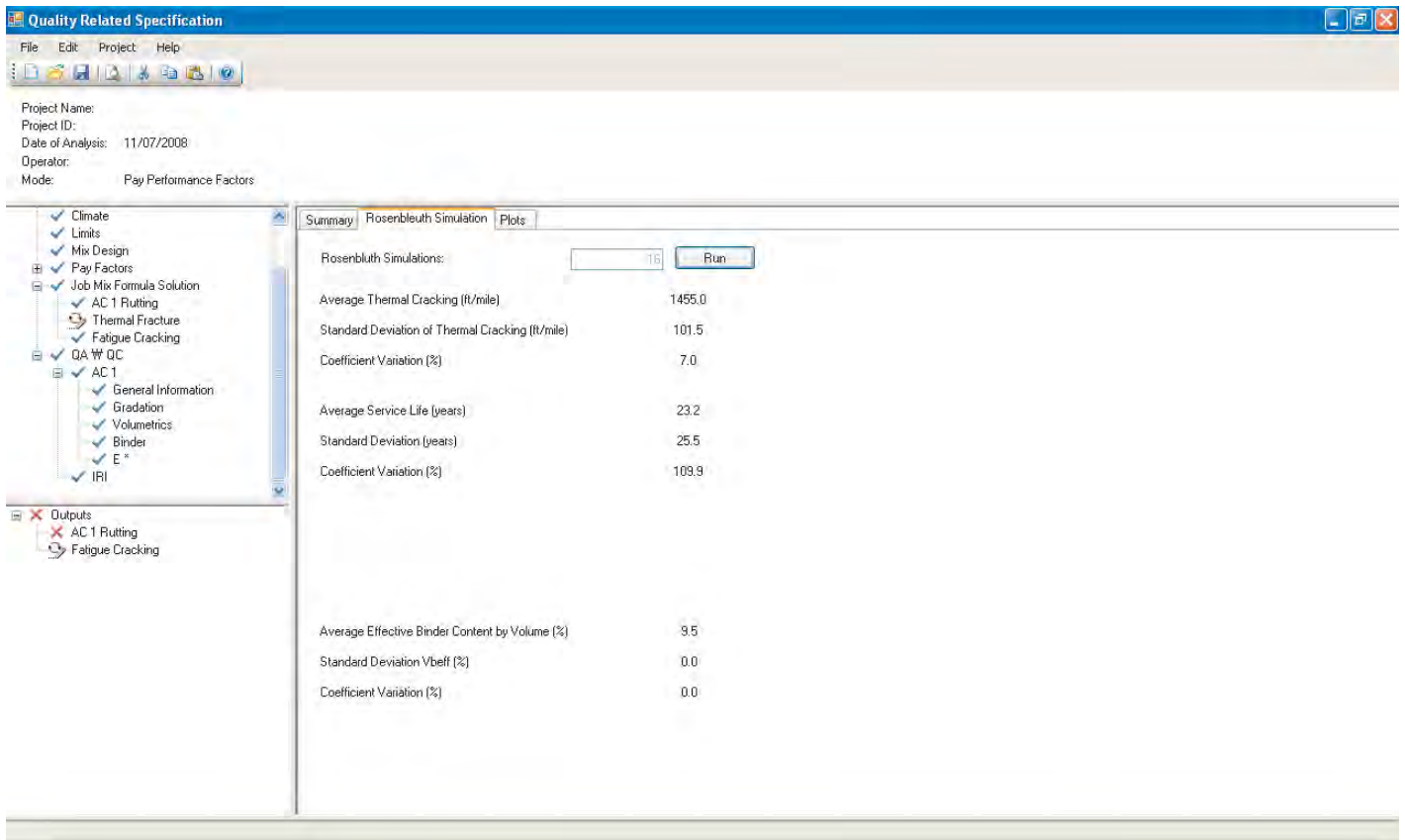


Figure 100. Rosenbluth simulation for TC.

```

C:\Program Files\WCHRP9-22\tcp\tcnew.exe
5
Time begin= 0.000000000000000E+000
No. months crack [in] TC [ft/mile]
1 240 0.8 629.0
Time end= 1.015625000000000
ihac= 1 5.801000 6
5845
500
1000
1500
2000
2500
3000
3500
4000
4500
5000
5500
9999
ihac= 1 4.199000 6
5845
500
1000
1500
2000
2500
3000
3500
4000
4500
5000
5500
9999
Time begin= 113.2031250000000
No. months crack [in] TC [ft/mile]
1 240 1.3 862.7
2 304 1.0 691.1
3 240 1.6 999.8
4 242 0.9 639.0
5 240 1.2 798.5
6 338 0.9 645.3
7 240 1.4 904.2
8 304 1.1 728.3
9 240 0.9 803.7
10 315 0.7 640.1

```

Figure 101. Creating temperature files for stochastic solution of TC.

These temperature files are used to run the 16 ($= 2^4$) Rosenblueth simulations for both TC and service life. The results—the mean, variance, and coefficient of variation of the thermal cracking and the service life—are displayed in the same screen. The relevant plots are presented on the third tab (Plots) where the beta frequency distributions for both predicted TC and service life are presented, similar to the beta distribution plots for fatigue cracking shown in Figures 98 and 99.

4.2.5 Pay Performance Analysis (Stochastic Analysis for As-Built Mix)

The general information for the actual project site and the as-built mix property information are entered from the

branches of the QA tree for use in the analysis of the as-built mix quality. The user must enter the relevant data in five input sections for each AC mix layer, with the exception of the E^* section. In the E^* section, the critical volumetric properties (In Situ V_a , V_{beff} , and the four critical gradations) are calculated from data entered into the other as-built mix property sections (i.e., Gradation and Volumetrics) for use in the WPE. The next sections discuss the requirements of each data branch:

- General Information
- Gradation
- Volumetrics
- Binder
- E^*

4.2.5.1 General Information

The first user input section under QA/QC is the general information for the project. The user selects whether a Superpave Gyratory or Marshall mix design is used, or the program allows the user to directly enter another mix design type by choosing the Other button as shown in Figure 102. This mix design information does not affect the analysis of the mix quality determination; it is only used for informational purposes.

The next user inputs in this section are the lot definition and the number of lots. Lot definition varies by agency. Some agencies use a constant tonnage as one lot, while others use the daily production as one lot. Therefore, the program allows the user to select either definition. If the constant tonnage definition is selected, the user must specify the amount of constant tonnage. Also, the program requires the user to select the number of lots using the drop-down menu. The maximum allowable lot number is 50. Finally, the user enters the tonnage and production date for each lot in the daily production table as shown in Figure 102.

4.2.5.2 QA/QC Gradation

The next branch is for entry of the in-situ gradation data. The window (Figure 103) contains a range of gradation tabs from 1½" to #200. The highlighted gradation tabs in the window are the four sieve sizes needed for the calculation of E*

with the WPE. The other sieve sizes are stored for the purpose of the project inventory record. Each gradation tab has the following information:

- Number of Samples: The user selects this number. The program allows up to 10 samples per lot.
- Historical Standard Deviation: For the four main gradations which are used for the E* prediction, the historical standard deviation values provided are the same as those of the as-designed mix.
- Reliability (%): The default reliability value is set to 99% and the user can re-define it. This reliability is used for the analysis of variance. This topic is discussed in detail in Section 3.3.1.
- Significance Interval (-R and +R): These interval values are determined based on the number of samples and the reliability level; they are used in the generation of the control charts.
- Target Value (JMF Average): This value is transferred from information on the as-designed mix. It is used as the target value (reference value) to monitor the quality of the as-built mix.

Each gradation tab has four sub-tabs: Samples, Summary, ANOVA, and Control Charts. In the Samples tab, the user enters the actual as-built gradation (% passing) in the empty cells for each lot and each sample. The program

The screenshot shows the 'Quality Related Specification' software interface. The 'Project Name' is blank, 'Project ID' is blank, 'Date of Analysis' is 11/07/2008, 'Operator' is blank, and 'Mode' is 'Pay Performance Factors'. The 'Select Mix Design' section has 'Gyratory Design' selected. The 'Select Lot Definition' section has 'Daily Production' selected with a 'Lots' dropdown set to 30. The 'Daily Production Table' is visible on the right, listing 21 lots with their respective dates and tonnage (2000).

Lot #	Date	Tonnage
1	7/17/2000	2000
2	7/18/2000	2000
3	7/20/2000	2000
4	7/21/2000	2000
5	7/22/2000	2000
6	7/24/2000	2000
7	7/25/2000	2000
8	7/26/2000	2000
9	7/27/2000	2000
10	7/28/2000	2000
11	7/31/2000	2000
12	8/1/2000	2000
13	8/2/2000	2000
14	8/4/2000	2000
15	10/18/2001	2000
16	1/23/2001	2000
17	10/24/2001	2000
18	10/25/2001	2000
19	10/26/2001	2000
20	10/29/2001	2000
21	10/30/2001	2000

Figure 102. QA/QC general job site information.

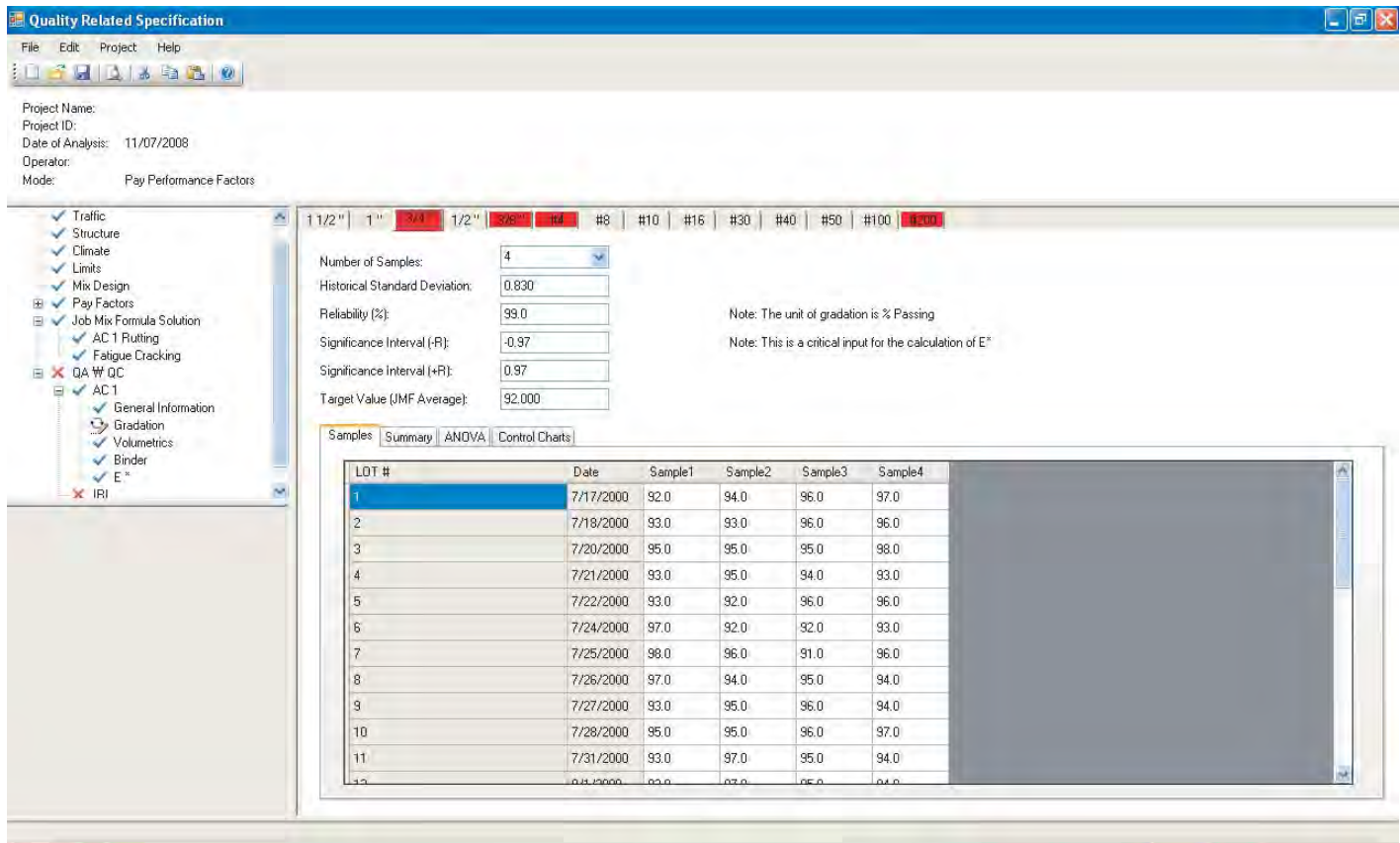


Figure 103. QA/QC as-built gradation input.

calculates the relevant statistics and displays them in the other three tabs, as shown in Figures 104 through 108. This format (i.e., each property tab has the four sub-tabs) applies to all other volumetric properties with the exception of the Binder tab.

The Summary table (Figure 104) contains critical statistics that are automatically computed by the program based on each measured parameter stored in the “Samples” tab. The statistics are displayed in a table. Section 3.3.1 provides details about how these statistics are calculated. The statistics include the following:

- Average, Variance, and Coefficient of Variation
- Range
- Lower and Upper Control Limits (LCL and UCL)
- Lower and Upper Limits (LL and UL)
- Target Value (TV)

The program also performs a One-Way ANOVA based on the measured as-built sample for each lot and property. The ANOVA is completed at two significance levels, 95% and 99%. The “ANOVA” tab (Figures 105 and 106) contains the following information:

- Summary of Pooled Variance
 - Total Average of All Samples
 - Total Average of All Lots
 - Pooled Sample Variance, S
 - Sample Coefficient of Variation, CV
 - Pooled Lot Variance
 - Lot Coefficient of Variation
- ANOVA Variance Estimates
 - Lot Variance Estimate
 - Sample Variance Estimate
- Project Variance
 - Variance at $\alpha = 0.05$ (Significance Level of 95%)
 - Variance at $\alpha = 0.01$ (Significance Level of 99%)
- Analysis of Variance Table
 - Sum of Squares
 - Degree of Freedom
 - Mean Square
 - F-value
 - Critical F-value at $\alpha = 0.05$ and 0.01
- Final Decision

The program automatically develops the average and range control charts based on the sample values for all lots. These

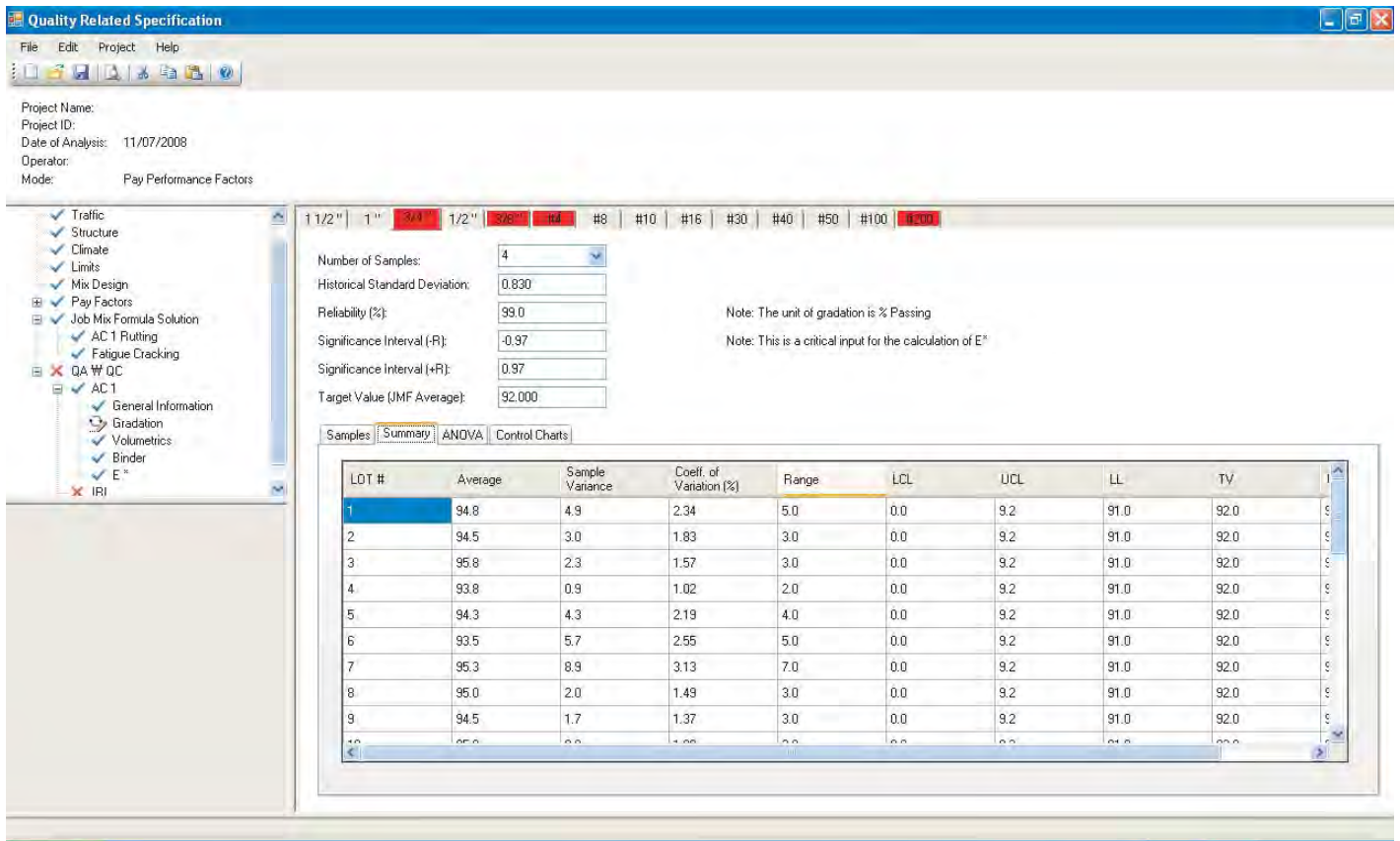


Figure 104. QA/QC summary table.

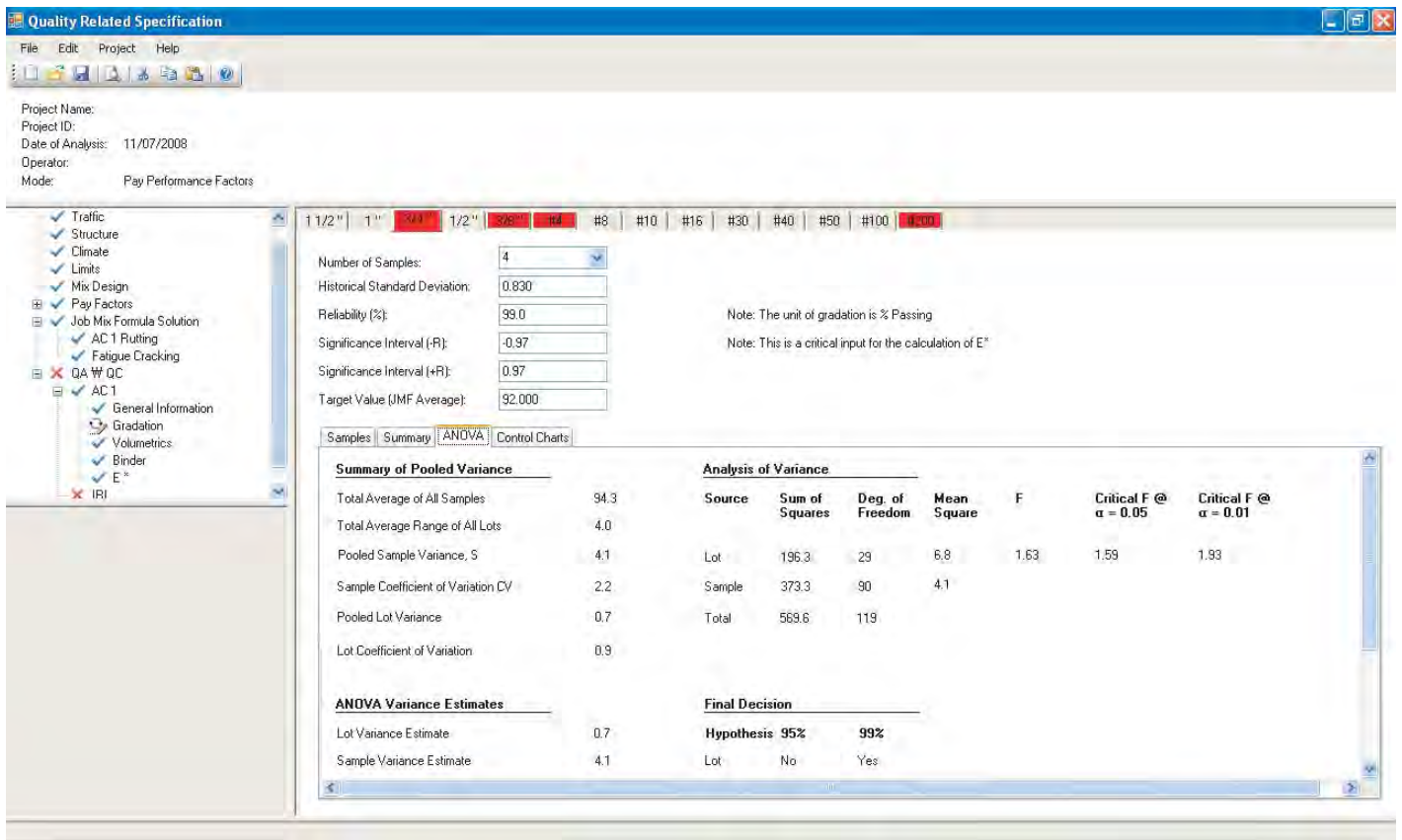


Figure 105. QA/QC ANOVA table.

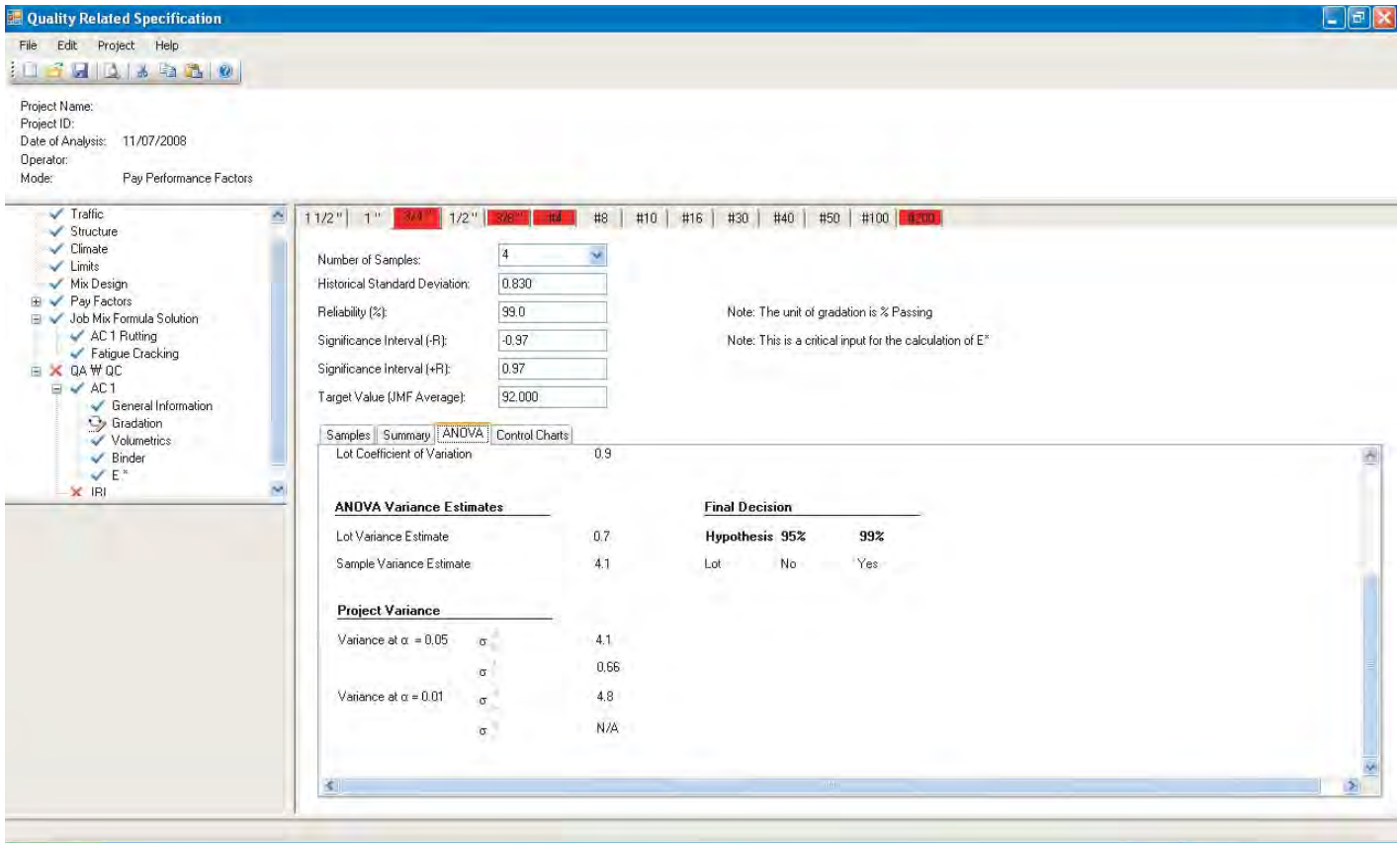


Figure 106. QA/QC ANOVA table (continued).

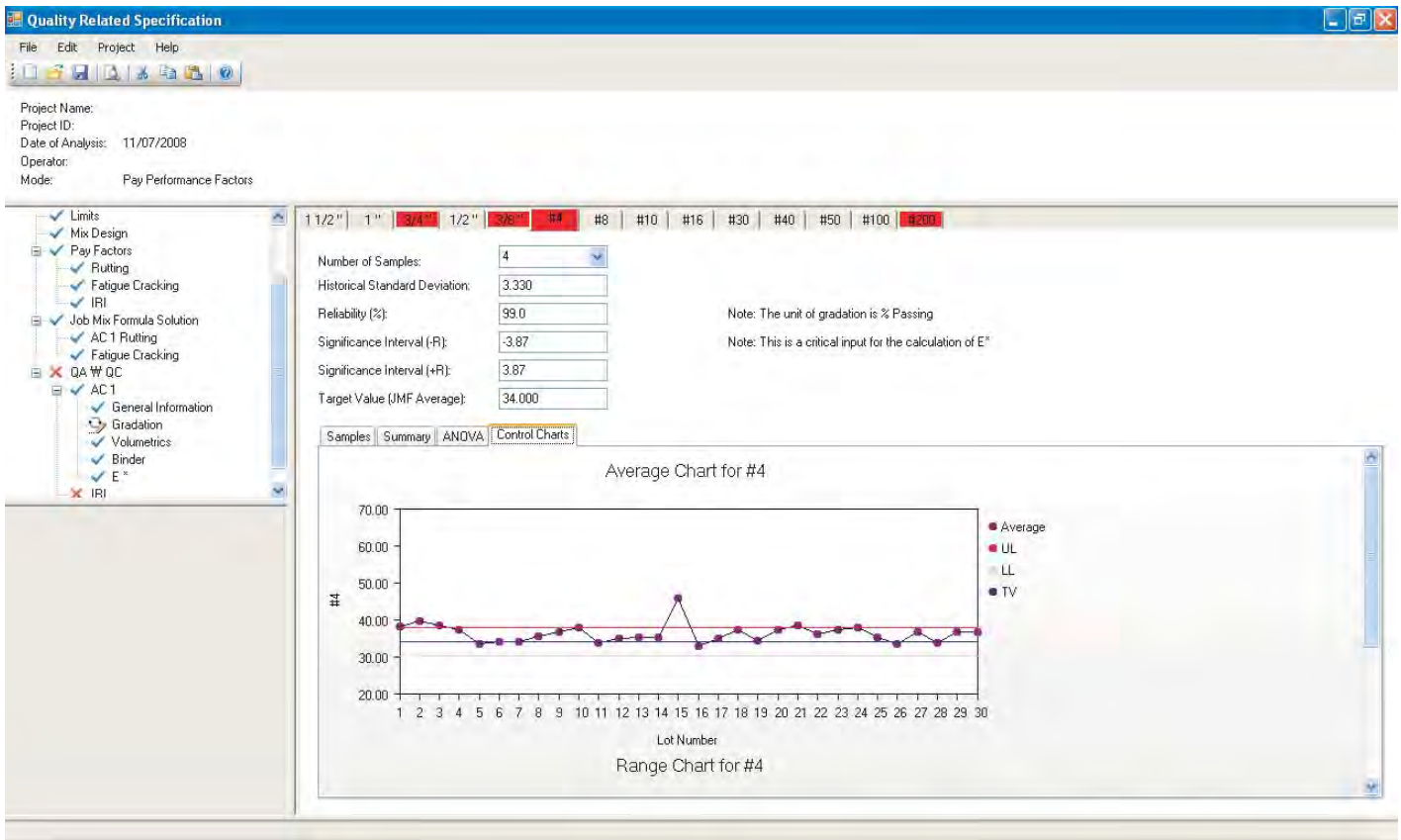


Figure 107. QA/QC control chart (average).

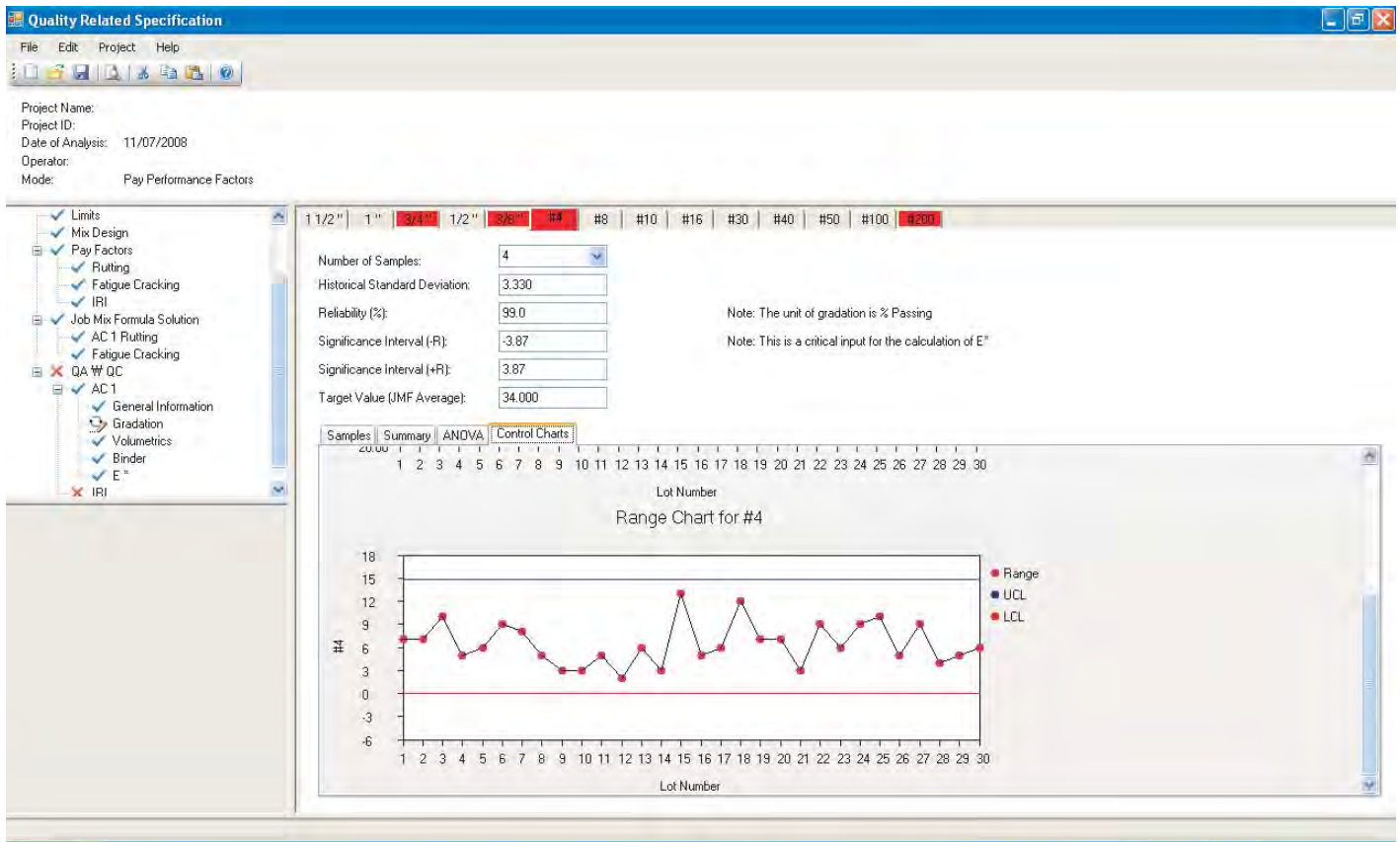


Figure 108. QA/QC control chart (range).

charts are helpful in verifying if the process is under control or not. Observing the trend of averages or ranges in the control charts can help in recognizing potential sources of high variability or problems in the materials, production, or construction. Figures 107 and 108 depict example plots of the average and range control charts for the #4 sieve size in the aggregate gradation.

4.2.5.3 QA/QC Volumetrics

In the QA/QC volumetrics branch (Figure 109), the user enters the as-built volumetric mix properties. These property values measured in the field are used to calculate the mean and variance of each volumetric property. The mean and variance are then used as critical variables in the E^* predictive equations. Like the gradation, all relevant statistics are internally analyzed by the program and summarized and displayed in the Summary, ANOVA, and Control Charts tabs. The volumetric properties include the following:

- Asphalt Content (%)
- Maximum Theoretical Specific Gravity (G_{mm})
- In-Situ Bulk Density (PCF)
- In-Situ Air Voids

- Thickness
- G_{sb}

Note that the in-situ AC layer thickness is not used in the analysis of rutting and fatigue cracking, but is included for information purposes; the thickness is used in the thermal cracking analysis in the creation of the two temperature files ($\mu - \sigma$ and $\mu + \sigma$). If there is more than one AC layer (i.e., two or three AC layers), the TC analysis assumes that the as-built total AC thickness is the same as the AC thickness of the design structure; that is, the same temperature files used in the as-designed mix analysis are used for the as-built mix analysis. New temperature files are not created because it is not possible to define the total AC thickness considering all AC layers by lot.

4.2.5.4 QA/QC Binder

In the Binder branch (Figure 110), the user simply selects the as-built binder type from the drop-down menu and the program displays the corresponding A and VTS values at the RTFO condition. It is assumed that there is little probability of using a binder type different than that used in the as-designed mix for the as-built mix. Furthermore, the short-term aging of the binder is seldom measured at the plant mixing stage.

LOT #	Date	Sample1	Sample2	Sample3	Sample4
1	10/28/2003	2.400	2.400	2.400	2.400
2	10/30/2003	2.400	2.400	2.400	2.400
3	11/5/2003	2.400	2.400	2.400	2.400
4	11/7/2003	2.400	2.400	2.400	2.300

Figure 109. QA/QC volumetric mix property input.

4.2.5.5 QA/QC Dynamic Modulus

This E* branch window (Figure 111) summarizes the critical variables used in the calculation of E*. All necessary, previously entered sample data (i.e., air voids and gradation) are automatically transferred here, except for the effective binder contents (V_{beff}). The V_{beff} is calculated by the following equation:

$$\%V_{beff} = \left(\frac{100 - \%V_a}{100} \right) \left(\frac{100G_{sb} - 100G_{mm} + \%AC G_{mm}}{G_{sb}} \right) \quad (133)$$

where

$\%V_a$ = average in-situ air voids (%)

G_{sb} = average bulk aggregate specific gravity

G_{mm} = average maximum theoretical mix specific gravity
 $\%AC$ = average asphalt content by weight (%)

The standard deviation of the V_{beff} is also calculated. Since Equation 133 is essentially a multivariate function having the specified key volumetric properties as independent variables, it can be expanded by a Taylor series to obtain the standard deviation of the dependent variable, V_{beff} . Therefore, the partial derivative of V_{beff} with respect to each variable was obtained as shown in Equations 134 through 137. Then the variance of V_{beff} can be calculated using Equation 138. Note that the average and variance of each volumetric property used in the equations are measured for each lot of the as-built mix.

$$\frac{\partial V_{beff}}{\partial V_a} = \frac{100G_{mm} - \%AC G_{mm} - 100G_{sb}}{100G_{sb}} \quad (134)$$

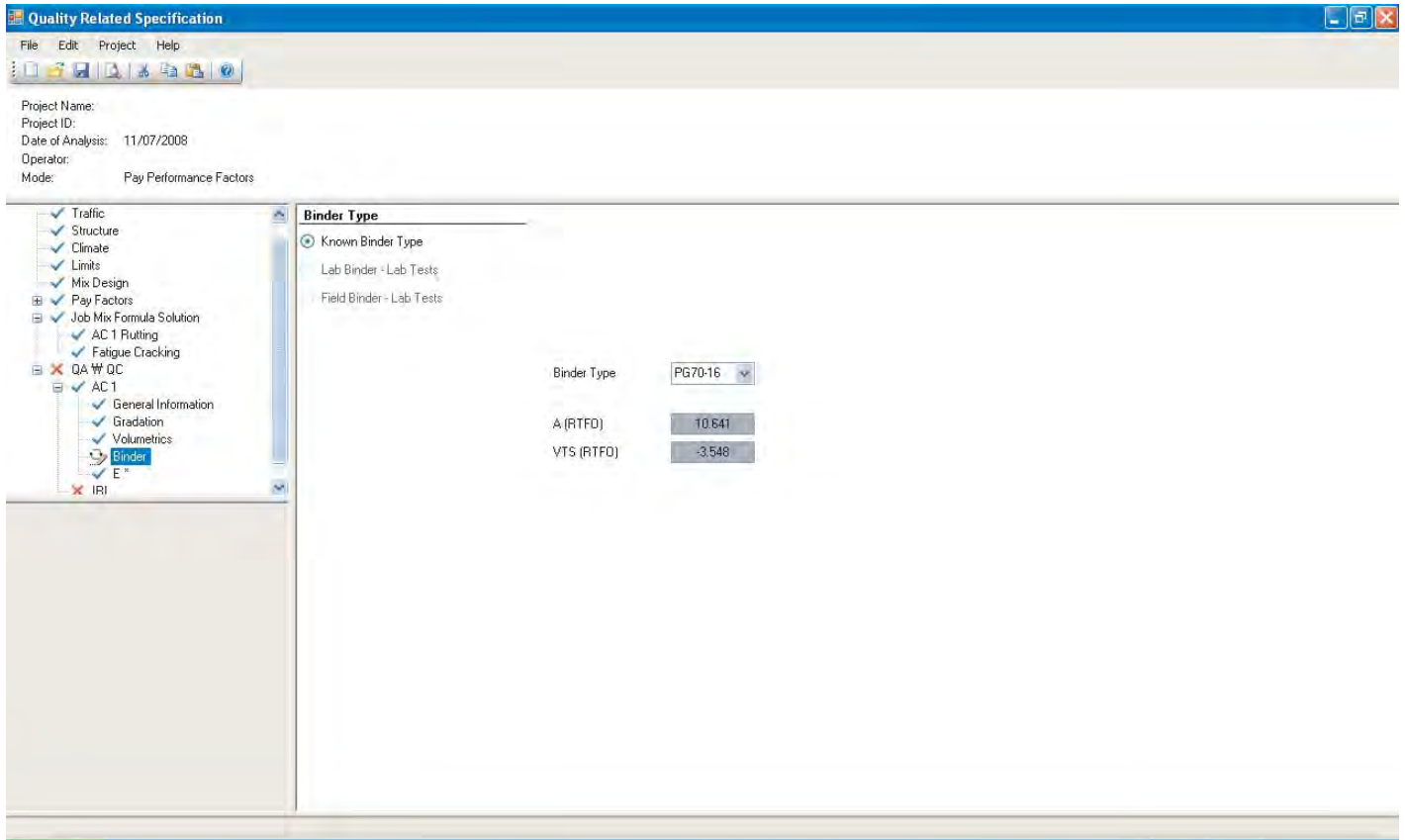


Figure 110. QA/QC binder selection.

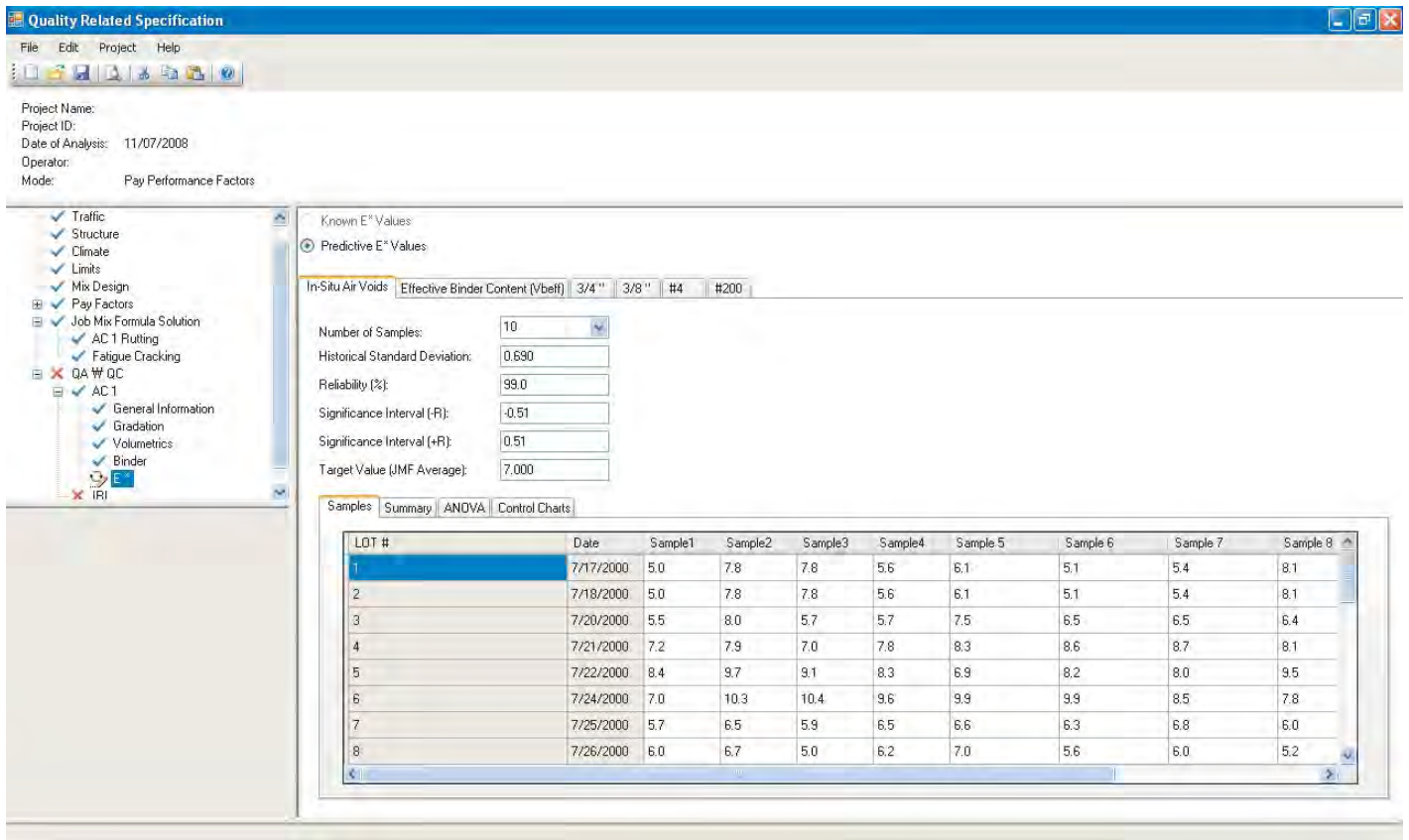


Figure 111. QA/QC E* variable summary.

$$\frac{\partial V_{beff}}{\partial G_{sb}} = \frac{100 - \%V_a}{G_{sb}} + \frac{(100G_{mm} - \%AC \ G_{mm} - 100G_{sb})(100 - \%V_a)}{100G_{sb}^2} \quad (135)$$

$$\frac{\partial V_{beff}}{\partial G_{mm}} = \frac{(\%AC - 100)(100 - \%V_a)}{100G_{sb}} \quad (136)$$

$$\frac{\partial V_{beff}}{\partial AC} = \frac{G_{mm}(100 - \%V_a)}{100G_{sb}} \quad (137)$$

$$\sigma_{V_{beff}}^2 = \left(\frac{\partial V_{beff}}{\partial V_a} \right)^2 \sigma_{V_a}^2 + \left(\frac{\partial V_{beff}}{\partial G_{sb}} \right)^2 \sigma_{G_{sb}}^2 + \left(\frac{\partial V_{beff}}{\partial G_{mm}} \right)^2 \sigma_{G_{mm}}^2 + \left(\frac{\partial V_{beff}}{\partial AC} \right)^2 \sigma_{AC}^2 \quad (138)$$

Although the values of the volumetric properties used in these calculations are ordinarily supplied by the program from those values entered in the Volumetrics window (Figure 109), the program does allow the user to manually overwrite these values in the E* variable summary table, except for V_{beff} . However, the use of this capability is not recommended unless dictated by unique circumstances of the project or specific lot.

4.2.5.6 QA/QC IRI

The last input branch related to as-built mix quality is that for IRI. The program uses IRI as an indicator of the ride quality of the pavement surface. The program requires the user to enter the initial IRI (IRI_0) to characterize the roughness measured prior to opening the road to traffic. Since the penalty/bonus arrangement is directly tied to the initial IRI (IRI_0), the measurement of compliance for IRI is always done before traffic has used the facility. The IRI_0 values should be entered at every mile post by lane in the prepared table as shown in Figure 112. As described in Chapter 3, the user-defined pay adjustment schedule individually converts each IRI_0 value to an amount of penalty or bonus that is then totaled and combined with the penalties and bonuses arising from the other predicted distresses.

4.2.6 Run Solution

At this point in the program, the user has entered all the required data for the as-designed and as-built mixes. This section explains how the QRSS outputs the results of the analyses of these data to assess the quality of each lot of the as-built mix.

Mile Post	Unit Mileage	Average IRI (in/mile) - Lane 1	Average IRI (in/mile) - Lane 2	Average IRI (in/mile) - Lane 3	Average IRI (in/mile) - Lane 4
1	0.1	77	70	78	78
2	0.1	69	75	75	76
3	0.1	71	73	73	75
4	0.1	71	72	69	68
5	0.1	76	65	62	70

Figure 112. QA/QC IRI.

Once all data entry is finished, the program indicates that it is ready to run a solution by showing the message box seen in Figure 113.

The user presses the “OK” button and then goes to Run Solution in the Project drop-down menu at the upper left hand corner of the program window. The program then performs all required calculations for the selected distresses and generates the Outputs tree on the lower left side of the program window (see Figure 114). The Outputs tree contains an overall summary and detailed results for each distress.

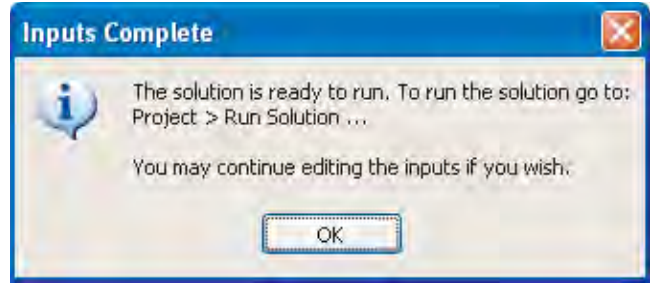


Figure 113. Inputs complete message box.

4.2.6.1 Overall Output Summary

The overall output summary for the project is displayed immediately after completion of the program run, as shown Figure 114. In addition to displaying the predicted service life difference between the as-designed and as-built mixes for the selected distresses, this window opens several empty cells

that permit the user to define, if necessary, several important factors affecting the projects final penalty or bonus.

If multiple distresses are selected for analysis, the user enters weighting factors that assign a relative significance to each distress for the project. Also, if the project uses multiple AC layers and rutting is selected as a distress to be analyzed, the user defines the relative significance of each AC layer by entering

Project Information

Project Name: Tuscumbia, Colbert County
 Project ID: NHF-0013(509)
 Date of Analysis: 04/30/2009
 Operator: Mainey
 Mode: Pay Performance Factors

Distress Summary

Distress	Predicted Life Difference (years)	Penalty/Bonus (%)
Surface Rutting (rk)	-0.03	100.00
Binder Rutting (rl)	-0.04	100.00
Base Rutting (rm)		
Fatigue Cracking (f)		
Thermal Cracking (t)		

Weighting Factor (%) by distress

Rutting (β_r) = 60
 Fatigue Cracking (β_f) = 20
 Thermal Cracking (β_t) = 20

Construction Cost

Surface cost (C_{ac_s}) = \$ 150,000
 Binder cost (C_{ac_m}) = \$ 100,000
 Base cost (C_{ac_b}) = \$ 0
 Total cost (C_{ac}) = \$ 250,000

Rut weighting factor ratios by layer

Surface Rutting (P_{r_s}) = 0.06
 Binder Rutting (P_{r_m}) = 1.00
 Base Rutting (P_{r_b}) = 1.00

Distress Pay Adjustment

$$C_{PB1} = \beta_r \left\{ P_{r_s} \left(\frac{\sum n_k (P/B)_{rk} - 1}{N_{(AC_s)}} \right) C_{AC_s} + P_{r_m} \left(\frac{\sum n_l (P/B)_{rl} - 1}{N_{(AC_m)}} \right) C_{AC_m} + P_{r_b} \left(\frac{\sum n_m (P/B)_{rm} - 1}{N_{(AC_b)}} \right) C_{AC_b} \right\} + \beta_f \left(\frac{\sum n_n (P/B)_{fn} - 1}{N_{(AC_b)}} \right) C_{AC_b} + \beta_t \left(\frac{\sum n_k (P/B)_{tk} - 1}{N_{(AC_s)}} \right) C_{AC_s}$$

C_{pb1} = 0.60 * (0.06 * (1.00 - 1.00) * 150,000.00 + 0.94 * (1.00 - 1.00) * 100,000.00) = 0.00

IRI Pay Adjustment

$$C_{PB2} = \sum_{i=1}^L \sum_{j=1}^{Lp/0.1} (P/B)_{IRI_{ij}}$$

C_{pb2} = 0.00

Total Pay Adjustment

$$C_{PB} = C_{PB1} + C_{PB2}$$

C_{pb} = 0.00 + 0.00 = 0.00

Figure 114. Overall output summary.

the rut weighting factor by layer. In both these cases, the weighting factors must sum to unity or 100%.

Finally, the user must enter the unit construction cost per ton by layer. The unit cost and weighting factors are the key variables in the pay adjustment equation, as derived in Section 3.6.1, and repeated here:

$$C_{PB1} = \beta_r \left\{ P_{r_s} \left(\frac{\sum n_k (P/B)_{rk}}{N_{t(AC_s)}} - 1 \right) C_{AC_s} \right. \\ \left. + P_{r_m} \left(\frac{\sum n_l (P/B)_{rl}}{N_{t(AC_m)}} - 1 \right) C_{AC_m} \right. \\ \left. + P_{r_b} \left(\frac{\sum n_m (P/B)_{rm}}{N_{t(AC_b)}} - 1 \right) C_{AC_b} \right\} \\ + \beta_f \left(\frac{\sum n_m (P/B)_{fm}}{N_{t(AC_b)}} - 1 \right) C_{AC_b} \\ + \beta_{tf} \left(\frac{\sum n_k (P/B)_{tk}}{N_{t(AC_s)}} - 1 \right) C_{AC_s}$$

The pay adjustment calculation result for IRI is also presented in this overall summary window (Figure 115) based on the initial IRI input. The IRI pay adjustment equation is derived in Section 3.6.2 and repeated here:

$$C_{PB} = \sum_{i=1}^L \sum_{j=1}^{Lp/0.1} (P/B)_{IRI_{ij}}$$

The detailed items displayed in the summary window (Figures 114 and 115) are as follows:

- Distress Summary
 - Predicted Life Difference (years)
 - Penalty/Bonus (%)
- Rut Weighting Factor Ratios by Layer
 - Surface Rutting (P_{r_s})
 - Binder Rutting (P_{r_m})
 - Base Rutting (P_{r_b})
- Weighting Factor (%) by Distress
 - Rutting (β_r)
 - Fatigue Cracking (β_f)
 - Thermal Cracking (β_t)
- Construction Cost
 - Surface Cost (C_{ac_s})
 - Binder Cost (C_{ac_m})
 - Base Cost (C_{ac_b})
 - Total Cost (C_{ac})
- Distress Pay Adjustment
- IRI Pay Adjustment
- Total Pay Adjustment

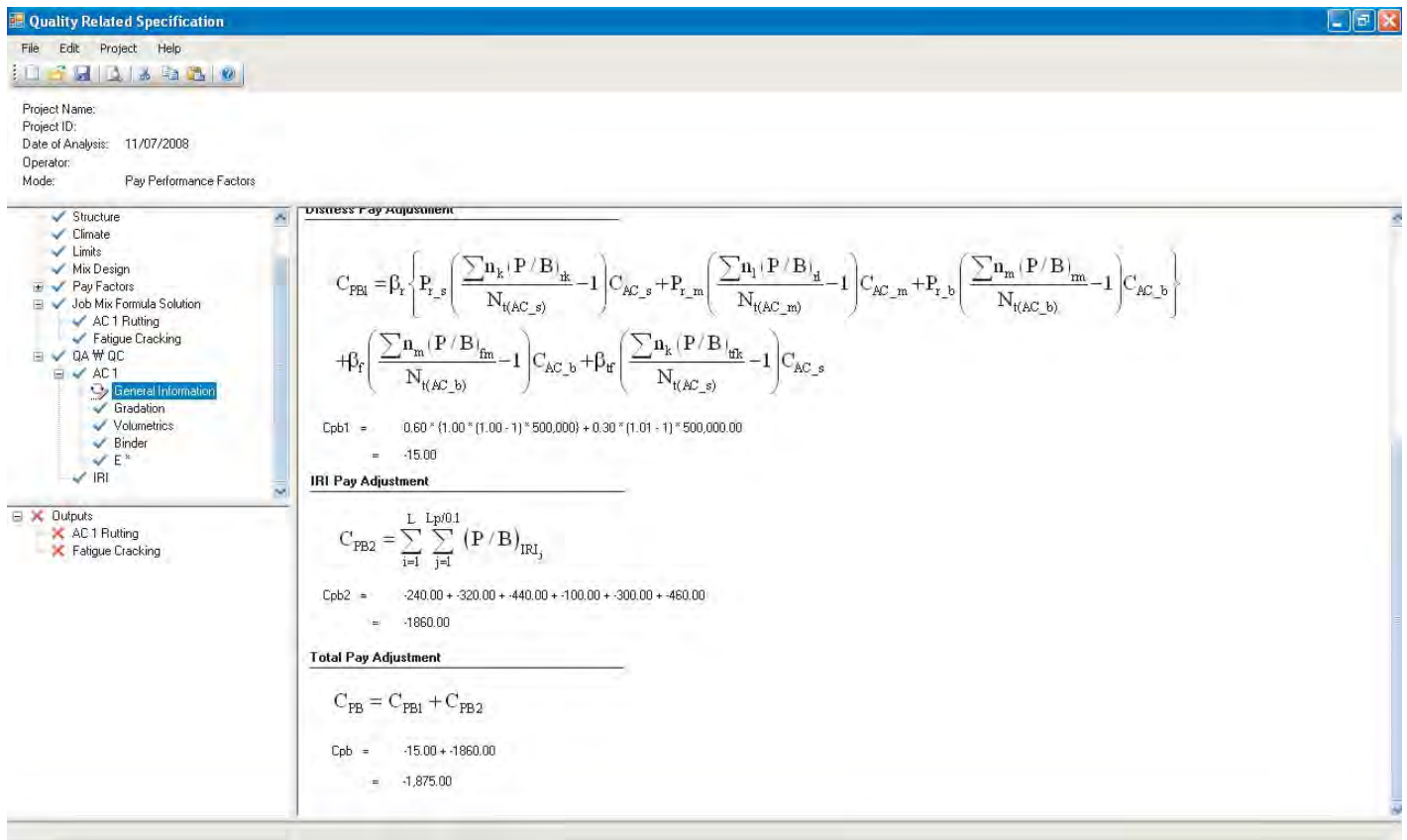


Figure 115. Overall output summary (continued).

4.2.6.2 Output Summary for Each Distress

The user can select a specific distress under the “Outputs” tree to see the detailed results for that distress. Each summary window for a specific distress provides three tabs: Summary, Detailed Outputs, and Plots.

Summary: The Summary tab presents the detailed inputted data and outputted results for the selected distress. Figure 116 is a screen shot of a summary window for rutting; the items displayed are as follows:

- Project Traffic Condition
 - Design Speed (mph)
 - Design ESALs
- Layer Description
- Summary of Results

- Average Project Life Difference (yrs)
- Project Penalty/Bonus (%)
- Project Climatic Conditions
 - Mean Annual Air Temperature (°F)
 - Mean Monthly Air Temperature Standard Deviation (°F)
 - Mean Annual Wind Speed (mph)
 - Mean Annual Sunshine (%)
 - Annual Cumulative Rainfall Depth (in.)
- Summary of Output
 - Allowable Layer Distress (various)
 - Allowable Layer E* (ksi)
 - Effective Temperature (°F)
 - Effective Frequency (Hz)
 - Recommended Temperature (°F)
 - Recommended Frequency (Hz)

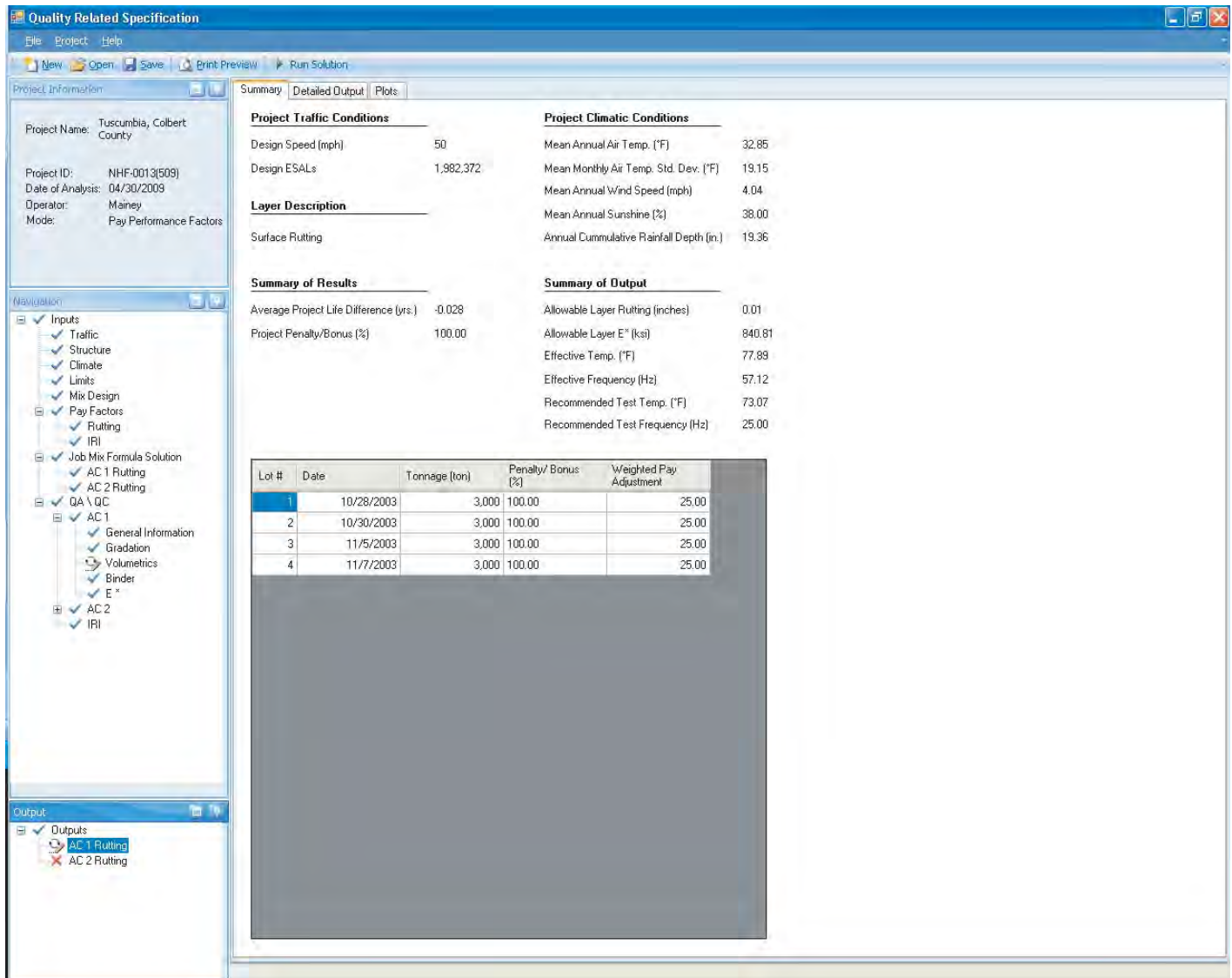


Figure 116. Output summary table.

- Summary Table
 - Lot Number
 - Date
 - Tonnage (ton)
 - Penalty/Bonus (%)
 - Weighted Pay Adjustment

Detailed Output: The second tab in the distress output window (Figures 117 to 119) takes the user to a table that contains detailed results of the analysis of both the as-designed and as-built mix quality in terms of dynamic modulus, predicted distress, predicted service life, and, most importantly, the penalty or bonus by lot. The following output data types are displayed in the table; each distress has its own output table.

- Lot Number
- Date
- Tonnage
- Air Voids (%)
- Effective Binder Content (%)
- Effective Temperature (°F)
- Effective Frequency (Hz)
- Target E* (ksi)
- Predicted E* (ksi)

- E* Variance
- E* Coefficient of Variation (%)
- Target Distress (various)
- Predicted Distress (various)
- Distress Standard Deviation
- Distress Coefficient of Variation (%)
- Target Service Life (yrs)
- Predicted Service Life (yrs)
- Service Life Standard Deviation
- Service Life Coefficient of Variation (%)
- Predicted Life Difference (yrs)
- Reliability
- Bonus/Penalty
- Weighted Pay Adjustment

Plots: The last tab in the distress output window is a plot comparing the as-designed mix and the as-built mix. A cumulative frequency distribution associated with the predicted service life is presented for both mix types by lot as shown in Figure 120. The user can select different lots by using the drop-down menu in the window. The distribution curve for the as-designed (JMF) mix is the same for all lots (i.e., the as-designed mix is a reference), while the curve for the as-built mix varies by lot.

Target E* (ksi)	Predicted E* (ksi)	E* Variance	E* Coefficient of Variation (%)	Target Distress (m.)	Predicted Distress (m.)	Distress Standard Deviation
374.057	343.095	101.336	29.536	0.446	0.480	0.093
374.057	360.208	95.610	26.543	0.446	0.461	0.079
374.057	335.410	97.972	29.210	0.446	0.487	0.093
374.057	309.567	70.566	22.795	0.446	0.503	0.073
374.057	304.293	76.653	25.191	0.446	0.512	0.083
374.057	294.884	88.721	30.087	0.446	0.530	0.105
374.057	353.122	95.967	27.177	0.446	0.468	0.081
374.057	344.216	80.281	23.323	0.446	0.470	0.070
374.057	348.964	79.727	22.847	0.446	0.466	0.067
374.057	351.725	78.792	22.401	0.446	0.463	0.065
374.057	327.072	75.897	23.205	0.446	0.496	0.072
374.057	313.031	70.882	22.644	0.446	0.499	0.071
374.057	350.458	84.674	24.161	0.446	0.466	0.071
374.057	336.141	75.368	22.422	0.446	0.476	0.067
374.057	257.382	97.442	37.859	0.446	0.597	0.156
374.057	358.631	85.354	23.800	0.446	0.459	0.068
374.057	362.733	95.894	26.437	0.446	0.459	0.077
374.057	352.712	147.089	41.702	0.446	0.499	0.156
374.057	372.057	89.346	24.014	0.446	0.449	0.068
374.057	376.757	95.208	25.270	0.446	0.447	0.071
374.057	348.754	89.086	25.544	0.446	0.469	0.077
374.057	369.884	97.950	26.481	0.446	0.454	0.078

Figure 117. Detailed output table.

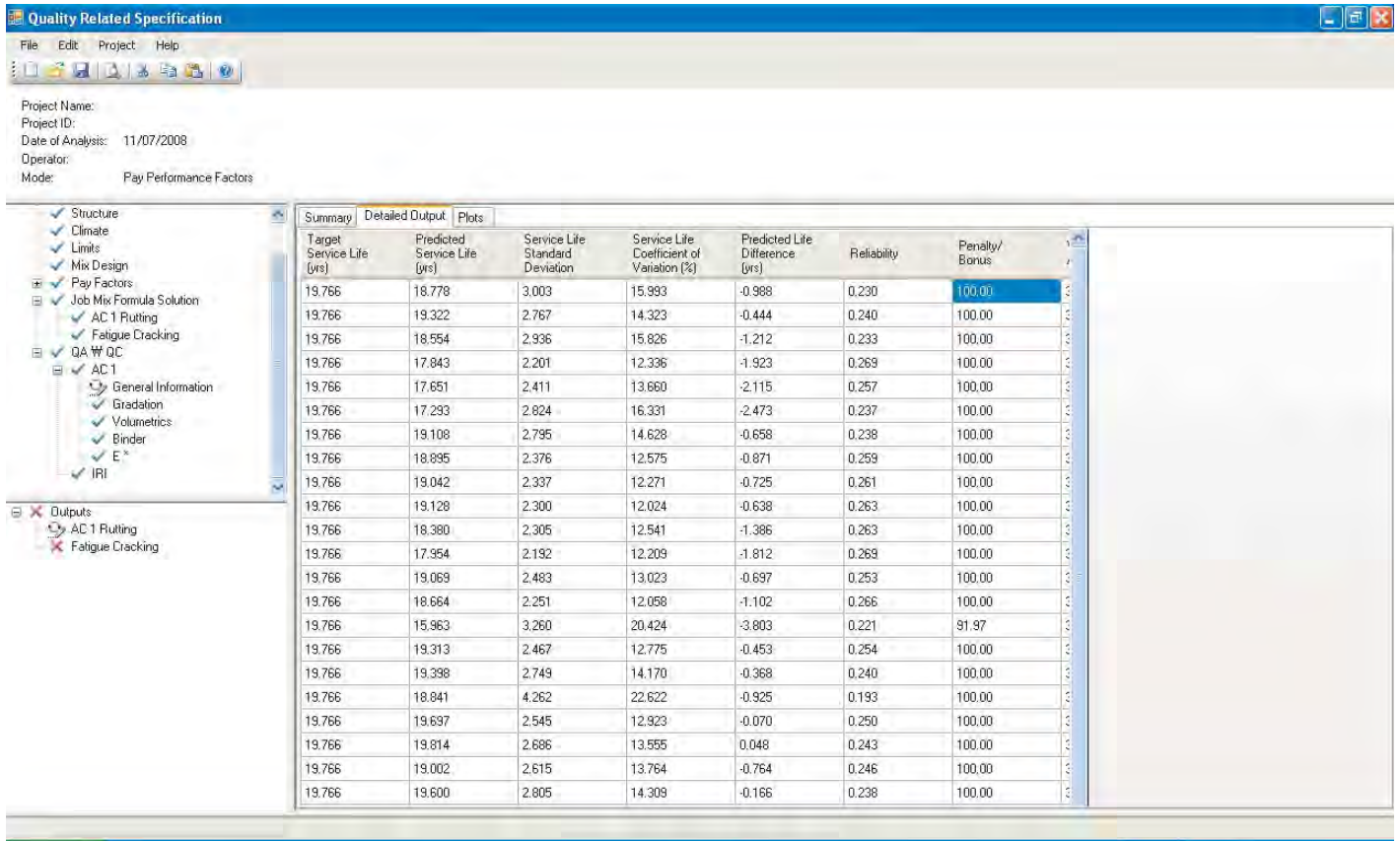


Figure 118. Detailed output table (continued).

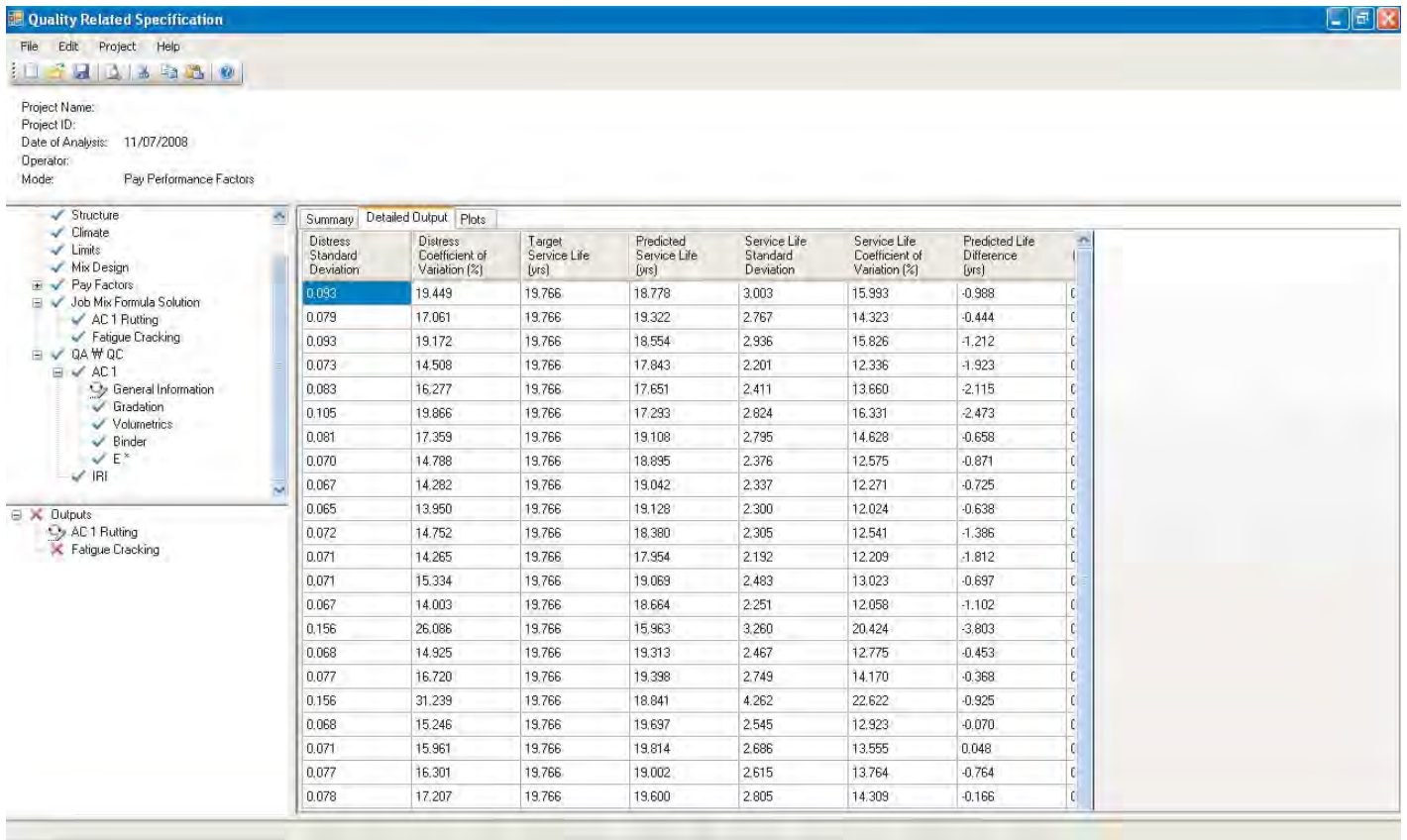


Figure 119. Detailed output table (continued).

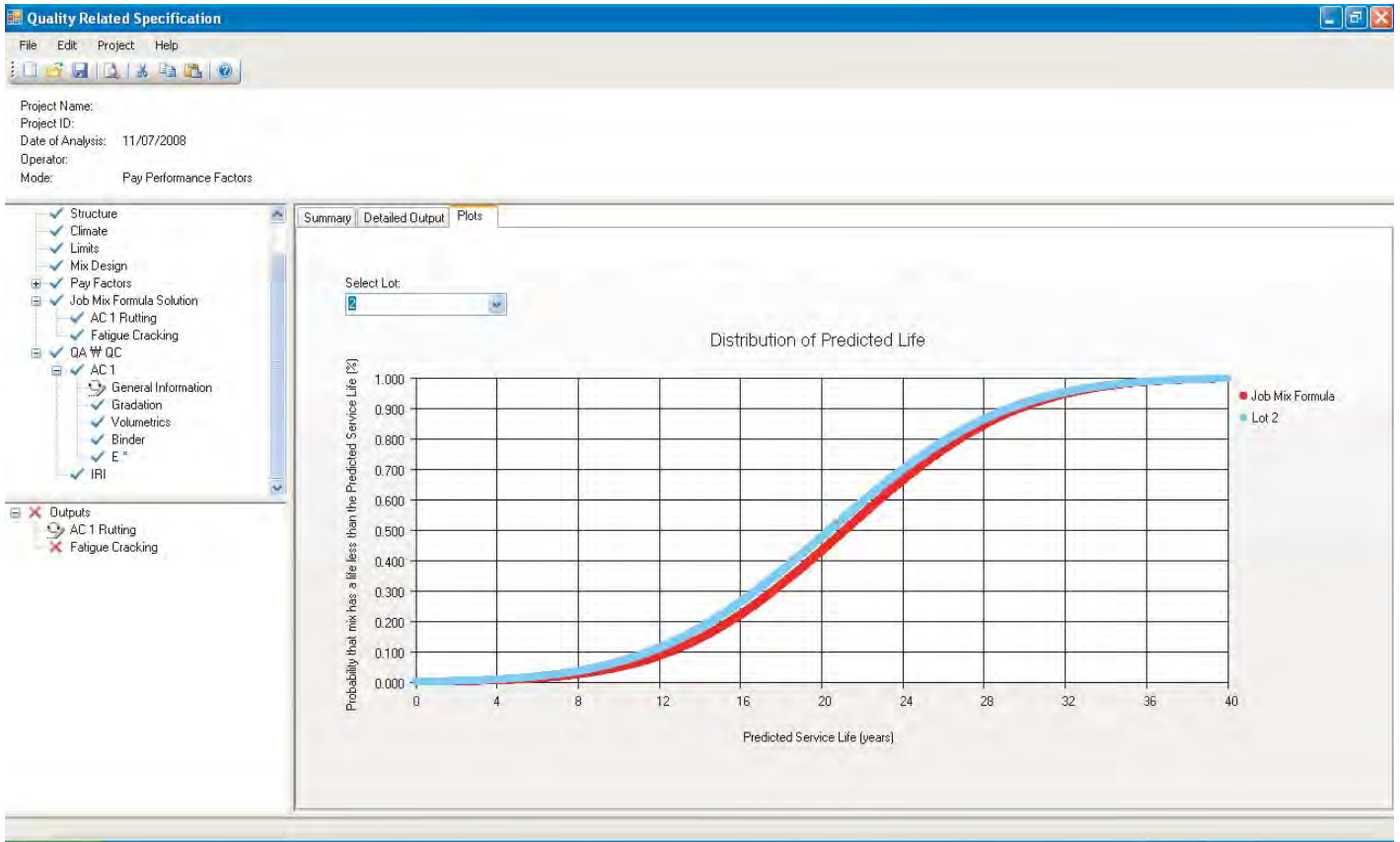


Figure 120. Comparison of cumulative frequency distribution between as-designed and as-built mix quality.

CHAPTER 5

Summary, Conclusions, and Future Research

5.1 Summary

Traditionally, HMA production and construction specifications require the measurement of volumetric properties (typically air voids, asphalt content, and aggregate gradation) that are assumed to be related to some arbitrary level of performance. Specifications where M&C variables, also known as AQC, are used to control quality are primarily tied to performance through intuition, engineering judgment, or both. A PRS is one that ties AQCs to performance (distress) through the medium of fundamental engineering properties (such as dynamic modulus and creep compliance) and quantified relationships such as distress prediction models and so provides the basis for rational acceptance and pay adjustment decisions.

In 1994 the FHWA funded the WesTrack Project to provide a prototype PRS that would quantify the effects of deviations in M&C properties on the overall performance of HMA layers. WesTrack's primary performance emphasis was on the load-associated distresses of rutting and fatigue cracking. The data collected during the construction and loading of the track was used to develop simple empirical relationships for performance prediction that provided the basis for the prediction models used in the supporting software, HMA Spec.

The original WesTrack team identified numerous limitations of the alpha version of the HMA Spec software. The original objectives of NCHRP Project 9-22, "Beta Testing and Validation of HMA PRS," was to evaluate and refine the HMA PRS and supporting HMA Spec software developed through the WesTrack project in a series of field trials and calibrate and validate the Level I and II performance models in HMA Spec.

Over the course of NCHRP Project 9-22, the objective was first changed to an evaluation of the use of the MEPDG Version 1.0 models for distress predictions in HMA specification. This evaluation ultimately led to the development of a new program called QRSS that is founded on pre-solved solutions of the MEPDG for rutting, FC, and TC. This foundation

directly links measured M&C variables such as air voids and asphalt content with models that predict pavement distress from the calculated engineering properties dynamic modulus, E^* , and creep compliance, D .

This report has documented the development, technical features, and use of the QRSS as a pay adjustment system for HMA construction as well as a tool for interactive HMA mix and structural design. The following sections present key conclusions and recommendations of the project.

5.2 Conclusions

The QRSS developed in this study provides agencies and industry responsible for HMA construction industry with a scientific approach for computing penalties or bonuses based on the predicted life difference between the as-designed and as-built HMA pavement. The QRSS applies the following concepts in computing penalties or bonuses for HMA pavement construction.

- The effective temperature concept is applied to evaluate climatic effects on the HMA dynamic modulus and determine the critical temperatures (moduli) needed to predict the rutting and FC for a particular pavement structure and design location. Each distress has an unique effective temperature.
- The simulation of the MEPDG distress predictions is the basis for developing CFS for the three major distresses (rutting, FC, and TC). The CFS are based on relating the dynamic modulus calculated using the effective temperature with rutting and FC and the calculated creep compliance with TC. Evaluation of these CFS show that they agree with good accuracy with the MEPDG Version 1.0
- For the as-designed mix (the job mix formula, JMF), in addition to the distress prediction using CFS, a Monte Carlo simulation of the dynamic modulus is run using the mean and historical variance of the HMA volumetric and aggregate gradation properties. For the as-built mix, information

from each lot is used to run the Monte Carlo simulation to estimate the distresses and the predicted pavement life.

- A methodology to relate the level of the predicted distress to the pavement life was developed. This methodology estimates the as-designed pavement life and compares it with as-built pavement life on a lot by lot basis. For each lot, a comparison between the cumulative probability distribution of the as-designed pavement life and the as-built pavement life is conducted to calculate the PLD.
- Finally, the pay factor and the penalty or bonus are estimated from the PLD for each lot. The criterion relating the PLD and pay factor for each distress is solely defined by the user agency. The summation of the pay factors for the lots provides a total project pay factor. The user has the option of using the IRI to further adjust the pay factor.

5.3 Proposed Future Research

Based on the results of this project, the following future research studies are proposed:

- Evaluate the QRSS using real-world field data in order to validate that the software solutions meet the test of engineering reasonableness.
 - Using field data, compare the QRSS pay adjustment criteria to the current pay adjustment criteria specified by state DOTs.
 - Since the national calibration of the MEPDG was limited to HMA mixtures prepared with unmodified asphalt binders, test the QRSS with data from field projects incorporating modified binders, recycled asphalt pavement, recycled asphalt shingles, and warm mix asphalt.
 - In a future version of the QRSS, provide the ability to enter measured values of E^* and D and compare these results to those computed using the WPE (for rutting and FC) and the equations for D in Section 2.5 of this report (for TC).
 - Since the current TC module is coded in the Fortran language, re-code this module in the same language as the main portion of the QRSS to provide better program stability, a more user-friendly interface, and better computing speed.
-

References

1. Witczak, M. W., D. Andrei, and W. Mirza. *Development of Revised Predictive Model for the Dynamic (Complex) Modulus of Asphalt Mixtures*. Interim technical report, NCHRP Project 1-37A, University of Maryland, 1999.
2. El-Basyouny, M. and M. G. Jeong. Effective Temperature for Permanent Deformation and Fatigue Distress Analysis on Asphalt Mixtures. In *Transportation Research Record: Journal of the Transportation Research Board*, No. 2127, Transportation Research Board of the National Academies, Washington, D.C., 2009, pp. 155–163.
3. Sotil, A. *Use of the Dynamic Modulus E^* Test as Permanent Deformation Performance Criteria for Asphalt Pavement Systems*. Ph.D. dissertation, Arizona State University, Tempe, 2005.
4. El-Basyouny, M. and M. G. Jeong. Development of Database Solution for Prediction of the MEPDG Permanent Deformation. Presented at 89th Annual Meeting of the Transportation Research Board, Washington, D.C., 2010.
5. El-Badawy, S., M. G. Jeong, and M. El-Basyouny. Methodology to Predict Alligator Fatigue Cracking Distress Based on AC Dynamic Modulus. In *Transportation Research Record: Journal of the Transportation Research Board*, No. 2095, Transportation Research Board of the National Academies, Washington, D.C., 2009, pp. 115–124.
6. Jeong, M., J. Uzan, and M. W. Witczak. Development of a Stochastic Framework of the Thermal Cracking Distress on Asphaltic Pavement. Presented at 89th Annual Meeting of the Transportation Research Board, Washington, D.C., 2010.
7. Jeong, M. and M. El-Basyouny. Statistical Applications and Stochastic Analysis for Performance Related Specification of Asphalt Pavement Quality Assurance. In *Transportation Research Record: Journal of the Transportation Research Board of the National Academies*, No. 2151, Transportation Research Board of the National Academies, Washington, D.C., 2010, pp. 84–92.
8. Rosenblueth, E. Point Estimates for Probability Moments. *Proceeding of National Academy of Sciences of the United States of America*, Vol. 72, No. 10, 1975, pp. 3812–3814.
9. Harr, M. E. *Reliability-Based Design in Civil Engineering*. McGraw-Hill, Inc., New York, 1987.
10. M. W. Witczak. A-001 MIDAS Study. *Effective Temperature Analysis for Permanent Deformation of Asphaltic Mixtures*. September 1992.
11. *The Superpave Mix Design Manual for New Construction and Overlays*. SHRP A-407 Report, Strategic Highway Research Program, National Research Council, Washington D.C. 1994.
12. *Guide for Mechanistic-Empirical Design of New and Rehabilitated Pavement Structures*. NCHRP 1-37A Final Report, Transportation Research Board, National Research Council, Washington, D.C., 2004.
13. El-Basyouny, M. M. *Calibration and Validation of Asphalt Concrete Pavements Distress Models for 2002 Design Guide*. Ph.D. dissertation. Department of Civil and Environmental Engineering, Arizona State University, Tempe, AZ, 2004.
14. Deacon, J., J. Coplantz, A. Tayebali, and C. Monismith. Temperature Considerations in Asphalt-Aggregate Mixture Analysis and Design. In *Transportation Research Record: Journal of the Transportation Research Board*, No. 1454, Transportation Research Board of the National Academies, Washington, D.C., 1994, pp. 97–112.
15. Shook, J. F., and B. F. Kallas. Factors Influencing Dynamic Modulus of Asphalt Concrete, *Proceedings of the Association of Asphalt Paving Technologists*, Vol. 38, 1969.
16. Witczak, M. W., K. E. Kaloush, T. Pellinen, M. El-Basyouny, and H. Von Quintus. *NCHRP Report 465: Simple Performance Test for Superpave Mix Design*. TRB, National Research Council, Washington D.C. 2002.
17. Bonnaure, F., G. Gest, A. Garvois, and P. Uge. A New Method of Predicting the Stiffness of Asphalt Paving Mixes. *Journal of the Association of Asphalt Paving Technologists*, Vol. 46, 1977, pp. 64–104.
18. Fonseca, O. A., and M. W. Witczak. A Prediction Methodology for the Dynamic Modulus of In-Placed Aged Asphalt Mixtures. *Journal of the Association of the Asphalt Paving Technologists*, Vol. 65, 1996, pp. 393–430.
19. *The AASHO Road Test Report 5: Pavement Research*. Highway Research Board Special Report 61E, National Research Council, Washington, D.C., 1962.
20. Hiltunen, D. R. and R. Roque. A Mechanics-Based Prediction Model for Thermal Cracking of Asphaltic Concrete Pavements. *Journal of the Association of Asphalt Paving Technologists*, Vol. 63, 1994, pp. 81–117.
21. Ullidtz, P. *Modeling Flexible Pavement Response and Performance*. Polyteknisk Forlag, Denmark, 1998.
22. Montgomery, D. C. *Design and Analysis of Experiments*, 5th Edition. John Wiley and Sons, Inc., 2001.
23. Montgomery, D. C., E. A. Peck, and G. G. Vining. *Introduction to Linear Regression Analysis*, 3rd Edition. John Wiley and Sons, Inc., 2001.
24. *Assessment of Statistical Variability of Asphalt Concrete Mixture Components*, ASU-ADOT Research Program unpublished report, Arizona State University, 2005.
25. Klemunes, Jr., J. A. *Determining Soil Volumetric Moisture Content Using Time Domain Reflectometry*. Master of science thesis. University of Maryland, College Park, MD 1995.

26. Federal Highway Administration. *Quality Assurance Procedures for Construction*, FHWA FAPG-23 CFR 637B, 1995.
 27. Epps, J. A., M. S. Gardiner, and D. Newcomb. *Review of ADOT's Quality Assurance Asphalt Concrete Specification*, Arizona Department of Transportation, 1989.
 28. Witczak M. W. and E. J. Yoder. *Principles of Pavement Design*, 2nd Edition, John Wiley and Sons, Inc., 1975.
 29. Witczak, M. W. and M. W. Mirza. Development of a Global Aging System for Short and Long Term Aging of Asphalt Cements. *Journal of the Association of the Asphalt Paving Technologists*, Vol. 64, 1995, pp. 532–572.
 30. Mirza, M. W. *Development of a Global Aging System for Short and Long Term Aging of Asphalt Cements*. Ph.D. dissertation. Department of Civil Engineering, University of Maryland, College Park, 1993.
 31. Patni, A. *Development of Performance Related Pay Factors for Asphalt Mixture Permanent Deformation Distress*. Master thesis. Arizona State University, Tempe, 2007.
 32. Patni, A. *Transportation Research Circular E-C137: Glossary of Highway Quality Assurance Terms, 4th Update*, Transportation Research Board, National Research Council, Washington, D.C., May 2009.
-

APPENDICES A THROUGH D

Appendices A through D are not published herein, but are available on the project description web page at: <http://apps.trb.org/cmsfeed/TRBNetProjectDisplay.asp?ProjectID=958>. The appendices titles are:

Appendix A: Raw Data for Permanent Deformation Model Analysis

Appendix B: Raw Data for Fatigue Cracking Model Analysis

Appendix C: Summary of Results for Level 3 Creep Compliance Predictive Equations

Appendix D: Hardening Ratio Database

APPENDIX E

Quality Related Specification Software (QRSS) User's Manual

This material also is available at <http://apps.trb.org/cmsfeed/TRBNetProjectDisplay.asp?ProjectID=958>. Material provided by contractor.

SI* (MODERN METRIC) CONVERSION FACTORS				
APPROXIMATE CONVERSIONS TO SI UNITS				
Symbol	When You Know	Multiply By	To Find	Symbol
LENGTH				
in	Inches	25.4	millimeters	mm
ft	Feet	0.305	meters	m
yd	Yards	0.914	meters	m
mi	Miles	1.61	kilometers	km
AREA				
in ²	square inches	645.2	square millimeters	mm ²
ft ²	square feet	0.093	square meters	m ²
yd ²	square yards	0.836	square meters	m ²
ac	Acres	0.405	hectares	ha
mi ²	square miles	2.59	square kilometers	km ²
VOLUME				
fl oz	fluid ounces	29.57	milliliters	mL
gal	Gallons	3.785	Liters	L
ft ³	cubic feet	0.028	cubic meters	m ³
yd ³	cubic yards	0.765	cubic meters	m ³
NOTE: Volumes greater than 1,000 L shall be shown in m ³				
MASS				
oz	Ounces	28.35	grams	g
lb	Pounds	0.454	kilograms	kg
T	short tons (2,000 lb)	0.907	megagrams (or "metric ton")	Mg ("t")
TEMPERATURE (Exact Degrees)				
oF	Fahrenheit	5 (-32)/9 or (F-32)/1.8	Celsius	oC
ILLUMINATION				
fc	foot-candles	10.76	Lux	lx
fl	foot-lamberts	3.426	candela/m ²	cd/m ²
FORCE and PRESSURE or STRESS				
lbf	Poundforce	4.45	newtons	N
lbf/in ²	poundforce per square inch	6.89	kilopascals	kPa
APPROXIMATE CONVERSIONS FROM SI UNITS				
Symbol	When You Know	Multiply By	To Find	Symbol
LENGTH				
mm	millimeters	0.039	inches	in
m	meters	3.28	Feet	ft
m	meters	1.09	yards	yd
km	kilometers	0.621	miles	mi
AREA				
mm ²	square millimeters	0.0016	square inches	in ²
m ²	square meters	10.764	square feet	ft ²
m ²	square meters	1.195	square yards	yd ²
ha	hectares	2.47	acres	Ac
km ²	square kilometers	0.386	square miles	mi ²
VOLUME				
mL	milliliters	0.034	fluid ounces	fl oz
L	liters	0.264	gallons	Gal
m ³	cubic meters	35.314	cubic feet	ft ³
m ³	cubic meters	1.307	cubic yards	yd ³
MASS				
g	grams	0.035	ounces	Oz
kg	kilograms	2.202	pounds	Lb
Mg ("t")	megagrams (or "metric ton")	1.103	short tons (2,000 lb)	T
TEMPERATURE (Exact Degrees)				
oC	Celsius	1.8C+32	Fahrenheit	oF
ILLUMINATION				
lx	lux	0.0929	foot-candles	Fc
cd/m ²	candela/m ²	0.2919	foot-lamberts	Fl
FORCE and PRESSURE or STRESS				
N	newtons	0.225	poundforce	Lbf
kPa	kilopascals	0.145	poundforce per square inch	lbf/in ²
*SI is the symbol for the International System of Units. Appropriate rounding should be made to comply with Section 4 of ASTM E380. (Revised March 2003)				

TABLE OF CONTENTS

CHAPTER 1–INTRODUCTION.....	1
Background.....	1
Quality Related Specification (QRS).....	1
QRSS Overview.....	2
Field of Application.....	4
CHAPTER 2 – GETTING STARTED	6
System Requirements	6
Installation Drive.....	6
Installation Procedure	7
CHAPTER 3 – USING THE SOFTWARE	9
Software Program Overview	9
Creating a new project	9
Open an Existing Project.....	12
Save a Project.....	13
Pavement Parameters	13
Traffic.....	13
Structure	14
Material Properties	16
Climate.....	18
Limits.....	21
Mix Design.....	22
Pay Factors	23
Pay factor for each distress	23
IRI Pay factor	25
Job Mix Formula Solution	26
Summary.....	26
Monte Carlo and Rosenbleuth simulation	27
Job Mix Formula plots	28
QA Data	28
General information.....	29
Gradation	30
Volumetric	33
Binder.....	34
Dynamic Modulus (E*).....	35
IRI including input parameters.....	36
Output.....	36
Output Parameters.....	38
Detailed and summarized results each distress.....	40
Predicted Life distribution plots.....	42
APPENDICES	44
Example Input Data.....	44
QA/QC Inputs.....	45

LIST OF FIGURES

Figure 1: QRSS Overview - Flow Diagram	3
Figure 2: Install.bat file	7
Figure 3: Screen shot - .Net install	7
Figure 4: Screen shot - Set install directory	7
Figure 5: Screen shot - Install components.....	8
Figure 6: Screen shot - Install finish.....	8
Figure 7: Screen shot - Create a new project	9
Figure 8: Screen shot – Showing left tabs minimized	10
Figure 9: Screen shot - Use an Existing Mix Design Project?	10
Figure 10: Screen shot - New Project	11
Figure 11: Screen shot - Open File Dialog.....	12
Figure 12: Screen shot - Save current project?	12
Figure 13: Screen shot - Save Project	13
Figure 14: Screen shot - Traffic Screen	14
Figure 15: Screen shot - Completed Structure.....	15
Figure 16: Screen shot – Historical and Lab Measured SPT Option	16
Figure 17: Screen shot - Job Mix Formula inputs	17
Figure 18: Screen shot - Climate	18
Figure 19: Screen shot - Climate Interpolation.....	19
Figure 20: Screen shot - Unable to load HCD File	20
Figure 21: Screen shot – Limits	21
Figure 22: Screen shot - Mix Design run-time warning	22
Figure 23: Screen shot - Mix Design analysis.....	22
Figure 24: Screen shot - Pay factors	23
Figure 25: Screen shot - Pay factor plot	24
Figure 26: Screen shot - IRI Pay Factor	25
Figure 27: Screen shot - JMF summary.....	26
Figure 28: Screen shot - JMF Simulation.....	27
Figure 29: Screen shot - JMF Plots	28
Figure 30: Screen shot - General Information.....	30
Figure 31: Screen shot – Gradation.....	31
Figure 32: Screen shot - Sample data Summary	31
Figure 33: Screen shot - Sample data ANOVA.....	32
Figure 34: Screen shot - Sample data Control Charts	32
Figure 35: Screen shot – Volumetric	33
Figure 36: Screen shot – Binder	34
Figure 37: Screen shot - Dynamic Modulus (E*)	35
Figure 38: Screen shot - IRI input parameters	36
Figure 39: Screen shot - Inputs Complete	37
Figure 40: Screen shot - Project > Run Solution.....	37
Figure 41: Screen shot - Outputs navigation.....	37
Figure 42: Screen shot - Output summary	39
Figure 43: Equation - Pay Factor (Cpb1)	39
Figure 44: Equation - Individual distress Pay Factor.....	41
Figure 45: Screen shot - Individual distress summary	41
Figure 46: Screen shot - Detailed output	42
Figure 47: Screen shot - Predicted Life distribution plots.....	43

LIST OF TABLES

Table 1: System Requirements 6

CHAPTER 1—INTRODUCTION

The Quality Related Specification Software (QRSS) is a Windows® based program capable of (1) evaluating an hot-mix asphalt (HMA) mix design (the job mix formula or *as-designed mix*) in terms of distress criteria defined by the state highway agency and (2) determining a pay adjustment system, including incentives and disincentives, for the *as-built mix* in terms of the same agency-defined distress criteria. Specifically, the QRSS can assist agencies in checking a mix design for a given pavement structure to satisfy the required design criteria and determine appropriate pay adjustments to a contractor's bid price based on the predicted performance of the as-constructed pavement.

Background

The current practice of quality assurance (QA) in the HMA pavement industry varies widely and is based on field measurement of several HMA properties. Generally, HMA quality is typically defined by how closely the as-built mixture meets the mix design requirements.

Expected future performance may be inferred from the difference between the as-designed and as-built HMA properties. The field-measured properties are not a direct measure of pavement performance. There has been progress in the paving industry in defining the quality of the mixture and the pavement in terms of performance, where the contractor responsible for production and placement would then be paid based on the difference in predicted life between the as-designed and as-constructed pavement. In these types of specifications, the Acceptance Quality Characteristics (AQC)s specify the amount of time (i.e., 20 years) the pavement structure is expected to perform. However, this type of performance-related specification is new and relatively untried, and has not been widely used in the industry.

Quality Related Specification (QRS)

The purpose of the new approach used in the QRSS program is to establish a specification that determines the quality of HMA construction by measuring and evaluating AQC)s directly related to pavement performance. These AQC)s are tied to performance through prediction models and measured fundamental engineering characteristics. The quality of the as-built mix is expressed in terms of its predicted service life and is then compared with the predicted service life of the as-designed mix. The difference in performance between the two mixes becomes the basis of the payment adjustment system.

The QRSS uses performance models developed from the results of the Mechanistic Empirical Pavement Design Guide (MEPDG) to predict rutting, fatigue cracking, and thermal cracking. The predicted life of each lot is statistically compared to that of the as-designed mix and the predicted life difference is used to calculate the pay adjustment factor. The final pay adjustment for each lot is the summation of the pay adjustments estimated for each distress for each HMA layer. Unlike other distresses the pay adjustment for International Roughness Index

(IRI) is estimated separately using the user input values of initial IRI measured in the field for the surface layer.

Pay factor values for each distress are defined by the agency, based on the percent of maximum and minimum incentive and disincentive allowed for each distress. The QRSS is capable of applying an agency-defined weighting factor for each distress as the relative importance of each distress varies with the climate in different geographical regions. The final pay factor equation combines each distress component to calculate the incentives and disincentives. The approach taken by the QRSS establishes a new paradigm in calculating the pay adjustment based on the Predicted Life Difference (PLD) of the pavement between the as-designed mix and the as-constructed mix.

QRSS Overview

The QRSS has two modes of operation: (1) the mix design mode and (2) the pay performance mode. The flow chart in Figure 1 provides an overview of the different software components.

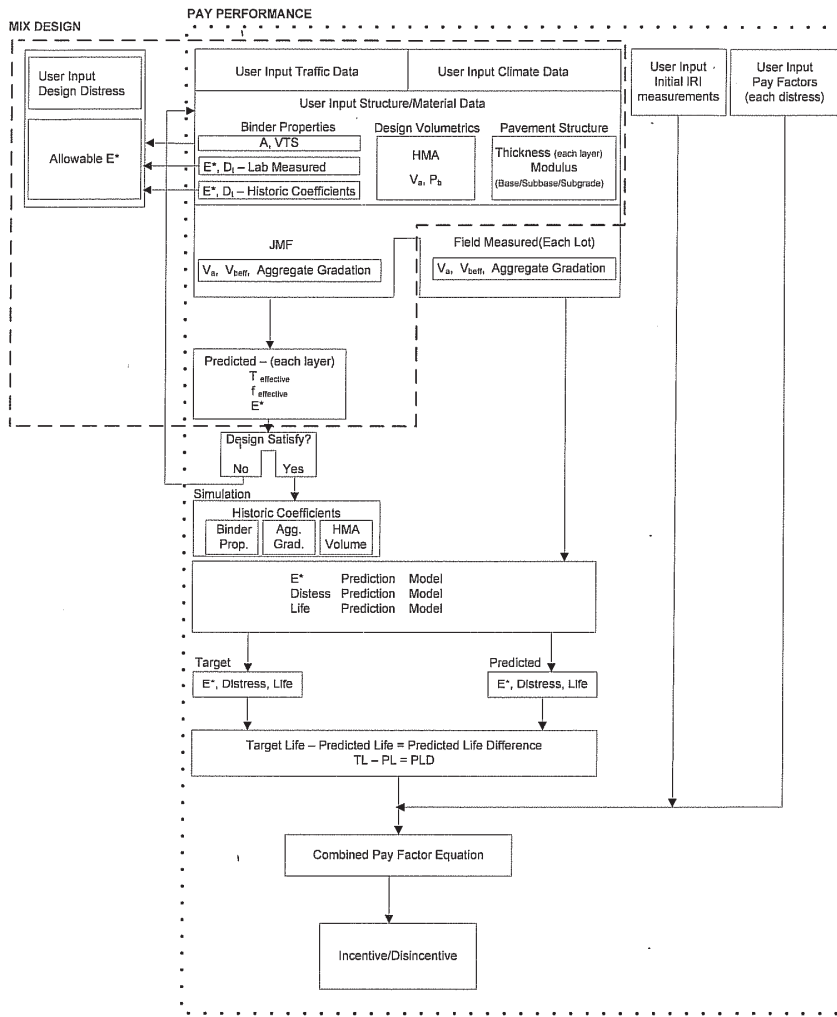


Figure 1: QRSS Overview - Flow Diagram

The user inputs common to both modes include traffic, climate, structure, and material properties of the as-designed mix. In the mix design mode the inputted design distress limits are only required for verifying that the as-designed mix meets these agency-defined criteria. In the pay performance mode, additional user inputs are required; most importantly the measured QA properties of each lot of the as-built mix, the pay factors for each distress type, and initial IRI measurements at each milepost of the project.

In the mix design mode, the predicted dynamic modulus (E^*) is compared to the allowable E^* (master curve) and the predicted distress values to the allowable distress limits entered by the user. If the predicted values of E^* is greater than the allowable E^* and the predicted distresses are less than the specified allowable limits, the design criteria is satisfied and the program proceeds to the next step of accepting pay factor and QA inputs for the pay performance calculation. If the as-designed mix does not satisfy the E^* and distress criteria, the mix properties, the pavement structure, or both must be adjusted depending on the project requirements to obtain an as-designed mix that satisfies the performance criteria.

In the pay performance mode, historical measures of variability of the volumetric properties of the as-designed mix are used to simulate their effects on the pavement performance. The QA information for each as-constructed lot, including aggregate gradation, mixture volumetrics (asphalt content, specific gravity, bulk density, in situ air voids), layer thickness, and binder type are used to predict the E^* , distress, and life of the lot. These predicted values are compared and the predicted life difference is used to calculate the final incentive or disincentive to the contractor. The distresses evaluated are the predicted rutting in each HMA layer, fatigue cracking in the bottom HMA layer, thermal cracking of the top HMA layer and the initial IRI data supplied by the user. Unlike the other distresses, the software does not predict IRI distress; instead, the user provides the initial IRI to include in the final pay factor calculation. Including IRI in the final pay calculation is a user option.

Applicability

The QRSS can be used for all new construction flexible pavement projects in checking the design criteria and calculating the incentives or disincentives of each lot constructed. For each distress, the QRSS prediction models (pre-solved solutions based on multiple MEPDG runs) yield results that closely match those predicted with the MEPDG. Details of how the parameters influencing each distress, including climate and subsurface conditions, have been accounted for in developing the models and the accuracy of the prediction models are presented in the project final report.

Since the models used in the MEPDG for predicting the rutting performance were calibrated and validated with data from new pavements, there is uncertainty whether the rutting model in the QRSS is applicable to overlay projects. This issue is being further explored in NCHRP Project 9-22A, "Evaluation of the Quality-Related Specification Software (QRSS) Version 1.0." In NCHRP Project 9-22, the QRSS is being used to (1) evaluate the quality of as-built mix compared to the as-designed mix on several field projects that involve the placement of HMA overlays on existing pavements and (2) retrospectively evaluate QA data from several

completed field projects and compare the results to those of the usual QA analysis conducted by the respective state agencies.

CHAPTER 2 – GETTING STARTED

System Requirements

Processor	Minimum: 400 megahertz (MHz) Pentium processor Recommended: 1 gigahertz (GHz) Pentium processor
Operating System	.NET Framework 3.0 can be installed on any of the following systems: Microsoft Windows 2003 Server Service Pack 1 (SP1) Windows XP SP2 Windows Vista * *Windows Vista comes with .NET Framework 3.0. There is no separate installation package required. The standalone .NET Framework 3.0 packages are not supported on Vista.
RAM	Minimum: 96 megabytes (MB) Recommended: 256 MB
Hard Disk	Up to 500 MB of available space may be required.
Display	Minimum: 800 x 600, 256 colors Recommended: 1024 x 768 high color, 32-bit
Mouse	Not required

Table 1: System Requirements

Installation Drive

When you start the .NET Framework 3.0 installer, the default installation location is on your system drive, which is the drive that boots your system. Please ensure that the required amount of space (up to 500 MB) is available on your system drive.

Installation Procedure

The application should begin installing when the CD is inserted into the drive. If the application does not immediately begin installing, click the install.bat file on the CD.



Figure 2: Install.bat file

When the application begins installing, it will first check for the existence of the Microsoft .Net Framework; if necessary, follow the instructions to complete the installation of the required version of Microsoft .Net.

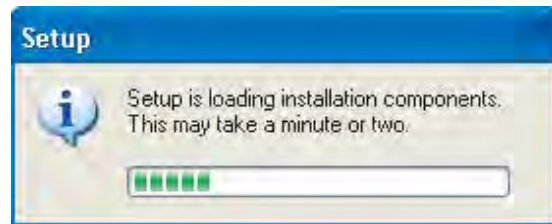


Figure 3: Screen shot - .Net install

Set the directory where the application is to be installed. The default install directory of the application is **C:\Program Files\NCHRP9-22**; this can be changed by either clicking the **Browse...** button or directly entering the new directory. Once the directory has been set, click the **Next>>** button.

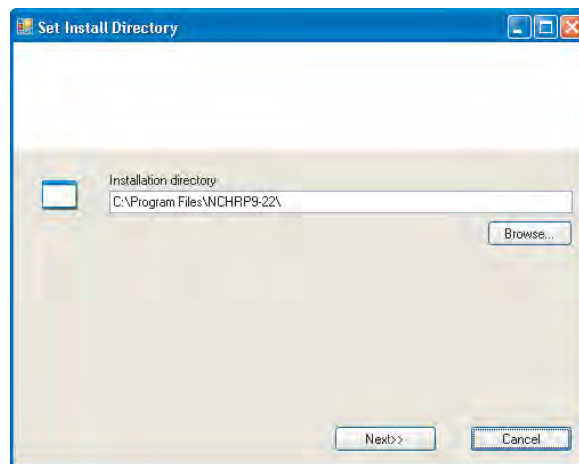


Figure 4: Screen shot - Set install directory

Before the application can be run, other components must be first installed. Click the **Install** button to begin the installation of the components.

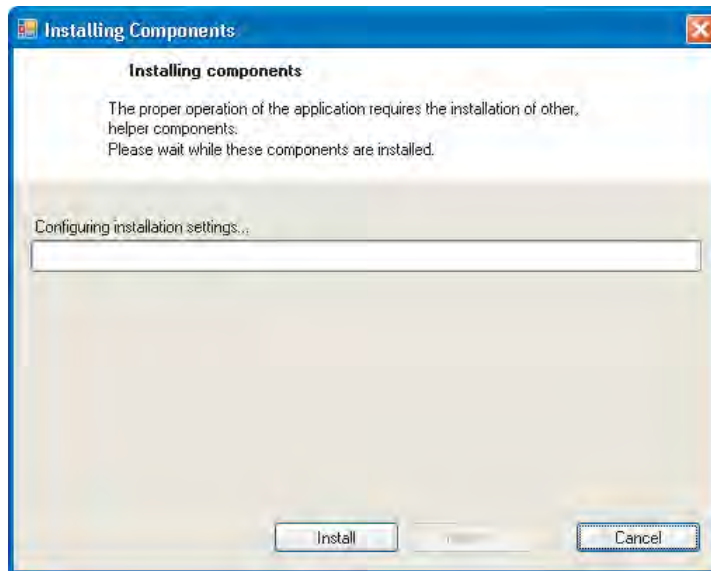


Figure 5: Screen shot - Install components

After the application is installed, the final install screen will be displayed. Check the checkbox to launch the application on Finishing. Click the **Finish** button.

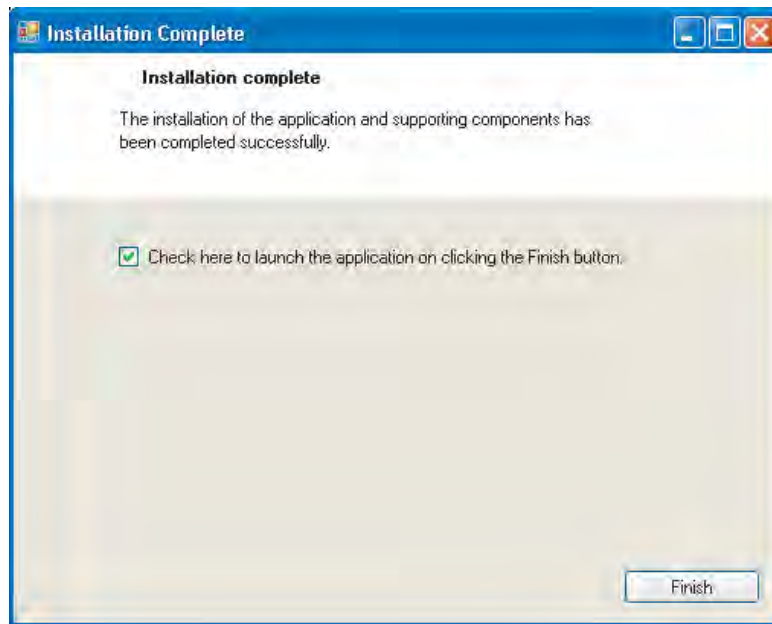



Figure 6: Screen shot - Install finish

CHAPTER 3 – USING THE SOFTWARE

Software Program Overview

As noted in the QRSS Overview in Chapter 1, the QRSS can be run in either of two modes: Mix Design and Pay Performance Factors. The example discussed in this manual is focused on running the QRSS in the “Pay Performance Factors” mode. The example also discusses the Mix Design mode inputs and outputs, as the output of mix design mode is an input for pay performance mode.

Creating a new project

After starting the application or clicking on the new project icon () the screen should resemble Figure 7. It has two main sections, the left tab and a display area. The left tab has three separate windows named “Project Information”, “Navigation”, and “Output”. Once the general project information is entered in the first screen (Figure 7), the “Project Information” tab displays this information throughout the project. The “Navigation” tab displays the tree structure of the data input process and helps navigate between different stages of the input process. The “Output” window lists the tree structure of the calculated results once the solution is run. Selecting a particular file in the “Navigation” or “Output” window will display its contents in the display area.

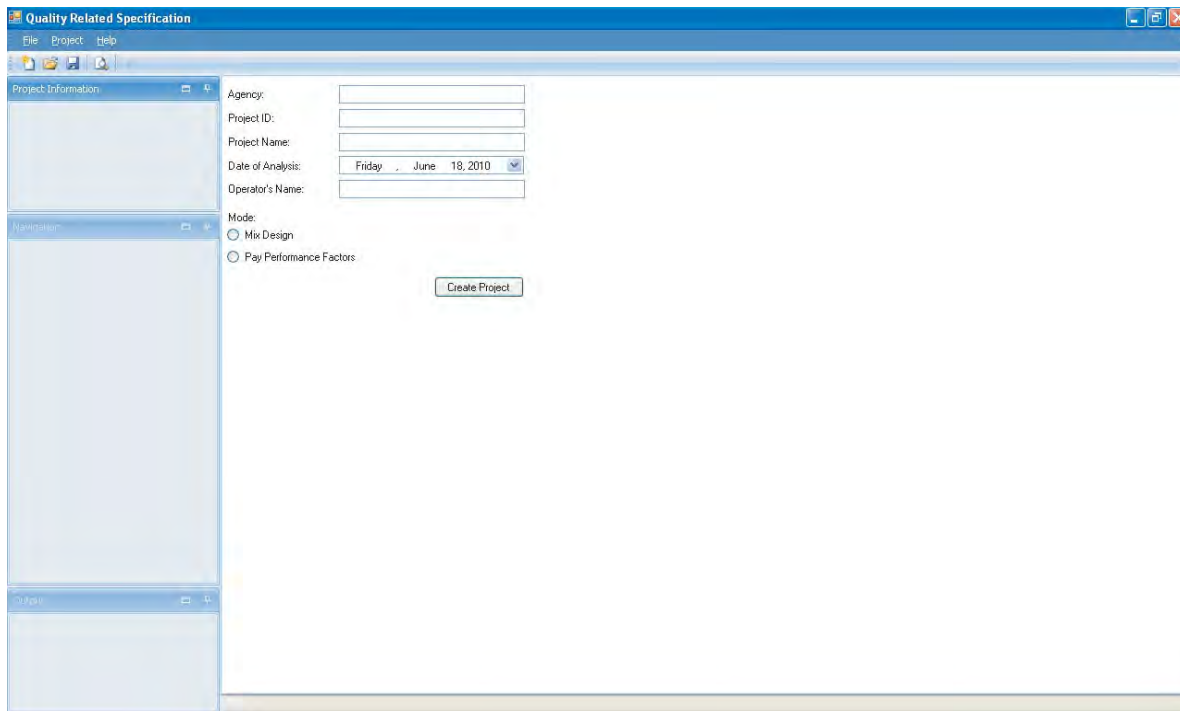


Figure 7: Screen shot - Create a new project

The three left tabs can be minimized to increase the display area as shown in Figure 8 below. Clicking a minimized tab will display its contents to make a selection. These tabs can be opened, moved, and minimized as required.

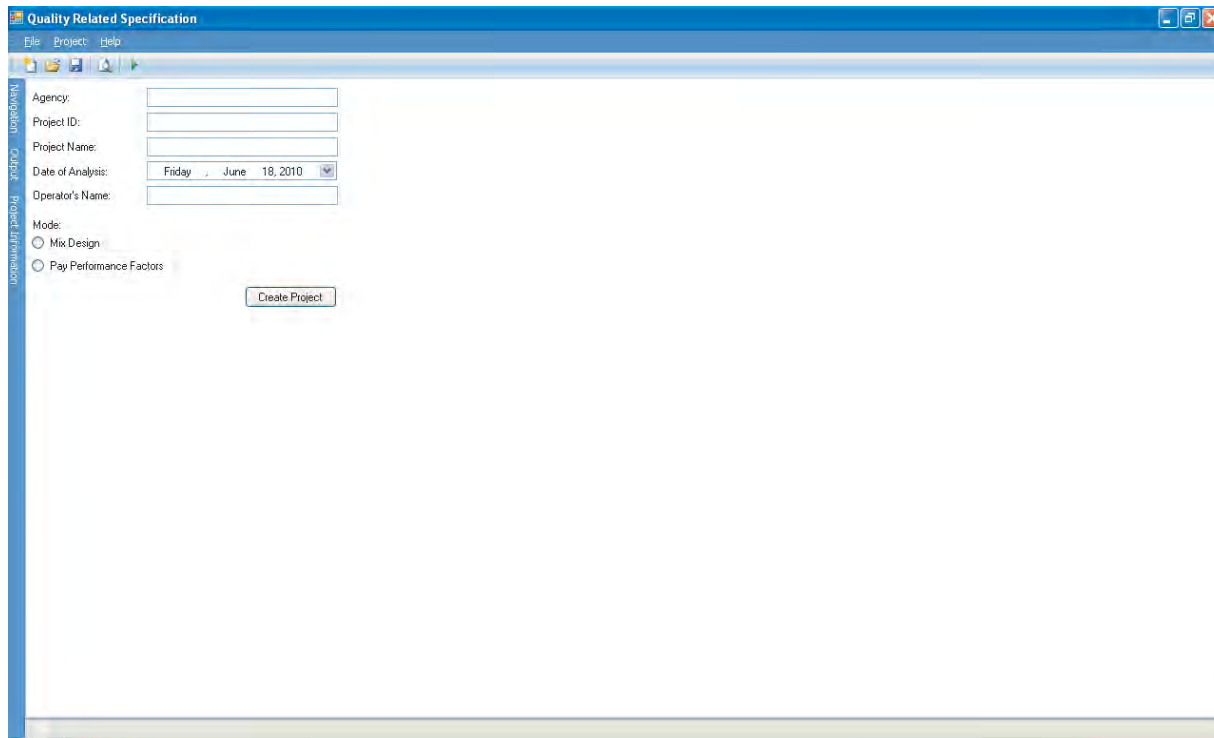


Figure 8: Screen shot – Showing left tabs minimized

Enter the Agency, Project ID, Project Name, Date of Analysis, and Operators Name. Then select the project mode, either Mix Design or Pay Performance Factors. If “Pay Performance Factors” mode is selected, the Question dialog box of Figure 9 will appear. Selecting Yes opens a file dialog box that allows selection of an existing Mix Design project. Then the “Pavement Parameters” (see Chapter 3: Pavement Parameters) of the existing Mix Design project will be used for this project; If No is selected the “Pavement Parameters” will need to be entered manually for the new project.

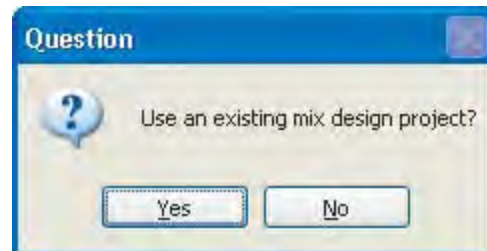


Figure 9: Screen shot - Use an Existing Mix Design Project?

Click the Create Project button as shown in Figure 7 to start the new project. The general project information will be displayed in the “Project Information” window along the left tab of the screen and the inputs tree will become available on the “Navigation” window (Figure 10).

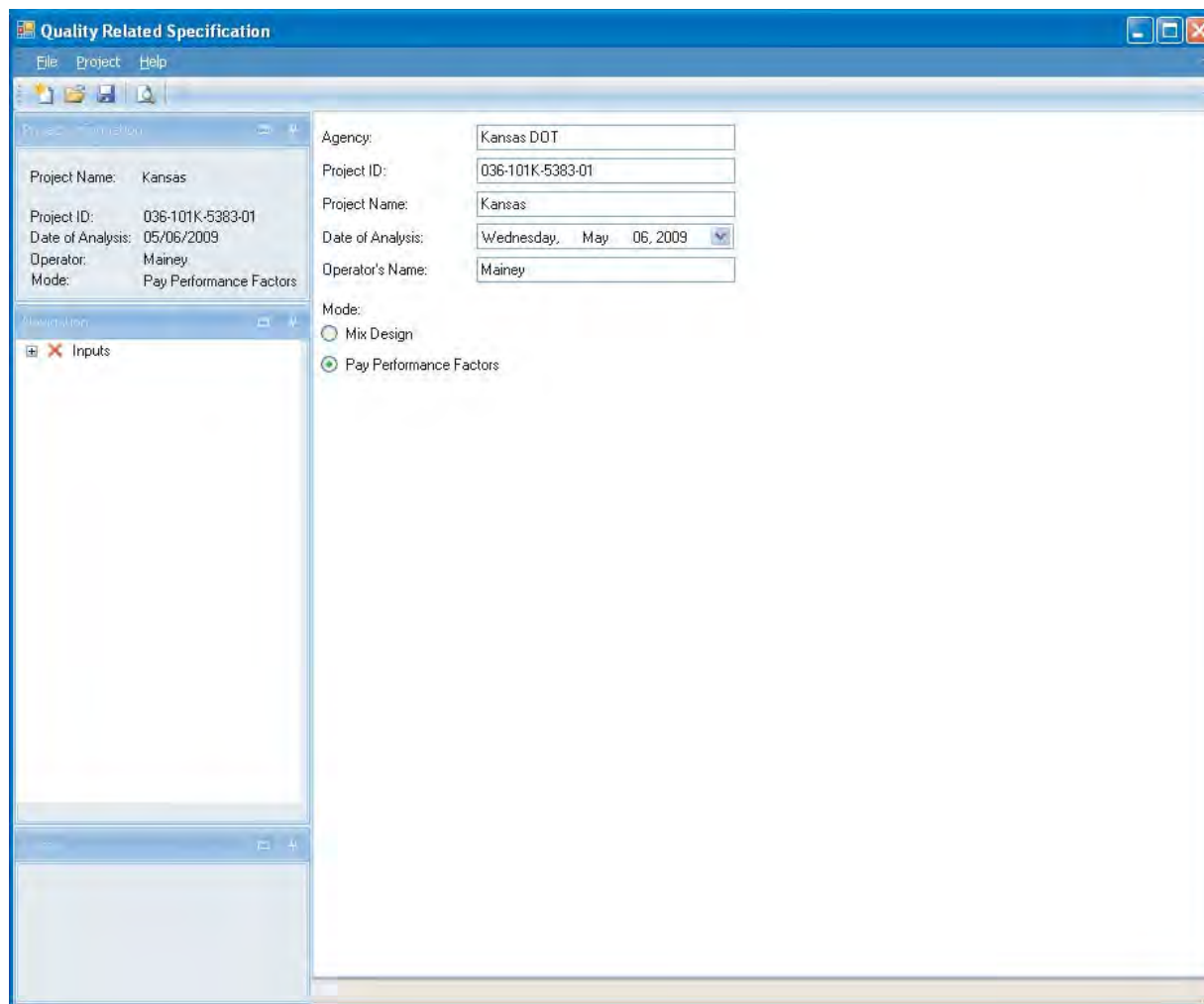
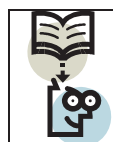



Figure 10: Screen shot - New Project



Example:

Enter values for **Project ID**, **Project Description**, **Date of Analysis** and **Operators Name**.
 Select the **Pay Performance Factors** option.
 Click **No** when prompted to use an existing mix design project.
 Click the **Create Project** button.

Open an Existing Project

At any point during the operation of the QRSS, clicking either the open file icon () or navigating to File > Open in the menu bar will launch the Open File dialog box (Figure 11). If another project is already open, the “Save Current Project” dialog box (Figure 12) will be displayed; selecting Yes will save the changes to the current project, selecting No, will discard any changes.

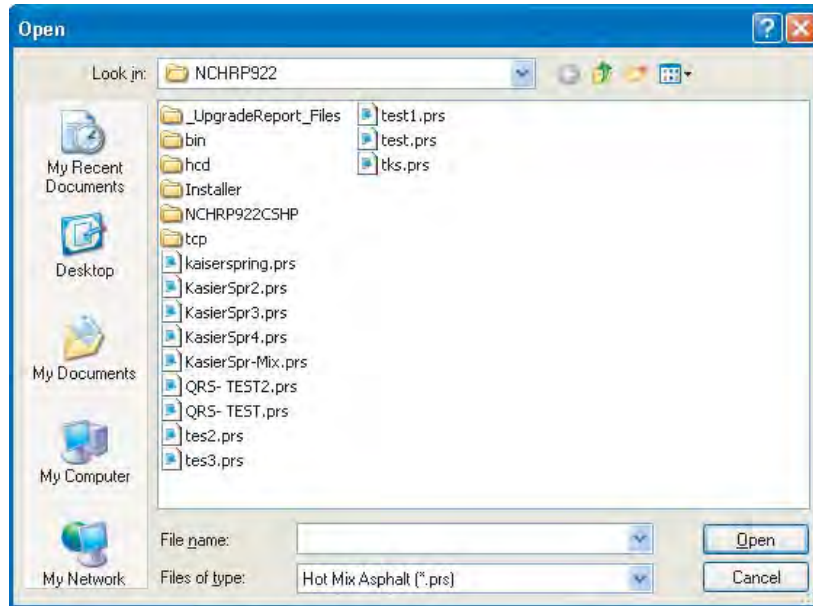


Figure 11: Screen shot - Open File Dialog



NOTE: Only files with a “.prs” extension are displayed in the Open File dialog window and can be opened.

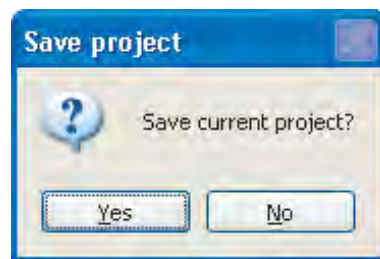



Figure 12: Screen shot - Save current project?

Save a Project

Clicking on the **Save File** button () in the toolbar, or navigating to File > Save will cause the **Save As** dialog to appear (Figure 13). Type in the file name to save the project, then click the **Save** button.

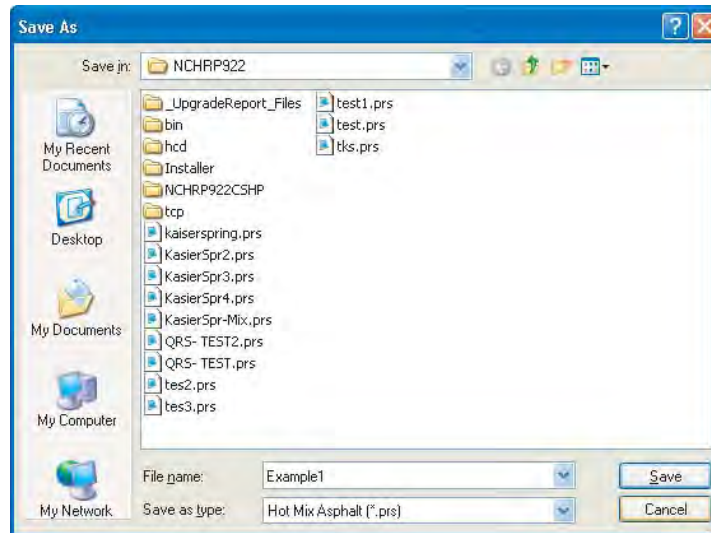


Figure 13: Screen shot - Save Project

Pavement Parameters

Clicking the input icon on the left tab will open up the input tree that includes the pavement parameters required for design and performance prediction, namely: **Traffic**, **Structure** including the **Material Properties**, **Climate**, and the distress **Limits** for the mix design check. As noted in Chapter 1, these parameters are common to both the mix design mode and pay performance mode.

Traffic

In the traffic input screen (Figure 14) all values are required to be entered. The shaded area indicates that it is not a user input, but a parameter computed by the software. In this screen the Total ESALs is shaded to indicate that it is calculated by the software based on the design life, initial year daily ESALs, and annual percentage growth rate entered by the user.

Quality Related Specification

File Project Help

Project Name: Kansas

Project ID: 036-101K-5383-01

Date of Analysis: 05/06/2009

Operator: Mainey

Mode: Pay Performance Factors

Design Speed (mph): 70

Design Life (yrs): 20

Design ESALs

Year 1 Daily ESALs (Design Lane): 175

Annual Growth Rate Y (%): 1.5

Total ESALs: 1,488,074

Navigation:

- Inputs
 - Traffic
 - Structure
 - Climate
 - Limits
 - Mix Design
 - Pay Factors
 - Job Mix Formula Solution
 - QA \ QC

Figure 14: Screen shot - Traffic Screen

If all details are entered correctly, the icon for Traffic in the input tree will turn to a check.

	<p>Example:</p> <p>Expand the Inputs tree and select Traffic</p> <ul style="list-style-type: none"> ○ Set: <table style="margin-left: 20px;"> <tr> <td>Design Speed</td> <td style="text-align: right;">70</td> </tr> <tr> <td>Design Life</td> <td style="text-align: right;">20</td> </tr> <tr> <td>Initial ESALs</td> <td style="text-align: right;">175</td> </tr> <tr> <td>Annual Growth Rate</td> <td style="text-align: right;">1.5</td> </tr> </table> <p>Total ESALs should be 1,488,074</p> <p>The resultant Traffic Screen should resemble Figure 14.</p>	Design Speed	70	Design Life	20	Initial ESALs	175	Annual Growth Rate	1.5
Design Speed	70								
Design Life	20								
Initial ESALs	175								
Annual Growth Rate	1.5								

Structure

The “Structure” input screen (Figure 15) allows the input of the pavement structure, including thickness and material properties. This screen is also used to select the distress types considered in the analysis.

The QRSS is capable of allowing up to three (3) AC layers (AC Surface, AC Binder, and AC Base). By default the AC Binder and AC Base layers are not enabled (shown as shaded that does not allow user inputs). Checking or un-checking the AC Binder and AC Base check boxes in the “Material Properties” screen enables or disables the option to edit the material properties of these layers. Enabling or disabling the AC Binder and AC Base check boxes

defines the number of AC layers in the project, which will also determine the range of distress that can be included in the analysis. Project specific thickness (in inches) of the asphalt layers and modulus (in psi) of the unbound layers (base, subbase, and subgrade) are input using this screen.

Depending on the number of AC layers in the project, the QRSS is capable of analyzing the rutting distress in each of the AC layers, fatigue in the bottom AC layer, and thermal cracking in the top AC layer. If the initial IRI data of the surface layer is also a distress parameter in deciding the contractor’s incentive or disincentive, the IRI for the surface layer must also be checked in the “Desired Distress” field. This will add the tabs to input tree for entering IRI pay factors and the initial IRI at the time of construction.

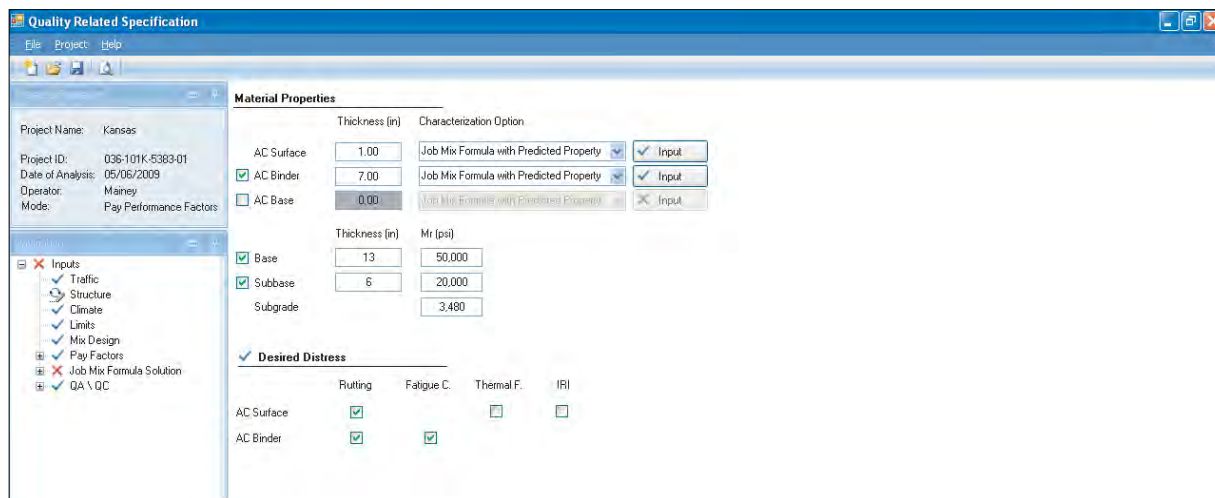




Figure 15: Screen shot - Completed Structure

For layer information to be deemed complete, the thickness of the layer needs to be entered in the corresponding “Thickness” field and the material properties need to be entered using the “Input” button. Clicking on the “Input” button of each layer seen in Figure 15 brings up the Material Properties dialog (Figure 17).

 **NOTE:** At least one of the Desired Distress checkboxes must be selected in order for the “Desired Distress” section shown below the “Material Properties” to turn to a checked status.

 **Example:**
 Check the **AC Binder**, **AC Base**, **Base** and **Subbase** checkboxes.
 Set the **Thicknesses** of the AC Surface and AC Binder to 1.00, and 7.00 respectively.

	<p>Set all Characterization Option drop-downs to Job Mix Formula.</p> <p>Set the Thickness of the Base and Subbase to 13 and 6 respectively.</p> <p>Set the Mr (psi) of the Base, Subbase, and Subgrade to 50000, 20000 and 3480 respectively.</p> <p>Check the Desired Distress checkboxes for AC Surface Rutting, AC Binder Rutting, and Fatigue Cracking.</p> <p>The Structure screen should resemble Figure 15.</p>
--	--

Material Properties

The “Characterization Option” available for each AC layer decides the method used to determine the Simple Performance Test (SPT) coefficients that describe the E^* master curve. Currently only the option of “Job Mix Formula with Predicted Property Models” is available in QRSS. The other two options, “Lab Measured SPT Property” and “Historically known SPT Property coefficient,” are not implemented in the current version of the QRS software. Selecting the “Lab Measured SPT Property” or “Historically known SPT Property coefficient” option brings up a Material properties dialog (Figure 16).

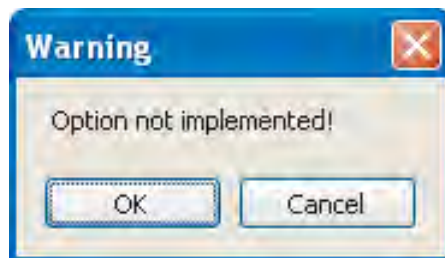


Figure 16: Screen shot – Historical and Lab Measured SPT Option

Job Mix Formula with Predicted Property Models

The Job Mix Formula **Material Properties** screen inputs are structured into four (4) sections: **Design Volumetrics**, **Binder Characteristics**, **Target In Situ Volumetrics**, and **Gradation**.

Design Volumetrics

A user input includes the mix design air voids in percent and asphalt content by weight in percent. Both these values are taken from the laboratory mixture design volumetrics.

Binder Characteristics

QRSS-required binder characteristics are the viscosity-temperature susceptibility (VTS) and A (intercept) after the Rolling Thin Film Oven (RTFO) test along with the binder specific

gravity (G_b). Since these values, for a given binder type, are pre-determined and loaded in the software database, it is only required to select the “Binder Type” from the drop down menu. If the binder type is not available in the drop-down menu, but the A and VTS values are known, they can be entered by selecting the option “Direct Input (A and VTS)”. Selecting this option will enable the A (RTFO) and V (RTFO) field to be modified.

The screenshot shows the 'Material Properties' dialog box with the following sections and values:

- Design Volumetrics:**
 - Air Voids (%): 4.0
 - Asphalt Content by Weight (%): 6.5
- Binder Characteristics:**
 - Binder Type: PG58-28
 - Direct Input (A and VTS): (Selected)
 - A (RTFO): 11.010
 - VTS (RTFO): -3.701
 - G_b : 1.030
- Target In-Situ Volumetrics:**
 - Air Voids - V_a (%): 6.0
 - G_{sb} : 2.500
 - G_{mm} : 2.360
 - Bulk Density - G_{mb} : 2.218
 - Asphalt Content by Weight (%): 6.5
 - Effective Binder Content by Volume - V_{beff} (%): 11.032
 - VMA (%): 17.0
 - VFA (%): 64.9

On the right side, there is a sieve analysis table:

Sieve	% Passing
* 1 1/2 "	
1 "	
* 3/4 "	100
1/2 "	
* 3/8 "	98
* #4	61
#8	
#10	
#16	
#30	
#40	
#50	
#100	
* #200	3.4

* Required Field

Figure 17: Screen shot - Job Mix Formula inputs


Target In Situ Volumetrics

The required as-built asphalt mixture properties are the target in-situ air voids in percent (V_a), Bulk Specific Gravity (G_{mb}), Bulk Aggregate Specific Gravity (G_{sb}), and Maximum Theoretical Specific Gravity (G_{mm}). The other volumetric properties including the “Asphalt Content by Weight (%)”, “Effective Binder Content by Volume – V_{beff} (%)”, “VMA,” and “VFA” that are listed under this section are computed by the software based on volumetric properties previously entered by the user and hence are not editable.

Gradation

QRSS provides the option to input the aggregate gradation information for all sieve sizes. However, for the computation of the dynamic modulus, four (4) of the gradation sizes (3/4", 3/8", #4, and #200) are mandatory and hence marked with an asterisk to indicate that each is a required field.

Click the “OK” button once you completed entering the information for a particular layer. The same procedure for inputting material properties as detailed above applies to all AC layers in the project.



Example:

- Click the **Inputs** button for the **AC Surface** layer.
- Set the inputs of the AC Surface layer to those displayed in Figure 15.
- Click the **OK** button.
- Repeat the process for the **AC Binder** layer.
- Full inputs for all layers are available in the APPENDICES example input (page 41).

Climate

Clicking **Climate** under **Inputs** on the left hand navigation menu displays the climate screen (Figure 18). The aim of the climate screen is to determine the climate summary statistics, namely, Mean Annual Air Temperature; Mean Monthly Air Temperature standard deviation; Mean Annual Wind Speed; Mean Annual Sunshine percentage; and the Annual Cumulative Rainfall Depth.

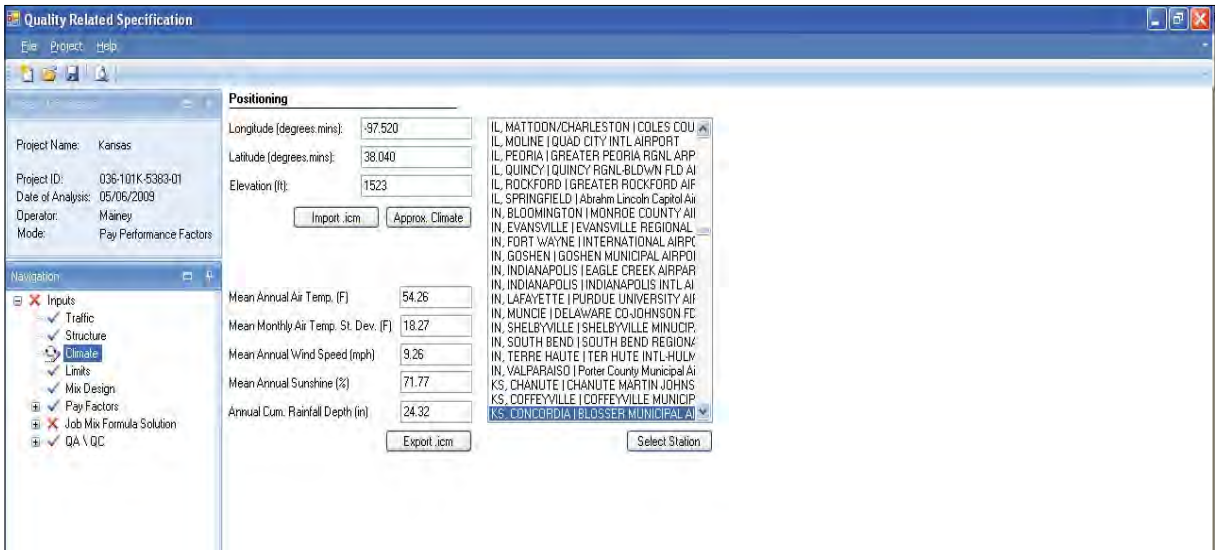



Figure 18: Screen shot - Climate

The required climate data can be entered in one or a combination of four ways:

1. Import the Integrated Climatic Model (ICM) file
2. Select a weather station
3. Enter Latitude, Longitude, and Elevation to permit interpolation among several nearest weather stations
4. Direct input.



Example:

- Ensure you have downloaded the latest hourly climatic data files from the NCHRP website at http://onlinepubs.trb.org/onlinepubs/archive/mepdg/climatic_state.htm.
- Click **Climate** from the **Inputs** tree.
- Set the **Longitude**, **Latitude** and **Elevation** to -97.39, 39.33, and 1472 respectively.
- Click the **Approx. Climate** button.

Import of Integrated Climatic Model file

An ICM file can be imported as the project's climatic data by clicking the **Import .icm** button. Clicking the Import .icm will display an Open File dialog, navigate to the directory containing the ICM file and select it. The data in the ICM file will then be used to populate the positioning data and climate summary statistics as required by the software.

Interpolate Climate

Clicking the "Approx. Climate" button will display the Climate Station Interpolation dialog (Figure 19) and display the five nearest climate stations to the position inputted in the latitude, longitude, and elevation fields.

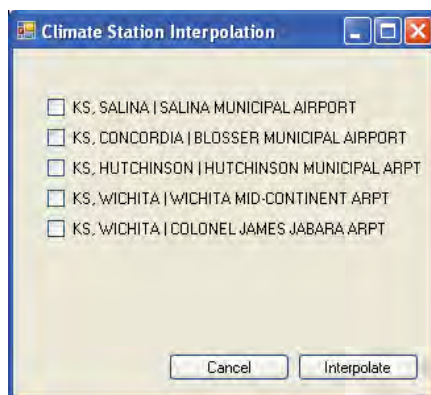


Figure 19: Screen shot - Climate Interpolation

Check the desired climate stations, which will then be used to create an interpolated set of climate summary statistics. The Hourly Climatic Data (HCD) file corresponding to the selected climate stations must exist in the HCD directory, which is the “hcd” subfolder within the installation directory (see installation procedure). If a HCD file does not exist, the error message in Figure 20 is displayed.

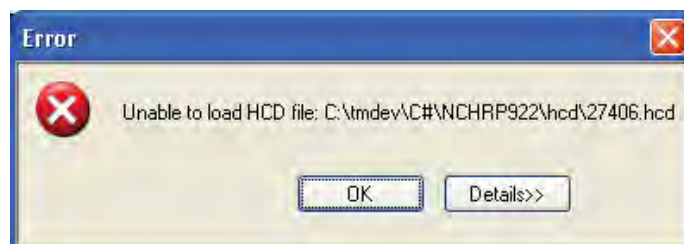


Figure 20: Screen shot - Unable to load HCD File


Select climate station


The weather station.dat files that exist in the HCD directory are used to populate the list of weather stations seen in Figure 18. On selecting the climate station from the list, the coordinates (latitude, longitude, and elevation) of the station are displayed in the appropriate fields. Clicking the **Select station** button will then use the associated HCD file to calculate the climate summary statistics. If no corresponding HCD file can be found in the HCD directory, the error message in Figure 20 is displayed.

Direct input

It is also possible to directly input the climate summary statistics, including the Mean Annual Air Temperature, Mean Monthly Air Temperature standard deviation, Mean Annual Wind Speed, Mean Annual Sunshine percentage, and the Annual Cumulative Rainfall Depth, if the project specific information is available.

The climate inputs tree will be deemed complete (change from cross mark to check mark) when all of the previously mentioned data are entered.

	<p>NOTE: Updated HCD files can be downloaded from the Transportation Research Boards web page on the Mechanistic Empirical Pavement Design Guide, or at http://www.trb.org/mepdq/climatic_state.htm</p>
---	--

	<p>Example:</p> <ul style="list-style-type: none"> • Check each of the nearby climate stations. • Click the Interpolate button.
---	---

Limits

This tab inputs the limits established for the rutting, fatigue cracking, and thermal cracking distresses in the design. The values entered in the Limits screen (Figure 21) will be used in the Mix Design mode to determine if the mix is acceptable. Selection of distress type in the **Structure** screen enables or disables the option to edit the related distress limit values. Hence, only the distress limits values corresponding to the distress type selected in the **Structure** screen are editable.

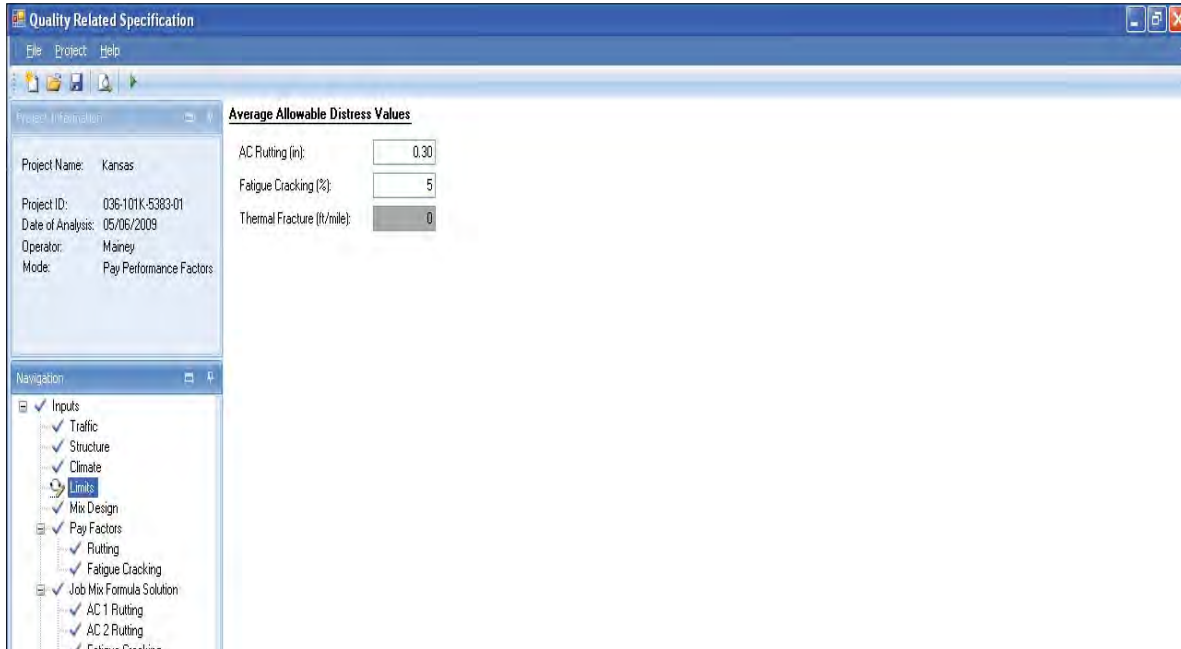


Figure 21: Screen shot – Limits



Example:

- Click on the **Limits** node from the **Inputs** tree.
- Set the **Rutting** to 0.3 inches, and **Fatigue Cracking** to 5%.

Mix Design

Clicking on **Mix Design** in the left hand navigation menu will cause the warning dialog box in Figure 22 to be displayed, advising the user that the analysis may take several minutes. Click **OK** and the Mix Design analysis will run.

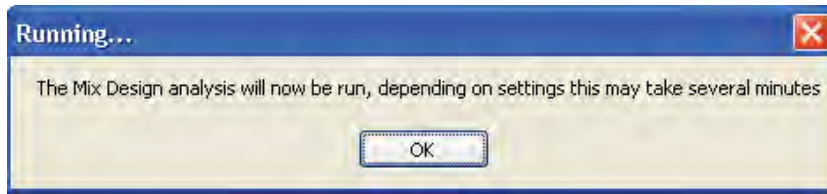


Figure 22: Screen shot - Mix Design run-time warning


The Mix Design analysis is a deterministic analysis of the as-designed mix using the previously entered data for traffic, structure, material properties, and climate to determine if the mix is acceptable (Figure 23).

	Surface Rutting	Binder Rutting	Fatigue Cracking
Project Name: Kansas			
Project ID: 036-101K-5383-01			
Date of Analysis: 05/06/2009			
Operator: Mainey			
Mode: Pay Performance Factors			
Layer Thickness (in)	1.00	7.00	8.00
Effective Frequency (Hz)	92.63	71.69	45.61
Effective Temperature (°F)	110.02	102.68	70.94
SPT Recom. Frequency (Hz)	<input type="text" value="25"/>	<input type="text" value="25"/>	<input type="text" value="25"/>
SPT Recom. Temp. (°F)	99.71	90.72	67.46
Allowable Distress*	0.03	0.27	5
Allowable Layer E* (ksi)	198.6	128.1	50.0
Predicted Distress*	0.01	0.12	0.14
Predicted Layer E* (ksi)	208.9	289.5	792.3
Acceptable Distress*	Yes	Yes	Yes
Acceptable E*?	Yes	Yes	Yes

*Rutting (in), Fatigue Cracking (%), and Thermal Cracking (ft/mile)

Figure 23: Screen shot - Mix Design analysis

If a predicted distress is greater than the level of distress entered in **Limits** tab by the user, the display screen shows “No” for Acceptable Distress; if it is lower, the display screen shows “Yes.” Similarly, when the predicted E* modulus is greater than the allowable E*, the screen displays “Yes” for Acceptable E*; it displays “No” when the predicted E* is lower than allowable E*.



Example:

- Click the **Mix Design** node from the **Inputs** tree.
- Click the **OK** button when the **Running...** dialog box (Figure 22) appears.

Pay Factors

Pay factors are inputs required for the “Pay Performance” mode that determine the incentive or disincentive for the contractor in the construction of AC layers. These “Pay Factors” are user-defined limits of distress varying from the target design value and the respective percents of incentive and disincentive for the contractor. It is also possible to set the range of values such that the contractor is paid neither an incentive nor a disincentive. These limits will vary for each state agency and the QRSS permits setting these limits as required.

Pay factor for each distress

Each distress has its own set of Pay Factor values and all Pay Factors (excluding IRI) are set based on the deviation of the service life of the as-built mix from the predicted service life of the as-designed mix. The Pay Factors are designed in such a way that a predicted increase in the service life of the as-built mix over the as-designed mix will award the contractor an incentive payment. Conversely, a predicted decrease in the service life of the as-built mix from that of the as-designed mix will incur a disincentive to the contractor or a requirement to remove and replace, depending on the pay factor criteria.

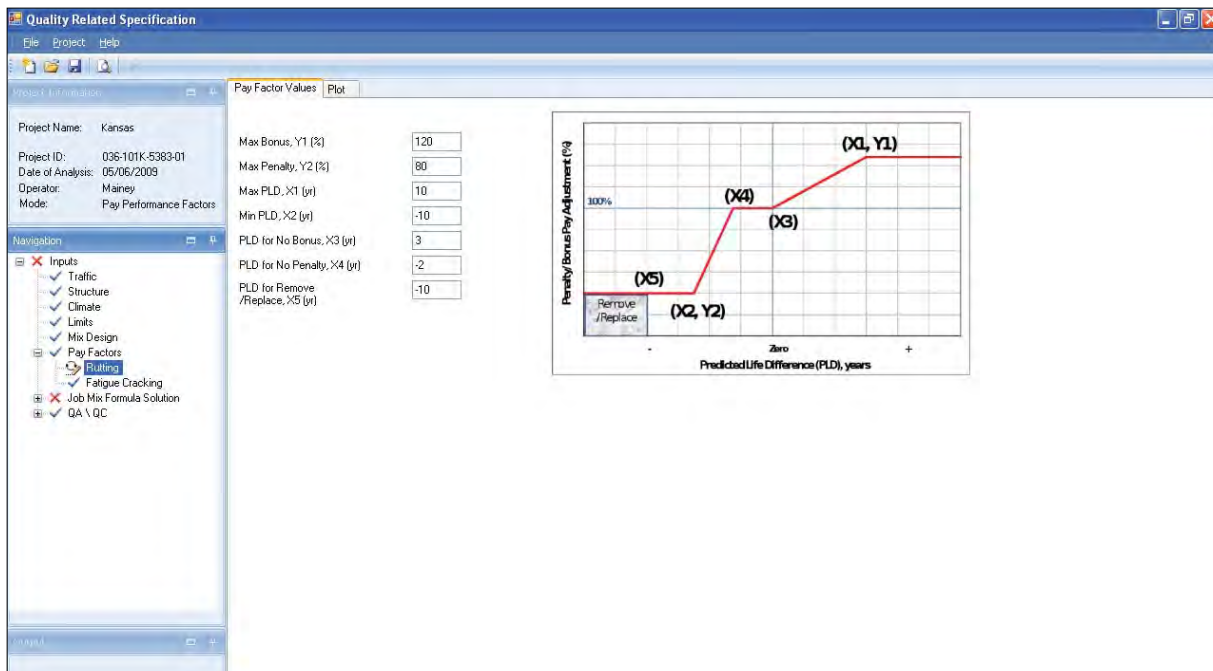
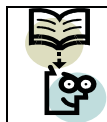


Figure 24: Screen shot - Pay factors

**Example:**

- Click the **Pay Factors > Rutting** node from the **Inputs** tree.
- The pay factor values for rutting are 120, 80, 10, -10, 3, -2, and -10 for the Y1, Y2, X1, X2, X3, X3, and X5 points respectively.
- Fatigue cracking also requires pay factor values to be entered, use the same values as rutting.

The final amount of the incentive or disincentive is computed by the five (5) points on the Pay Factor plot, called Pay Factor values. These five (5) points are defined as “Maximum positive service life difference for maximum bonus” (X1,Y1), “Maximum penalty for a negative service life difference” (X2,Y2), “Maximum positive service life difference for no bonus” (X3), “Maximum negative service life difference for no penalty” (X4), and “Negative service life difference for replacement” (X5). The Pay Factor values are entered in the Pay Factor screen (Figure 24). The Pay Factor values can be viewed graphically by clicking on the “Plot” tab of the “Pay Factor” screen (Figure 25).

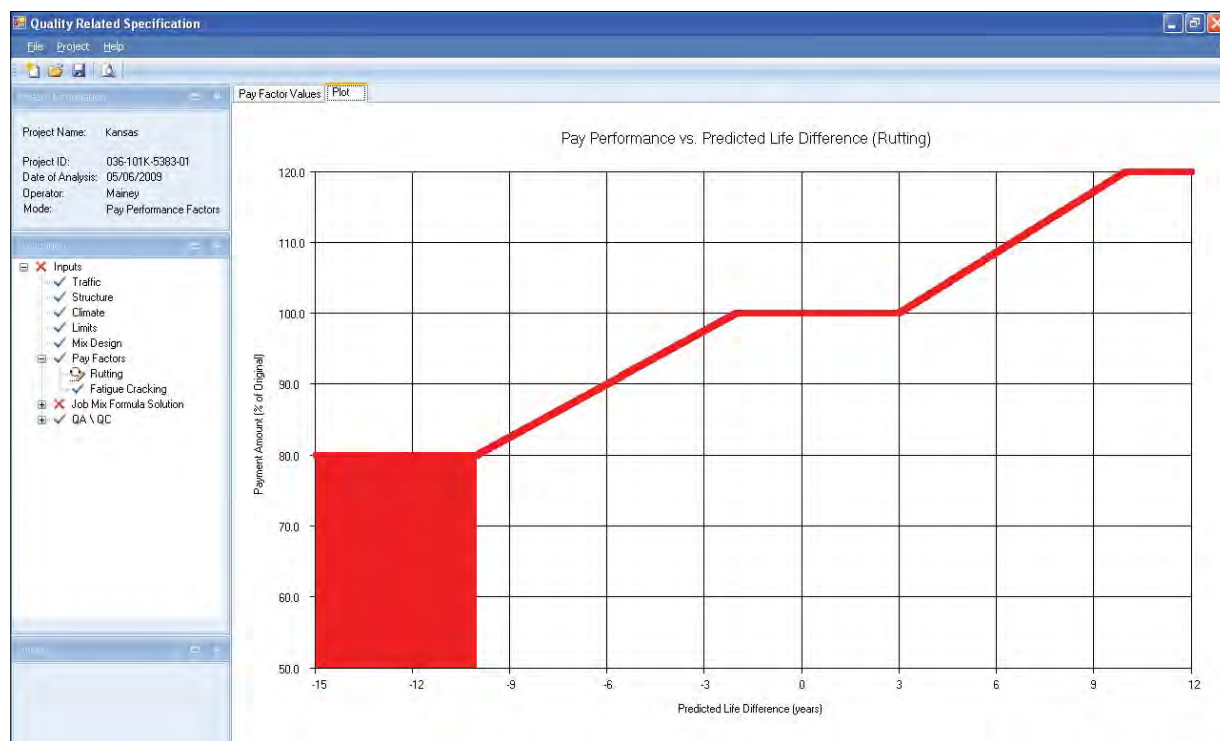


Figure 25: Screen shot - Pay factor plot

IRI Pay Factor

As noted previously, the QRSS does not predict the IRI distress data, but the initial IRI data measured at the time of construction inputted by the user are used in the final payment calculation. Including IRI in the pay factor calculation is a user option. The IRI Pay Factor uses a dollar (\$) amount to adjust the incentive or disincentive for the IRI. Three default payment options, for local roads, arterial roads, or highways, are provided based on the values used by the Texas Department of Transportation, from which the IRI payment system has been adopted (Figure 26).

The IRI Pay factor also uses a five point system to determine the pay factor scale:

- (X1, Y1) Minimum IRI for maximum bonus
- (X3, \$0) Minimum IRI for \$0 bonus
- (X4, \$0) Maximum IRI for \$0 penalty
- (X2, Y2) Minimum IRI for maximum penalty
- (X5, Y2) Minimum IRI for corrective action

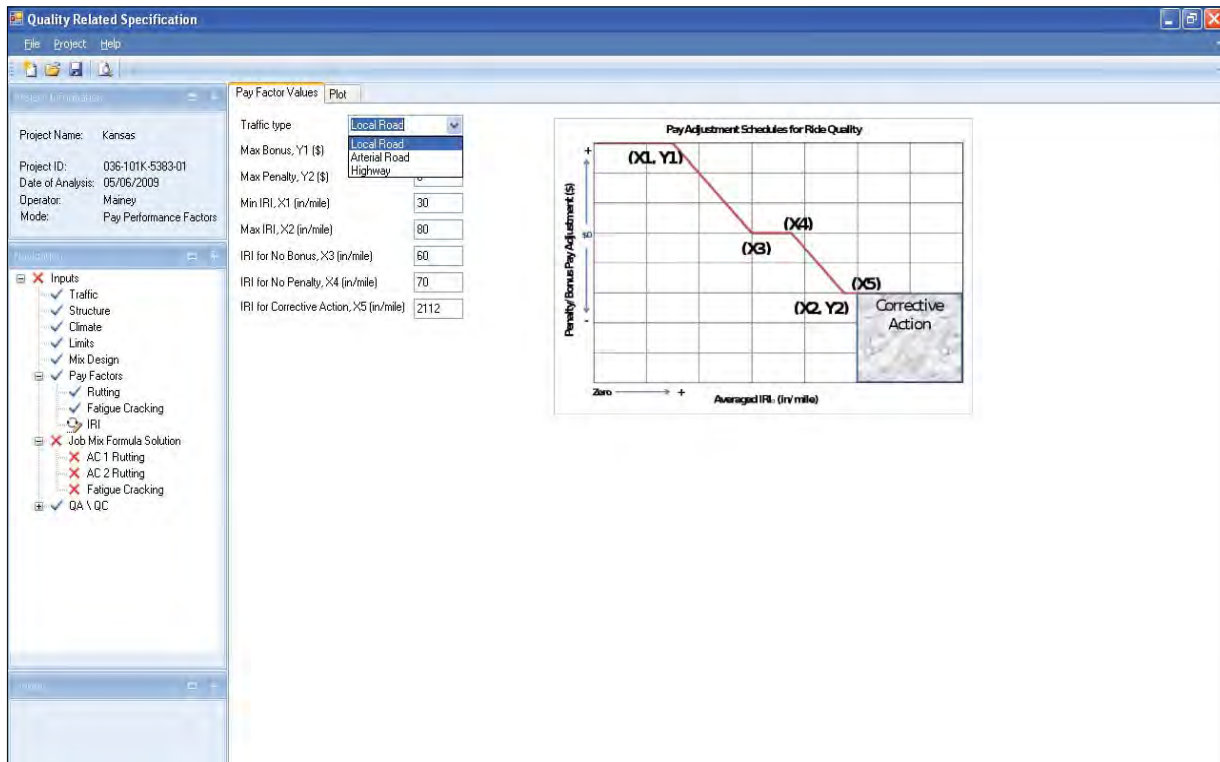


Figure 26: Screen shot - IRI Pay Factor

Job Mix Formula Solution

The Job Mix Formula solution menu item becomes enabled after the Mix Design process has been run (see Mix Design). For each distress selected in the “Structure” screen (see Structure) a new menu item is displayed in the left hand navigation tree under the “Job Mix Formula Solution” (Figure 27). Each of these items have three tabs, the first tab the summary of the inputs used, the second tab for the detail results of the simulation run, and the third tab for the plots of the simulation run results.

Summary

The Job Mix Formula solution summary screen displays the mean values entered in the Job Mix page of the Material Properties dialog (See Material Properties) Default historical values of standard deviation for the material properties are displayed in the “Summary” screen (Figure 27); these values are editable.

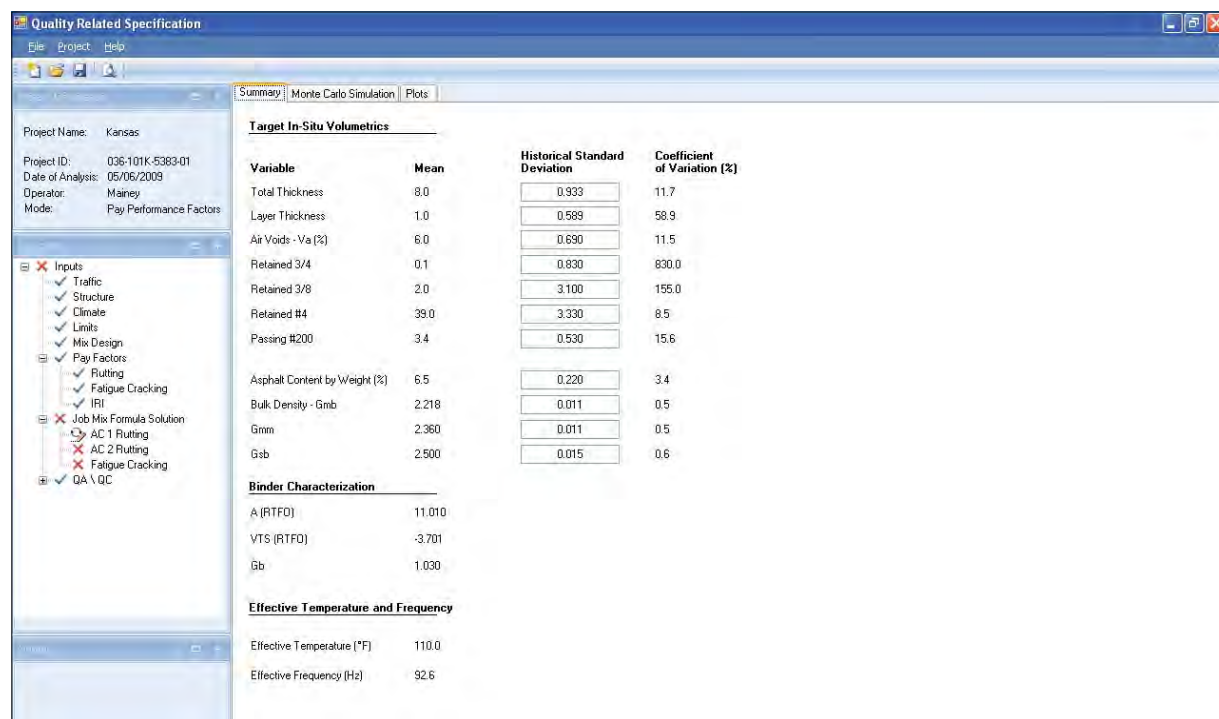
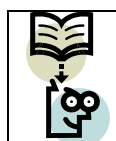


Figure 27: Screen shot - JMF summary



Example:

- Select **Job Mix Formula Solution > AC 1 Rutting** from the **Inputs** tree.

Monte Carlo and Rosenbleuth simulation

After all the inputs have been entered and confirmed on the Summary tab, click the simulation tab to display the simulation screen (Figure 28).

Clicking the **Run** button runs the Job Mix Formula simulation. Rutting and fatigue cracking distresses use a Monte Carlo simulation, while thermal cracking uses a Rosenblueth simulation. For the Monte Carlo simulations, the number of simulations to be run is set to 1000 by default, but can be edited by the user to enter values anywhere from 2 to 1000. Rosenblueth simulation runs are set to 16 by the program, which is not editable. Please refer to Chapter 3.3 of the final report for more details on the simulation types and number of runs used.

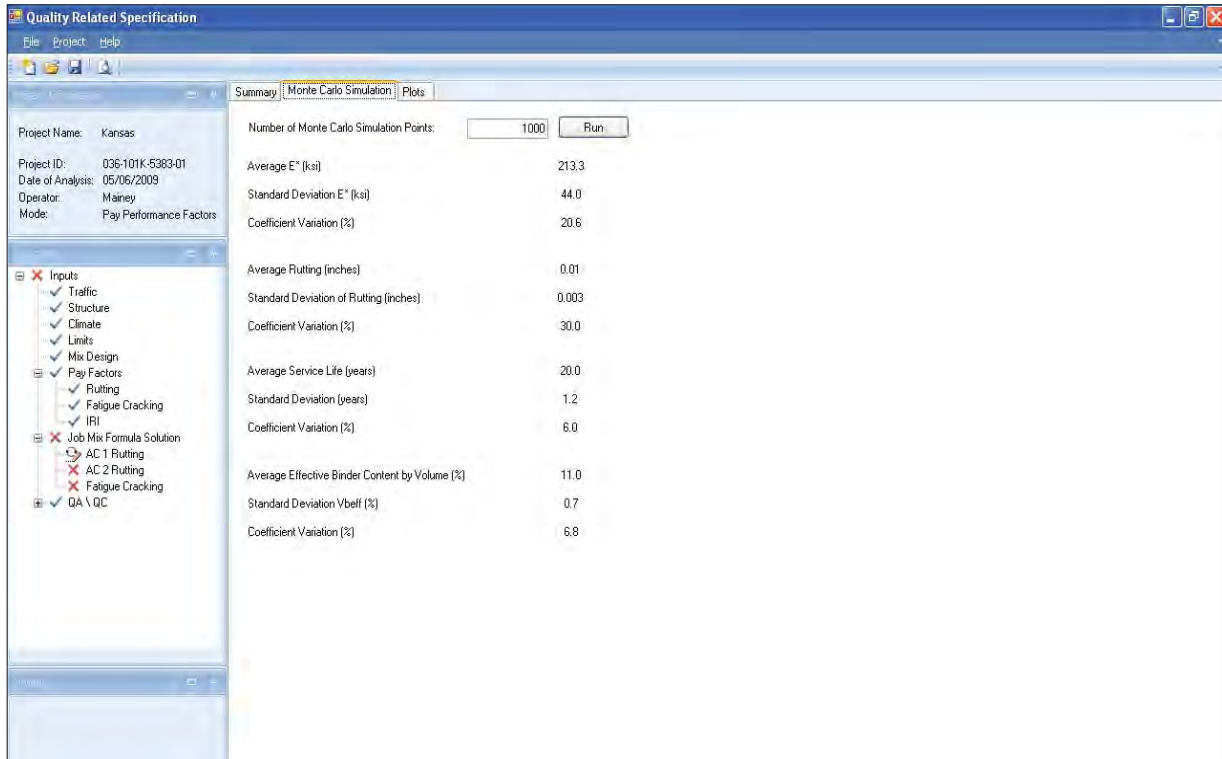


Figure 28: Screen shot - JMF Simulation



Example:

- Click the **Monte Carlo Simulation** tab.
- Click the **Run** button.
- The Monte Carlo simulation needs to be run for each of the measured distresses.

Job Mix Formula plots

After running the Job Mix Formula simulation, a range of plots generated by the program are displayed on the Plots tab (Figure 29). Simulation runs of the rutting and fatigue cracking modules display (in plots tab) the average, standard deviation, and coefficient of variation of the predicted distress, the dynamic modulus, and the service life. Thermal cracking only displays plots of the beta and cumulative beta distributions of the predicted distress and service life.



Figure 29: Screen shot - JMF Plots

QA Data

For each of the AC layers defined for the project, the QA data for the as-built mix must be entered. Listed below are five sets of data required for each AC layer:

1. General information
2. Gradation data
3. Volumetrics data
4. Binder information
5. Dynamic Modulus (E^*) data

The QA\QC screens are for entering the data collected for the as-built mix. Once these data have been entered, each lot is compared to the as-designed mix (see Job Mix Solution) to

determine the appropriate pay factor for the lot and eventually for the entire project (see Output).

General information

The General Information screen (Figure 30) allows for the entering of the basic lot information, such as: the number of lots; the tonnage of each lot, and the date the lot was placed.

Select Mix Design

Select the mix design procedure for the mix for which the QA data is recorded. The two general design options of Gyratory Design and Marshall Design options are available. If a different method is used, selecting the Other option enables the user to specify the mix design procedure used.

Select Lot Definition

The number of project lots are selected from the drop-down list Lots (Figure 30); if the Lot Definition is specified as Constant Tonnage, then the tonnage for all the newly created lots will be the value indicated in the constant tonnage field (2000 in Figure 30). The Daily Production Table is completely editable and data can be entered or copied into it from other sources.



Example:

- Click the **QA/QC > AC 1 > General Information** node from the **Inputs** tree.
- Set the number of **Lots** to three (3).
- Fill in the **Daily Production Table** to resemble Figure 30.

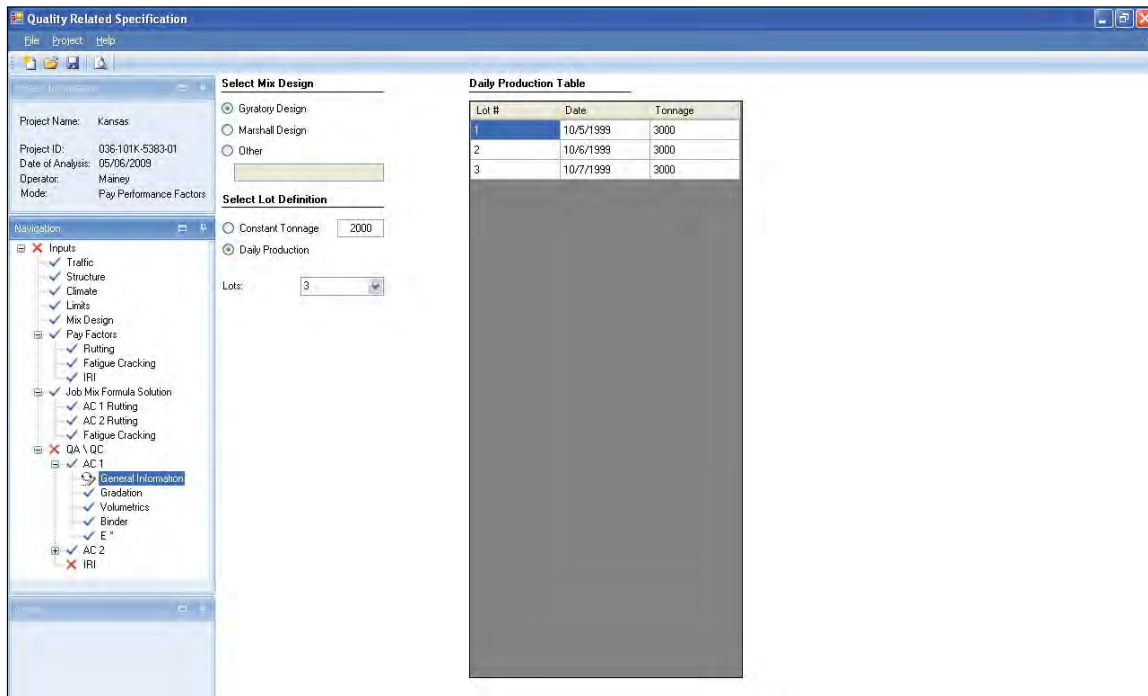


Figure 30: Screen shot - General Information

Gradation

On entering the Gradation screen, the number of lots, defined in the General Information screen (Figure 31), are displayed as rows. The number of samples are configurable for each gradation sieve; initially the sample number defaults to four (4), but can range anywhere from zero (0) to ten (10). The screen (Figure 31) also displays the Historical Standard Deviation and Target Value from the Job Mix Formula (Figure 27), while Reliability and the Significance Intervals (-R and +R) are calculated.

Once gradation data has been entered in the “Samples” tab, the “Summary” tab (Figure 32) and “ANOVA” tab (Figure 33) displays the calculated statistics of the input data. As mentioned in the JMF material properties screen, four of the gradation sizes (3/4”, 3/8” #4 and #200) are required for the computation of the dynamic modulus and hence required for the input data to be deemed complete. The control charts (Figure 34) show the variation between lots.



Example:

- Fill in the **Daily Production Table** to resemble Figure 30.
- Click the **QA/QC > AC 1 > Gradation** node from the **Inputs** tree.
- Click the **3/4”** tab.
- Set the **Number of Samples** to four (4) and enter the gradation data.
- Repeat for the 3/8”, #4 and #200 sieves.
- Sample data is available in the APPENDICES under QA/QC Inputs.

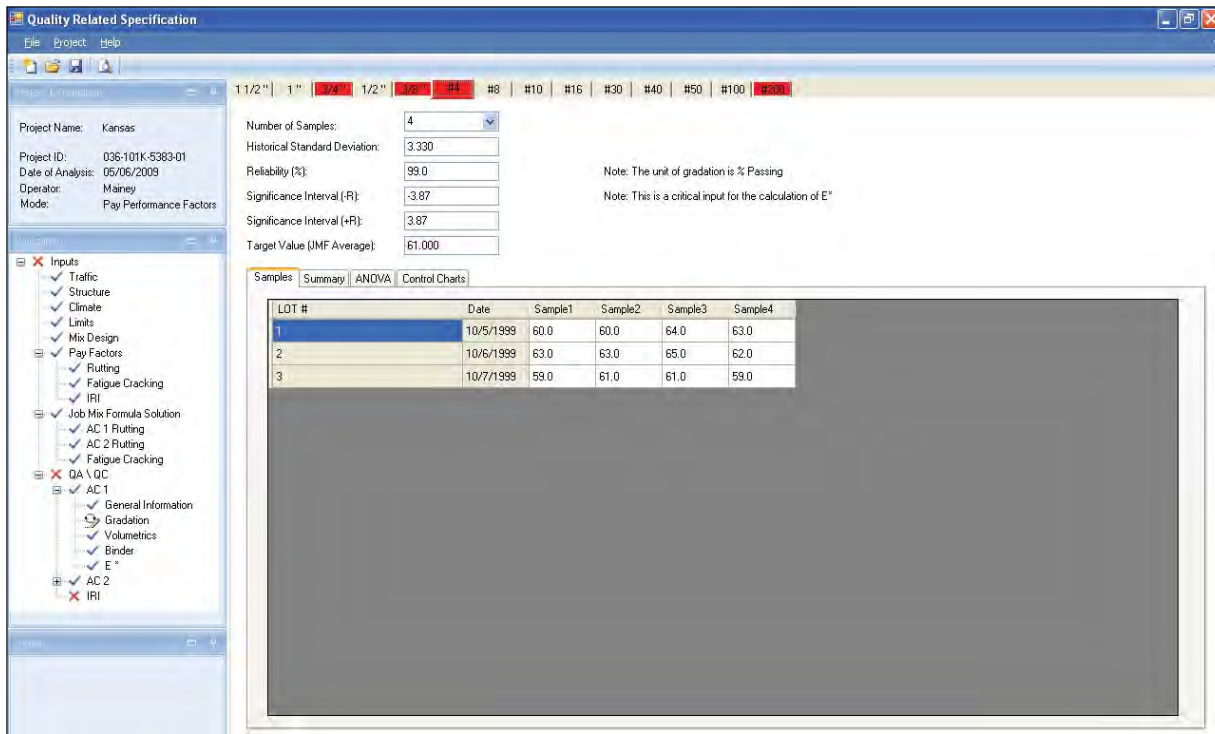


Figure 31: Screen shot – Gradation

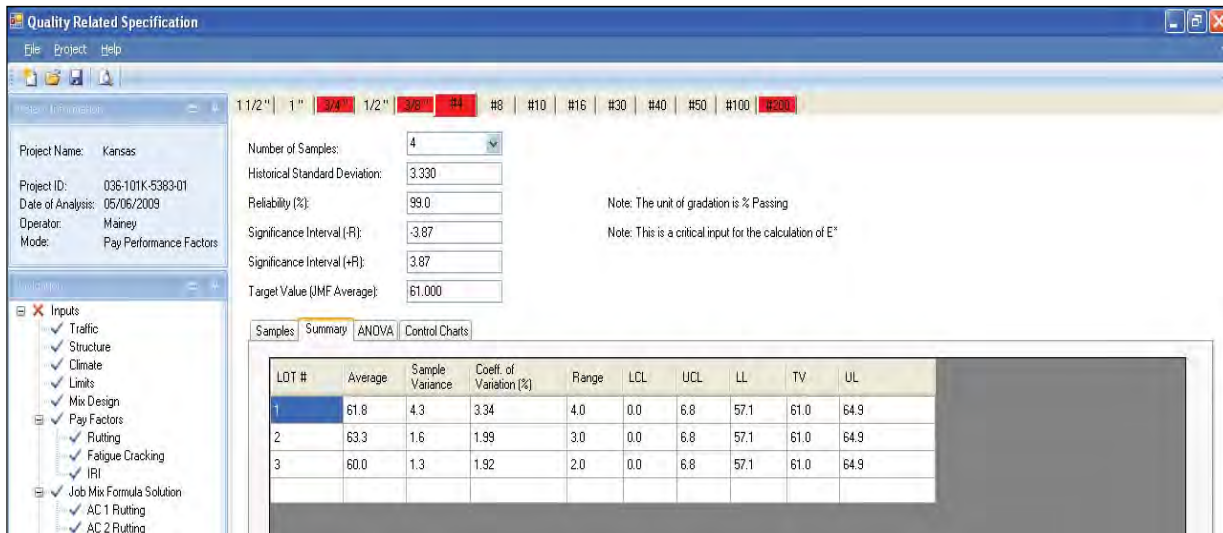


Figure 32: Screen shot - Sample data Summary

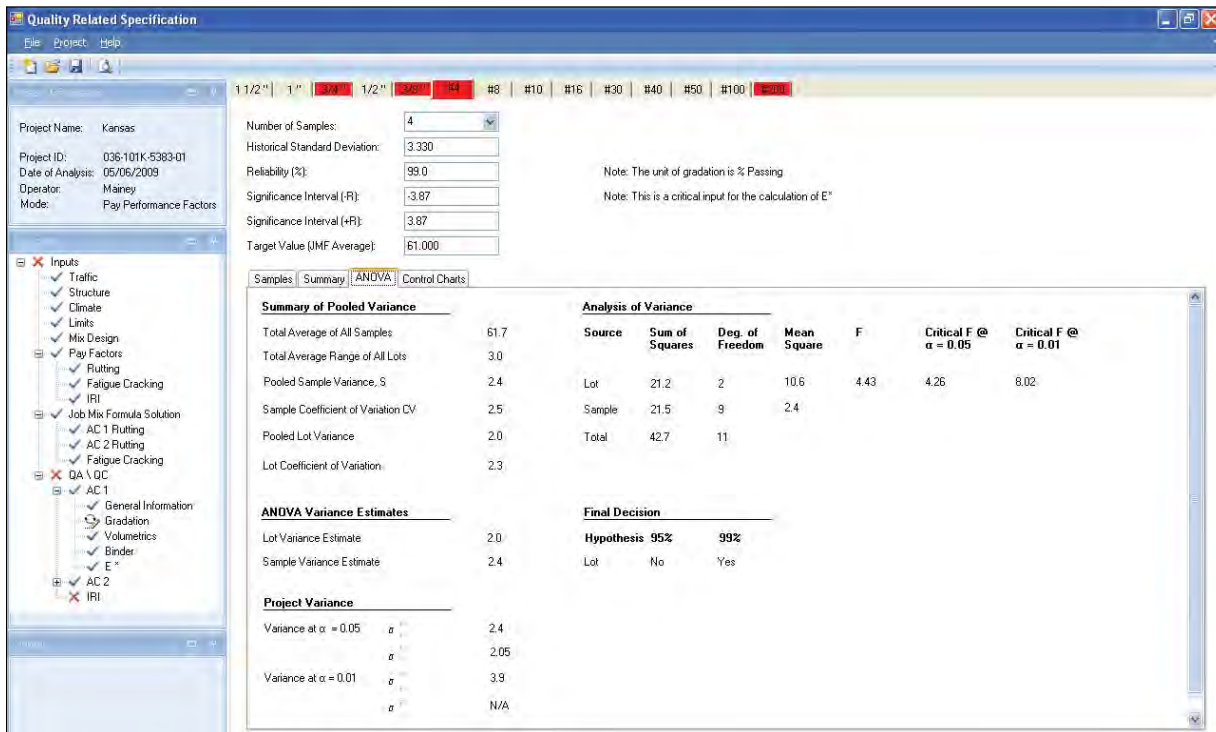


Figure 33: Screen shot - Sample data ANOVA

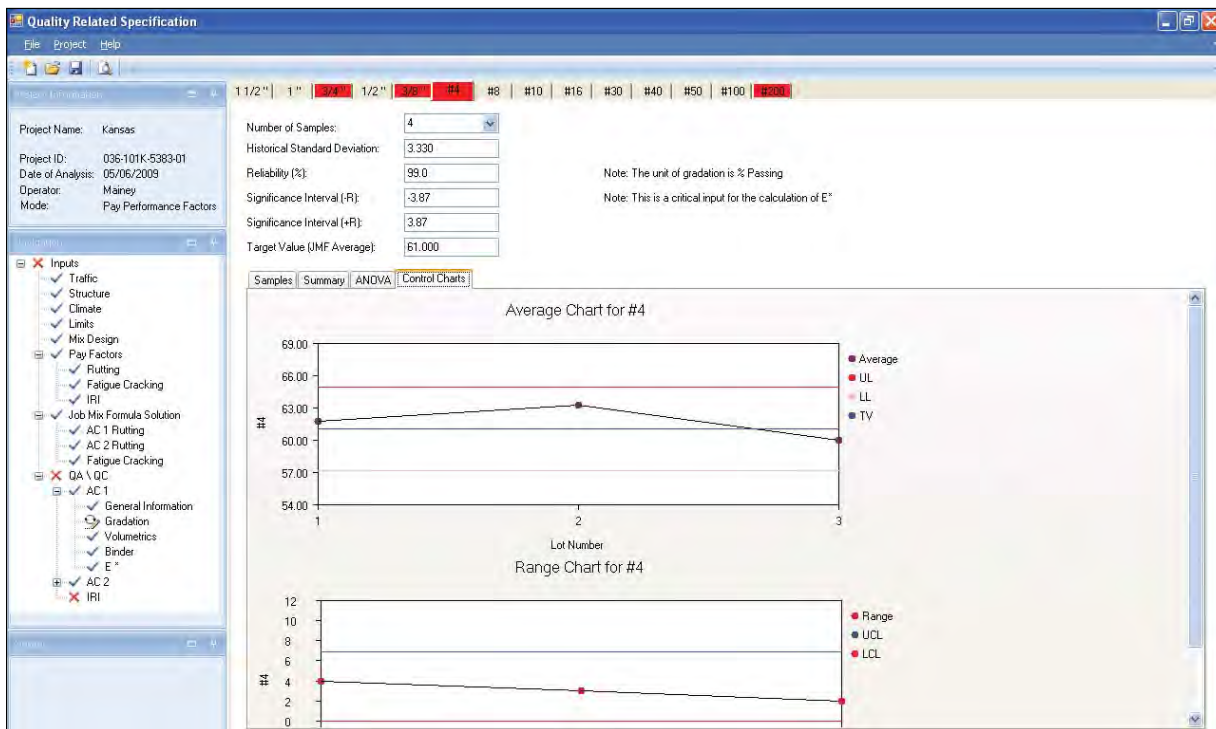


Figure 34: Screen shot - Sample data Control Charts



NOTE: The data to be entered in the QA\QC screen is the sample data taken from the as-built mix.

Volumetric

The “Volumetric” screen (Figure 35) is used to enter for the as-built volumetric sample data including the asphalt content, maximum theoretical specific gravity, HMA bulk density (in pcf), in situ air voids, thickness, and aggregate specific gravity. The corresponding six tabs function the same as the “Gradation” screen (Figure 31), but they require the input of the above-mentioned parameters for the respective lots.

The screenshot shows the 'Quality Related Specification' software window. The 'Volumetric' tab is selected in the navigation tree. The data entry form includes the following fields:

- Project Name: Kansas
- Project ID: 036-101K-5383-01
- Date of Analysis: 05/06/2009
- Operator: Mainey
- Mode: Pay Performance Factors
- Number of Samples: 4
- Historical Standard Deviation: 0.220
- Reliability (%): 99.0
- Significance Interval (-R): -0.26
- Significance Interval (+R): 0.26
- Target Value (JMF Average): 6.500

The 'Samples' table displays the following data:

LOT #	Date	Sample1	Sample2	Sample3	Sample4
1	10/5/1999	6.3	6.2	6.4	6.4
2	10/6/1999	6.4	6.6	6.7	6.6
3	10/7/1999	6.5	6.5	6.4	6.3

Figure 35: Screen shot – Volumetric



NOTE: Like the input of Gradation data, for each Volumetric Characteristic, the user can specify the number of samples.

Bulk density of HMA (in pcf) is required to input here unlike the bulk specific gravity required in the JMF material properties Figure 17).

**Example:**

- Click the **QA\QC > AC 1 > Volumetrics** node from the **Inputs** tree.
- Set the **Number of Samples** for the **Asphalt Content** to four (4).
- Fill in the **Production Table** to resemble Figure 35.
- Sample data is available in the APPENDICES QA/QC Inputs.
- Repeat data entry for other layers from the APPENDICES under QA/QC Inputs.

Binder

In this screen (Figure 36), the type of binder used for the currently selected AC layer needs to be specified. The binder type is selected from the drop-down list of performance grades (PG). Once the performance grade is selected, the A and VTS properties of the binder are displayed on the screen.

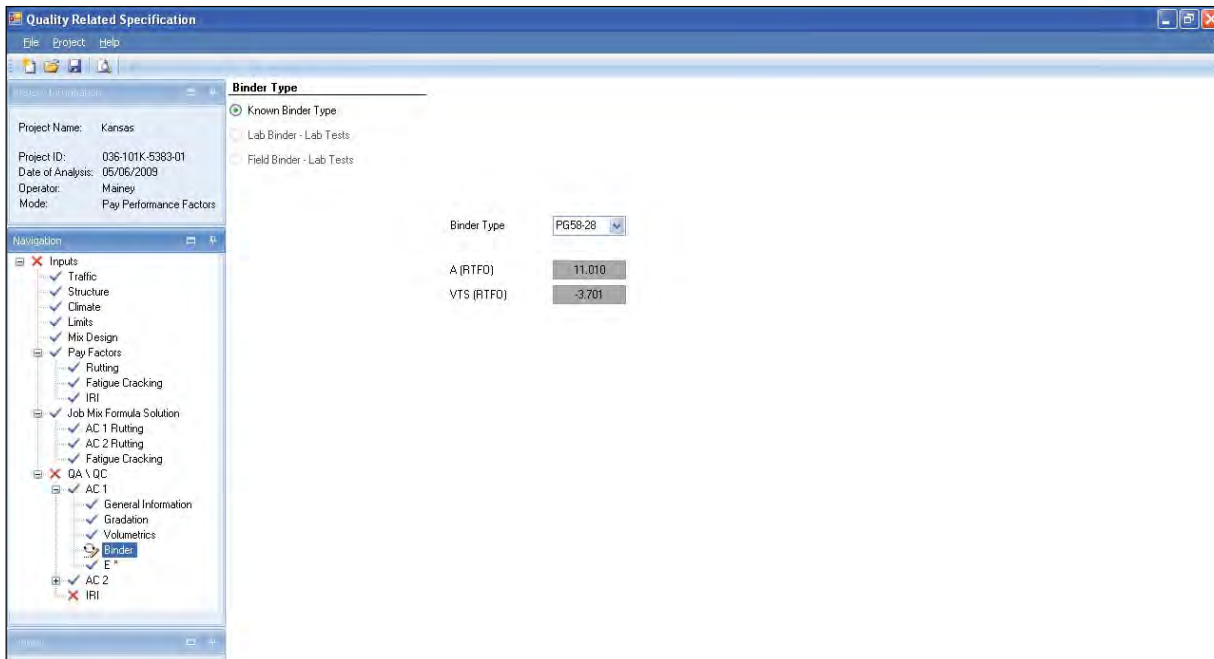


Figure 36: Screen shot – Binder

**Example:**

- Click the **QA\QC > AC 1 > Binder** node from the **Inputs** tree.
- Set the **Binder Type** from the drop down list to **PG58-28** to resemble Figure 36.



NOTE: The options to use the field binder and lab binder test inputs are not functional for this version of the software.

Dynamic Modulus (E^*)

The Dynamic Modulus or E^* screen (Figure 37) displays only those Gradations and Volumetrics that are specifically required for the calculation of E^* , which are

- In Situ Air Voids,
- Effective Binder Content (V_{beff}),
- 3/4" gradation sieve,
- 3/8" gradation sieve,
- #4 gradation sieve, and
- #200 gradation sieve.

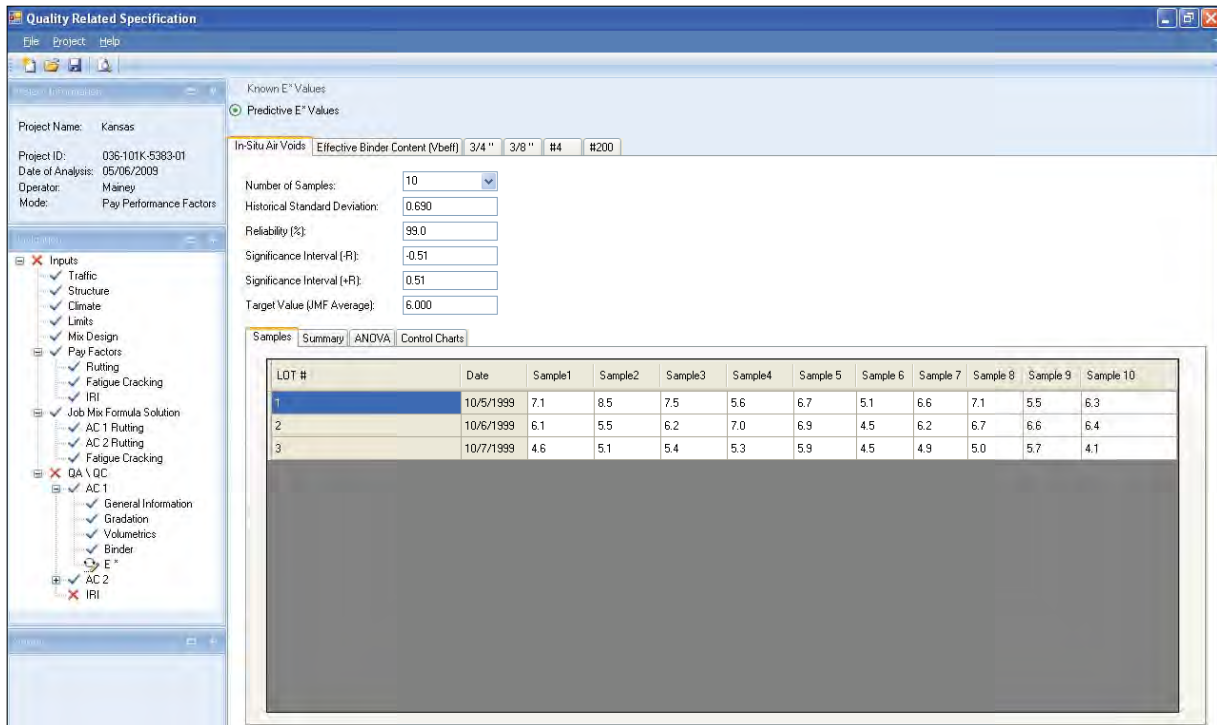


Figure 37: Screen shot - Dynamic Modulus (E^*)



NOTE: Values of air voids and gradation are displayed as entered in the "Gradation" and "Volumetrics" input tab and are editable. However, the "Effective Binder Content (V_{beff}) is computed from In Situ Air Voids (V_a), Asphalt Content (P_b), Bulk Density (G_{mb}), and G_{sb} entered in the "volumetrics" input tab and are not editable.



CAUTION: V_{beff} values do **NOT** reverse calculate for In Situ Air Voids, Asphalt Content, Bulk Density or G_{sb} .

IRI Including Input Parameters

The IRI (Figure 38) requires the input of the initial IRI (in/mile) at the time of construction for each lane. IRI in the pay factor calculation is a user option. The number of lanes can be specified by the Number of Lanes drop-down above the input table. All the data fields are editable including the unit mileage. Entering in any data for a single Mile Post will automatically generate a number for that mile post and create a new row for the input of the next mile post.

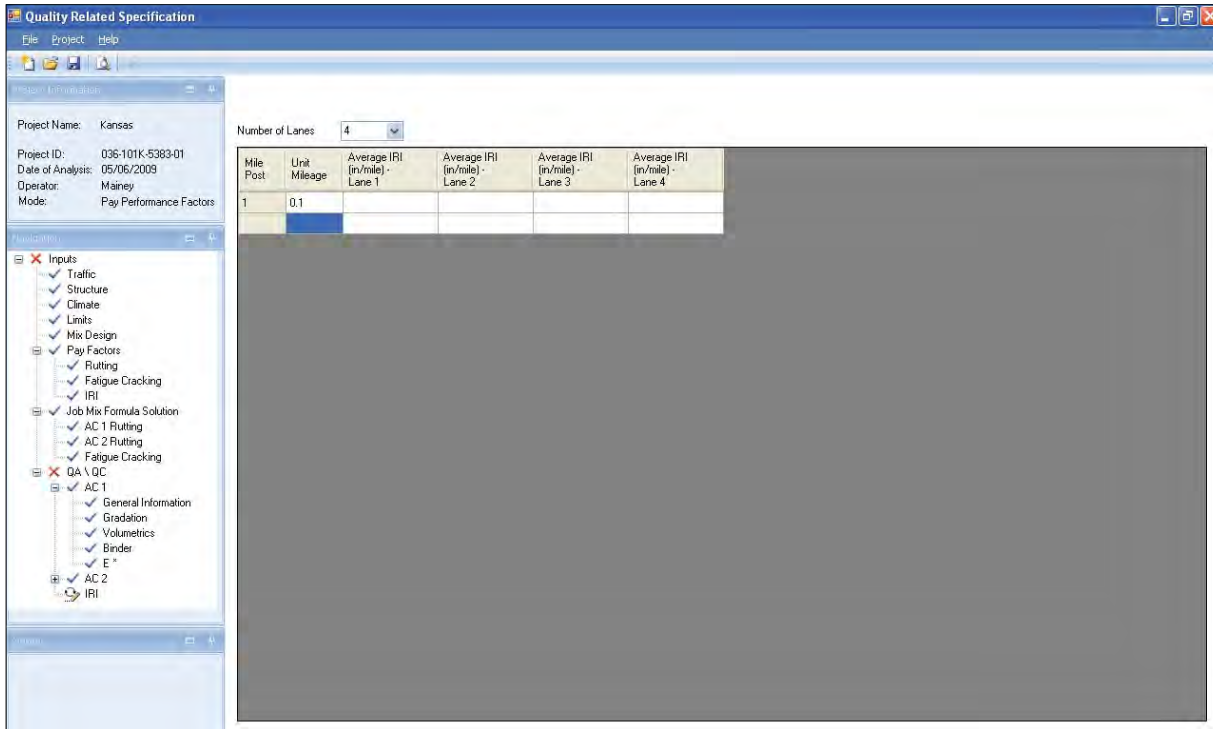


Figure 38: Screen shot - IRI input parameters

Output

After each set of data or screen is completed, the cross (✗) in the left hand navigation tree becomes a check (✓). That is, once all the sub nodes of a parent node become checked, the parent node is checked. Once all the required inputs are completed, the Inputs Complete dialog (Figure 39) is displayed.

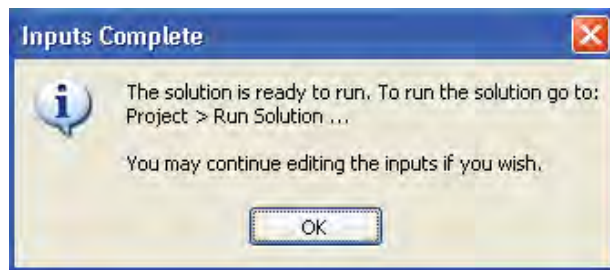


Figure 39: Screen shot - Inputs Complete

	<p>Example:</p> <ul style="list-style-type: none"> • After filling in all the inputs the dialog box of Figure 39 will appear. • Click the OK button.
--	--

Once all the inputs are completed, the project is ready to run. In the menu bar, go to the Project tab drop-down list and select “Run Solution” (Figure 40).



Figure 40: Screen shot - Project > Run Solution

	<p>Example:</p> <ul style="list-style-type: none"> • Navigate to Project > Run Solution ...
--	---

After the project has been run, the Outputs section of the left hand navigation menu is displayed (Figure 41) with a sub node for each distress analyzed as part of the project.

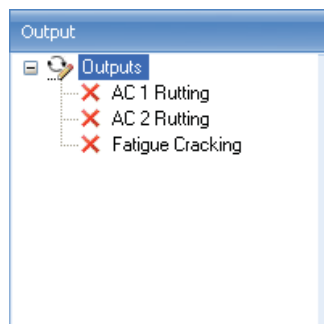


Figure 41: Screen shot - Outputs navigation

Output Parameters

The Output screen (Figure 42) is configured to calculate the contractor's final payment for the project. As mentioned in Chapter 1, the final incentives and disincentives are calculated using the Predicted Life Difference between the as-designed mix and each lot of the as-built mix and the Pay Factors for each distress. This screen (Figure 42) has seven (7) different sections as listed below.

- Distress Summary
- Rut weighting factor ratio by layer
- Weighting Factor (%) by distress
- Construction Cost
- Distress Pay Adjustment
- IRI Pay Adjustment
- Total Pay Adjustment

Distress Summary

This section lists the distresses evaluated with the computed Predicted Life Difference (PLD) and the corresponding incentive or disincentive percentage based on the pay factor values entered by the user.

Rut weighting factor ratio by layer

This section allows the user to edit the rut weighting factor ratio for the surface and binder AC layers displayed by the program with more accurate data, if available. Weighting factors for the surface, binder, and base are termed Pr_s, Pr_m, and Pr_b, respectively.

Weighting Factor (%) by distress

Since not all the evaluated distresses are weighted equally in all regions of varying climates, this option is available to enter a user-defined weighting factor for each distress is available.

Construction Cost

This section allows the user to input the total cost estimated for the construction of each of the AC layers. These are termed as Cac_s, Cac_m, and Cac_b for the surface, binder, and base layers respectively.

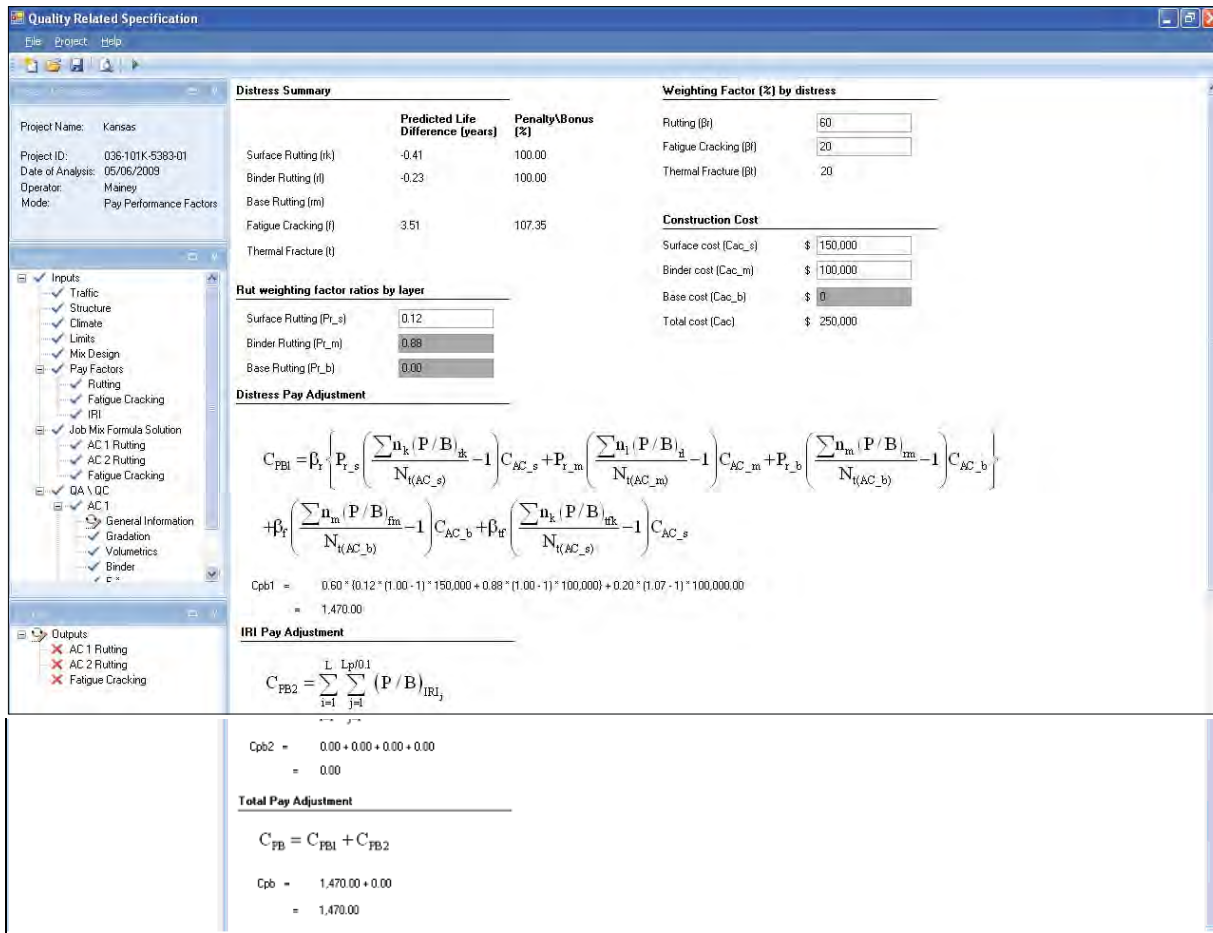


Figure 42: Screen shot - Output summary

Distress Pay Adjustment

This section displays the final pay adjustment equation considering the distresses of rutting in each layer, fatigue cracking, and thermal cracking. This pay adjustment calculation requires the input of the Rut weighting factor ratios (%) by layer, the Weighting Factor (%) by distress, and the Construction Cost of each layer. These data are displayed along with the computed distress summary data and are used in calculating the final pay adjustment for the contractor, termed Cpb1. The first part of the equation (Figure 43) is the weighting of each of the calculated distresses. The penalty/bonus (P/B) factor of each distress is weighted against the weighting factor for the distress and the construction cost for the layer associated with the distress.

$$C_{FB1} = \beta_r \left\{ P_{r_s} \left(\frac{\sum n_k (P/B)_{tk} - 1}{N_{i(AC_s)}} \right) C_{AC_s} + P_{r_m} \left(\frac{\sum n_l (P/B)_{tl} - 1}{N_{i(AC_m)}} \right) C_{AC_m} + P_{r_b} \left(\frac{\sum n_m (P/B)_{tm} - 1}{N_{i(AC_b)}} \right) C_{AC_b} \right\} + \beta_f \left(\frac{\sum n_n (P/B)_{fn} - 1}{N_{i(AC_b)}} \right) C_{AC_b} + \beta_{tf} \left(\frac{\sum n_k (P/B)_{tk} - 1}{N_{i(AC_s)}} \right) C_{AC_s}$$

Figure 43: Equation - Pay Factor (Cpb1)



NOTE: The overall rutting adjustment is further weighted by individual layer contributions as specified in the **Rut Weighting Factor (%) by layer inputs**.

IRI Pay Adjustment

When the IRI data is also considered in the final pay adjustment, from the initial IRI input and the pay factors provided before, the equation shown in this section calculates the pay adjustment for the same, termed as Cpb2.

Total Pay Adjustment

The total pay adjustment is the sum of the pay adjustment computed in the “Distress Pay Adjustment” section (Cpb1) for the rutting, fatigue cracking, and thermal cracking and the “IRI Pay Adjustment” section (Cpb2) for the initial IRI measured. This final pay adjustment is termed Cpb.



Example:

Rut Weighting factor ratios

Surface Rutting (Pr_s) = 0.12

Weighting Factor (%) by Distress

Rutting (β_r) = 60

Fatigue Cracking (β_f) = 20

Construction cost

Surface Cost (Cac_s) = 150,000

Binder Cost (Cac_m) = 100,000

After these values are entered, the pay adjustment values will be computed for the entered parameters.

Detailed and summarized results each distress

The net result of the analysis is the determination of the Pay Factor for each distress. The Pay Factor is the part detailed in Figure 44 from the complete equation in Figure 43. Individual distress contributions (Figure 44) are calculated as the sum of the predicted life of all lots as a percentage of the total tonnage. The Summary screen (Figure 45) for a distress displays the Weighted Pay Adjustment of each lot (last column of the table). These weighted pay adjustments are then summed to determine the incentive or disincentive for the particular distress (100% being no incentive or disincentive).

$$\frac{\sum_{rk} (P|B)_{rk}}{N_{r(ACI)}}$$

Figure 44: Equation - Individual distress Pay Factor

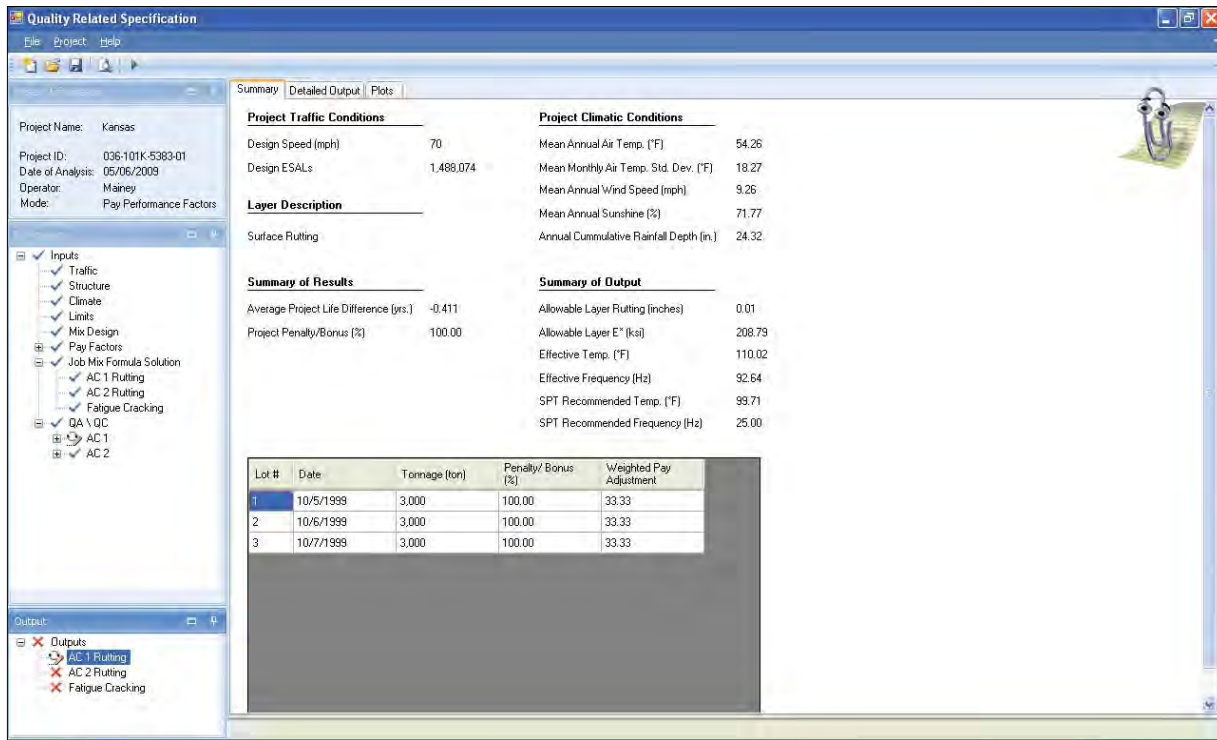


Figure 45: Screen shot - Individual distress summary

Statistical information for each lot (Figure 46) can be seen by clicking on the Detailed Output tab of the individual distress summary screen. The detailed output screen shows the important inputted data and calculated results for each lot, including Target Distress, Predicted Distress, Target Service Life, Predicted Service Life, Predicted Life Difference, Penalty/Bonus (see Pay Factors), and the Weighted Pay Adjustment.

Lot #	Date	Tonnage	Az Voids (%)	Binder Content (Vbeff %)	Effective Tempera (F)	Effectiv Freque (Hz)	Target E* (k.s)	Predictec E* (k.s)	E* Varianc	E* Coefficient of Variation (%)	Target Distress (in.)	Predictc Distress (in.)	Distrib Stand Devia	Distress Coefficient of Variation (%)	Target Service Life (yrs)	Predicted Service Life (yrs)	Service Life Standar Deviatic	Service Life Coefficient of Variation (%)	Predicted Life Difference (yrs)	Reliability	Penalty/Bonus	Weighted Pay Adjustment
3	10/7/1999	3,000	5.050	11.428	110.023	92.638	213.275	233.047	45.823	19.662	0.014	0.012	0.003	22.320	20.029	19.489	1.127	5.781	-0.541	0.376	100.00	33.333
2	10/6/1999	3,000	6.210	11.139	110.023	92.638	213.275	228.196	45.398	19.877	0.014	0.012	0.003	22.611	20.029	19.616	1.147	5.846	-0.414	0.373	100.00	33.333
1	10/5/1999	3,000	6.600	10.636	110.023	92.638	213.275	223.581	46.451	20.776	0.014	0.013	0.003	23.923	20.029	19.751	1.214	6.148	-0.279	0.362	100.00	33.333

Figure 46: Screen shot - Detailed output

Predicted Life distribution plots

The cumulative distribution of predicted life for each as-built lot and its comparison with the cumulative distribution of predicted life for the as-designed mix (Figure 47) can be seen by clicking on the Plots tab and selecting the lot number from the drop-down list.

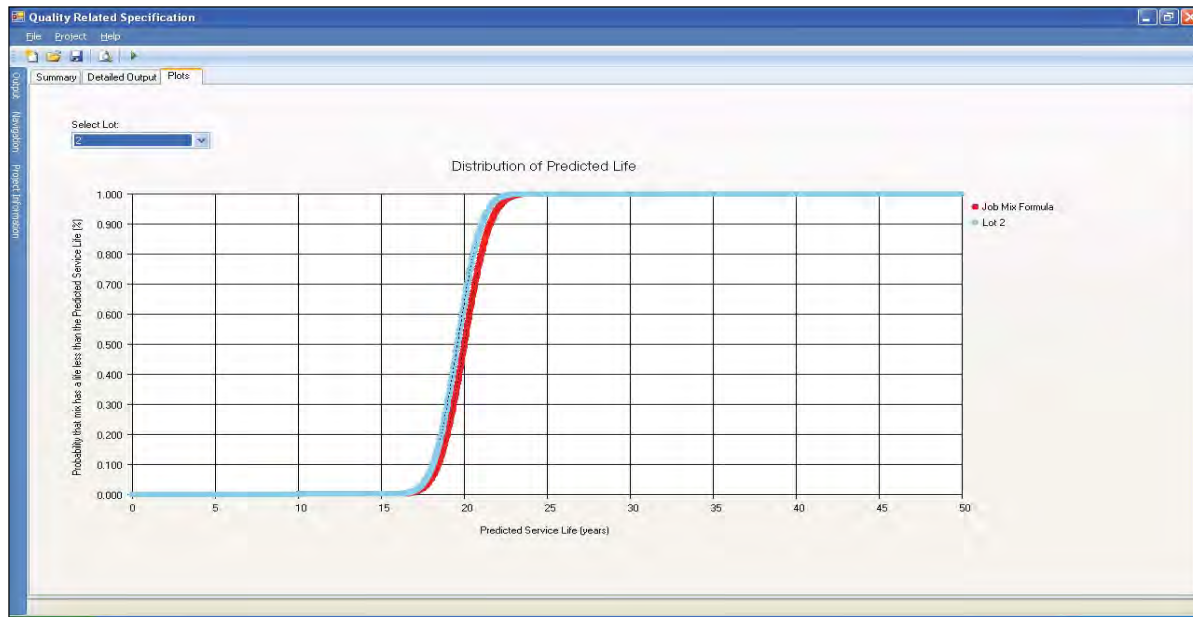


Figure 47: Screen shot - Predicted Life distribution plots

APPENDICES

Example Input Data

An example input data is provided below for the user to practice. Each tab is separated using the respective heading for convenience. These are not the default values to be used, but provided only for practice.

Material Properties

AC Surface

Gradations

1 1/2 "	
1 "	
3/4 "	100
1/2 "	
3/8 "	98
#4	61
#8	
#10	
#16	
#30	
#40	
#50	
#100	
#200	3.4

Design Volumetrics

Air voids	4.0
Asphalt Content by Wt	6.5

Binder Characteristics

Binder Type	PG58-28
Gb	1.03

Target In-Situ Volumetrics

Air_voids	6.0
Gsb	2.500
Gmm	2.360

AC Binder

Gradations

1 1/2 "	
1 "	
3/4 "	100
1/2 "	
3/8 "	80
#4	53
#8	
#10	
#16	
#30	
#40	
#50	
#100	
#200	4.0

Design Volumetrics

Air voids	4.0
Asphalt Content by Wt	5.4

Binder Characteristics

Binder Type	PG58-28
Gb	1.03

Target In-Situ Volumetrics

Air_voids	6.0
Gsb	2.471
Gmm	2.371

QA/QC Inputs

AC Surface

Daily Production

Lots 7

ID	Date	Tonnage
1	10/5/1999	3000
2	10/6/1999	3000
3	10/7/1999	3000

Gradation

3/4 "

Lot	1	2	3	4
1	100	100	100	100
2	100	100	100	100
3	100	100	100	100

3/8 "

Lot	1	2	3	4
1	98.0	97.0	98.0	98.0
2	98.0	97.0	98.0	98.0
3	97.0	98.0	97.0	97.0

#4

Lot	1	2	3	4
1	60.0	60.0	64.0	63.0
2	63.0	63.0	65.0	62.0
3	59.0	61.0	61.0	59.0

#200

Lot	1	2	3	4
1	3.7	3.9	3.5	3.4
2	3.4	3.4	3.7	3.3
3	3.0	2.7	3.4	3.0

Asphalt Lot	Content			
	1	2	3	4
1	6.3	6.2	6.4	6.4
2	6.4	6.6	6.7	6.6
3	6.5	6.5	6.4	6.3

Gmm Lot	1	2	3	4
	1	2.451	2.458	2.462
2	2.449	2.454	2.450	2.462
3	2.448	2.463	2.471	2.451

Bulk Density (PCF) Lot	1	2	3	4
	1	137.1	135.0	136.5
2	138.2	139.1	138.0	136.9
3	139.8	139.2	138.8	138.9

In-Situ Air Voids Lot	1	2	3	4
	1	7.0	8.5	7.5
2	6.1	5.5	6.2	7.0
3	4.6	5.1	5.4	5.3

Thickness Lot	1	2	3	4
	1	1.0	1.0	1.0
2	1.0	1.0	1.0	1.0
3	1.0	1.0	1.0	1.0

Gsb Lot	1	2	3	4
	1	2.500	2.500	2.500
2	2.500	2.500	2.500	2.500
3	2.500	2.500	2.500	2.500

AC Binder

Daily Production

Lots		7	
ID	Date	Tonnage	
1	8/5/1999	3000	
2	8/6/1999	3000	

Gradation

3/4 "

Lot	1	2	3	4
1	99.0	100.0	100.0	98.0
2	99.0	99.0	100.0	100.0

3/8 "

Lot	1	2	3	4
1	74.0	75.0	77.0	76.0
2	77.0	77.0	80.0	79.0

#4

Lot	1	2	3	4
1	50.0	49.0	50.0	51.0
2	51.0	51.0	52.0	54.0

#200

Lot	1	2	3	4
1	3.4	3.2	3.4	3.8
2	3.7	3.9	3.8	4.1

Asphalt Content

Lot	1	2	3	4
1	5.4	5.4	5.5	5.6
2	5.9	5.7	5.7	5.7

Gmm

Lot	1	2	3	4
1	2.363	2.363	2.362	2.357
2	2.346	2.363	2.359	2.356

Bulk Density (PCF)

Lot	1	2	3	4
1	138.1	140.5	139.8	135.4
2	139.1	137.5	136.2	135.3

In-Situ Air Voids

Lot		1	2	3	4
	1	6.1	4.5	4.9	7.9
	2	5.2	6.2	7.1	7.7

Thickness

Lot		1	2	3	4
	1	7.0	7.0	7.0	7.0
	2	7.0	7.0	7.0	7.0

Gsb

Lot		1	2	3	4
	1	2.471	2.471	2.471	2.471
	2	2.471	2.471	2.471	2.471

Abbreviations and acronyms used without definitions in TRB publications:

AAAE	American Association of Airport Executives
AASHO	American Association of State Highway Officials
AASHTO	American Association of State Highway and Transportation Officials
ACI-NA	Airports Council International-North America
ACRP	Airport Cooperative Research Program
ADA	Americans with Disabilities Act
APTA	American Public Transportation Association
ASCE	American Society of Civil Engineers
ASME	American Society of Mechanical Engineers
ASTM	American Society for Testing and Materials
ATA	Air Transport Association
ATA	American Trucking Associations
CTAA	Community Transportation Association of America
CTBSSP	Commercial Truck and Bus Safety Synthesis Program
DHS	Department of Homeland Security
DOE	Department of Energy
EPA	Environmental Protection Agency
FAA	Federal Aviation Administration
FHWA	Federal Highway Administration
FMCSA	Federal Motor Carrier Safety Administration
FRA	Federal Railroad Administration
FTA	Federal Transit Administration
HMCRP	Hazardous Materials Cooperative Research Program
IEEE	Institute of Electrical and Electronics Engineers
ISTEA	Intermodal Surface Transportation Efficiency Act of 1991
ITE	Institute of Transportation Engineers
NASA	National Aeronautics and Space Administration
NASAO	National Association of State Aviation Officials
NCFRP	National Cooperative Freight Research Program
NCHRP	National Cooperative Highway Research Program
NHTSA	National Highway Traffic Safety Administration
NTSB	National Transportation Safety Board
PHMSA	Pipeline and Hazardous Materials Safety Administration
RITA	Research and Innovative Technology Administration
SAE	Society of Automotive Engineers
SAFETEA-LU	Safe, Accountable, Flexible, Efficient Transportation Equity Act: A Legacy for Users (2005)
TCRP	Transit Cooperative Research Program
TEA-21	Transportation Equity Act for the 21st Century (1998)
TRB	Transportation Research Board
TSA	Transportation Security Administration
U.S.DOT	United States Department of Transportation